Platelets sequester extracellular DNA, capturing tumour-derived and free foetal DNA



Lauren Murphy

Exeter College

University of Oxford

A thesis submitted for the degree of

Doctor of Philosophy

Michaelmas 2024

Acknowledgements

Firstly, I would like to thank my supervisor Beth, for giving me the opportunity to complete my DPhil in the Psaila lab. Your help and guidance over the past five and a half years, positive attitude, and enthusiasm, especially for attending conferences in sunny locations, has been invaluable. I appreciate the confidence you've placed in me, your unfailing interest, and the freedom you've granted me to explore and develop my own ideas. I would also like to thank my co-supervisors Adam Mead and Simon Leedham for their support and encouragement throughout. I am also grateful to the flow and imaging facilities at the Weatherall Institute for Molecular Medicine, in particular Sally-Ann Clark, Christoffer Lagerholm and Jana Koth for training me and helping me to generate and analyse these data. I would also like to thank Jill Brown and Daniela Moralli for their incredible patience and assistance in helping me optimize the FISH protocols. Finally, I would like to extend my thanks to Pamela Holland, Chris Greggory, and Paul Rees for their unwavering support from the very start of this project through to its completion. Your cheerfulness and ability to make even Zoom meetings enjoyable have been very much appreciated.

To my Oxford lab colleagues, especially Jen, Aimee, Christina and Ravza - thank you for your day-to-day support, company, laughter and unwavering enthusiasm for ‘Doughnut Thursdays’. Thank you to my lab manager, Cristina- not only for your support but also for naming one of our tissue culture fridges ‘Taylor Swift.’ To Natalie, Camelia and Eleanor, thank you for being the dream team that helped me power through the revision experiments for the paper -I couldn’t have done it without you. And finally, to Jeanne, thank you for your kindness and invaluable bioinformatics expertise, which played a crucial role in bringing the manuscript to fruition.

I would also like to thank the many patients who generously donated samples to the study, as well as acknowledge the mice who were used in this research. Thank you to my funders: the Emerson Collective and Cancer Research UK.

Above all - to my family -my parents and sister. Thank you for listening to all of my practice presentations and continually reminding me how cool the project is. Thank you for also offering valuable perspective when I mix up samples, clog the flow machine or accidentally throw samples away. Your continual reminders that life extends beyond the lab have not only brought balance and joy but also averted many a late-night spiral. To Youcef, thank you for being my endless source of encouragement and for always knowing when to ask about my experiments- and, more importantly, when not to. Your late-night lab pickups, understanding of how "just five more minutes" somehow turns into three hours, and the smile you always greet me with when I finally emerge, have meant so much. Your patience and support through this PhD have been truly invaluable.

Finally, to my late friend Ciará Ward. Your enduring friendship, unwavering support, and genuine interest in the science I do have indelibly shaped the person I am today.

This thesis is dedicated to you.

Declaration

I declare that this thesis is entirely my own work, and except where otherwise stated, describes my own research. The following contributions were specifically made in this work and are acknowledged in relevant sections throughout:

Chapter 3

1. ITP mouse maintenance was carried out by Rong Li.
2. ChIPmentation data were generated by Jeanne Inchauspé (Fig. 3-9E & G).

Chapter 4

3. The generation, purification and amine labelling of extracellular vesicles from BL2 and BL2-bcl-2 cells was carried out by Pamela Holland from the University of Edinburgh. Pamela also performed platelet-EV co-cultures.
4. Natalie Jooss and Camelia Benlabioid assisted in flow cytometry experiments (Fig. 4-14 and Fig. 4-15D).
5. Co-localisation analysis of the Airyscan images were carried out by Paul Rees (Fig. 4-16B and Fig. 4-17B).

Chapter 5

6. Bioinformatics analysis was performed by Jeanne Inchauspé, Benjamin Schuster-Böeckler and Zohar Etzioni for whole genome sequencing analysis (Fig. 5-11- Fig. 5-15).
7. KPN mouse maintenance was carried out by Hayley Belnoue-Davis.
8. KPC mouse maintenance and p53 immunohistochemical staining were performed by Giampiero Valenzano (Fig. 5-17B).

Abstract

Platelets are small, anucleate cells with important roles in haemostasis and immunity. During cell death and aberrant mitosis, nucleated cells release chromosomal DNA, resulting in ‘cell free’ DNA in plasma (cfDNA). An excess of cfDNA is deleterious. Given their ability to sense and internalise pathogen-derived nucleic acids, we hypothesised that platelets may also clear endogenous cfDNA. Here I reveal that despite lacking a nucleus, platelets contain a repertoire of DNA fragments that map across the nuclear genome. I identify mechanisms by which platelets sequester DNA and demonstrate foetal DNA in maternal platelets and cancer cell-derived DNA in platelets from patients with pre-malignant lesions and overt cancers. As current liquid biopsy approaches utilise platelet-depleted plasma, this suggests that important genetic information within platelets is being missed. This study establishes a physiological role for platelets that has not previously been highlighted, with broad relevance in human biology and potential for clinical translation.

Table of contents

Acknowledgments 3
Declaration 5
Abstract 6
Table of contents 7
List of figures 14
List of tables 17
List of Videos 18
List of abbreviations 19

CHAPTER 1: INTRODUCTION 24
1-1 Platelet overview 24
1-1.1 Platelet production 24
i) Pro-platelet formation 25
ii) Megakaryocyte budding 26
iii) Neutrophil plucking 27
1-1.2 Platelet structure 28
i) Platelet cytoskeleton 29
ii) Open canalicular system 29
1-1.3 Platelet granules 30
i) Alpha granules 30
ii) Dense granules 31
iii) Lysosomes 32
iv) T-granules 32
1-1.4 Platelet nucleic acid content 32
i) Megakaryocyte- derived mRNA 33
ii) Non-megakaryocyte- derived RNA 33
iii) Micro RNA 33
iv) Mitochondrial DNA 34
1-2 Haemostasis 34
1-3 Non-canonical roles 38
1-3.1 Platelets in infection 38
i) Platelets recognise pathogens 38
ii) Platelets internalise pathogens 39

iii) Platelets facilitate removal of old and damaged cells 39
iv) Platelets secrete anti-microbial proteins 40
1-3.2 Platelets in inflammation 42
1-3.3 Platelets in cancer 44
i) Tumour initiation and growth 44
ii) Angiogenesis 44
iii) Invasion and metastasis 45
iv) Immune evasion 45
v) Extravasation and establishment of the metastatic niche 46
1-3.4 Tumour educated platelets 49
i) Platelet 'education' by cancer cells 49
a. Tumour induced activation 49
b. Uptake of tumour derived protein 50
c. RNA delivery and modifications to RNA processing 50
d. Tumour educated megakaryocytes 51
ii) TEP transcriptome as a biomarker for disease 53
1-4 Overview of cell free DNA 55
1-5 Hypothesis and Aims 57

CHAPTER 2: MATERIALS AND METHODS 60
2-1 Ethical approval, banking and processing of samples 60
2-1.1 Blood collection 60
i) Non cancer controls 60
ii) Sessile serrated lesions 61
iii) GI malignancies 61
iv) Immune thrombocytopenic purpura 61
v) Obstetric samples 62
2-1.2 Animals 62
i) Colorectal (KP and KPN) 62
ii) Pancreatic (KPC) 63
iii) Immune thrombocytopenic purpura 63
2-2 Blood cell isolation 64
2-2.1 Platelet and plasma isolation 64
i) Method optimisation 64
ii) Final protocol 65
iii) Purity assessment of isolated platelets 66
2-2.2 Murine platelet and plasma isolation 67

2-2.3 Human granulocyte, mononuclear and red blood cell isolation 67
2-3 Nucleic acid extraction and QC 68
2-3.1 Genomic DNA 68
2-3.2 Cell free DNA 68
2-3.3 Nucleic acid quantification 68
2-3.4 Conversion to genomic copies per µl 69
2-3.5 Automated electrophoresis 69
2-3.6 Polymerase chain reaction 69
2-4 Droplet digital PCR 70
2-4.1 Method overview 70
2-4.2 Human assays 72
2-4.3 Mouse assays 72
2-5 Cell lines 73
2-5.1 Cell maintenance 73
2-5.2 BL2-Bcl-2 cell generation 73
i) Generation of extracellular vesicles 74
ii) Purification of extracellular vesicles 74
iii) Fluorescent labelling of extracellular vesicles 75
2-6 Flow cytometry and fluorescence-activated cell sorting 75
2-6.1 Flow cytometry instrumentation 75
2-6.2 Platelet purity assessment 75
2-6.3 Platelet sorting from whole blood 76
2-6.4 Platelet nucleic acid content 76
2-6.5 Platelet activation 76
i) To evaluate the activation status and DNA content of healthy donor platelets 77
ii) To assess platelet reactivity to cargo trafficking and activation inhibitors 77
iii) To evaluate platelet reactivity in response to synthetic DNA exposure 77
iv) To determine changes in platelet DNA content upon activation 78
2-7 *In vitro* co-culture experiments 78
2-7.1 Blood cell-tumour incubation 78
i) Description of method 78
ii) Co-culture set up 79
2-7.2 Platelet- extracellular vesicle incubation 80
2-7.3 Platelet-synthetic DNA oligo 80
i) Synthetic oligo generation 80
ii) Platelet-DNA oligo incubation 81
2-7.4 DNase treatment to investigate DNA internalisation 82

2-7.5 Inhibition of platelets endocytosis and exocytosis 83
i) Description of inhibitors 83
ii) Platelet endocytosis 83
iii) Platelet exocytosis 84
2-7.6 Inhibition of platelet activation 85
2-8 Immunofluorescence microscopy 85
2-8.1 Live 86
i) Platelet-tumour cell 86
ii) Platelet-conditioned media 86
2-8.2 Fixed 87
i) Sorted platelet from whole blood 87
ii) Apoptotic extracellular vesicles 87
iii) Platelet-apoptotic extracellular vesicle incubation 88
iv) Histology, immunohistochemistry, and imaging of peripheral blood films 88
v) Fluorescence In Situ Hybridization 89
vi) ZEISS Airyscan imaging of platelet ultrastructure 90
2-8.3 Image analysis 91
2-9 H3k27ac ChIPmentation of platelet chromatin 92
2-10 Whole genome sequencing 94
2-10.1 Library preparation 94
i) Platelet DNA size selection 94
ii) Genomic DNA fragmentation 94
iii) NEBNext® UltraTM II DNA Library Prep 95
2-11 Bioinformatics analysis 95
2-11.1 Data pre-processing 95
2-11.2 Insert size distribution 96
2-11.3 Peak quantification 96
2-11.4 Coverage plotting 96
2-11.5 Gini index 96
2-11.6 Read depth around transcription start sites 96
2-11.7 ichorCNA 97
2-11.8 Targeted mutational analysis 97
i) Tumour tissue DNA sequencing and analysis 97
ii) Estimation of observed and expected tumour fragments 97
2-11.9 Data availability 98
2-11.10 Code availability 98
2-11.11 Statistical analysis 98

CHAPTER 3: PLATELETS CONTAIN DNA 99

3-1 Introduction 99

3-1.1 Indications that platelets may contain DNA 99

3-1.2 Platelets express nucleic acid sensing receptors 100

i) Toll-Like Receptor 9 100

ii) Receptor for Advanced Glycation End products 101

3-1.3 Anucleate red blood cells bind DNA via Toll-Like Receptor 9 103

3-1.4 Hypothesis and aims 104

3-2 Results 105

3-2.1 Healthy donor platelets associate with DNA 105

i) Platelets from peripheral blood 106

ii) Plateletpheresis and fluorescently sorted platelets 109

3-2.2 Assessment of DNA associated platelets using flow cytometry 111

i) Labelling of platelet DNA with DRAQ5 111

ii) Labelling of platelet RNA with Syto-13 111

iii) DNA containing platelets show increased expression of activation markers 112

3-2.3 Platelets capture DNA during circulation 113

i) Maternal platelets sequester foetal DNA 113

ii) Rise in plasma cell free DNA after acute platelet depletion in healthy mice 113

iii) Increased plasma cell free DNA in patients with ITP 114

3-2.4 Platelets sequester DNA from nucleated cells 116

i) Platelet-tumour cell incubation 116

ii) Platelet-tumour cell conditioned media incubation 122

3-2.5 Box 1. Summary of findings in Aim1 124

3-3 Discussion 125

CHAPTER 4: MECHANISMS OF DNA UPTAKE BY PLATELETS 128

4-1 Introduction 128

4-1.1 Platelet endocytosis 128

4-1.2 Platelets sequester extracellular vesicles 132

4-1.3 Platelet exocytosis 136

4-1.4 Platelet activation 137

i) Pharmacological inhibition of platelet activation 139

4-1.5 Platelet lifespan 141

4-1.6 Hypothesis and aims 145

4-2 Results 146

4-2.1 Nucleic acid transfer via DNA-loaded extracellular vesicles 146
i) Extracellular vesicles contain DNA 146
ii) Platelets internalise DNA loaded apoptotic extracellular vesicles 147
4-2.2 Platelet uptake of 'membrane free' DNA fragments of different lengths 150
4-2.3 Impact of DNA exposure on platelet immunophenotype and response to agonists 150
4-2.4 Inhibition of platelet cargo trafficking 152
4-2.5 Inhibition of platelet activation 154
4-2.6 DNA is internalised by the platelets 157
i) DNA fragments are protected from enzymatic degradation 163
4-2.7 Box 2. Summary of findings in Aim 2 164
4-3 Discussion 165

CHAPTER 5: CLINICAL UTILITY OF PLATELET DNA 173
5-1 Introduction 173
5-1.1 Liquid biopsy 173
5-1.2 Cell free DNA 174
5-1.3 Origin of cell free DNA 175
5-1.4 Cell free DNA production 175
5-1.5 Cell free DNA clearance 177
5-1.6 Deleterious effects of excess circulating cell free DNA 179
5-1.7 Hypothesis and aims 181
5-2 Results 182
5-2.1 Detection of mutant alleles in platelets 182
5-2.2 Platelets are more efficient at capturing DNA compared to other blood cell types 183
5-2.3 Mutant alleles captured by platelets are protected from degradation 184
5-2.4 Genomic distribution and origin of platelet DNA 186
i) Size distribution 186
ii) Genomic distribution and origin of platelet DNA 187
iii) Nuclear genomic coverage of platelet DNA mirrors cell free DNA 192
5-2.5 Copy number variations are detectable in platelet DNA 193
5-2.6 Deeper sequencing reveals mutant alleles are detectable in platelet DNA 195
5-2.7 Inferring gene expression and cell of origin from platelet DNA and cell free DNA 196
5-2.8 High abundance of mutant alleles in platelets in colorectal and pancreatic carcinoma 198
5-2.9 Detection of *BRAF*V600E in platelets from patients with pre-malignant lesions 201
5-2.10 Box 3. Summary of findings in Aim 3 203
5-3 Discussion 204

CHAPTER 6: DISCUSSION 207

6-1 Outcomes of this research 207

6-1.1 Despite being anucleate, platelets contain DNA 207

6-1.2 Platelets sequester DNA via multiple mechanisms 207

6-1.3 Platelets contain clinically important tumour- derived DNA 208

6-2 Implications and wider relevance 209

6-3 Limitations of this research 210

6-4 Future research 212

6-4.1 Question 1: Do platelets transfer sequestered DNA to other cell types? 212

6-4.2 Question 2: Do platelets release DNA at sites of activation to elicit an immune response? 214

6-4.3 Question 3: Can we inhibit platelet exocytosis in whole blood? 215

6-4.4 Question 4: Are DNA sensing receptors involved in platelet DNA uptake? 215

6-5 Conclusion 216

BIBLIOGRAPHY 217

APPENDIX 244

List of Figures

Chapter 1: Introduction

1-1 Schematic of platelet production mechanisms

1-2 Schematic illustrating the platelet cytoskeletal structure and internal membrane system, the OCS

1-3 Schematic illustrating platelet interactions with exposed extracellular matrix components in the vessel wall

1-4 Representative platelet receptors that mediate bacterial and viral interactions

1-5 Platelets mediate the immune response via multiple mechanisms

1-6 The role of platelets in tumour development

1-7 Mechanisms of tumour-induced platelet education

1-8 Summary of aims

Chapter 2: Materials and Methods

2-1 Schematic showing sources of purified platelets

2-2 Droplet digital PCR workflow

2-3 *In vitro* co-culture set up

2-4 Design of synthetic DNA fragments

2-5 Method used to explore mechanisms of DNA uptake

2-6 Method used to investigate platelet DNA release

Chapter 3: Platelets contain DNA

3-1 Hypothetical role for platelet RAGE and TLR9 in DNA sensing and internalisation based on published literature

3-2 Schematic showing sources of purified platelets

3-3 Detection of DNA from peripheral blood

3-4 DNA extraction from plateletpheresis samples and platelets sorted from whole blood

3-5 Detection of DNA in circulating platelets using DRAQ5

3-6 DNA containing platelets are younger and more activated

3-7 Platelets capture DNA during circulation

3-8 Platelets sequestration of DNA released from nucleated tumour cells

3-9 Platelets sequester nucleosomes

3-10 Platelet uptake of tumour derived DNA is rapid

Chapter 4: Mechanisms of DNA uptake by platelets

4-1 Cargo trafficking in platelets and common drugs used to inhibit them
4-2 Production of extracellular vesicles and apoptotic bodies
4-3 Proposed mechanism of platelet uptake of extracellular vesicles
4-4 Platelet exocytosis via fusion pore formation
4-5 Schematic of platelet activation
4-6 Mechanism of aspirin inhibition
4-7 The effects of ibrutinib on platelet function
4-8 Proposed mechanisms of platelet clearance
4-9 Apoptotic platelets communicate with circulating phagocytes
4-10 Extracellular vesicles contain genomic DNA
4-11 Platelets sequester DNA containing vesicles
4-12 Platelet uptake of 'free' DNA fragments
4-13 Platelet uptake of DNA-loaded extracellular vesicles and 'free' DNA fragments can be pharmacologically modulated
4-14 Inhibition of alpha granule secretion by Dynole and amiloride
4-15 Inhibition of platelet activation increases platelet DNA content
4-16 Platelets internalise DNA
4-17 Platelet DNA is localised at the centre of platelets
4-18 Platelet DNA is protected from nucleases
4-19 Proposed mechanism of action showing amiloride inhibition of the sodium-hydrogen exchanger (NHE) in the platelet plasma membrane
4-20 Proposed mechanism of action illustrating how treatment with Dynole and amiloride reduces platelet secretion
4-21 Proposed mechanism of DNA uptake by platelets

Chapter 5: Clinical utility of platelet DNA

5-1 Advantages and disadvantages of current liquid biopsy biomarkers
5-2 Fragmentation characteristics of cell free DNA
5-3 Fragmentation characteristics of circulating tumour DNA
5-4 Characteristics of cell free DNA in circulation
5-5 Immune sensing of cell free DNA
5-6 Platelets contain tumour -derived DNA bearing cancer-associated gene mutations
5-7 Platelets are more efficient at capturing tumour-derived DNA compared to other blood cell types
5-8 Impact of DNase treatment on the detection of *JAK2* mutant alleles
5-9 Platelets contain both short and long fragments of DNA

5-10 Bead separation of platelet DNA
5-11 Platelets capture fragments of DNA that map across the human genome
5-12 Fragmentomic analysis reveals platelets contain shorter, tumour -derived DNA
5-13 Platelet DNA analysis reveals copy number variations
5-14 Platelets contain tumour-derived DNA bearing cancer-associated gene mutations
5-15 Platelet DNA analysis reveals gene activity in cell-of-origin
5-16 Detection of driver mutations in pDNA and cfDNA from mice with localised and metastatic colorectal adenocarcinoma
5-17 Detection of driver mutations in pDNA and cfDNA from mice with localised pancreatic cancer
5-18 Detection of driver mutations in patients with pre-malignant colonic lesions

Chapter 6: Discussion

6-1 Schematic illustrating how immediate inhibition of platelet secretion may enhance the yield of tumour-derived biomarkers, thereby improving the sensitivity of tumour detection

Appendix

A1 Platelet sequestration of DNA released by nucleated cells
A2 PBS control for vesicle imaging
A3 Flow cytometric analysis of resting platelets
A4 Comparison of total DNA isolated from platelets using two different extraction kits
A5 Comparison of DNA yield from platelet poor plasma (PPP) and platelet rich plasma (PRP)

List of Tables

A1 Platelet wash buffer and HEPES-modified Tyrode's buffer
A2 Droplet digital PCR assays
A3 Antibodies and nucleic acid stains used for flow cytometry
A4 Reagents used to assess platelet reactivity
A5 Details of synthetic DNA fragments synthesised
A6 Antibodies and nucleic acid stains used for microscopy
A7 Clinical information for the control cohort (n=14, including patients with ulcerative colitis, Crohn's disease and individuals on the bowel cancer screening programme)
A8 Clinical information for patients with pre-malignant sessile serrated lesions (n=34)
A9 Clinical information for patients with gastrointestinal carcinoma (n=15)
A10 Clinical information for patients with gastrointestinal carcinoma used for whole genome sequencing study (n=13)
A11 Clinical information for obstetric cohort (n=30)
A12 Clinical information for the immune thrombocytopenic purpura (ITP) and controls cohort (n=23)

List of Videos

Chapter 3: Platelets contain DNA

Video 1: Maternal platelets sequester male foetal DNA

Video 2: A healthy donor platelet sequesters tumour- derived DNA

Video 3: Multiple platelets sequester COLO205 tumour- derived DNA

Video 4A and 4B: Healthy donor platelets physically interact with colorectal tumour cells

Video 5: Platelets sequester tumour-derived, DNA bound histone proteins

Chapter 4: Mechanisms of DNA uptake by platelets

Video 6: Platelets interact with DNA containing extracellular vesicles

Video 7: Platelets internalise DNA containing extracellular vesicles

List of Abbreviations

Abbreviation	Expansion
3D	3 dimensional
AA	Arachidonic acid
ACD	Acid citrate dextrose
AdV	Adenovirus
AMP	Adenosine monophosphate
AMR	Ashwell-Morell receptor
APO EV	Apoptotic extracellular vesicle
ASA	Aspirin
ATP	Adenosine triphosphate
AU	Arbitrary units
AUC	Area under curve
BSA	Bovine serum albumin
Btk	Bruton's tyrosine kinase
bp	Base pair
$CaCl_2$	Calcium chloride
CALR	Calreticulin
cAMP	Cyclic adenosine monophosphate
cfDNA	Cell-free DNA
cGMP	Cyclic guanosine monophosphate
Chr	Chromosome
CLEC-2	C-type lectin domain family 2
CNA	Copy number alterations
CNV	Copy number variations
CMV	Cytomegalovirus
COX-1	Cyclooxygenase-1
CRC	Colorectal cancer
CR	Complement receptor
ctDNA	Circulating tumour derived DNA

ctRNA	Circulating tumour derived RNA
CXCR4	C–X–C chemokine receptor type 4
CYTO D	Cytochalasin D
DAMPs	Damage-associated molecular patterns
DAPI	4′,6-diamidino-2-phenylindole
DC-SIGN	DC-specific intercellular adhesion molecule-3-grapping non-integrin
ddPCR	Droplet digital PCR
DMSO	Dimethyl sulfoxide
DNA	Deoxyribonucleic acid
DNM1L	Dynamin-1-like protein
dsDNA	Double stranded DNA
DTS	Dense tubular system
DV	Dengue virus
EDTA	Ethylenediaminetetraacetic acid
EGFR	Epidermal growth factor receptor
EMCV	Encephalomyocarditis virus
EMT	Epithelial-mesenchymal transition
EV	Extracellular vesicle
FACS	Fluorescence activated cell sorting
FAM	Fluorescein
FBS	Foetal bovine serum
FCγRII	Fc receptor γ II
FISH	Fluorescence in situ hybridization
FGF	Fibroblast growth factors
FSC	Forward scatter channel
GPVI	Glycoprotein VI
GRA	Granulocyte
gDNA	Genomic DNA
GP	Glycoprotein
GTP	Guanosine triphosphate
H2B	Histone H2B
HBSS	Hank’s Balanced Salt Solution
HCV	Hepatitis virus C
HEX	Hexachlorofluorescein
HIV	Human immunodeficient virus
HSC	Haematopoietic stem cell

HSPC	Haematopoietic stem and progenitor cell
IgG	Immunoglobulin G
IL	Interleukin
ILV	Intraluminal vesicles
IMDM	Iscove′s Modified Dulbecco′s Medium
IMS	Invaginated membrane system
IP_3	Inositol 1,4,5- trisphosphate
IP_3R	Inositol 1,4,5- trisphosphate receptor
ITP	Immune thrombocytopenic purpura
kb	Kilobase
KP	$villinCre^{ER}$ $Kras^{G12D/+}$ $Trp53^{fl/fl}$
KPC	$Kras^{G12D/+}$ $Trp53^{R172H/+}$ P48-Cre
KPN	$villinCre^{ER}$ $Kras^{G12D/+}$ $Trp53^{fl/fl}$ $R26^{N1icd/+}$
LN_2	Liquid nitrogen
l-pDNA	Long platelet DNA
Mb	Megabase
MK	Megakaryocyte
MNC	Mononuclear cell
mRNA	Messenger ribonucleic acid
MU	Mutant
MVB	Multivesicular bodies
NADH	Nicotinamide adenine dinucleotide
NCX	Sodium-calcium exchanger
NET	Neutrophil extracellular trap
NGS	Next-generation sequencing
NHE	Sodium-hydrogen exchanger
NHSBT	NHS Blood and Transplant
non-apo-EV	Non-apoptotic extracellular vesicle
NM	Nanometer
OCS	Open canalicular system
ORB	Oxford Research Biobank
OUH	Oxford University Hospitals
PAF	Platelet activating factor
PAMPs	Pathogen-associated molecular patterns
PB	Peripheral blood
PBMNC	Peripheral blood mononuclear cells

PBS	Phosphate-buffered saline
PCR	Polymerase chain reaction
PDGF	Platelet-derived growth factor
PFA	Paraformaldehyde
PGE1	Prostaglandin E1
PGE2	Prostaglandin E2
PGH2	Prostaglandin H2
PGI_2	Prostacyclin
PGSL-1	P-selectin glycoprotein ligand-1
PI3K	Phosphatidylinositide-3-kinase
PLA	Plasma
PLA	Platelet leukocyte aggregate
PLT	Platelet
PMP	Platelet microparticle
POV	Point of view
PPP	Platelet poor plasma
PRP	Platelet rich plasma
PS	Phosphatidylserine
RAGE	Receptor for Advanced Glycation Endproducts
RANTES	Regulated upon Activation, Normal T cell Expressed and Secreted
RBC	Red blood cell
RNA	Ribonucleic acid
SE	Succinimidyl ester
s-pDNA	Short platelet DNA
SRY	Sex-determining region Y
SSC	Side scatter channel
ssDNA	Single stranded DNA
SSL	Sessile serrated lesions
TGFβ	Transforming growth factor-beta
TGU	Translational Gastroenterology Unit
TC	Tissue culture
TF	Tissue factor
TLR	Toll like receptor
TPO	Thrombopoietin
TRAP-6	Thrombin Receptor Activator for Peptide 6
TSS	Transcription start site

TxA_2	Thromboxane A_2
VAF	Variant allele frequency
VEGF	Vascular endothelial growth factor
vSNAREs	Vesicles SNAp REceptor
vWF	von Willebrand factor
WGS	Whole genome sequencing
WT	Wild type

Chapter 1: Introduction

1-1 Platelets

1-1.1 Platelet production

Platelets are the smallest cells in the blood, about 2-5 μm in size produced by megakaryocytes (MKs). The majority of MKs reside in the bone marrow, however they have also been identified in other organs, including the liver, spleen, and lungs[1-3]. Notably, a 2017 study in mice suggested that the lungs serve as a significant site of platelet biogenesis, contributing up to 50% of circulating platelets[2,4]. However, subsequent research has since indicated that this contribution is likely much smaller, confirming that while MKs may be detected in other tissues, the bone marrow remains the primary site of platelet production[5].

MKs are continually replenished throughout life by haematopoietic stem cells. After commitment to the MK lineage, maturing cells switch to a variant of the normal cell cycle called ‘endomitosis’, in which they continue to replicate their nuclear DNA without completing cytokinesis, generating large, polyploid cells. MK differentiation and maturation is primarily controlled by the cytokine thrombopoietin (TPO)[6,7]. Endomitosis is essential for producing the large quantities of mRNA, proteins, cytoplasmic membrane and organelles for platelet biogenesis. The synthesis of these proteins and lipids also facilitates the development of an extensive invaginated membrane system (IMS), which is continuous with the plasma membrane. This complex membrane network, supported by cytoskeletal fibres, serves as a membrane reservoir for proplatelet formation.

i) Proplatelet formation

As the MK matures, it degrades the basement membrane[8] and extends long, branching protrusions called proplatelets into the sinusoidal blood vessels of the bone marrow. These extensions elongate and narrow to form proplatelet shafts. This is driven primarily by the sliding of microtubule fibres, a process facilitated by the motor protein, dynein[8,9]. The microtubule cytoskeleton lines the entire length of the proplatelet and loops back towards the MK.

These microtubule dynamics also allow the transport of organelles and granules from the MK cell body into the proplatelet shaft, where they are directed towards tandem arrays of platelet-sized swellings[10,11]. Once the appropriate allotment of organelles, proteins, and RNA is packaged into the proplatelet tips, the shear force of blood flow detaches the protrusions into the vascular lumen (Fig.1-1A). Although the proplatelet shaft has multiple platelet sized swellings, fragmentation and release only occurs from the tips of proplatelets[10].

Initially, these protrusions circulate as preplatelets, which are typically larger than mature platelets. However, they quickly undergo fission in the circulation, dividing into smaller, individual platelets[12,13]. This process continues until the megakaryocyte's entire intracellular contents is trafficked along the microtubules, through the platelet shaft and packaged into the proplatelet tips[11]. Once this is complete, the MK nucleus is extruded and degraded[14,15]. Since platelets have a short lifespan of only 7-10 days before being cleared by macrophages in the spleen and liver[16], continuous replenishment of apoptotic MKs is essential to maintain MK homeostasis and ensure sustained platelet production[17]. Interestingly, Gaertner *et al.,* recently established plasmacytoid dendritic cells (pDCs) as key players in mediating the replenishment of platelet-producing MKs[17]. Their findings suggest that this subset of immune cells, bind MK- derived cfDNA through TLR9 which results in the delivery of interferon alpha (INFα) to MK progenitors, triggering their proliferation and maturation[17].

ii) Megakaryocyte budding

In contrast to the widely recognised mechanism of proplatelet fragmentation, the 'MK budding theory' offers an alternative perspective on platelet biogenesis[18-20]. Proposed by Potts *et al.,* this theory suggests that platelets are generated from localised membrane protrusions, or blebs, on the surface of MKs (Fig.1-1B)[19]. These blebs bud outward and detach directly into the bone marrow sinusoids, forming platelets without the formation of proplatelet extensions and tip fragmentation, as described above.

However, this model remains controversial, as several reports question whether MK buds contain the structural features of mature platelets, such as α-granules, an open canalicular system, a discoid shape, and a circumferential microtubule coil[21]. Italiano *et al.,* have suggested that these buds may not be platelet precursors but rather MK-derived microvesicles (MVs) lacking essential organelles[21]. This view contrasts with the findings of Potts e*t al.,* who showed that MK buds are similar in size to circulating platelets and possess platelet granule markers, including von Willebrand factor (vWF) and platelet factor 4[19].

Despite initial scepticism, the MK budding theory has recently gained support, with studies reporting findings consistent with earlier observations[18,20,22-24]. Ellis *et al.,* confirmed the presence of MK membrane buds with platelet-like ultrastructure[22] and addressed concerns raised by Italiano *et al.,* regarding some buds lacking typical platelet features[21]. They identified three distinct MK-derived structures in the bone marrow:

1. Platelet-sized, vWF-positive buds containing internal αIIbβ3 and F-actin
2. vWF-negative membrane blebs lacking internal CD41 and F-actin, likely formed at MK edges, as previously described by Italiano *et al.,*[21]
3. Scattered CD41-positive MVs, similar to those observed in circulation by Flaumenhaft *et al.,*[25]

These findings support at least two distinct mechanisms for platelet release from bone marrow MKs: the well-established proplatelet formation and the recently supported MK budding theory. Additionally, emerging research indicates the possibility of a third pathway for platelet generation.

iii) Neutrophil "plucking"

In 2022, Petzold *et al.,* presented evidence suggesting neutrophils contribute to platelet production by "plucking" on MK proplatelet extensions, accelerating their growth and driving the release of preplatelets into circulation (Fig.1-1C)[26]. Building on this, further research into neutrophil-induced platelet production, revealed that CXCR4-expressing neutrophils within the bone marrow sinusoid recognise the chemokine CXCL12, produced by MKs. This interaction facilitates neutrophil-MK adhesion, allowing neutrophils to mechanically 'pull' on MK proplatelet extensions. The resulting force fragments the proplatelet membrane, releasing preplatelets into the bloodstream. During this process, neutrophils also generate reactive oxygen species (ROS), which phosphorylate MK intracellular proteins in involved in their maturation and proplatelet formation, further enhancing platelet production[26,27].

Like the MK budding theory, neutrophil plucking presents an alternative mechanism to the classical proplatelet formation theory of platelet production. However, a key distinction is that while MK budding has been observed in human bone marrow, neutrophil plucking has not yet been demonstrated in humans[27]. Thus, further research is needed to determine the relative contribution of neutrophil-mediated platelet production to human thrombopoiesis.

In summary, proplatelet formation is well-characterized, whereas the MK budding and neutrophil plucking theories require further investigation to fully elucidate their role in platelet production.

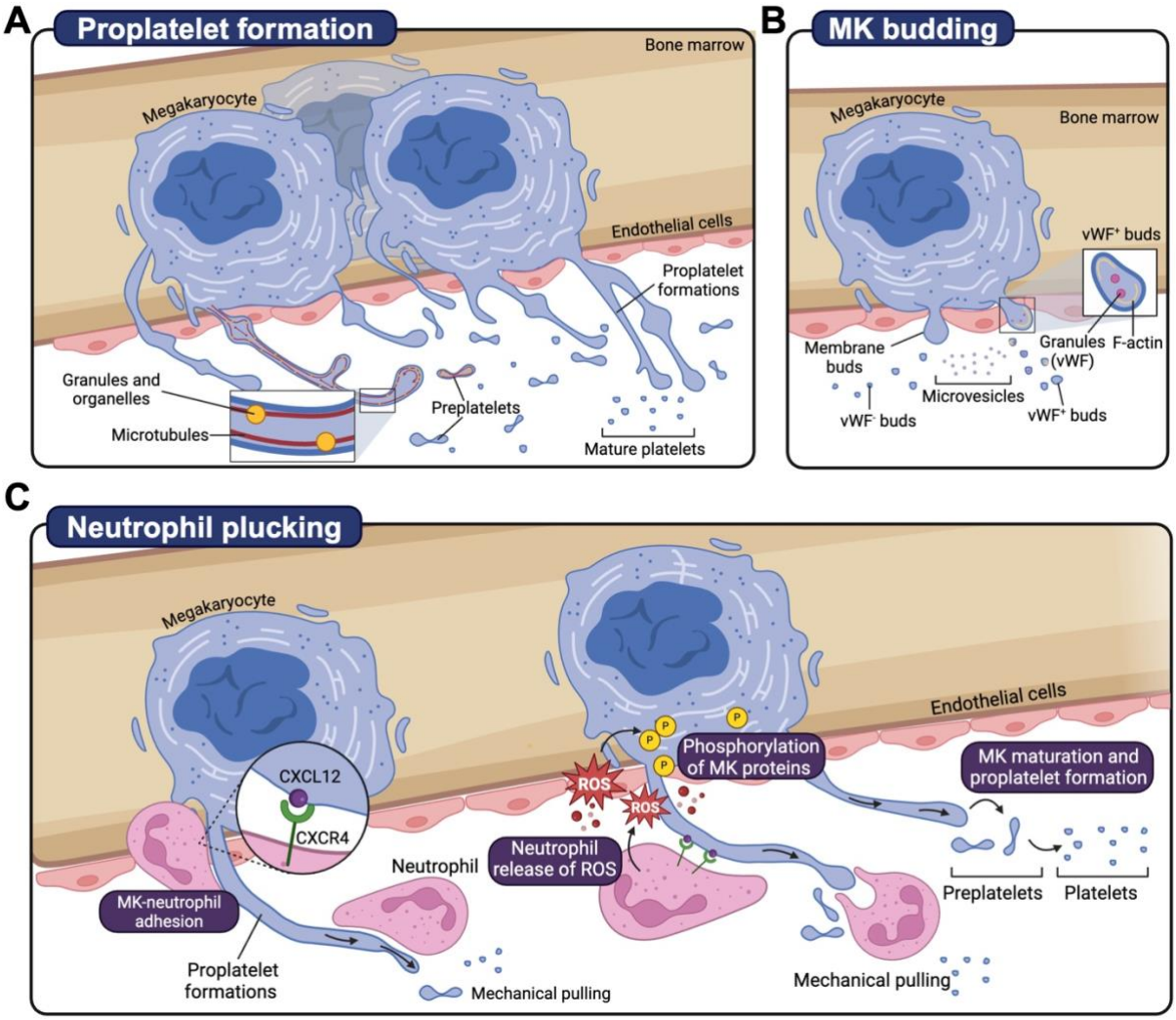


Figure 1-1. Schematic of platelet production mechanisms. (A) Long, irregularly shaped cytoplasmic protrusions extend from MKs into sinusoids. Organelles and platelet-specific granules are trafficked to platelet sized swellings via microtubules that line the length of the proplatelet[11]. The shear flow of blood causes the tips of the proplatelet to be released into the circulation. **(B)** Platelet-sized protrusions are directly released from the MK surface. Membrane buds have been shown to contain platelet-specific components such as vWF, CD41 and filamentous actin. Buds are distinct from membrane blebs and microvesicles (MVs), which lack platelet-specific internal components[18]. **(C)** Neutrophil plucking of MK proplatelet extensions. In the bone marrow sinusoids, neutrophils interact with MK proplatelet protrusions through the binding of neutrophil CXCR4 to MK-derived CXCL12. This tethering enables neutrophils to pull on and elongate the proplatelet extensions. Neutrophils also release ROS, which induce the phosphorylation of proteins essential for MK maturation and proplatelet formation. Adapted from Petzold *et al.,* (2022)[26] and Van Grinsven & Udalova (2022)[27].Created using Biorender.com.

1-1.2 Platelet structure

Despite being the smallest cells in circulation, platelets are packed with various cellular components, most of which are derived from parent MKs during thrombopoiesis. Platelets harbour a complex repertoire of RNA along with the necessary machinery for protein synthesis. They also contain typical

cytoplasmic organelles, including mitochondria, lysosomes, the Golgi apparatus, and a modified endoplasmic reticulum known as the dense tubular system (DTS). Additionally, platelets possess specialized structures essential to their function, such as the open canalicular system (OCS), alpha granules, dense granules, and an extensive cytoskeletal network composed of actin and tubulin.

i) Platelet cytoskeleton

Platelets are the only human cells that contain a marginal band (MB)- a closed ring structure composed of 7–12 microtubule filaments, located just beneath the plasma membrane[28,29]. The MB plays a crucial role in maintaining resting platelets in their discoid form.

Platelets also contain a high concentration of actin, with 60-70% existing in its unpolymerized form in resting platelets[30]. Upon activation, actin polymerizes rapidly, causing significant cytoskeletal rearrangement that leads to the formation of membrane extensions known as filopodia or lamellipodia, and an increase in surface area (Fig. 1-2A)[31,32].

ii) Open canalicular system

The open canalicular system (OCS) is a complex intracellular network of surface-connected membrane channels that facilitates the efficient uptake and release of cellular components, such as plasma proteins (Fig. 1-2B)[33,34]. Once within the OCS, these proteins are transported to the platelet's interior and directed to granules for storage. Upon activation-induced exocytosis, alpha and dense granules can fuse with the OCS membrane, releasing their contents into the extracellular environment[35]. The extensive distribution of the OCS throughout the platelet ensures close proximity of the granules to the channels, allowing for rapid content release.

Beyond cargo trafficking, the OCS also serves as a membrane reservoir, providing additional plasma membrane required during platelet activation and spreading. This enables the formation of filopodia and lamellipodia, which can increase the platelet’s surface area by up to 420%[35,36].

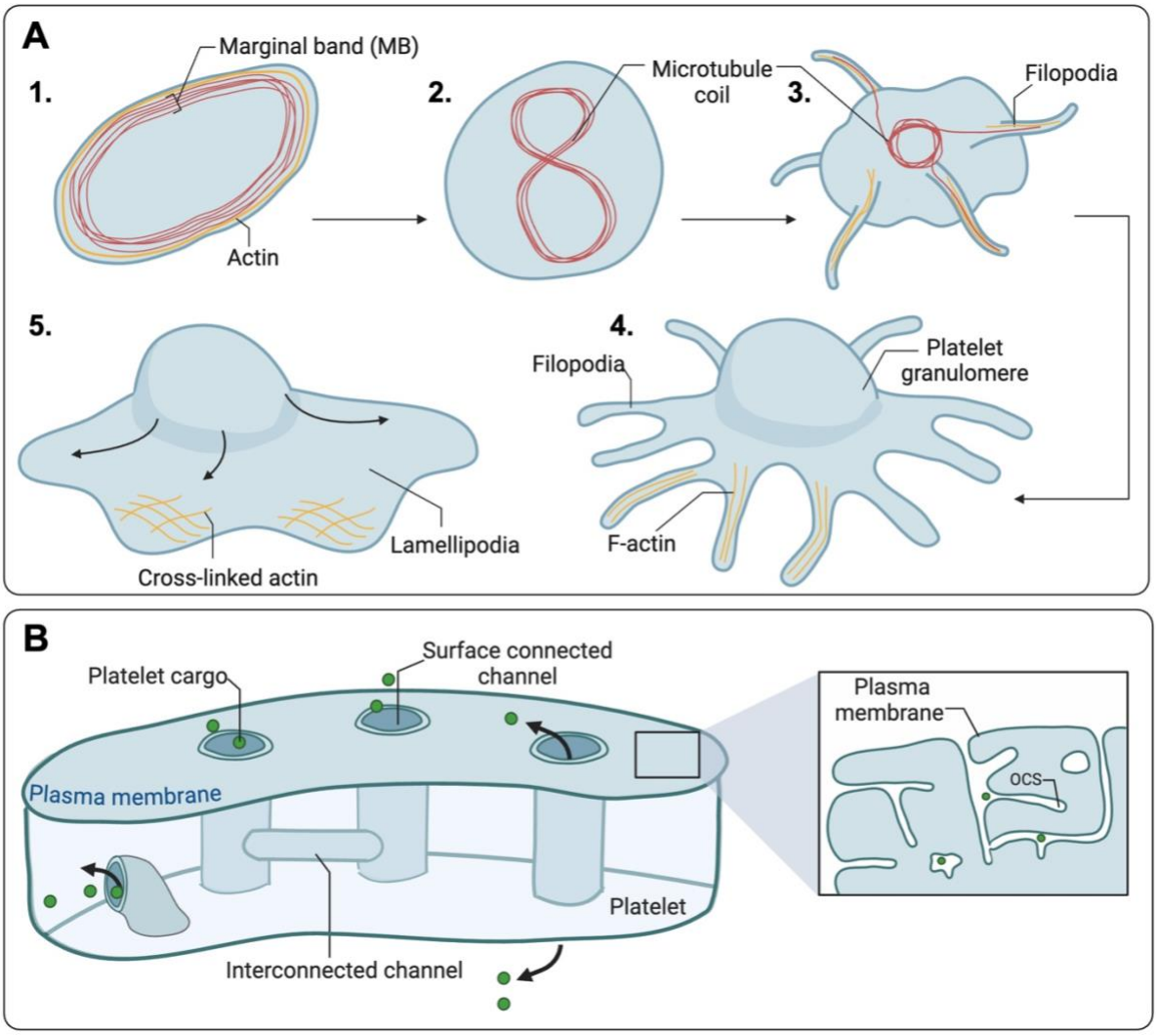


Figure 1-2. Schematic illustrating the platelet cytoskeletal structure and internal membrane system, the OCS. (A) 1) Resting platelets maintain a discoid shape due to a circumferential marginal band of microtubules. 2) Upon activation, this band coils, leading to a spherical shape. 3-4) Further activation triggers polymerization of microtubule and actin filaments, resulting in membrane protrusions that facilitate platelet aggregation, called filopodia. 5) Platelets can also extend laterally, forming lamellipodia composed of cross-linked actin filament networks[37]. Lamellipodia enable platelets to spread effectively. Figure adapted from Liu *et al.,* (2024)[38]. **(B)** The OCS is depicted as a network of surface-connected and interconnected tunnels extending throughout the platelet, providing a route for cargo transport into and out of the cell. Created using BioRender.com.

1-1.3 Platelet granules

i) Alpha granules

Alpha granules are the largest and most abundant granule type present in platelets. Each platelet contains about 50-80 alpha granules, ranging from 200-500 nm in diameter[35,39]. These granules store a

diverse[1] array of bioactive molecules, including growth factors (platelet derived growth factor [PDGF] and transforming growth factor-beta [TGF-β]), cytokines (platelet factor 4 [PF4]), coagulation proteins (fibrinogen), soluble adhesion molecules (von Willebrand Factor [vWF]), membrane adhesion molecules (P-Selectin) and pro- and anti-angiogenic factors (vascular endothelial growth factor [VEGF] and endostatin)[40-43]. Some alpha granules also contain exosomes, small vesicles of 40-200 nm that are released upon platelet activation[44].

The majority of alpha granule cargo is synthesised in the parent MK (or acquired by the MK through endocytosis) and trafficked through multivesicular bodies (MVBs) as the granules develop and mature[41]. These granules and their contents are then directed into proplatelet extensions and packaged into preplatelets before being released into the circulation[10,11,41].

While most alpha granule content originates from MKs, platelets also acquire some granule contents through endocytosis as they circulate. For example, the proteins, IgG and albumin are acquired through fluid-phase endocytosis, while fibrinogen is endocytosed via αIIbβ3 integrins[39].

ii) Dense granules

Dense granules, like alpha granules, are unique to platelets but are less abundant and smaller. Each platelet contains approximately 3-8 dense granules, each measuring about 150 nm in diameter[35,41]. While their contents are less diverse than alpha granules, dense granules are acidic and store high concentrations of crucial secondary mediators that play a vital role in amplifying platelet aggregation and coagulation, including ADP, ATP and serotonin[39,45-47]. Dense granules also contain 70% of the total platelet bivalent cations, predominantly calcium, which is present at concentrations over 100 times higher than that found in the rest of the platelet interior[48].

[1] Recent studies have suggested that platelets contain different sub-populations of alpha granules that undergo differential release upon platelet activation. However, the pathways by which platelets develop distinct alpha granule populations remain unclear. Italiano & Battinelli (2009).

The biogenesis of dense granules is less well understood than alpha granules. Unlike alpha granules, which primarily originate from the trans-Golgi network, dense granules are thought to share a similar pathway with lysosomes, originating from the late endosome/MVB compartment of MKs[48,49]. However, like alpha granules, dense granules undergo maturation in MVBs before being packaged into platelets[35,50,51].

iii) Lysosomes

Lysosomes are another type of secretory granule found in platelets, with each platelet containing approximately 2-3 lysosomes measuring around 200-250 nm in size[35]. These organelles store a range of digestive enzymes, including glycosidases, proteases and cationic proteins with bactericidal activity[48,52]. Although the specific functions of platelet lysosomes are not well understood, they are thought to participate in the digestion of phagocytic and cytosolic components, similar to the role lysosomes play in nucleated cells[48].

iv) T- granules

T-granules, a recently identified type of platelet granule, are characterized by the presence of Toll-Like Receptor 9 (TLR9)[47,48,53]. While our understanding of T-granule biology is limited, they have also been found to contain protein disulphide isomerase (PDI). This composition suggests that T-granules may originate from the endoplasmic reticulum of megakaryocytes and could be related to the dense tubular system in platelets. However, further research is needed to fully elucidate their origin, function, and relationship to other platelet structures.

1-1.4 Platelet nucleic acid content

Platelets, like mature red blood cells, are anucleate, a characteristic that likely serves two purposes. First, it allows platelets to maintain their small size and flexibility, enabling them to navigate through narrow capillaries and undergo significant morphological change[54]. Second, the absence of a nucleus provides more internal space for platelets to store the wide range of active biomolecules necessary for their various functions.

Interestingly, unlike mammals, non-mammalian vertebrates such as birds have nucleated thrombocytes. The presence of a nucleus in avian thrombocytes makes them larger and less efficient compared to mammalian platelets. For instance, avian thrombocytes spread less effectively on collagen and express significantly lower levels of the α2bβ3 integrin, which is essential for aggregate formation[54].

i) Megakaryocyte-derived mRNA

Platelets, being anucleate, lack the machinery for RNA synthesis. Therefore, during thrombopoiesis, they are selectively packed with essential RNA and processing machinery to enable protein synthesis for their various functions. For instance, platelets can translate inherited megakaryocyte mRNA to synthesize inflammatory cytokines like interleukin-1 beta (IL-1β)[55]. Although, without transcriptional machinery or DNA templates, this inherited RNA gradually degrades as platelets circulate, making platelet RNA content a useful marker to distinguish between 'young' and 'old' platelets[56-58].

ii) Non-megakaryocyte-derived RNA

It was recently shown that platelets can supplement their RNA pool by acquiring transcripts after platelet biogenesis, by taking up RNAs shed from other cells in microvesicles[59,60]. This ability to sequester RNA has led to the suggestion that the platelet transcriptome could serve as a potential biomarker for various diseases, a topic further explored in section 1-3.4.

iii) Micro RNA

In addition to mRNA, platelets contain small non-coding RNAs known as microRNAs (miRNAs)[61,62]. These miRNAs play a crucial role as key regulators of mRNA translation. Consequently, there is significant research interest in understanding how these miRNAs influence protein synthesis in platelets and, by extension, modulate platelet reactivity[62,63].

iv) Mitochondrial DNA

Finally, platelets contain a small number of mitochondria[2], with an estimated 5-8 mitochondria per platelet[54,64-66]. Human mitochondrial DNA is double-stranded, circular, small at 16.6 kb, and enclosed by a double membrane[67].

Just as in nucleated cells, platelet mitochondria are involved in metabolism, platelet activation, ATP production, and regulation of platelet viability. Due to their crucial role in energy production and the inability of platelets to replenish mitochondria proteins encoded by nuclear DNA, the lifespan of platelet mitochondria likely influences the overall lifespan of platelets[54,68].

Overall, despite being anucleate, platelets possess a diverse array of nucleic acids, including RNA inherited from parent megakaryocytes, RNA acquired from external sources, and mitochondrial DNA. However, prior to the research presented in this thesis, the presence of nuclear DNA in platelets had not been investigated.

1-2 Haemostasis

The role of platelets in haemostasis has been recognised since their discovery by Giulio Bizzozero in 1882[69]. His observations of platelet aggregation and leukocyte recruitment at sites of vessel injury, were instrumental in shaping the current understanding of haemostasis. Today, haemostasis is defined as a tightly regulated process that prevents excessive bleeding, maintains vascular integrity, and provides a protective barrier against infection.

Haemostasis consists of two components. Primary haemostasis involves platelet activation, adhesion, and aggregation, culminating in the formation of a platelet plug at the site of vascular injury. Secondary

[2]Interestingly, platelets have been reported to act as mitochondrial donors, for example transferring respiratory competent mitochondria to mesenchymal stem cells (MSCs)! This transfer improved the wound-healing capacity of MSCs via increased angiogenesis (Levoux, J. *et al.,* 2021).

haemostasis refers to the formation and deposition of insoluble fibrin, generated through the coagulation cascade. This fibrin network strengthens the platelet plug, resulting in a stable clot[70]. A summary of primary haemostasis is described below.

During circulation, platelets continuously monitor their environment, by interacting with various endogenous factors through their surface receptors. This ongoing communication enables rapid response to vascular damage. Vascular injury exposes collagen and extracellular matrix (ECM) proteins, initiating platelet tethering. This process is primarily mediated by vWF, which circulates in the plasma in an inactive form[71]. Upon vessel damage, vWF adheres to exposed collagen fibres. The shear force of blood flow then induces conformational changes in vWF, exposing binding sites for the GPIbα subunit of the platelet GPIb-IX-V complex[72-74].

Initially, the vWF- GPIbα interaction is weak, causing platelets to roll along the vessel wall. This rolling continues until the interaction is stabilised by the binding of additional subunits in the GPIb-IX-V complex. This stabilisation facilitates the binding of collagen to the platelet GPVI receptor, further strengthening platelet adhesion[71,75].

GPVI -collagen binding triggers robust platelet activation, granule secretion, release of calcium from internal stores, and calcium influx through plasma membrane channels[76]. The rise in intracellular calcium not only drives secretion of secondary mediators like ADP and thromboxane A_2 (TxA_2), which amplify the haemostatic response by activating additional circulating platelets, but also induces cytoskeletal rearrangement and spreading[72]. This occurs in two phases: initial extension of filopodia, followed by the formation of lamellipodia, resulting in platelet flattening and increased surface area. This enhances their adhesive capacity and strengthens their contact with the ECM[31,32,77].

This monolayer of platelets serves as a foundation for further platelet aggregation. Secondary mediators activate the αIIbβ3 integrin, inducing a conformational change that allows binding to its primary ligand, fibrinogen as well as vWF, collagen and fibronectin. As a bivalent ligand, fibrinogen connects two

platelets by binding to αIIbβ3 on each, promoting platelet aggregation and stabilising the growing platelet plug, thereby reinforcing the haemostatic response[77].

In summary, platelet adhesion is initiated when GPIbα binds to immobilized vWF. GPVI then binds to exposed collagen at the site of vessel injury which activates the local platelets and recruits additional platelets. Platelet adhesion and aggregation are then enhanced through inter-platelet connections mediated by αIIbβ3 binding to fibrinogen and other ligands (Fig. 1-3). The platelet plug is further stabilised by the deposition of insoluble fibrin formed during secondary haemostasis, the coagulation cascade[70].

Platelet activation during haemostasis induces the expression of membrane components like CD62P and CD40L[72,76]. These proteins facilitate the formation of platelet-leukocyte aggregates (PLA) through CD62P-PSGL-1 and CD40L-CD40/CD154 interactions[72,76,78]. Leukocytes amplify the haemostatic response by releasing pro-inflammatory cytokines, chemokines, and enzymes that promote inflammation[79]. Additionally, leukocytes express tissue factor, which boosts thrombin generation and the conversion of fibrinogen to fibrin, further stabilising the developing thrombus[79,80].

Overall, the interplay between leukocytes and platelets ensures an effective haemostatic response to vascular injury. However, beyond haemostasis, platelets are increasingly recognised for their role in intercellular communication, mediating inflammatory and immunomodulatory activities.

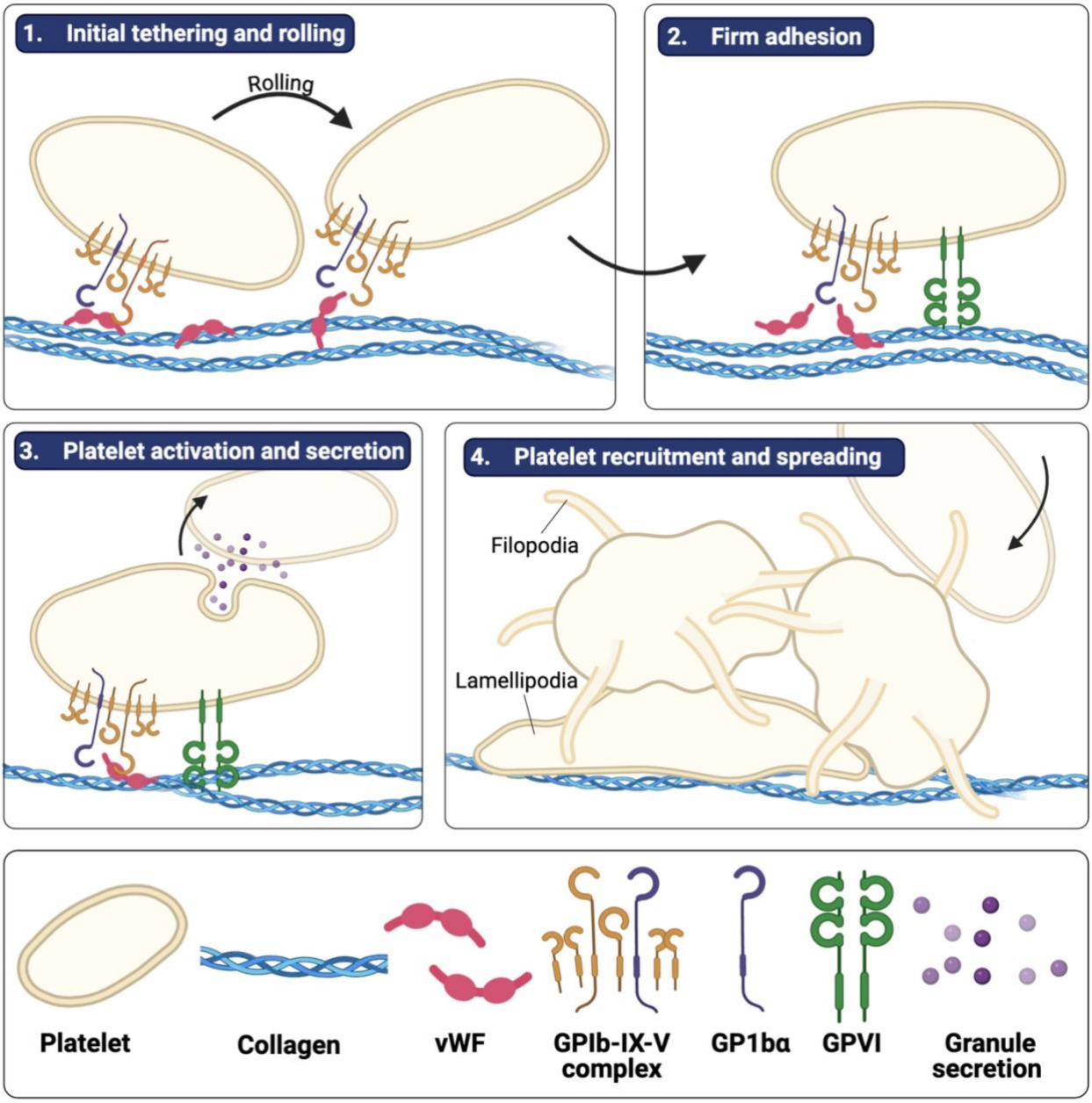


Figure 1-3. Schematic illustrating platelet interactions with exposed extracellular matrix components in the vessel wall. 1) Initial tethering: vWF binds to platelet GPIbα within the GPIb-V-IX complex, enabling weak adhesion and platelet rolling along the vessel wall. 2) Stable adhesion: GPVI on the platelet surface establishes a stronger interaction with exposed collagen. 3) Platelet activation: GPVI-collagen binding triggers robust platelet activation, leading to the secretion of contents from alpha and dense granules and platelet spreading. 4) The release of secondary mediators (e.g. ADP and TxA_2) causes further platelet activation and recruitment of additional platelets. The accumulation and activation of platelets leads to thrombus formation and stabilisation. Created using Biorender.com.

1-3 Non-canonical roles

Beyond haemostasis and thrombosis, platelets are increasingly recognised as key players in infection and inflammation. In infection, platelets primarily interact with pathogens, contributing to their clearance, while in inflammation, they play a broader role by recruiting immune cells and releasing inflammatory mediators to regulate the response. The following section will briefly describe the roles of platelets in each process.

1-3.1 Platelets in infection

i) Platelets recognise pathogens

Platelets express numerous receptors that enable their interactions with pathogens, including lectins (e.g., CLEC-2), integrins (e.g., αIIbβ3), and FcγRIIA receptors that bind pathogen-IgG complexes (Fig. 1-4A)[81,82]. In addition to these, platelets also express toll-like receptors (TLRs), which are crucial in detecting pathogen-associated molecular patterns (PAMPs) such as lipids, proteins and nucleic acids from viruses, bacteria, fungi, and parasites. Multiple studies have identified the presence of all 10 TLRs in human platelets[833], with several TLRs, including TLR2, TLR3, TLR4, TLR7, and TLR9 shown to be functional in modulating platelet responses during infections[84].

TLR4 is the most abundantly expressed TLR on platelets and recognises lipopolysaccharides (LPS), a key component of Gram-negative bacterial membranes. It has also been shown to mediate platelet-neutrophil interactions, leading to the formation of neutrophil extracellular traps (NETs)[85] and bacterial 'trapping'[86]. TLR2 binds a wide variety of PAMPs and forms heterodimers with TLR1 and TLR6. The TLR2/TLR1 complex preferentially binds triacylated lipopeptides from Gram-negative bacteria, while the TLR2/TLR6 complex targets diacylated lipopeptides from Gram-positive bacteria[87]. TLR2 also facilitates platelet binding to cytomegalovirus (CMV), triggering platelet activation, degranulation, and enhanced interactions with neutrophils[88]. TLR7 resides in platelet endosomes and recognises single-

[3]Interestingly, TLR expression is significantly higher in platelets from women than from platelets in men. Koupenova *et al.,* (2015).

stranded RNA, requiring viral particle internalisation for activation[89,90]. TLR7 has also been shown to enhance platelet uptake of viruses such as influenza and contribute to NETosis[82]. TLR3 is also endosomal but binds viral dsRNA, a by-product of ssRNA virus replication[91,92]. TLR9 primarily recognises unmethylated CpG motifs in bacterial and viral DNA, but has recently been shown to bind various forms of mammalian DNA[93] including, foetal DNA[94] and circulating tumour DNA (ctDNA)[95,96]. Although traditionally considered endosomal, recent evidence indicates that TLR9 is also expressed at low levels on the platelet surface, increasing upon activation[53].

ii) Platelets internalise pathogens

Upon recognition and binding, pathogens can be internalised into platelets[97,98,99]. Viral particles have been detected inside platelets isolated from patients infected with HIV[100-102], influenza[103,104], dengue virus[105], and hepatitis C[106]. Similarly, platelets have been observed to internalise whole bacteria such as *S. aureus*[107] and *P. gingivalis*[108] as well as their toxins[109]. However, the nature of this internalisation remains debated[36]. It's unclear whether platelets actively phagocytose pathogens or simply trap them within the membrane folds of the OCS[110].

Recent studies have provided evidence supporting active internalisation. Youssefian *et al.,* demonstrated that platelets can extend membrane pseudopods around *S. aureus,* capturing the bacteria in a phagocytic-like manner[107]. Similarly, Koupenova *et al.,* observed influenza virions within phagosome-like structures (PLS) distinct from the platelet OCS[104]. Furthermore, the authors noted fusion of the PLS with platelet granules leading to digestion of the viral particles, indicating active internalisation[103,104]. HIV particles have also been detected within the OCS and in vacuoles near the plasma membrane, some of which are enclosed by endosome-like structures, suggesting that platelets may engage in phagocytosis in addition to passive uptake[111,112].

iii) Platelets facilitate removal of old and damaged cells

Platelets play a crucial role in removing pathogens from circulation and have recently been shown to contribute to the clearance of aged and damaged red blood cells[113]. This is achieved through the

formation of prophagocytic platelet-cell complexes, which are then selectively engulfed by professional erythrophagocytes[113]. Similarly, platelets can bind to malarial-infected red blood cells through platelet CD36 receptors[114-117]. This interaction triggers the release of PF4 from platelet alpha granules, which is subsequently internalised by the infected red blood cells via their Fcγ receptor[118]. The accumulation of PF4 within red cells directly induces the killing of *Plasmodium falciparum*, one of the six species of malarial parasites that cause disease in humans (Fig. 1-4B)[119].

iv) Platelets secrete anti-microbial proteins

As described earlier in this chapter, platelets contain secretory granules that store proteins involved in adhesion, aggregation, and coagulation. However, some proteins stored in alpha granules also possess antimicrobial properties capable of killing bacteria and fungi[120]. For example, molecules known as thrombocidins are released following pathogen-induced platelet activation[97]. Platelet thrombocidin-1 and -2 demonstrate broad-spectrum antimicrobial activity and are effective against both Gram-positive bacteria such as *S. aureus* and Gram-negative bacteria such as *E. coli*, as well as fungi like *C. neoformans*[121,122,].

In addition to their direct antimicrobial action, activated platelets coordinate the chemotaxis of other immune cells. This is achieved through the release of microbicidal chemokines, including CXC chemokine ligand 4 (CXCL4), also known as PF4 and CCL5, also known as RANTES (Regulated upon Activation, Normal T cell Expressed and Secreted)[123].

In summary, platelets actively contribute to host defence against infections through multiple mechanisms:

1. Physical containment: Platelets trap and encapsulate pathogens, limiting their spread in the bloodstream[100,103,104,114,124,125].
2. Antimicrobial action: Upon activation, platelets release antimicrobial proteins that directly eliminate pathogens.
3. Immune support: Platelets assist professional phagocytes in pathogen clearance.

Moreover, it is possible that one of the reasons that platelets have evolved to bear nucleic acid sensing machinery is due to their roles in sensing pathogen-derived DNA and RNAs.

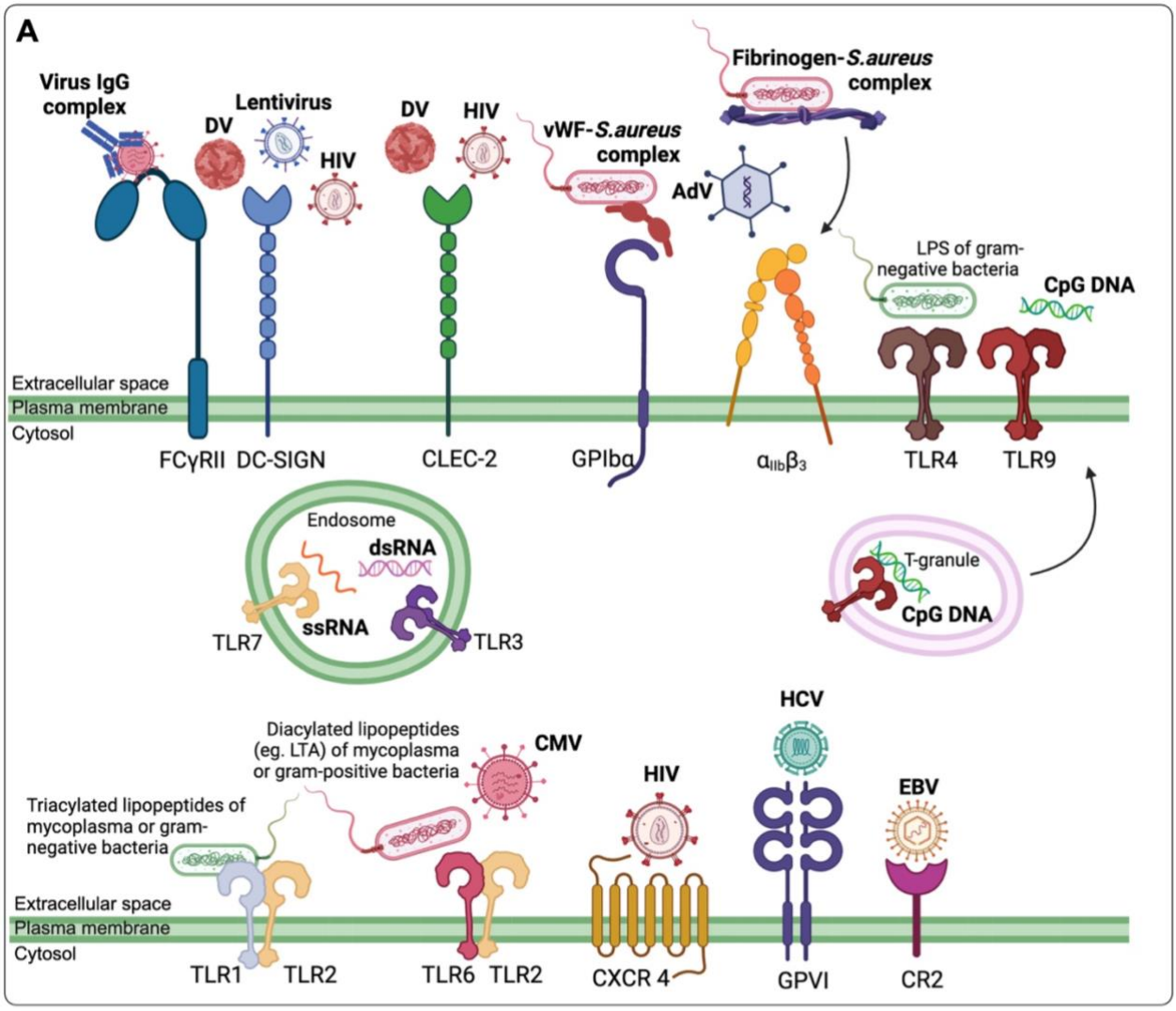


Figure 1-4. Representative platelet receptors that mediate bacterial and viral interactions. (A) Platelets express numerous receptors, a subset of which are shown here, that facilitate direct or indirect (via plasma proteins such as fibrinogen and vWF) binding to pathogens. This schematic representation is not exhaustive. Figure adapted from[81,82,87,126,127]. See abbreviations on page 18. **(B)** Activated platelets bind malaria infected platelets through platelet CD36 and possibly *P. falciparum* erythrocyte membrane protein 1 (PfEMP-1). Upon binding, PF4 is released from platelet alpha granules which binds to the Fcγ receptor. The PF4- Fcγ receptor complex is internalised into the red blood cell where it kills the parasite directly, leading to cell lysis and death. Adapted from Engwerda & Good (2012)[119]. Created using Biorender.com.

1-3.2 Platelets in inflammation

As described above, platelets play a critical role in the inflammatory response by releasing chemoattractants like RANTES and PF4, which recruit leukocytes to sites of injury and infection (Fig. 1-5). They also enhance leukocyte recruitment by altering vascular permeability through the secretion of pro-permeability factors such as serotonin, VEGF-A, and platelet-activating factor (PAF)[128].

In parallel, platelets upregulate adhesion molecules on their surface, directly binding to leukocytes and guiding them to sites of inflammation. Specifically, platelet P-selectin binds to leukocyte PSGL-1, and CD40L interacts with CD40/CD154 on leukocytes, while the activated GpIIb/IIIa integrin receptor on platelets binds fibrinogen, crosslinking with neutrophil integrin receptor Mac-1[129]. These interactions lead to the formation of platelet-leukocyte aggregates (PLAs), which further enhance leukocyte recruitment and amplify inflammatory signalling[130].

After recruitment, platelets modulate leukocyte functions by secreting inflammatory mediators such as, macrophage inflammatory protein-1 (MIP-1) and IL-1β, synthesised in the platelet from pre-mRNA. Additionally, platelet activation of TLR4 promotes the formation of neutrophil extracellular traps (NETs), driving local inflammation by causing neutrophils to expel chromatin and granular proteins like elastase and myeloperoxidase (MPO), which form web-like structures to trap and kill pathogens[85,91,127].

Beyond their pro-inflammatory roles, platelets can also exert anti-inflammatory effects by releasing immunosuppressive mediators such as TGF-β and prostaglandin E2 (PGE2)[122,131-133]. High levels of PGE2 stimulate monocytes and macrophages to produce the anti-inflammatory cytokine IL-10, which

inhibits the release of tumour necrosis factor (TNF) and other pro-inflammatory cytokines, thereby dampening the inflammatory response[134].

As the most abundant immune cells in circulation, platelets serve as first responders to injury and infection[104]. They recruit professional immune cells and modulate their activity by releasing a balance of pro- and anti-inflammatory signals, highlighting their crucial role in regulating inflammation and supporting the body's first line of defence against pathogens.

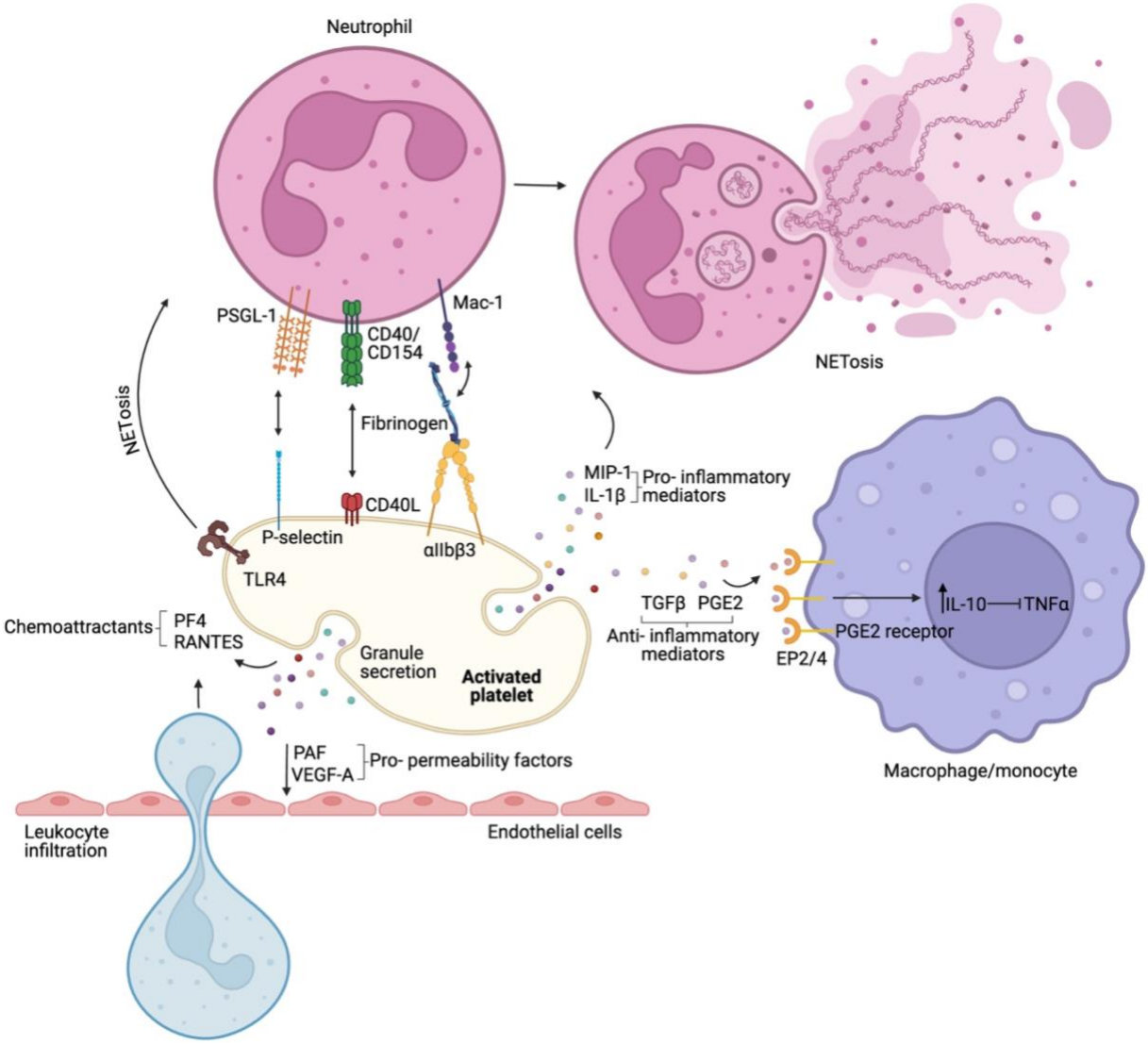


Figure 1-5. Platelets mediate the immune response via multiple mechanisms. Platelets bind neutrophils directly through their receptors CD40L and P-selectin or indirectly via αIIbβ3 binding to fibrinogen. Platelets also secrete mediators into the extracellular environment which can increase the permeability of the endothelial cell wall to allow for the infiltration of leukocytes. Platelets secrete pro- and anti-inflammatory signals which can drive inflammatory processes such as NETosis or dampen the inflammatory response by increasing the production of anti-inflammatory cytokines like IL-10. Adapted from Deppermann & Kubes (2018) and Ludwig *et al.,* (2022). Created using Biorender.com.

1-3.3 Platelets in cancer

Platelets have long been recognised for their role in cancer pathogenesis, with early clinical evidence linking elevated platelet counts to the presence of occult malignancy as well as to inferior survival[135-139]. Conversely, lower circulating platelet counts, and the use of antiplatelet therapies, such as aspirin[140-145] have been associated with better prognoses[139,146-148].

Platelets are involved in multiple stages of cancer development. They not only promote growth of the primary tumour, but also facilitate immune evasion and metastasis. The following sections detail the key stages of tumourigenesis, and the critical roles platelets play in each (Fig. 1-6).

i) Tumour Initiation and growth

In the early stages of cancer development, tumour cells are confined within their tissue-of-origin. Here, they release factors that activate endothelial cells and induce local inflammation, and thereby attract circulating platelets. Tumour cells then activate recruited platelets through direct binding or by releasing mediators like ADP and TxA_2. Some cancer cells express tissue factor (TF), mimicking vessel injury to further induce platelet aggregation and activation[149]. Upon activation, platelets release growth factors such as TGF-β, PDGF, and VEGF that drive tumour cell proliferation and inhibit apoptosis, thereby enhancing tumour cell survival. For example, platelet derived TGF-β was shown to directly increase the proliferation of ovarian cancer cells *in vitro* and *in vivo*[150,151] .

ii) Angiogenesis

Without vascularization, solid tumours cannot grow beyond 1–2 mm^3 in volume, as the surrounding tissue resources become insufficient to sustain growth[152]. At this stage, vascularization becomes essential for continued expansion[153]. The formation of new blood vessels is locally driven by the release of pro-angiogenic factors from activated platelets.

Platelets store both pro- and anti-angiogenic proteins in distinct subpopulations of α-granules[154]. Pro-angiogenic factors such as VEGF, fibroblast growth factor (FGF), and TGF-β promote tumour infiltrating blood vessel formation, while anti-angiogenic proteins, including endostatin[155],

angiostatin[156], PF4[157], and thrombospondin[158], inhibit this. Some studies indicate that these factors are selectively released from platelets in response to specific stimuli, enabling fine-tuned regulation of the angiogenic process[159,160]. However, this remains a subject of debate, and further research is needed to fully understand the underlying mechanisms.

iii) Invasion and metastasis

Platelets play a significant role in cancer metastasis by promoting epithelial-mesenchymal transition (EMT), a process in which epithelial cells lose their adhesion properties and gain migratory and invasive characteristics[161]. This shift to a mesenchymal phenotype enables cancer cells to detach from the primary tumour, invade surrounding tissues, and enter the bloodstream. Platelets drive EMT through direct binding, such as CLEC-2 to tumour cell podoplanin[162] and integrin α6β1 on platelets to ADAM9[163], as well as by secreting TGF-β, which has been shown to induce EMT and enhance metastasis in breast, colon, and ovarian cancer cells[161,164,165].

Additionally, platelets promote metastasis by releasing matrix metalloproteinases (MMPs), which degrade components of the ECM like collagen, breaking down the basement membrane and allowing tumour cells to penetrate the subendothelial layer and enter the vasculature[149,166].

Once in the bloodstream, circulating tumour cells are often destroyed by the shear forces generated by blood flow[153]. Platelets counter this by rapidly adhering to circulating tumour cells, forming aggregates that act as a 'physical shield' protecting them from shear-induced damage[139]. Key interactions that facilitate this include platelet P-selectin binding to tumour PSGL-1, and platelet αIIbβ3 integrin linking with fibrin and tumour αVβ3 integrin[167-170].

iv) Immune evasion

Tumour-induced platelet aggregation aids cancer cells in evading immune detection through several mechanisms. First, platelets secrete TGF-β, which suppresses natural killer (NK) cell cytotoxicity by downregulating the activating immunoreceptor NKG2D, thereby inhibiting NK cell antitumour functions, including IFN-γ secretion and granule mobilization[139,171,172]. TGF-β also inhibits activation

of the kinase mTOR, a central regulator of NK cellular metabolism and function, further supressing the innate immune response[173]. Additionally, platelets transfer major histocompatibility complex (MHC) class I molecules to tumour cells, creating a "false self"-signal that helps cancer cells escape recognition by circulating T-lymphocytes and NK cells[174,175].

v) Extravasation and establishment of the metastatic niche

Platelets play an essential role in helping cancer cells adhere to blood vessel walls by mediating interactions between tumour cells and the vascular endothelium[176]. Platelet-tumour cell aggregates release a mix of growth factors and cytokines (IL1- β and CD40L)[177] that activate endothelial cells, leading to the expression of adhesion molecules such as E-selectin, P-selectin and vascular and intercellular cell adhesion molecules 1 (VCAM-1 and ICAM-1)[178].

These endothelial adhesion molecules bind to specific ligands on the tumour-platelet aggregates[176,179]. For example, tumour Sialyl Lewis X (sLeX) binds to endothelial E-selectin[180], platelet GPIbα and PSGL-1 interacts with endothelial P-selectin, platelet αIIbβ3 recognises endothelial ICAM-1[181] and tumour α4β1 binds to endothelial VCAM-1[162]. After tumour cells dock to the endothelium, platelets secrete TGF-β, which induces EMT in tumour cells, promoting a migratory phenotype. Activated platelets also release ADP from their dense granules, which binds to $P2Y_2$ receptors on endothelial cells, increasing endothelial permeability and facilitating tumour cell transmigration[182-184].

Platelets contribute to the establishment of a metastatic niche by releasing various factors that create a supportive microenvironment for tumour development[185]. For instance, platelet-derived chemokines CXCL5 and CXCL7 recruit host cells such as granulocytes, which eventually form the tumour stroma[185,186]. Immunomodulatory factors also released by platelets, including TGF-β and PF4, suppress local anti-tumour immune responses, fostering an immunosuppressive environment that supports metastatic cell survival. Additionally, activated platelets can form microthrombi that trap circulating tumour cells (CTCs), providing a protective niche that aids their initial survival and growth. Tumour

cell proliferation is further supported by platelets through the secretion of pro-angiogenic factors that promote new blood vessel formation[185].

Recent studies have shown that platelets can transfer functional RNA transcripts to recipient cells[187-190] through microparticles and exosomes[191]. Platelet-derived microparticles (PMPs) serve as key mediators of cell-cell communication, while the role of platelet-derived exosomes is less clear[59,192,193]. As the uptake of platelet-derived transcripts can alter the gene expression of recipient cells, platelets can significantly influence tumour development within the metastatic niche, by delivering PMPs to cells in the microenvironment. For example, platelet- derived mRNA uptake by cancer cells enhances their migration[194], invasion[195], angiogenesis[196], and proliferation[197]. Moreover, the uptake of transcripts by macrophages, results in the reprogramming of the macrophages' immunosurveillance functions[198].

Together, this body of literature highlights the close association between platelets and cancer cells at every step of the malignant process – providing ample opportunity for the exchange of biomolecules between platelets and malignant cells and highlighting their role as cancer biomarkers. The final section of this introduction explores the platelet transcriptome and its modulation by cancer cells. This has been the focus of recent work indicating that platelet RNA content may indicate the presence and type of cancer, therefore is relevant to my work.

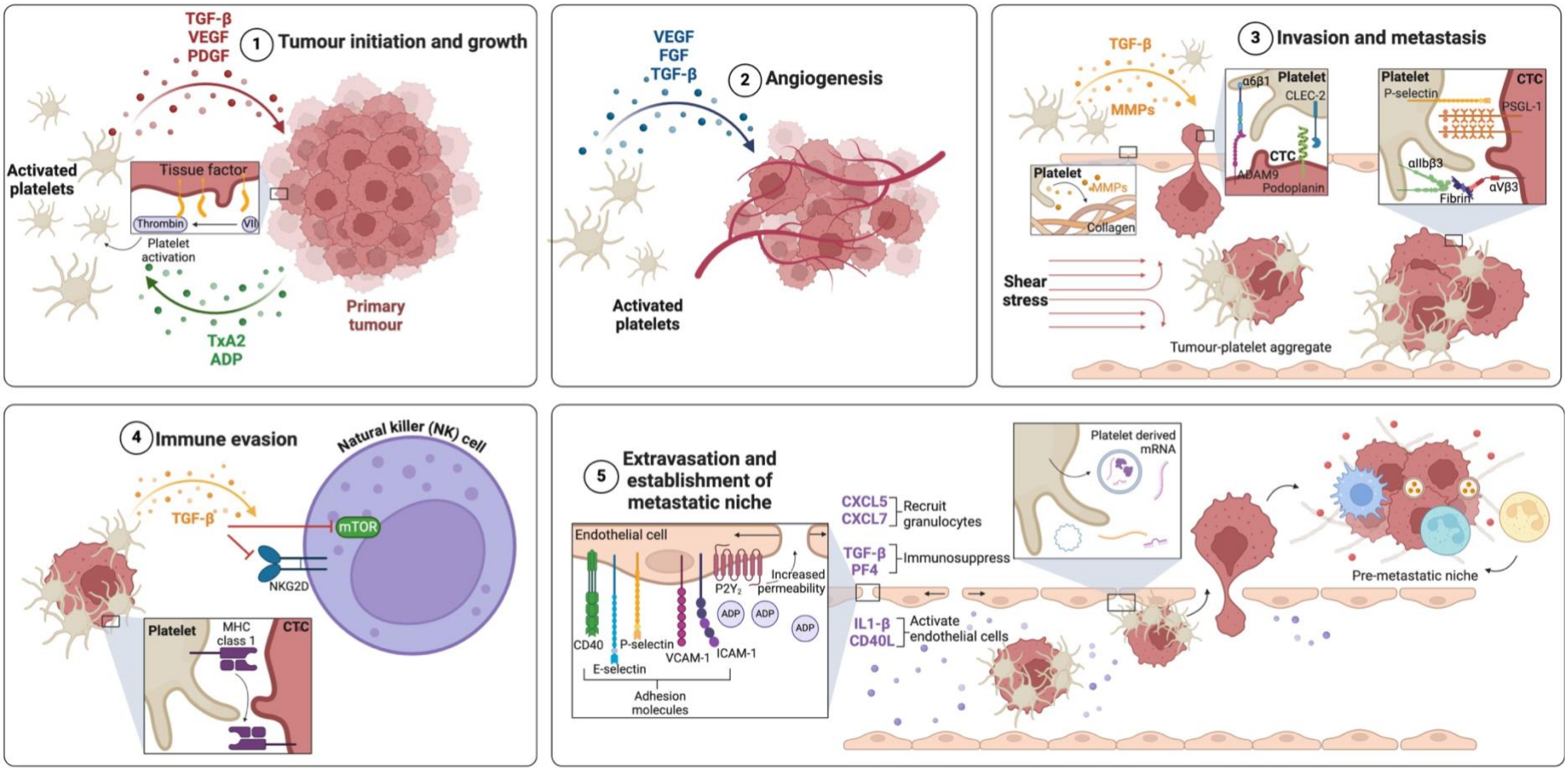


Figure 1-6. The role of platelets in tumour development. This diagram illustrates the primary functions of platelets in cancer progression, from tumour initiation to extravasation into the metastatic niche. The figure is not exhaustive but highlights the key roles discussed in the text above. 1) Platelets are activated by tumour cells and release growth factors that promote tumour cell proliferation and survival. 2) Activated platelets secrete pro-angiogenic factors that stimulate new blood vessel formation, supporting tumour vascularization. 3) Platelets encourage EMT through direct binding and TGF-β secretion, facilitating tumour cell detachment and invasion. Platelet-derived MMPs degrade the extracellular matrix, enabling tumour cells to enter blood vessels. 4) Platelets form aggregates with circulating tumour cells, shielding them from shear stress and immune attack. 5) Platelets assist tumour cells in adhering to the endothelium and extravasating into the metastatic niche. Created using Biorender.com.

1-3.4 Tumour educated platelets

In 1966 Warshaw *et al.,* suggested that platelets had the ability to synthesise protein, even though they lacked a cell nucleus[199-201]. In 1988 it was confirmed that platelets were able to translate protein from a pool of mRNA[202], which was 10 years later, found to occur in response to signal-induced platelet activation[203].

Since these initial discoveries, we now know that the majority of platelet RNAs are derived from the parent megakaryocytes, along with the RNA processing machinery. However, it's also clear that platelets supplement their RNA pool with plasma-derived RNA transcripts encountered during circulation[59,190]. This can include tumour cell-derived RNAs, taken up either in peripheral circulation or within the tumour microenvironment[54].

Moreover, the interactions between platelets and tumour cells (or tumour cell-derived biomolecules) have been suggested to provide 'educational' signals to platelets. This means that exposure to cancer signals can alter platelet behaviour and induce specific splicing of platelet pre-mRNA, leading to distinctive mRNA profiles in the context of certain cancers.[204]. This led to coining of the term 'tumour-educated' platelets (TEP), and studies largely led by the Wurdinger Group have demonstrated the potential of TEP- derived RNA profiling for cancer detection (Fig. 1-7) [205-208].

i) Platelet 'education' by cancer cells

While the exact mechanisms through which tumour cells "educate" platelets remain unclear, it likely involves a combination of factors[59,140].

a. Tumour-induced platelet activation

Tumour cells activate platelets through both direct and indirect mechanisms. Direct activation involves platelet adhesion molecules, such as glycoproteins, integrins, P-selectin, and CLEC-2, binding to specific ligands on tumour cell surfaces[209,210]. Indirect activation occurs when tumour cells release bioactive factors like TF, ADP, and TxA_2, which interact with platelet receptors. Tumour induced

activation results in altered platelet phenotypes[160]. This includes increased secretion of granular contents, altered expression of surface receptors, synthesis and release of proinflammatory mediators, and enhanced binding to immune cells, particularly neutrophils.

b. Uptake of tumour derived protein

Tumour cells can induce platelets to sequester proteins, encouraging the platelets to be become pro-tumourigenic as they can release these factors into local and distal tissues to encourage tumour growth[211]. Clinical studies have shown that platelets from cancer patients contain elevated levels of pro-angiogenic proteins such as VEGF and PDGF, along with the immunosuppressive factor PF4[212-214]. Additionally, as mentioned above, activated platelets release vesicles, including exosomes and PMPs[215]. Platelets have been shown to mediate crosstalk between primary tumours, metastatic tumours and the bone marrow niche, via the uptake and selective delivery of tumour-secreted proteins contained within EVs[211,216]. Notably, higher levels of circulating PMPs are associated with more aggressive tumours [217,218].

c. RNA delivery and modifications to RNA processing

Cancer also affects the platelet transcriptome and proteome, for example they can stimulate de novo protein synthesis[219,220] and trigger specific splicing of platelet pre-mRNA[221]. Calverley *et al.,* were the first to identify differential RNA splicing events in TEPs isolated from patients with metastatic lung cancer[222]. Platelet microRNAs can also be altered, leading to changes in mRNA translation and protein synthesis[223]. Moreover, platelets can sequester tumour RNA via the uptake of tumour-derived, RNA-laden EVs[224-226]. Nilsson *et al.,* demonstrated that membrane vesicles secreted by glioma and prostate cancer cells transferred tumour-derived RNA into platelets[59,60]. The mechanisms behind platelet uptake of tumour-derived EVs remain unclear but may involve processes such as plasma membrane fusion, clathrin-mediated endocytosis, phagocytosis, and micropinocytosis (see Fig. 4-3, chapter 4)[140,224]. Of note, it is not known whether sequestered tumour-derived spliced RNA is translated into protein that modifies platelet function[211].

d. Tumour educated megakaryocytes

Tumour-derived factors can also influence MK biology, which in turn impacts their platelet progeny. For instance, cytokines released by tumour cells such as colony stimulating factor (CSF), can directly increase thrombocytosis and subsequently, platelet counts[227]. Cancer cells can also modulate platelet content. A study in 2002 found that IL-6 derived from metastatic breast cancer cells increased VEGF expression in patients' megakaryocytes. This resulted in increased VEGF content within circulating platelet alpha granules, suggesting that tumour cells can indirectly promote angiogenesis through MKs[228].

In summary, tumour cells substantially alter various aspects of platelet biology, and these cancer-associated changes hold potential as early biomarkers for cancer screening.

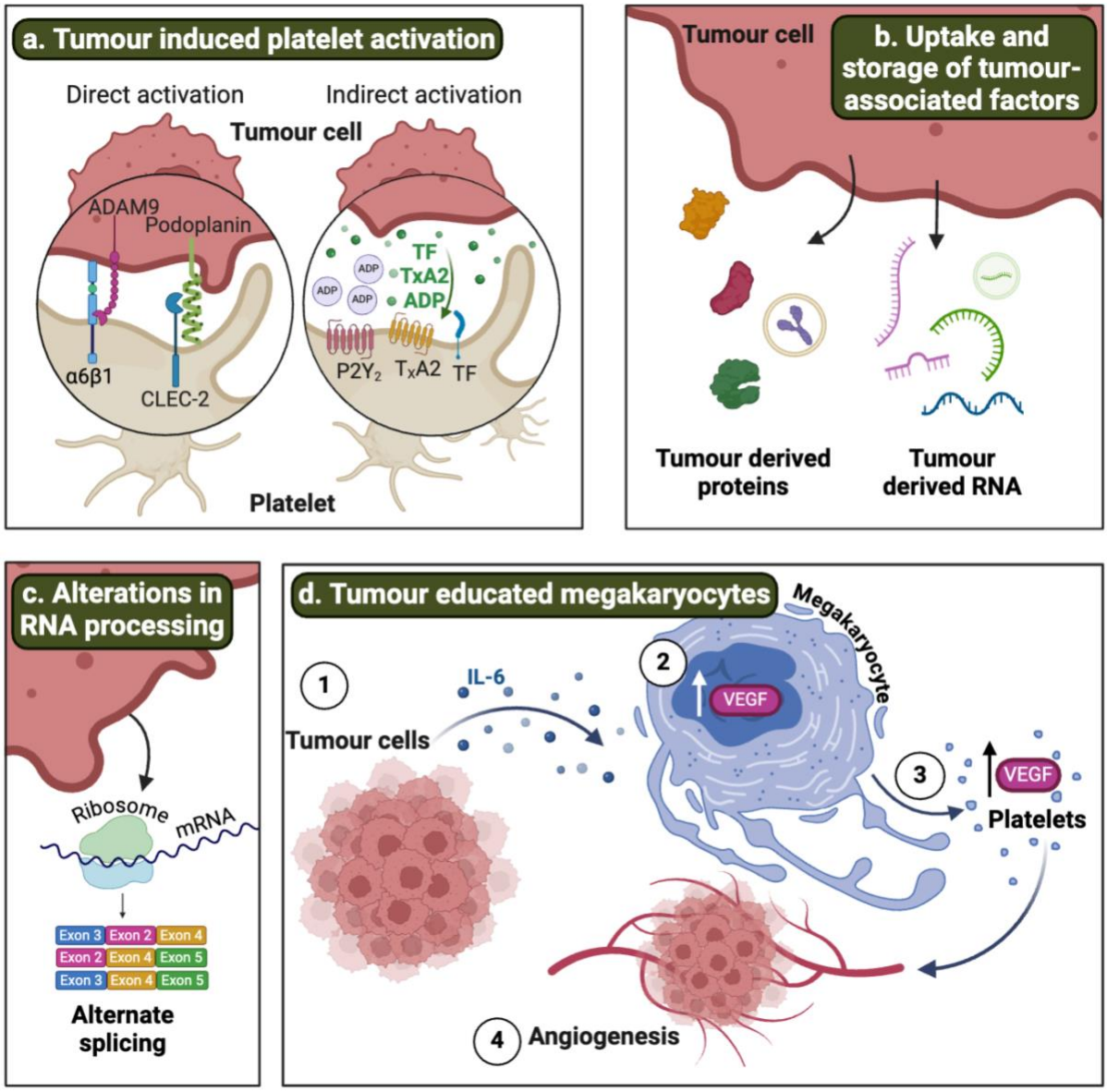


Figure 1-7. Mechanisms of tumour-induced platelet education. Tumour cells modify platelets through multiple pathways. They induce direct and indirect platelet activation via receptor binding and release of activating factors. Platelets sequester and store tumour-derived molecules, including proteins, RNA transcripts, and extracellular vesicles (EVs). Tumour cells trigger alternative splicing of platelet pre-mRNA and induce de novo protein synthesis within platelets. Additionally, tumour cells can alter platelet production by influencing megakaryocytes (MKs), thereby modifying the content of newly formed platelets. Created using Biorender.com.

ii) TEP transcriptome as a biomarker for disease

Given platelets' abundance, ease of isolation, and short lifespan, they have potential to offer 'real-time' insights into disease states. Furthermore, their unique ability to undergo specific splicing events in response to external signals, coupled with their capacity to directly ingest circulating mRNA, has made the TEP transcriptome one of the most extensively studied platelet biomarkers.

In 2010, Calverley *et al.,* were the first to profile platelet mRNA from metastatic lung cancer patients and healthy donors, identifying altered expression levels in 200 RNAs and 608 splicing events[222]. Building on this, Nilsson *et al.,* discovered that platelets from cancer patients contained tumour-associated RNA biomarkers, such as epidermal growth factor receptor (EGFR) vIII, PCA3, and the fusion transcript EML4-ALK, linked to glioma, prostate, and lung cancers, respectively[60,229].

These initial discoveries prompted Best *et al.,* in 2015, to develop an algorithm based on platelet transcriptomes, which classified cancer patients across six cancer types with 96% accuracy and identified the primary tumour location with 71% accuracy[205]. Two years later, the same group demonstrated the algorithm's ability to accurately detect both early- and late-stage non-small cell lung cancer (NSCLC)[230].

While the diagnostic potential of platelet RNA profiles for cancer screening is promising, several limitations should be acknowledged. One key challenge is their sensitivity in detecting early-stage cancers, particularly when tumour burden is low. This is especially relevant given that, despite being anucleate, platelets are rich in RNA, which may dilute mutant RNA transcripts. For instance, a recent study showed that platelets isolated from melanoma patients contained more wild-type RNA transcripts compared to EV-derived RNAs isolated from plasma, resulting in a lower tumour-to-non-tumour RNA ratio in the platelets[231].

Specificity is another concern, as the platelet's RNA profile can be "educated" by various conditions beyond cancer. Inflammatory diseases[232,233], cardiovascular conditions[234], and other non-cancer

pathologies such as kidney disease[235] may all alter platelet RNA profiles via similar inflammatory signals to those operating in cancer, increasing the risk of false positives. Additionally, changes in platelet mRNA profiles have been linked to factors like obesity[236], race[237] and medication use[238].

Furthermore, the dynamic nature of platelets *in vivo* and the instability of RNA can introduce temporal variations in RNA profiles, impacting reproducibility. A 2023 study examining RNA profiles of platelets isolated from breast cancer patients found that gene expression was significantly influenced by hospital site[239]. The researchers attributed this variability largely to pre-analytical handling of blood samples, with patient factors such as medication use and possible undiagnosed systemic conditions also playing a role[239].

1-4 Overview of cell free DNA

Please note, more information on cfDNA can be found in chapter 5-1.

Genomic material is released into body fluids by nucleated cells through processes such as cell death, abnormal mitotic cycles, or regulated DNA extrusion, resulting in the presence of extracellular DNA known as cell-free DNA (cfDNA). Blood plasma cfDNA analysis has been widley implemented in various clinical settings, including cancer care pathways[240-246] and prenatal genetic testing[247]. For example, Dennis Lo *et al.,* (while working at the John Radcliffe Hospital in Oxford), demonstrated the potential to detect foetal origin circulating DNA in the blood of pregnant women[248,249]. Since its discovery, non-invasive prenatal diagnosis (NIPD), has become a routine method for identifying chromosomal abnormalities and determining foetal sex[250]. Recent studies have shown that when performed after the 10th week of gestation, NIPD can identify Down syndrome (trisomy 21) with high accuracy. Specifically, cfDNA is reported to have a 99.4% detection rate for trisomy 21, while only producing false positive results in 0.16% of cases[251].

The concentration of cfDNA in the blood can vary widely and is influenced by a range of factors, including physiological conditions (e.g., exercise)[252] and non-malignant pathological processes such as inflammation[253], stroke[254], diabetes[255] and sepsis[256]. Typically, cfDNA levels range from 0–5 ng/ml to over 1000 ng/ml in cancer patients, while levels in healthy individuals are usually between 0 and 100 ng/ml[256-258].

Although cfDNA concentrations are generally higher in cancer patients[259,260], the majority of cfDNA in circulation originates from healthy tissues and consists mostly of wild-type DNA[261]. This makes the detection of circulating tumour DNA (ctDNA), which specifically originates from the tumour cells, challenging due to the high background of non-malignant cfDNA.

To overcome this obstacle, recent research efforts have focused on several approaches. These include increasing sequencing depth, or more broadly capturing cancer-associated genetic aberrations through techniques such as whole genome sequencing (WGS)[262,263] or epigenetic analysis[264-267]. Additionally, studies have revealed that ctDNA fragments tend to be shorter in length compared to typical cfDNA fragments[268,269,270]. This discovery has sparked new research exploring the possibility of enriching ctDNA through fragment size selection, potentially offering a novel method to improve ctDNA detection and analysis in cancer diagnostics and monitoring[263,267,268,271-273].

Improved pre-analytical methods that increase the capture of cfDNA would also be highly beneficial. Crucially, as standard methods isolate cfDNA from platelet-depleted plasma, any DNA fragments sequestered within platelets are currently being missed using the commonly implemented protocols.

1-5 Hypothesis and Aims

As outlined above, platelets have recently emerged as a potential source of tumour derived biomarkers, with the majority of current approaches focusing on the platelet transcriptome – primarily on detecting cancer-specific transcriptomic signatures that result from differential mRNA splicing by platelets in response to signals released by the primary tumour. However, these approaches are likely to be poorly specific for cancer, and hard to distinguish from non-malignant inflammatory pathologies.

We know that platelets have a high capacity for intracellular trafficking and endocytosis. During peripheral circulation, they actively internalise and decipher biomolecules encountered – including proteins and nucleic acids released during tissue damage or by viral pathogens – enabling them to interpret and respond to signals in their immediate environment. Therefore, in addition to their crucial role in blood clotting and vascular maintenance, I hypothesise that platelets also sequester cfDNA from plasma including tumour derived DNA, and that important clinical insights may be derived from the analysis of genetic material contained within platelets relating to cell types encountered during their peripheral circulation. Given their lack of nuclear DNA, approaches to detect cancer-specific gene mutations have not yet focused specifically on platelets. Furthermore, there is an unmet need to improve the sensitivity of current liquid biopsy approaches which are often limited by the low abundance of cancer cell-derived DNA present in the plasma.

The specific aims of my thesis are as follows, and are summarised in Figure 1-8:

Aim 1: To evaluate whether, despite lacking a nucleus, platelets contain DNA

1.1: To confirm whether, irrespective of platelet preparation or source, platelets contain genomic DNA

1.2: To investigate potential correlations between DNA uptake, platelet activation and age

1.3: To determine the origin of platelet DNA (megakaryocyte derived vs. sequestered from the plasma)

Aim 2: To investigate the mechanism(s) platelets use to sequester DNA

2.1: To confirm whether platelets sequester DNA-loaded EVs

2.2: To determine whether DNA uptake by platelets is an active or a passive process and investigate the impact of inhibitors on platelet cargo trafficking, DNA uptake and release

2.3: To investigate the trafficking and location of DNA following platelet internalisation

Aim 3: To investigate the utility of platelet DNA in detecting cancer associated gene mutations

3.1: To determine if mutant alleles derived from tumour cells are sequestered by platelets

3.2: To explore the genomic distribution of DNA within platelets

3.3: To assess the potential utility of platelet DNA in various cancer models and patient cohorts, including both low and high tumour burden disease

Please note that in addition to this broad introductory chapter, each results chapter contains a further, detailed introduction specific to each section.

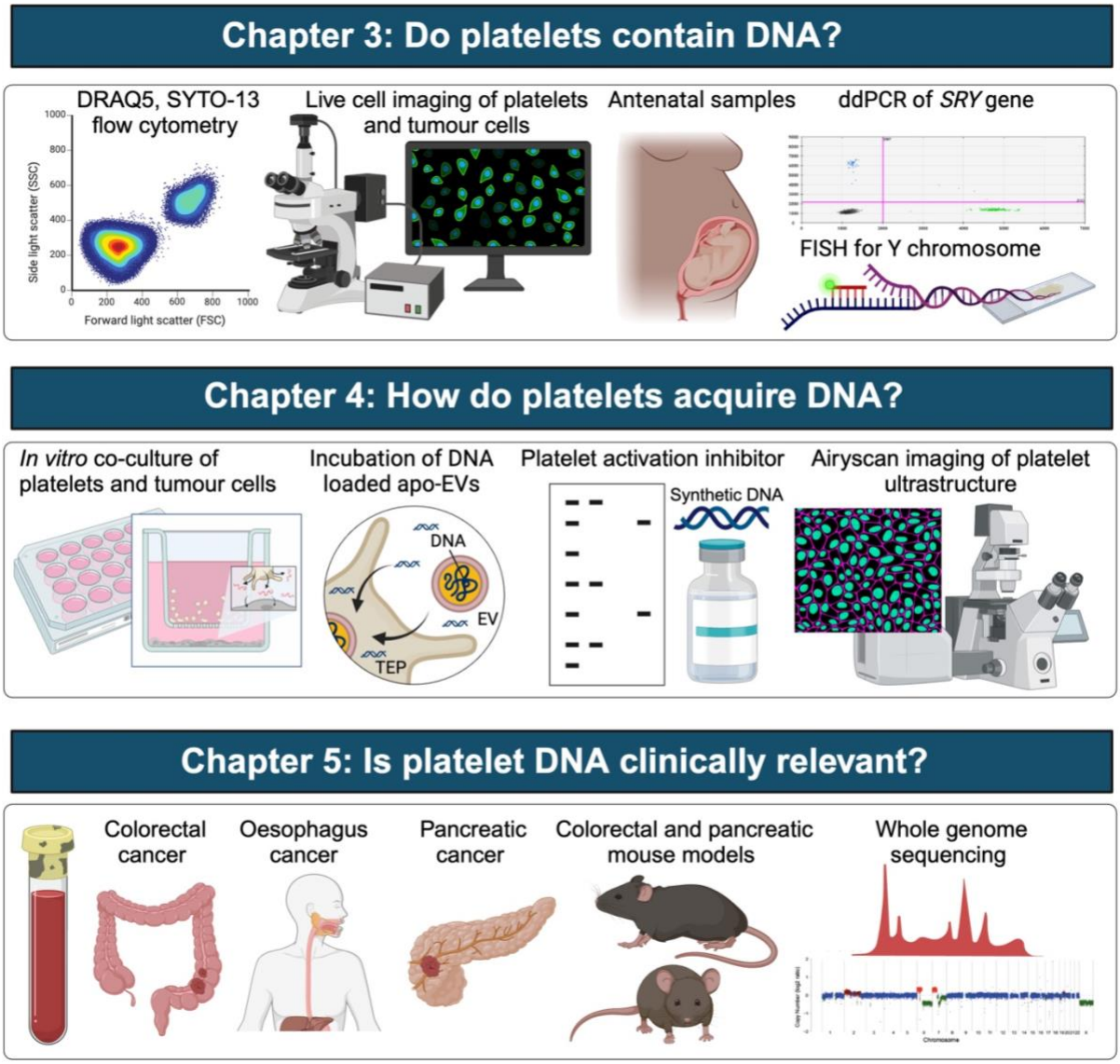


Figure 1-8. **Summary of aims.** Overview of thesis, highlighting experimental sequence outlined in results chapters 3-5. Created using Biorender.com.

Chapter 2: Materials and Methods

2-1 Ethical approval, banking and processing of samples

2-1.1 Blood collection

All procedures were performed in accordance with the ethical standards of the Declaration of Helsinki. Aside from healthy controls, the majority of patient blood samples were collected into Cell-Free DNA (Streck, cat # 218997) blood tubes. I chose to collect into these tubes as they are considered the gold standard for cell-free DNA (cfDNA) isolation. The tubes contain a proprietary preservative that limits the release of genomic DNA from nucleated cells, allowing for the isolation of pure cfDNA from the plasma. Although the addition of this preservative did not affect the recovery of DNA from pelleted platelets, I chose not to use this blood for platelet functional studies and opted for EDTA and citrate whole blood instead, as the impact of the preservative in Streck tubes on platelet function is unknown.

i) Non cancer controls

For healthy controls in Oxford, fully anonymised blood samples were collected from the Oxford Biomedical Research Laboratory under The INForMeD Study (REC reference 16/LO/1376). All donors provided informed consent, and blood was drawn into EDTA-coated tubes (Fisher Scientific, cat # 367839). However, BD Vacutainer® Citrate Tubes (Becton, Dickinson and Company, cat # 363080 were used to collect platelets for activation studies.

The usage and collection of healthy human donor blood samples in Edinburgh was authorised under the project "21-EMREC-041 – The Role of Inflammation in Human Immunity". Freshly drawn blood from

healthy human donors was collected into 50 ml BD Falcon tubes containing 4 ml of CPD buffer (16 mM citric acid, 90 mM sodium citrate, 16 mM NaH_2PO_4, 142 mM dextrose, pH 7.4).

Healthy donor platelet apheresis samples were provided by Oxford NHS Blood and Transplant (NHSBT) through the Non-Clinical Issue (NCI) service.

ii) Sessile serrated lesions

10 ml of peripheral blood was collected into Cell-Free DNA (Streck, cat # 218997) blood tubes, from patients with sessile serrated lesions (SSL) and from those on the bowel cancer screening pathway or those with inflammatory bowel disease undergoing colonoscopy. All patients provided informed consent, and procedures were approved by Yorkshire & The Humber - Sheffield Research Ethics Committee (REC reference 16/YH/0247), ORB research tissue bank ethics (REC reference 19/SC/0173) and Oxford GI Cohort ethics (REC reference 21\YH\0206).

iii) GI malignancies

Patient samples were collected by the Oxford Translational Gastroenterology Unit (TGU) and the Oxford Radcliffe Biobank (ORB). All patients provided informed consent, and procedures were approved by Yorkshire & The Humber - Sheffield Research Ethics Committee (REC reference 16/YH/0247), ORB research tissue bank ethics (REC reference 19/SC/0173) and Oxford GI Cohort ethics (REC reference 21\YH\0206). 10 or 20 ml of peripheral blood was drawn into EDTA-coated or Cell-Free DNA blood collection tubes from patients presenting with colorectal, oesophageal or pancreatic cancer.

iv) Immune thrombocytopenic purpura

Patients with immune thrombocytopenic purpura (ITP) were consented under the INForMeD Study (REC reference 16/LO/1376) and 10 ml of peripheral blood was collected into Streck tubes.

v) Obstetric samples

For obstetric samples, 10 ml of blood was collected from mothers at the time of caesarean delivery, and postnatally at 24 and 48 hours after delivery into Cell-Free DNA blood collection tubes. Samples were taken at the Department of Women's and Reproductive Health at the John Radcliffe Hospital Oxford and approved by the Oxfordshire Research Ethics Committee (REC reference 07/H0607/74). Sex of the neonate was confirmed after delivery and all mothers provided written informed consent.

vi) Suspected cancer samples

Patients with suspected cancer were recruited to the Suspected CANcer (SCAN) Diagnostic Pathway. 10 ml of peripheral blood was collected into Cell-Free DNA blood collection tubes. All patients provided informed consent, and procedures were approved by ORB research tissue bank ethics (REC reference 19/SC/0173).

2-1.2 Animals

All mice were bred and maintained in accordance with UK Home Office regulations. All experiments were performed under Project Licenses P2FF90EE8, P0B63BC4D and PP6460882 and approved by the University of Oxford Animal Welfare and Ethical Review Body. All mice were housed in individually ventilated cages at the animal unit either at Functional Genetics Facility (Wellcome Centre for Human Genetics, University of Oxford) or the Biomedical Services Facility at the John Radcliffe Hospital (The MRC Weatherall Institute of Molecular Medicine, University of Oxford), in a specific-pathogen-free (SPF) facility, with unrestricted access to food and water, and were not involved in any previous procedures.

i) Colorectal (KP and KPN)

KPN mouse maintenance was carried out by Hayley Belnoue-Davis from the Wellcome Centre for Human Genetics.

For the colorectal cancer (CRC) model, murine blood was drawn from KPN (villinCre^{ER} Kras$^{G12D/+}$ Trp53$^{fl/fl}$ R26$^{N1icd/+}$) and KP (villinCre^{ER} Kras$^{G12D/+}$ Trp53$^{fl/fl}$) mice via cardiac puncture into EDTA coated microvettes (Sarstedt, cat # 20.1288). All strains used in this model were maintained on C57BL/6J background. Both male and female KP and KPN mice were used.

ii) Pancreatic (KPC)

KPC (Kras$^{G12D/+}$ Trp53$^{R172H/+}$ P48-Cre) mouse maintenance was carried out by Giampiero Valenzano, a DPhil student in the Department of Oncology.

For the orthotopic pancreatic cancer model, a total of 500 KPC-F cells (passages 9-11) were injected in a volume of 10 µl in a mixture of 50% Matrigel and 50% DMEM (Gibco) using a 0.5 ml Micro-fine insulin syringe (BD). Following anaesthesia of the mice using 4% isoflurane/oxygen and clipping of hair, an incision of 1 cm was made in the left abdominal site. The spleen and pancreas were exteriorized using forceps and KPC-F cells were injected in the tail of the pancreas. Successful injection was verified by the appearance of a wheal at the injection site with no leakage through the pancreatic capsule. Spleen and pancreas were gently moved back into the peritoneal cavity; the abdominal wall was sutured with absorbable 4.0 Vicryl suture (Ethicon) and the skin was closed using a 7 mm wound clip. Two weeks post-surgery, after the mice had recovered, blood was drawn via cardiac puncture into EDTA-coated microtainer tubes (BD).

For the aspirin treatment of the KPC mice, aspirin (NSC 27223; Selleck Chemicals, cat #. S3017) was administered via intraperitoneal injection at a dose of 10 mg/kg. Treatment began on day 4 post-tumour cell implantation and continued every other day until day 14. Control animals received intraperitoneal injections of vehicle (2% DMSO in PBS) on the same schedule.

iii) Immune thrombocytopenic purpura

Immune thrombocytopenic purpura (ITP) mouse maintenance was carried out by Rong Li, a former postdoctoral researcher in Beth Psaila's Lab.

For the immune thrombocytopenia model, CD45.2 female, wild-type mice were injected intravenously with either an anti-platelet antibody to reduce platelet count (Emfret, cat # R300) or an IgG control that had no cytotoxic effects on platelets in mice (Emfret, cat # C301). Mice were humanely culled and then blood was collected via cardiac puncture into EDTA coated microvettes (Sarstedt, cat # 20.1288) at 24, 72 and 120 hours post treatment. Platelet counts were determined using an automated blood cell counter. cfDNA was extracted from plasma and quantified using the Qubit Fluorometer 2.0 (Thermo Fisher Scientific Inc.).

2-2 Blood cell isolation

2-2.1 Platelet and plasma isolation

i) Method optimisation

These platelet isolation studies were carried out in collaboration with Nikolaos Sousos, a former DPhil student in Adam Mead's lab.

As platelet isolation and downstream analysis was an integral part of the project, I wanted to ensure that the platelets I collected were as pure as possible. To achieve this, I compared the purity of different platelet isolation methods:

The approaches evaluated included:

1. A widely used density gradient centrifugation method for the isolation of different blood components, including plasma, platelets, mononuclear cells and granulocytes from peripheral blood.
2. An alternative published method designed to minimize platelet adhesion, aggregation, and activation[104]. This method incorporates platelet stabilisers, specifically: acid-citrate-dextrose (ACD) (Sigma Aldrich, cat # C3821-50ML) and prostaglandin E1 (PGE1) (Sigma Aldrich, cat # 538903). See final protocol below for detailed steps.

3. Leukodepletion of whole blood or platelet-rich plasma by depleting nucleated CD45+ cells and enriching for CD42b+ platelets using magnetic Dynabeads (Invitrogen; Thermo Fisher Scientific Inc.).
4. Physical removal of larger leukocytes using Pall Sterile Acrodisc WBC syringe filters (Pall Corporation).

Despite the theoretical advantages of approaches 3 and 4, neither significantly improved platelet recovery nor purity compared to the first two methods. Moreover, these approaches were considerably more expensive, making them less practical for routine use in this study.

ii) Final protocol

The final three-step centrifugation protocol is summarised in Figure 2-1. See Appendix Data Table A1 for details of platelet wash buffer and HEPES-modified Tyrode's buffer. Blood tubes were kept at room temperature and handled gently to avoid platelet activation. For human samples, platelets were isolated within 48 hours of blood sampling. Briefly, whole blood was supplemented with ACD and centrifuged at 180 x g for 20 minutes at room temperature. Eighty % of the supernatant was removed, diluted with platelet wash buffer and prostaglandin and centrifuged at 600 x g for 20 minutes at room temperature. The resulting platelet pellet was resuspended in pre-warmed (37 °C) HEPES-modified Tyrode's buffer. The remaining platelet poor plasma was centrifuged at 16'000 x g for 10 minutes at 4°C to ensure the pelleting of all cellular components and the isolation of pure cfDNA.

For the collection of platelets from healthy donor platelet apheresis bags, samples were pelleted at 600 x g for 20 minutes at room temperature. Platelet numbers were determined using an automated blood cell counter (Horiba, Pentra ES 60 Cell Counter).

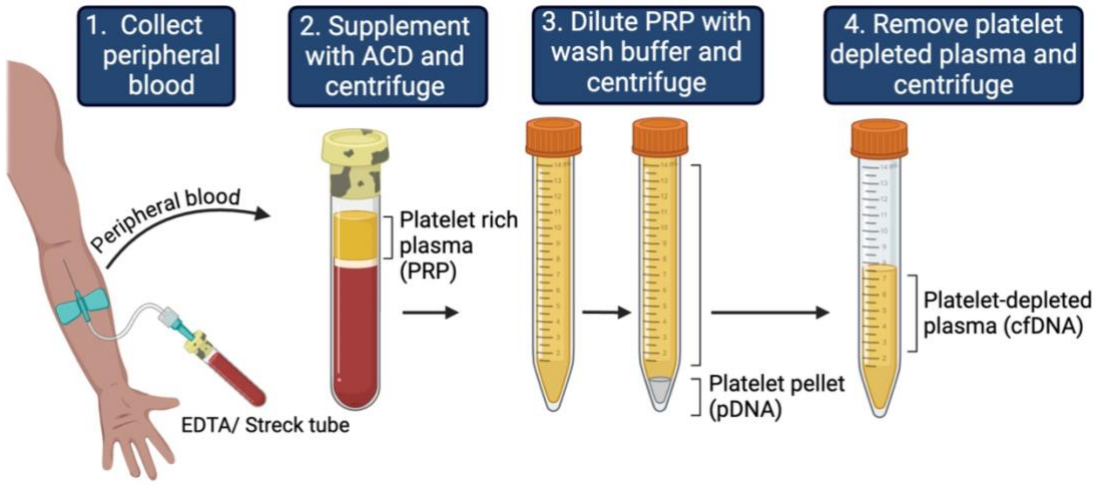


Figure 2-1. Schematic showing sources of purified platelets. Sequential centrifugation of peripheral blood to simultaneously extract DNA from pelleted platelets (pDNA) and platelet-depleted plasma (cfDNA). Created using Biorender.com.

iii) Purity assessment of isolated platelets

Blood cell contamination in the isolated platelet population was assessed by cytocentrifugation. Cytospins were prepared in a two-step cytocentrifugation process, using Polysine-coated microscope slides (VWR International; Avantor Inc.) and the Thermo Scientific Shandon Cytospin®4 Cytocentrifuge (Thermo Fisher Scientific Inc.). Cytospin filter cards were prepared with 50 µl phosphate-buffered saline (PBS) and centrifuged at 350 rpm for 2 min. 100 µl of the platelet resuspension was pipetted onto the slide and centrifuged at 1000 rpm for 10 min. Cytospins were air dried and subsequently stained using the Richard-Allan Scientific Three-Step Stain Set (Thermo Fisher Scientific Inc.). Fixation and staining times were optimised to 60 s for methanol fixative (Fixative), 2.5 minutes for aqueous Eosin Y solution (Solution A), and 3 minutes for aqueous Methylene Blue/Azure A solution (Solution B). After completion of the staining, the slides were washed with deionised water, air dried, and stored for imaging (section 2-8).

Following microscopy, contamination was assessed using ImageJ v2.1.0 (National Institute of Health, US-MD). At the time of optimising this method, based on previous publications[205,274], we considered ≤ 5 nucleated cells per 10 million platelets to be the optimal cut-off to exclude contamination.

Purity of the isolated platelet population was also assessed via flow cytometry. Details of sample preparation, the antibody panel, flow cytometry instrumentation, and data analysis are provided in section 2-6 Flow cytometry and fluorescence-activated cell sorting (FACS).

2-2.2 Murine platelet and plasma isolation

Mouse platelets were isolated within four hours of blood collection via cardiac puncture. Whole blood was supplemented with ACD and centrifuged at 100 x g for 10 minutes at room temperature. The plasma was removed and collected into a 1.5 ml Eppendorf tube. The plasma was then diluted with platelet wash buffer and centrifuged at 3500 x g for 11 minutes to pellet the platelets. The platelet pellet was resuspended in pre-warmed (37 °C) HEPES-modified Tyrode's buffer. The platelet poor plasma was removed and centrifuged at 1300 x g - 16'000 x g for 10 minutes at 4°C to remove all cells and debris, and the final supernatant collected for cfDNA isolation.

2-2.3 Human granulocyte, mononuclear and red blood cell isolation

Human mononuclear cells (MNCs) were isolated from freshly drawn venous blood into EDTA coated tubes. Whole blood was supplemented with ACD and centrifuged at 180 x g for 20 minutes at room temperature. The supernatant was removed and the remaining layer diluted with wash buffer (PBS pH 7.4 0.5% FBS, 2 mM EDTA). Diluted blood was layered onto Ficoll density gradient media (GE Healthcare, cat # 5442-03) and centrifuged for 20 minutes at 600 x g, low brake. MNCs were collected from the white inter-phase 'buffy coat' using a Pasteur pipette and transferred to a Falcon tube. Human red blood cells (RBCs) were sampled from the upper layer of the RBC/granulocyte pellet and diluted with wash buffer. The remaining RBC/granulocyte pellet was resuspended with chilled RBC Lysis Buffer (eBioscience, cat # 00-4300-54) and incubated at 4°C for 5 min. The lysed sample was centrifuged at 1000 x g for 5 min, the supernatant discarded, and the granulocyte pellet diluted with wash buffer. The remaining white granulocyte pellet was washed, centrifuged and stored at -80°C until required. Purity studies using an automated cell counter provided no evidence of MNC or RBC contamination in the granulocyte pellet.

2.3 Nucleic acid extraction and QC

2-3.1 Genomic DNA

Genomic DNA was extracted from nucleated cells using the DNeasy Blood & Tissue Kit (Qiagen, cat # 51104), as per the manufacturer's recommendations.

2-3.2 Cell free DNA

DNA was extracted from equal volumes of fresh platelets (resuspended in HEPES-modified Tyrode's buffer) and 'platelet poor plasma' using the QIAamp Circulating Nucleic Acid Kit (Qiagen, cat # 55114), as per manufacturer's instructions.

2-3.3 Nucleic acid quantification

DNA quantification is often measured by the NanoDrop One Spectrophotometer or the Qubit Fluorometer 2.0 (Thermo Fisher Scientific Inc.). I opted to use the Qubit assay to measure DNA concentration as there are several drawbacks associated with the use of the NanoDrop for example, low specificity. The NanoDrop measures the amount of light passing through the sample and although nucleic acids absorb light at a wavelength of 260 nm, other DNA species, proteins, RNA and contaminants in the buffer can interfere with this reading resulting in an incorrect concentration. However, the Qubit Fluorometer relies on dyes that bind specifically to double stranded DNA. As these reagents are specific to their target and will only fluoresce when bound, contaminants in the sample will not impact the readout.

Extracted DNA was quantified using a Qubit Fluorometer 2.0 (Thermo Fisher Scientific). Depending on the expected DNA yield samples were prepared for fluorometry using either the Qubit 1X dsDNA HS Assay Kit (quantitation range 0.1-120 ng) or the Qubit dsDNA BR Assay Kit (quantitation range 4-2,000 ng). DNA was stored at -80°C until required.

2-3.4 Conversion to genomic copies per µl

The nuclear genome comprises of approximately 3.2 billion nucleotides of DNA. This equates to 290 copies of the human genome per ng of DNA. Therefore, by measuring the ng of platelet DNA per µl of platelet-rich plasma, I was able to approximate the total number of copies of the genome per sample.

In addition to this, as I knew the platelet counts of 14 non-cancer controls, I calculated the approximate amount of DNA in picograms per individual platelet (0.000303848 pg). Each human diploid cell has 6.6 pg of DNA which equates to 2 copies of the genome. Based on this, I estimated that each platelet contained 0.0000921 copies of the genome which is roughly 1/22'000th of the DNA content of a 2N nucleated cell.

2-3.5 Automated electrophoresis

Fragment size was determined using the Agilent TapeStation 2200 system (Agilent Technologies). Cell-free DNA Reagents (Agilent, cat # 5067-5631) and High Sensitivity D1000 Reagents (Agilent, cat # 5067-5585) were used to analyse DNA extracted from plasma and platelets. Genomic DNA Reagents (Agilent, cat # 5067-5366) were used to analyse genomic DNA isolated from nucleated cells.

2-3.6 Polymerase chain reaction

All PCRs were performed using KAPA2G Fast HotStart PCR Kit (Roche, cat # KK5512). Each reaction was prepared as follows: 12.5 µl KAPA2G Robust HotStart ReadyMix, 1.25 µl of each primer at 10 µM, DNA template as required and PCR-grade water to a final volume of 25 µl.

Given the frequently low concentrations of platelet DNA in my samples, I aimed to optimise the detection of subtle variations in DNA recovery without the risk of losing information due to overamplification. To achieve this, I modified the standard protocol by reducing the number of PCR cycles from the recommended 35 to 8.

This adjustment served two purposes:

1. It ensured sufficient amplification of low DNA concentrations, allowing detection by the TapeStation (>5 cycles were needed for this).
2. It prevented overamplification, which could have obscured differences in DNA uptake between platelet samples (>10 cycles made this difficult).

8 cycles struck an optimal balance, providing enough amplification for detection while maintaining the sensitivity needed to discern sample-to-sample variations. The final protocol included an initial denaturation for 3 minutes at 95°C, then 8 cycles of denaturation for 15 seconds at 95°C, annealing for 15 seconds at 54°C and extension for 15 seconds at 72°C. Following this, the final extension was 3 minutes at 72°C.

2-4 Droplet digital PCR

2-4.1 Method overview

All droplet digital PCR (ddPCR) assays were conducted on a QX200 Droplet Digital PCR System using, unless otherwise stated, the manufacturer's recommended protocol and reagents (Bio-Rad Laboratories). Positive and negative controls, listed in Appendix Data Table A2 were included in every assay. Figure 2-2 summarises the ddPCR workflow.

Firstly, reactions are prepared in 96-well semi skirted plates (Bio-Rad, cat # 12001925) by combining genomic DNA template, forward and reverse primers, dual-labelled probes and Supermix for Probes (no dUTP) (Bio-Rad, cat # 1863023). Each probe is dual labelled as it contains a reporter dye (FAM or HEX) at the 5' end and a quencher molecule (BHQ1 or Iowa Black) at the 3' end. Except for the SRY assay, which utilized a single FAM probe, all other ddPCR experiments followed a 'duplex' approach. In this setup, both targets (wild-type and mutant) are simultaneously PCR amplified. Wild-type DNA is recognised by, and binds to a HEX fluorescent labelled probe, whereas mutant DNA binds to a FAM labelled probe.

Following sample preparation, the plate is loaded onto the Automated Droplet Generator (Bio-Rad Laboratories). Microfluidics partition the sample in each well into approximately 20'000 nanolitre-sized droplets, of which, the target and background DNA molecules are randomly distributed. The plate is then sealed and transferred to a Bio-Rad C1000 Touch Thermal Cycler. Each droplet contains the reagents necessary for PCR amplification.

While the probe remains intact, the close proximity of the 3' quencher suppresses the fluorescence of the reporter molecule. However, during PCR amplification, the exonuclease activity of the Taq polymerase cleaves the probe, releasing the reporter. Consequently, the reporter emits fluorescence, a signal that is then detected in the final step of the ddPCR workflow.

Amplified material is loaded onto the QX200 Droplet Reader, where fluorescence in both channels is measured for individual droplets. Positive droplets (containing at least one copy of the target DNA molecule) and negative droplets are counted, and using the Poisson algorithm, the QuantaSoft software (Bio-Rad Laboratories) determines the concentration of the target molecules as copies /µl.

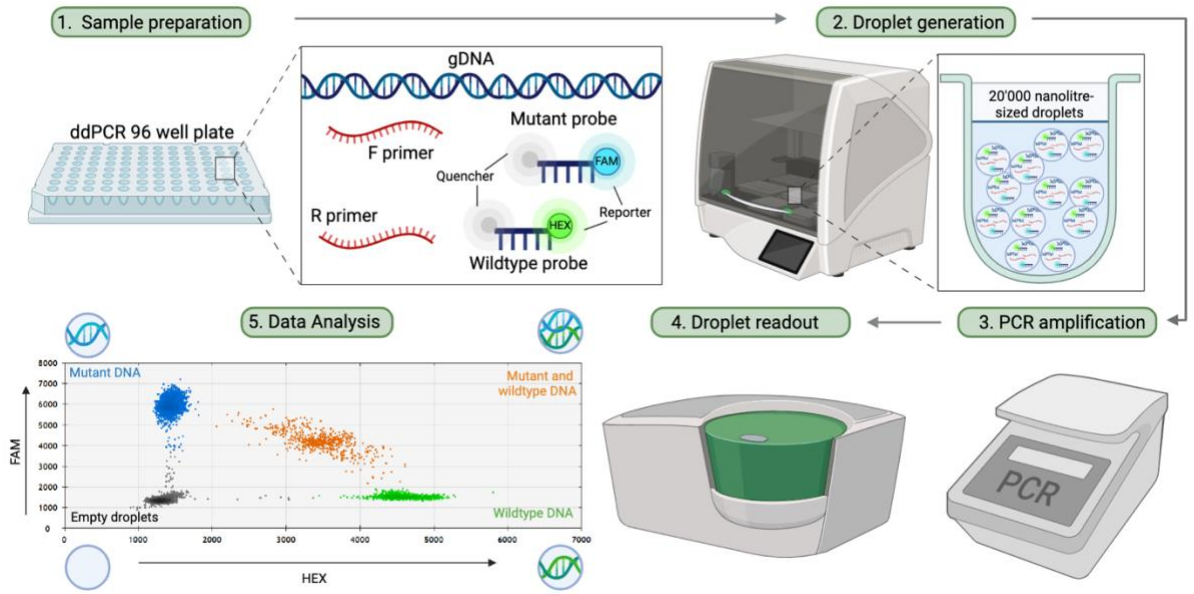


Figure 2-2. Droplet digital PCR workflow. 1) ddPCR reactions are prepared in 96 well plates and include primers, probes, DNA template and the ddPCR Supermix. 2) The plate is then transferred to the droplet generator, which partitions samples into thousands of nanolitre-sized droplets per well. 3) PCR

amplification is carried out within each droplet using a thermal cycler. 4) Lastly, the plate is transferred to the droplet reader where fluorescent positive and negative events are counted to calculate DNA concentration. 5) ddPCR data from a duplex experiment can be viewed as a 2D plot. Here the HEX signal (x axis) is plotted against the FAM signal (y axis). Double positive droplets are shown in orange, HEX only in green, FAM only in blue and double negative (empty droplets) are in grey. Created using Biorender.com.

2-4.2 Human assays

Nikolaos Sousos, a former DPhil student in Adam Mead's lab, designed the *JAK2*V617F ddPCR assays for genomic DNA.

For *JAK2*V617F, each reaction contained 11 µl of the Supermix (2X), primers at 900 nM each, probes at 250 nM each, DNA template and PCR-grade water to a final reaction volume of 22 µl. PCR amplification used the following optimised cycling protocol: initial enzyme activation for 10 minutes at 95°C, 43 cycles of denaturation for 30 seconds at 94°C, annealing/extension for 1 minute at 57°C and enzyme deactivation for 10 minutes at 98°C (ramp rate 2°C/s at all steps).

All other ddPCR assays were ordered directly from Bio-Rad and used the recommended cycling conditions. Details for each assay can be found in Appendix Data Table A2.

2-4.3 Mouse assays

I designed and optimised a ddPCR assay for the detection of *KRAS* in gDNA from KPC and KPN mice. This assay targeted both the wild-type sequence and point mutation present on codon 12 of exon 2 (*KRAS* p.G12D c.35G>A). The primers are as follows: forward 5'-GCCTGCTGAAAATGACTGAG-3' and reverse 5'-CGTAGGGTCATACTCATCCAC-3'.

When designing the dual labelled probes, I opted to include locked nucleic acid (LNA) bases to increase thermal stability and hybridization specificity. LNAs are nucleic acid analogues featuring modified ribose sugars characterized by a chemical bridge that connects the 2' oxygen and 4' carbon. This introduced methylene bridge serves to stabilise the nucleotide, effectively 'locking' it into an optimal conformation for binding. The probes are as follows:

Wild-type: 5'-HEX- ACGCC[+A][+C]CAG[+C]TCCAA-BHQ1-3'

Mutant: 5'-6FAM-AC[+G]CC[+A][+T][+C]AG[+C]TCCAA-BHQ1-3'

Square brackets indicate LNA bases (Merck Life Sciences).

For mouse samples, each reaction contained 11 µl of the Supermix (2×), primers at 900 nM each, probes at 250 nM each, DNA template and PCR-grade water to a final reaction volume of 22 µl. PCR amplification used the following optimised cycling protocol: initial enzyme activation for 10 minutes at 95°C, 40 cycles of denaturation for 30 seconds at 94°C, annealing/extension for 1 minute at 54°C and enzyme deactivation for 10 minutes at 98°C (ramp rate 2°C/second at all steps).

2-5 Cell Lines

2-5.1 Cell maintenance

The following cancer cell lines were used as positive and negative controls for common cancer-associated mutations; HCT116 (CVCL S744) *PIK3CA*H1047R, LS180 (CVCL 0397) *KRAS*G12D, COLO 205 (CVCL 0218) *BRAF*V600E, HEL (CVCL_0001) *JAK2*V617F. All cell lines were purchased from American Type Culture Collection (cat # CCL-247, CL-187, CCL-222 and TIB-180 for HCT116, LS180, COLO 205 and HEL cells respectively). All cells were cultured according to American Type Culture Collection recommendations and tested monthly for mycoplasma contamination.

NKPCB-NBC12.1F (KPC-F) cells, derived from a KPC mouse (LSLKras$^{G12D/+}$; LSLTrp53$^{R172H/+}$; Pdx1-Cre) were cultured in DMEM (Gibco) supplemented with 10% FBS, 2 mM glutamine, 100 U/ml penicillin, 100 µg/ml streptomycin and maintained under at 37 °C with 5% CO_2.

2-5.2 BL2-Bcl-2 cell generation

BL2 and BL2-Bcl-2 cells were maintained by Pamela Holland from the University of Edinburgh.

The human Burkitt's lymphoma cell line, BL2 (CVCL 1966, cat # CRL-2959) was used to generate tumour cell-derived extracellular vesicles (EVs). Standard BL2 cells, were used to obtain apoptotic

(apo-EV) from BL2 cells. BL2 cells stably transfected with the apoptosis-suppressing gene bcl-2 (termed BL2-Bcl-2 cells) were used to obtain non-apoptotic EVs. Protein expression was regularly tested by flow cytometry, confirming that 98% of the BL2-bcl-2 cells expressed Bcl-2. Both cell lines were maintained in 50% X-VIVO medium (50% Gibco RPMI-1640, 50% X-VIVO-20 medium; Lonza, Basel, Switzerland), supplemented with 50 U/ml penicillin and 50 µg/ml streptomycin at 37 °C with 5% CO_2.

The generation, purification and labelling of extracellular vesicles (EVs) was carried out by Pamela Holland from the University of Edinburgh.

i) Generation of extracellular vesicles

BL2 and BL2-Bcl-2 cells were cultured at 20 x 10^6/ml in 0.1 µm filtered 50% X-vivo 20 and irradiated with ultraviolet light to induce apoptosis with 6 doses at 50mJ/cm^2, for a total of 300mJ/cm^2. Apoptosis was monitored hourly by Annexin V and Sytox Blue staining. To isolate EVs, the culture supernatant was centrifuged at 25 x g for 1 hour followed by sequential filtering through a 5 µm mesh filter and a 1.2 µm syringe filter.

ii) Purification of extracellular vesicles

The EVs were purified from soluble factors and proteins from the cell culture by size exclusion chromatography using in-house prepared sepharose columns (Thermo Fisher, cat # 45-000-067 and Sigma Aldrich, cat # CL6B200-100ML). After purification, EV concentration and size profile was measured by Nanoparticle Tracking Analysis using a NanoSight LM10 and Malvern NanoSight software v.3.3. The software analyses each sample 5 times to give the average concentration, mean and mode size of each sample. EV size ranged between 150 – 200 nm and the concentration was between 100- 200 x 10^8/ml. The number of EVs added to platelets was standardised across experiments, using a ratio of 50 x 10^8 EVs with 1 x 10^7 healthy donor platelets.

iii) Fluorescent labelling of extracellular vesicles

For imaging experiments, prior to incubation with platelets, the purified EVs were suspended in 0.1 μm filtered HBSS were stained with Biotium CF568 NHS ester with a covalent attachment of the dye on the EV proteins, according to the manufacturer's protocol (Biotium, cat # NC1542764). To remove unbound dye, the EVs were purified again by size exclusion chromatography through Sepharose columns.

2-6 Flow cytometry and fluorescence-activated cell sorting

2-6.1 Flow cytometry instrumentation

All experiments were carried out using an LSRFortessa™ X-20 flow cytometer (Becton, Dickinson and Company). The BD FACSymphony™ S6 was used for cell sorting. Single colour-stained controls and fluorescence minus one (FMO) controls were used. FACS data were collected using BD FACSDiva software (version 9.0) and gates were set using FMO-controls and negative populations. All antibodies and nucleic acid stains used for flow cytometry are detailed in Appendix Data Table A3.

2-6.2 Purity assessment

Samples were prepared as previously described, pelleted and resuspended in HEPES-modified Tyrode's buffer. The samples were stained with a cocktail of antibodies for 20 minutes at room temperature in the dark, prior to being washed and resuspended in fresh buffer for flow cytometric analysis. The antibodies used are as follows, CD42 FITC, CD41 PE-Cy7, CD3 PE, CD11b and CD33 APC, CD19 APC-Cy7 and CD235a BV650.

I used two gating strategies to simultaneously compare the abundance of small platelets and large leukocytes in each sample. The first setting used a threshold of 1000 to focus on platelets. The second setting used a higher threshold of 5000 to capture the larger contaminating cells that would otherwise extend beyond the axes of the platelet setting. Each sample was analysed twice for 60 second at low speed.

2-6.3 Platelet sorting from whole blood

30 µl of healthy donor whole blood was diluted with an antibody cocktail to a final volume of 100 µl. The platelets were incubated for 20 minutes at room temperature in the dark, washed and resuspended in fresh buffer. The staining solution included the following antibodies, CD42 FITC, CD3 BV421, CD11b and CD33 APC, CD19 APC-Cy7 and CD235a FITC. Platelets ($CD42^+$, $CD3^-$, $CD11b^-$, $CD33^-$, $CD19^-$ and $CD235a^-$) were sorted into 15 ml falcon tubes containing HEPES-modified Tyrode's buffer. The platelets (20×10^6) were centrifuged at 600 x g for 20 minutes, the supernatant removed, and pellet frozen at -20°C.

2-6.4 Platelet nucleic acid content

To assess the nucleic acid content of platelets, healthy donor blood was drawn into EDTA-coated tubes and platelets were isolated as previously described. The platelets were stained with the antibody CD42 FITC or PeCy7 and nucleic acid stains DRAQ5 (DNA) and Syto-13 (RNA) for 20 minutes at room temperature in the dark. After incubation, the platelets were washed and resuspended in fresh HEPES-modified Tyrode's buffer for analysis. MACS compensation beads were stained and analysed in parallel, as an additional negative control to FMOs to confirm no non-specific binding of the nucleic acid stains.

2-6.5 Platelet activation

To assess platelet activation, healthy donor blood was drawn into citrate tubes. Where possible, a 'discard' tube was obtained from the donor before collecting the blood used for analysis. This order of sampling is recommended to avoid potential platelet activation via tissue factor, which becomes exposed during vessel injury such as venepuncture. After collection, the blood was allowed to rest for 30 minutes before platelet isolation. Special care was taken to avoid unintentionally knocking the tube, creating air bubbles or overly pipetting. After the second spin, the platelets were counted and maintained at a physiological concentration of ~300×10^6 /ml. Platelets were either incubated with a synthetic DNA oligo to assess reactivity or immediately stained and analysed.

i) To evaluate the activation status and DNA content of healthy donor platelets

After isolation, platelets were stained with CD42 FITC and antibodies for activation; CD63 PB and CD62P BV857. The DNA content of platelets was simultaneously assessed by the inclusion of the DNA marker, DRAQ5. After a 20 minute incubation at room temperature, the platelets were washed twice, resuspended in HEPES-modified Tyrode's buffer and analysed. DRAQ5 is a permeable anthraquinone dye with a capacity to intercalate between A-T bases of double-stranded DNA. Despite the presence of mitochondria in platelets, no existing literature, at the time of these experiments, documented DRAQ5 binding to mitochondrial DNA which made it an optimal stain for investigating DNA content using flow cytometry.

ii) To assess platelet reactivity to cargo trafficking and activation inhibitors

After isolation, platelets were pre- treated with 5 µM Ibrutinib (PCI-32765) (Stratech Scientific Ltd, cat # S2680-SEL-5mg), 500 µM amiloride (Abcam cat # ab120281) or 30 µM Dynole 34-2 (Abcam, cat # ab120463, 30 µM) for 20 minutes at room temperature. Following treatment, platelets were added to FACS tubes already containing the following staining antibodies, CD42 PE-Cy5, CD63 PB, CD62P BV857 and PAC-1 FITC. The platelets were then spiked with 3 µl of resting or activation mix (Appendix Data Table A4) and incubated in the dark for 15 minutes. After incubation, the platelets were diluted with 300 µl of HEPES-modified Tyrode's buffer and analysed immediately.

iii) To evaluate platelet reactivity in response to synthetic DNA exposure

980 µl platelets at ~300 x 10^6 /ml were incubated for 1 hour at 37°C with 20 µl of synthetic DNA (final concentration 10 ng/ml) or water. Following incubation, 10 µl of platelets were subsampled and added to FACS tubes containing the antibody cocktail described above. The platelets were then spiked with 3 µl of resting or activation mix and incubated in the dark for 15 minutes. After incubation, the platelets were diluted with 300 µl of HEPES-modified Tyrode's buffer and analysed immediately.

iv) To determine changes in platelet DNA content upon activation

Platelets were isolated as described above and resuspended at ~300 x 10^6 /ml. 10 µl of platelets were added to Eppendorf tubes containing the antibodies CD42 FITC, CD63 PB and CD62P BV857 and the DNA stain DRAQ5. The platelets were then spiked with 3 µl of resting or activation mix. After a 15 minute incubation at room temperature, the platelets were washed twice (to ensure complete removal of DRAQ5), resuspended in HEPES-modified Tyrode's buffer and analysed.

Details of the resting and activation mix are listed in Appendix Data Table A4. Briefly, HEPES-modified Tyrode's buffer was supplemented with calcium at 20 mM (Sigma Aldrich, cat # 21115-100ML) or calcium and the agonist, TRAP-6 at 5, 10, 50 and 100 µM (10X the final concentration) (Bachem AG, cat # 4031274.0025).

2-7 *In vitro* co-culture experiments

All blood cell and tumour cell co-culture experiments were conducted using 3 x 10^5/µl, platelets (PLTs) 0.075 x 10^5/µl mononuclear cells (MNCs), 3 x 10^5/µl red blood cells (RBCs) and 0.03 x 10^5/µl tumour cells. All blood cells for functional studies were isolated from whole blood drawn into EDTA-coated blood collection tubes and re-suspended in Tyrode's salts (Sigma Aldrich, cat # T2397-100ML). Unless otherwise stated, the QIAamp Circulating Nucleic Acid Kit (Qiagen, cat # 55114) was used to extract DNA from both the cells and buffer in the following co-culture experiments.

2-7.1 Blood cell-tumour incubation

i) Description of method

Platelets, MNCs and RBCs from healthy donors were added to individual wells within a 24-well plate and a 1.0 µm TC Insert (Sartstedt, cat # 83.3932.101) placed into the well. Tumour cells were carefully placed in the inserts and the plate incubated for approximately 8 hours at 37°C. Control samples were incubated simultaneously but without the addition of tumour cells. After incubation, the inserts were

removed and the blood cells transferred to Eppendorfs. To ensure complete removal of any contaminating tumour derived DNA in the media, all cell types were washed and centrifuged at 600 x g for 10 minutes. The supernatant was removed and the pelleted blood cells re-suspended in fresh buffer. The cells were washed for a total of three times and finally resuspended in 1 ml of fresh pre-warmed HEPES-modified Tyrode's buffer prior to DNA extraction.

ii) Co-culture set up

Tumour cell lines were separated from PLTs, MNCs, and RBCs using inserts with 1.0 µm pores. These pores allowed the exchange of biomolecules and small EVs between compartments while preventing nucleated cells from entering the lower compartment.

To validate this separation method, I conducted an experiment comparing the amount of DNA recovered from platelets using a range of membrane pores from 0.4 to 8.0 µm. The results showed that the amount of DNA extracted from the platelets remained consistent across all pore sizes, including the largest 8.0 µm pores. This consistency indicates that even at the largest pore size tested, cancer cells were unable to pass through the membrane. For context, the average size of cancer cells typically ranges from 10 to 30 µm in diameter, depending on the cell type. Therefore, pores significantly larger than 8.0 µm would be required for cancer cells to pass through the membrane.

This experiment confirms the effectiveness of the 1.0 µm pore size in allowing molecular exchange while maintaining physical separation of the cancer cells from the platelet fraction.

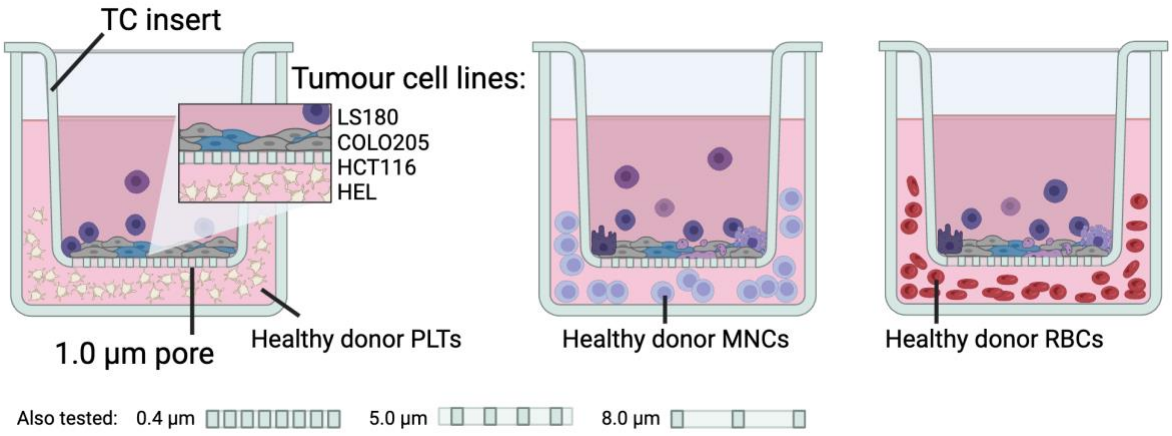


Figure 2-3. *In vitro* co-culture set up. Blood cells from healthy donors were co-cultured with tumour cells. Inserts with small membrane pores allowed for the exchange of biomolecules but prevented the cell types physically interacting. Created using Biorender.com.

2-7.2 Platelet-extracellular vesicle incubation

Platelet- extracellular vesicle incubation was carried out by Pamela Holland from the University of Edinburgh.

50 x 10^8 labelled, purified apo- and non-apo-EVs resuspended in in Tyrode's buffer were incubated with 0.1x 10^8 platelets for three hours at 37°C with gentle inversion every 30 minutes. Following incubation, the samples were centrifuged for 20 minutes at 800 x g. The supernatant was discarded, and the platelets re-suspended in 300 µl of PBS medium. EV and platelet pellets were treated with DNase before DNA extraction as per manufacturer's protocol (Sigma Aldrich, cat # AMPD1). DNA extraction was performed using a QiaAMP DNA blood kit as per manufacturer's protocol (Qiagen, cat # 51104), samples were eluted in 30 µl of elution buffer, and the DNA concentration was measured using a Qubit Fluorometer.

2-7.3 Platelet- synthetic DNA oligo

i) Synthetic DNA oligo generation

Double and single stranded DNA oligos were designed to include the mouse *KRAS*G12D genetic marker and synthesised by Integrated DNA Technologies (IDT, Iowa USA) (Fig. 2-4). I chose to base the DNA sequence of the synthetic oligo on the mutant mouse *KRAS* gene, for the added reassurance that I was highly unlikely to randomly amplify the same sequence in human platelets that had no exposure to the DNA fragment. Details of synthetic DNA oligos are listed in Appendix Data Table A5.

Synthesised DNA was reconstituted according to the manufacturer's protocol. PCR assays for the detection of *KRAS* were performed using the KAPA2G Fast HotStart PCR Kit. The primers were as follows:

Forward: 5'-GCCTGCTGAAAATGACTGAG-3'

Reverse: 5'-CGTAGGGTCATACTCATCCAC-3'.

Fragmentation profiles of DNA oligos were analysed using an Agilent TapeStation 2200 system. Electrophoresis data were analysed using the TapeStation Analysis Software (Agilent).

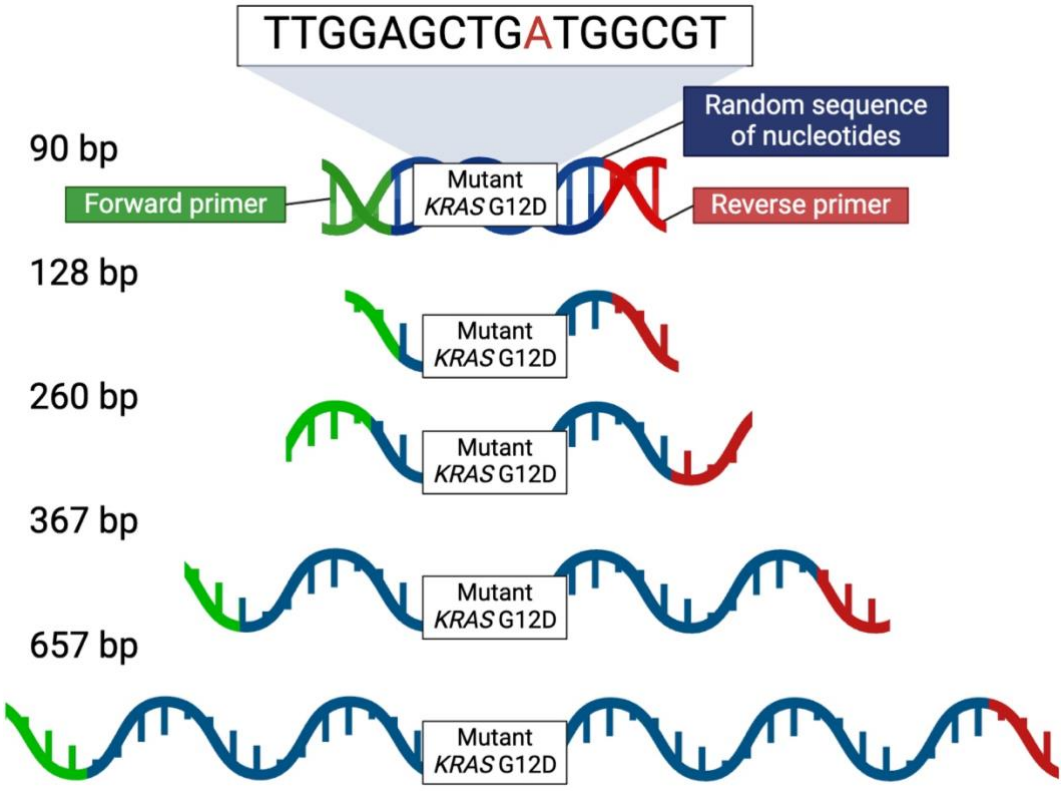


Figure 2-4. Design of synthetic DNA fragments. In each DNA sequence, mouse *KRAS*G12D was positioned at the centre, surrounded by random nucleotides. The length of DNA fragments ranged from 90 bp to 657 bp, determined by the quantity of random nucleotides. Amplification of each DNA sequence was achieved using a universal pair of forward and reverse primers. Created using Biorender.com.

ii) Platelet-DNA oligo incubation

All platelet-oligo experiments were conducted using 3 x 10^5 platelets/µl re-suspended in pre-warmed (37°C) HEPES-modified Tyrode's buffer. Healthy donor human platelets were aliquoted into Eppendorfs and spiked with reconstituted synthetic DNA oligos for a final concentration of 10 ng/ml. The platelets were mixed gently by pipetting and incubated at 37°C overnight. Following incubation, the platelets were centrifuged for 10 minutes at 600 x g. The supernatant (containing excess DNA oligo) was discarded, and the platelets re-suspended in fresh buffer. The platelets were washed for a total of

two times and finally resuspended in 1 ml of fresh pre-warmed HEPES-modified Tyrode's buffer prior to DNA extraction. Eluted DNA was PCR amplified and the Agilent TapeStation was used to confirm fragment length.

2-7.4 DNase treatment to investigate platelet DNA internalisation

Following incubation with HEL, erythroleukemia cells, platelets were treated with DNase according to the manufacturer's protocol (Ambion DNA-free Kit, cat # AM1906). To confirm catalytic activity of the enzyme, DNase was also added to conditioned media. Following DNase treatment, the platelet samples were washed with 500 µl of 5 mM EDTA and centrifuged at 600 x g for 10 minutes. The supernatant was removed, and the wash repeated. After the second centrifugation, the supernatant was discarded, and the platelet pellet resuspended in 1 ml of fresh pre-warmed HEPES-modified Tyrode's buffer. Following DNase inactivation of the conditioned media, 900 µl of HEPES buffer was added to a final volume of 1 ml in preparation for DNA extraction. For control samples, no DNase was added and 10 µl of 1M tris-HCL was added in replacement of 10X DNase I Buffer for the platelet samples.

In a separate experiment, healthy donor platelets or an equal volume of HEPES-modified Tyrode's buffer (to mimic cfDNA) was spiked with a 260 bp synthetic DNA oligo and incubated overnight. The samples were then treated with DNase according to the manufacturer's protocol (Life technologies, RapidOut DNA Removal Kit, cat # K2981). Following DNase treatment, the platelet samples were washed and centrifuged at 600 x g for 10 minutes. The supernatant was removed, and the wash repeated. After the second centrifugation, the supernatant was discarded, and the platelet pellet resuspended in 1 ml of fresh pre-warmed HEPES-modified Tyrode's buffer. For 'cfDNA' (buffer) samples, DNase was inactivated and 900 µl of HEPES buffer was added to a final volume of 1 ml. All samples were DNA extracted. Eluted DNA was PCR amplified and the Agilent TapeStation was used to confirm fragment length. For control samples, no DNase was added and 10 µl of 1M tris-HCL was added in replacement of 10X DNase I Buffer for the platelet samples.

2-7.5 Inhibition of platelet endocytosis and exocytosis

i) Description of inhibitors

To understand the mechanism(s) of DNA uptake, I tested a range of inhibitors (and paired negative controls) known to block specific components of cargo trafficking, including inhibitors of actin (cytochalasin D [Santa Cruz Biotechnology, cat # CAS 22144-77-0, 5 µM]), membrane ruffling (imipramine [Abcam, cat # ab141046, 5 µM]), caveolae-dependent endocytosis (nystatin [Merck Life Science UK, cat # N9150-20ML, 30 units/ml]), clathrin (Pitstop 2 [Abcam, cat # ab120687, 25 µM], Pitstop 2 Negative control, [Abcam, cat # ab120688, 25 µM]), dynamin (Dynole 34-2 [Abcam, cat # ab120463, 30 µM], Dynole 31-2, Negative control [Abcam, cat # ab120464-5mg, 30 µM]) and Na/H exchange/ micropinocytosis (amiloride, [Abcam cat # ab120281, 500 µM]).

ii) Platelet endocytosis

See Fig. 2-5 for a summarised overview. Healthy donor human platelets at 300 $x10^6$ /ml were treated with inhibitors or paired negative controls as described above. After treatment, platelets were spiked with a 260 bp synthetic DNA oligo for a final concentration of 10 ng/ml and incubated at 37°C overnight. Following incubation, the platelets were centrifuged for 10 minutes at 600 x g. The supernatant (containing excess inhibitor/ negative control and DNA oligo) was discarded, and the platelets re-suspended in fresh buffer. The platelets were washed for a total of two times and finally resuspended in 1 ml of fresh pre-warmed HEPES-modified Tyrode's buffer prior to DNA extraction. Eluted DNA was PCR amplified and the Agilent TapeStation was used to confirm fragment length.

Platelet- extracellular vesicle incubation was carried out by Pamela Holland from the University of Edinburgh.

To explore the impact of dynamin inhibition on platelet EV uptake, 0.1x 10^8 platelets were treated with either the dynamin inhibitor, paired negative control or DMSO for 30 minutes at 37°C. After incubation, 50 x 10^8 labelled, purified apo-EVs re-suspended in Tyrode's buffer were added to the treated platelets

and incubated as previously described prior to DNase treatment and DNA extraction. Eluted DNA was PCR amplified, and the Agilent TapeStation was used to confirm fragment length.

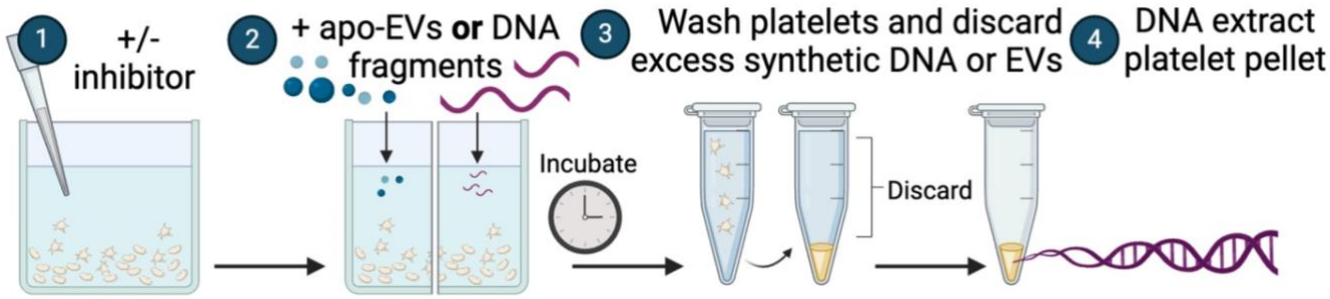


Figure 2-5. Method used to explore the mechanism(s) of DNA uptake. In brief, platelets were treated with inhibitors prior to incubation with DNA-laden EVs derived from apoptotic BL2 cells (apo-EVs) or 'free' synthetic DNA fragments. Platelets were washed and pelleted prior to DNA extraction. Created using Biorender.com.

iii) Platelet exocytosis

Healthy donor human platelets at 300 x10^6 /ml were treated with Dynole or paired negative control. After treatment, platelets were spiked with a 260 bp synthetic DNA oligo and incubated at 37°C overnight. Following incubation, the platelets were pelleted at 600 x g for 10 minutes and the supernatant discarded. The platelets were resuspended in fresh HEPES-modified Tyrode's buffer, re-treated with the inhibitor or negative control and incubated for 3 hours at 37°C. After the incubation, the platelets were pelleted, and the supernatant (platelet releasate) was collected. The supernatant was further centrifuged for 5 minutes at 16'000 x g to ensure complete removal of any contaminating platelets and subject to DNA extraction. Eluted DNA was PCR amplified and the Agilent TapeStation was used to confirm fragment length. The final method is summarised below.

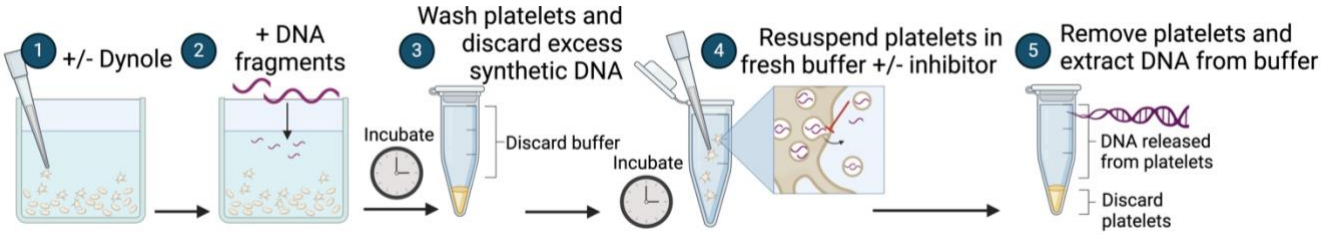


Figure 2-6. Method used to investigate platelet DNA release. Platelets were treated with/without Dynole and incubated with 260 bp DNA fragments. After incubation, the platelets were washed,

resuspended in fresh buffer and incubated again for 3 hours. The platelets were then pelleted, and DNA was extracted from the buffer. Created using Biorender.com.

2-7.6 Inhibition of platelet activation

Healthy donor platelets at 300 x10^6 /ml were treated with 500, 1000 or 2000 µM aspirin (Merck Life Sciences, cat # A2093-500G) or 5, 50, 100 or 200 µM Ibrutinib (PCI-32765) (Stratech Scientific Ltd, cat # S2680-SEL-5mg). Following treatment, platelets were spiked with a 260 or 367 bp synthetic DNA oligo for a final concentration of 10 ng/ml and incubated at 37°C overnight. Following incubation, the platelets were centrifuged for 10 minutes at 600 x g. The supernatant (containing excess inhibitor/ negative control and DNA oligo) was discarded, and the platelets re-suspended in fresh buffer. The platelets were washed for a total of two times and finally resuspended in 1 ml of fresh pre-warmed HEPES-modified Tyrode's buffer prior to DNA extraction. Eluted DNA was PCR amplified and the Agilent TapeStation was used to confirm fragment length.

For aspirin treatment of platelets co-cultured with COLO205 cells, instead of incubating with DNA oligonucleotides, platelets were treated with 2000 µM of aspirin and added to the bottom of a 24-well plate. A 1.0 µm TC Insert (Sartstedt, cat # 83.3932.101) was then placed into each well. COLO205 cells, resuspended in HEPES buffer at a concentration of 0.03 x 10^5 cells/µl, were carefully introduced into the inserts. This setup allowed for the exchange of soluble factors between the two cell types while maintaining their physical separation. The plate was incubated overnight at 37°C. Following incubation, the platelets were collected and washed as described in section 2-7.1.

2-8 Immunofluorescence microscopy

I employed multiple nucleic acid stains to validate platelet DNA content, including well-known markers like DAPI and Hoechst (Invitrogen, cat # H3570), as well as DRAQ5, SiR-DNA (Spirochrome, cat # CHF260.00), and NUCLEAR-ID® Red DNA stain (Enzo Life Sciences, cat # ENZ-52406). SiR-DNA, a live cell nuclear stain, binds reversibly to the minor grooves of double-stranded DNA with high

specificity. NUCLEAR-ID Red intercalates between the base pairs of double-stranded DNA through electrostatic interactions.

Platelets typically contain approximately 5-8 mitochondria, and although this is low compared to other cell types, there is no data suggesting that DRAQ5, SiR-DNA or NUCLEAR-ID Red bind to mitochondrial DNA. This suggests that the nucleic acid stains are unlikely to bind non-specifically to platelet mitochondrial DNA and therefore bind platelet genomic DNA. Details of the antibodies and nucleic acid stains used for imaging can be found in Appendix Data Table A6.

2-8.1 Live

i) Platelet-tumour cell

Human platelets were isolated from healthy donors as previously described and stained with anti-CD42 AF488 (BioLegend, cat # 303914) for 30 minutes at room temperature. Separately, COLO205 or H2B-mCherry HEL cells were labelled using either the highly specific live cell DNA stain, SiR-DNA, NUCLEAR-ID Red DNA stain or DAPI (HEL only) as per the manufacture's protocols. Stained COLO205 or H2B-mCherry HEL cells were then washed and added to collagen type-1 (Corning, cat # 354236)-coated microscopy slides (Greiner Bio-One, cat # 543079). Stained platelets were added to the wells containing tumour cells immediately before imaging. To analyse endogenous wild-type DNA within healthy donor platelets, platelets were co-stained with anti-CD42 AF488 and NUCLEAR-ID Red DNA and imaged alone. H2B-mCherry HEL cells were kindly provided by Antonio Rodriguez-Romera and Zoë Wong, both DPhil students in Beth Psaila's Lab.

ii) Platelet- conditioned media

COLO205 cells were labelled with NUCLEAR-ID Red DNA stain as previously described. Following staining, the cells were washed with MEM Alpha 5% FCS, pelleted and the supernatant removed. The cells were washed a further two times to ensure complete removal of any excess DNA stain in the media, and the COLO205 cells then resuspended in 200 µl of fresh MEM Alpha + 5% FCS. The cells were incubated at 37°C and vortexed periodically to encourage cell death and DNA release. After two hours,

the COLO205 cells were centrifuged at 16’000 x g for 10 minutes at 4°C. Supernatant was removed from the pelleted cells, transferred to a fresh Eppendorf and the COLO205 cell pellet discarded. Healthy donor platelets were stained with anti-CD42 AF488 as previously described and added to wells of Poly-L-lysine coated slides (Ibidi, cat # 81201). DNA labelled, COLO205 cell conditioned media was added to the platelets immediately before imaging. All cells were resolved by fluorescent microscopy using the Zeiss Spinning Disk Confocal with a 63X oil immersion objective.

2-8.2 Fixed

i) Sorted platelets from whole blood

Sorted platelets were spun onto slides and stained with CD42 AF488. The slides were mounted with a coverslip and then resolved by fluorescent microscopy using an Echo Revolve microscope with a 63X oil immersion objective.

ii) Apoptotic extracellular vesicles

BL2 cell-derived apo-EVs were isolated, labelled with an amine-reactive fluorescent dye (Biotium, cat # 92131) and frozen as previously described. Prior to imaging, the EVs were thawed and co-stained with DAPI for 30 minutes at room temperature. The EVs were washed twice, pelleted at 20’000 x g for 30 minutes at 4°C and resuspended in HBSS buffer (Thermo Fisher, cat # 88284). Labelled EVs were then added to Poly-L-lysine coated chamber slides (Ibidi, cat # 81201) and incubated overnight at 4°C. Following incubation, the supernatant was carefully removed and the EVs fixed with 4% formaldehyde at room temperature for 30 minutes. The fixative was then removed and the EVs gently washed three times with PBS. To confirm imaging of EVs and not auto-fluorescent debris, PBS was stained with DAPI, incubated overnight, and fixed onto slides alongside the EV preparations. The slides were mounted and the EVs and PBS controls, resolved by fluorescent microscopy using a Zeiss LSM900 with a 63X oil immersion objective.

iii) Platelet-apoptotic extracellular vesicle incubation

Human platelets were isolated from healthy donors as previously described and resuspended in 1 ml of HBSS buffer. BL2 cell-derived apo-EVs labelled with an amine-reactive fluorescent dye (Biotium, cat # 92131) were thawed and 5 x 10^9 EVs were added to 10 x 10^6 platelets and incubated for 3 hours at 37°C. To ensure adequate mixing, the cells were inverted gently every 30 minutes. Following incubation, the cells were centrifuged at 800 x g for 20 minutes, low brake. The supernatant (containing the EVs) was removed, and the platelets resuspended in 100 ml of PBS. Platelets were centrifuged onto a Poly-L-lysine coated chamber slide (Ibidi, cat # 81201) at 600 x g for 20 minutes and fixed in 2% formaldehyde/PBS for 10 minutes at room temperature. The fixative was then removed, and the platelets washed twice with PBS. The platelets were then labelled with stained with anti-CD42 AF488 (BioLegend, cat # 303914) for 20 minutes at room temperature. After labelling, the slides were washed, mounted with ProLong Gold Antifade Mountant (Thermo Fisher, cat # P36930) and imaged using the Zeiss LSM900.

iv) Histology, immunohistochemistry, and imaging of peripheral blood films

Cytospins prepared as previously described in section 2-2.1, were imaged using an Olympus BX60 Microscope.

P53 immunohistochemistry of KPC mouse tissue was carried out by Giampiero Valenzano, a DPhil student in the Department of Oncology.

KPC mice were sacrificed, and pancreatic tissue was taken for p53 immunohistochemical staining. Briefly, a total of 24 hours post fixation in 10% neutral buffered formalin at 4°C, tissues were transferred to 70% ethanol and stored overnight at 4°C. Fixed tissues were processed overnight using the STP120 Spin Tissue Processor (Thermo Fisher Scientific) and embedded the next day in paraffin wax. Tissues were cut into 4 μm sections using a Leica RM215 microtome and adhered onto SuperFrost Ultra Plus Adhesion slides (Thermo Fisher Scientific) before drying overnight in a 37°C incubator. After deparaffinization, rehydration in an ethanol gradient (100%, 70%, 50%), and antigen retrieval with

Citrate Buffer Antigen Retriever (Sigma-Aldrich), slides were incubated with Dual Endogenous Enzyme-Blocking Reagent (Dako) for 1 hour, washed in PBS, incubated with 5% goat serum for 30 minutes, washed in PBS again, and incubated with primary antibody (p53 1C12, Cell Signalling Technologies) diluted 1:2000 for 2 hours at room temperature. Slides were then washed in PBS with 0.05% Polysorbate 20 and incubated with secondary antibody (Anti-mouse IgG, HRP-linked, Cell Signalling Technologies) diluted 1:100 for 45 minutes at room temperature, washed in PBS with 0.05% Polysorbate 20 again, and incubated with 3,3′-Diaminobenzidine (DAB) chromogen for 3 minutes at room temperature. After staining, slides were dehydrated in an ethanol gradient (50% 70%, 100%), followed by tissue clearing in xylene (Thermo Fisher). Slides were mounted with dibutylphthalate polystyrene xylene (DPX; Sigma-Aldrich), dried for 24 hours and scanned using an Aperio ScanScope CS digital slide scanner (Leica Biosystems) at 20X magnification.

Healthy donor blood was used to prepare a peripheral blood film. The blood smear was fixed with 100% methanol for 30 seconds and stained with CD42 AF488 (BioLegend, cat # 303914) to identify platelets and the DNA stain Hoechst (Invitrogen, cat # H3570), to identify nucleated cells. The slide was mounted with a coverslip and imaged using the Leica SPE. These blood films were created and analysed with the help of Nikolaos Sousos, a former DPhil student in Adam Mead's lab.

v) Fluorescence In Situ Hybridization

Platelets in suspension were centrifuged onto Poly-L-lysine coated chamber slides (Ibidi, cat # 81201) at 600 x g for 20 minutes and fixed in 2% formaldehyde/PBS for 10 minutes at room temperature. The platelets were then permeabilised in 0.5% Triton X-100/PBS for 10 minutes at room temperature and washed twice in 0.05% Triton-X-100/PBS. The platelets were washed in 0.02% Tween20/PBS (PBST) and incubated with the primary anti-β-tubulin antibody (Sigma Aldrich, cat # T5201) diluted in blocking buffer for 30 minutes at 37ºC in a humid box. Following primary labelling, the platelets were washed with PBST and incubated with the secondary donkey anti-mouse IgG H&L AF405 antibody (Abcam, cat # ab175658) diluted in blocking buffer for 30 minutes at 37ºC. The labelled platelets were then washed with PBST, fixed and washed with PBS for 10 minutes at room temperature. Fluorescence In

Situ Hybridization (FISH) staining was carried out according to the manufacturer's protocol. Briefly, slides were incubated in 0.1N HCL, washed with 2x SSC and dehydrated in 70% ethanol for 3 minutes. Equal volumes of X- and Y-chromosome probes (Metasystems, cat # D-0323-050-FI and D-0324-100-OR) were added to the slide and covered with a 22 x 22 mm^2 coverslip. The slides were incubated at 85ºC for 5 minutes, sealed with rubber cement and incubated in a humidified chamber at 37°C overnight. Following hybridization, the rubber seal was removed, and the slides washed in 0.1x SSC at 60ºC. Slides were mounted and imaged using the Zeiss LSM900 with a 63X oil immersion objective. Control cells (HEL cells and MNCs) were fixed onto slides, permeabilised and labelled with the X- and Y- chromosome paints as previously described. Following overnight hybridization, the cells were washed and counterstained with DAPI.

vi) ZEISS Airyscan imaging of platelet ultrastructure

Glass coverslips (VWR, cat # 631-0150) were coated with 5 µg/ml fibrillar collagen-I (Horm), (Nycomed) and incubated at 4ºC overnight in a 24 well plate. The coverslips were blocked with 5 mg/ml BSA for 1 hour at room temp. After blocking, the BSA was removed and 300 µl of washed healthy donor platelets diluted to $10x10^6$/ml was added to the wells. The platelets were left to spread for 45 minutes in a humidified chamber at 37°C. Following incubation, the liquid was carefully removed and washed with PBS. The platelets were fixed with 5% formalin for 10 minutes at room temperature, washed with PBS and permeabilised with 0.1% Triton-X100 (Sigma, cat # SLCF5969) for 5 minutes. The slides were washed with PBS and blocked for 30 minutes with blocking buffer (1% BSA + 2% goat + 2% donkey serum). The primary antibodies: mouse anti- human CD63, mouse anti- human LAMP-2, rabbit anti- human TOM20, rabbit anti- human CD81 and mouse anti- human CD62P were diluted in blocking buffer and incubated with the platelets at 4ºC overnight. Following primary incubation, the coverslips were washed 3 times with PBS and incubated with the DNA stains (DRAQ5, NUCLEAR-ID Red or Hoechst) and the secondary antibodies; goat anti- mouse IgG H&L AF568 and goat anti- rabbit IgG H&L AF488 for 45 minutes at 37°C. Following incubation, the coverslips were washed and mounted onto imaging slides using Hydromount (Scientific Laboratory Supplies Ltd, cat #

NAT1324). The slides were imaged using the Airyscan function of a Zeiss LSM 980 confocal microscope (63X objective lens, NA 1.4).

2-8.3 Image analysis

Images were analysed using ImageJ v2.1.0 (National Institute of Health, US-MD) and 3D reconstructions were generated in Imaris Viewer v9.7.0 (Oxford Instruments, Abingdon). CellProfiler v4.0.7 (Broad Institute, US-MA) was used to quantitatively analyse platelet-tumour cell interaction. In brief, cells were segmented using the 'Identify Primary/secondary Object' module. Thresholding strategies were employed to accurately mask cells for segmentation. Platelets were tracked using the 'Track Objects' module. Finally, AF647 intensity was measured using 'Measure Object Intensity' and data 'Exported to Spreadsheet'. This image-analysis pipeline, as well as others can be recreated in Cell Profiler tool (freely available from the Broad Institute at www.cellprofiler.org).

ZEN Microscopy Software was used to create 3D masks using z stack images of platelets. After acquiring the images, I used the image processing module to create a maximum intensity projection of the Z-stack, which combines the brightest pixels from each slice into a single 2D image. Next, I used the software's segmentation tools to define the cell's boundaries. The 'Image Segmentation' feature in ZEN allows for the creation of a binary mask based on these boundaries. To extend this mask into three dimensions, the software's 3D construction tools can be utilized. By applying the 2D mask to each slice of the original Z-stack and interpolating between slices, ZEN generates a 3D volumetric mask of the cell. I then refined the mask of the platelet using manual editing in the software's 3D view.

Co-localisation analysis was conducted by Paul Rees from Swansea University.

For co-localisation analysis, we calculated the Pearson's correlation coefficient, r and Mander's overlap coefficient, R for each platelet by manually defining a cuboid (x=90pixels=3.8um, y=90pixels=3.8um) enclosing the fluorescence from all 3 channels. The coefficients are then calculated as defined by

$$r = \frac{\sum(I1_i - I1_{mean}) \times (I2_i - I2_{mean})}{\sqrt{\sum(I1_i - I1_{mean})^2 \times (I2_i - I2_{mean})^2}}$$

$$R = \frac{\sum I1_i \times I2_i}{\sqrt{\sum(I1_i)^2 \times (I2_i)^2}}$$

where $I1_i$ and $I2_i$ represent the fluorescence intensity of channel 1 and channel 2 in pixel i and $I1_{mean}$ and $I2_{mean}$ represent the mean fluorescence intensity of all pixels in channel 1 and channel 2 respectively. The coefficients were calculated using MATLAB scripts provided in Jung *et al,.*[275].

To assess the location of the DNA fluorescence within the platelet we developed a simple algorithm in MATLAB to calculate the total intensity of the DNA marker in a 3D platelet mask that was subsequently eroded away from the surface to the centre. First, we generated a 3-dimensional platelet mask by applying a one level Otsu thresholding algorithm to the CD62P fluorescence signal. The DNA intensity within the platelet was obtained by integrating the DRAQ5 fluorescence signal from pixels within the 3D platelet mask. To determine the position of the DNA fluorescence within the platelet, we use a series of one pixel erosion operations on the original 3D mask. After each erosion step, a convex hull was applied to ensure there were no 'holes' in the mask. The integrated DNA fluorescence intensity was then obtained within this new eroded mask. This procedure was repeated until a single pixel of the 3D platelet mask remained i.e. the centre of the platelet had been reached.

2-9 H3k27ac ChIPmentation of platelet chromatin

Platelet ChIPmentation, a technique that integrates chromatin immunoprecipitation (ChIP) with Tn5 transposase-based DNA tagmentation to study the genomic binding sites of proteins, was performed by Jeanne Inchauspé, a DPhil student under the co-supervision of Jim Hughes and Beth Psaila.

Three non-clinical research platelets samples were ordered from the NHS Blood and Transplant. Platelets were counted with an automated blood cell counter (Horiba, Pentra ES 60 Cell Counter). 13

ml of each sample was centrifuged at 600 x g for 30 minutes at room temperature, and the supernatant was removed. The platelet pellets were immediately used for H3K27ac ChIPmentation.

ChIPmentation was adapted from a published protocol[276], using the H3k27ac antibody (Diagenode, cat # C15410196). This protocol is tailored for low-input DNA samples, for samples with cell numbers as low as 2000 cells. Bead-bound chromatin undergoes a one-step adaptor insertion via Tn5 tagmentation. Only one post-PCR DNA purification is performed, which reduces sample loss.

For each reaction, 5 µl A-Dynabeads (Invitrogen cat # 10001D) were blocked with the H3K27ac antibody (Diagenode, cat # C15410196) (150 µl PBS, 0.5% BSA, 1x Proteinase inhibitor). The antibody bound-beads were then washed in PBS and 0.5% FBS, before being added to samples for overnight incubation.

Platelet pellets were obtained from two apheresis samples and were incubated in 600 µl lysis buffer (50 mM Tris pH 8, 10 mM EDTA, 0.5% SDS, 1x Protease Inhibitor) for 20 minutes on ice. Then, 1% Triton-X100 was added and the samples centrifuged to pellet insoluble material. The supernatant was split into three 200 µl sub-samples, which were pre-cleared with 5 µl A- Dynabeads and incubated overnight with the overnight antibody blocked-beads. Before incubation, 5% of the sample was kept aside for input control tagmentation.

After overnight incubation, beads underwent multiple rounds of washes with RIPA wash buffer (50 mM HEPES pH 7.6, 500 mM LiCl1, 1 mM EDTA, 1% NP-40 / IGEPAL CA-630, 0.7% Na-Deoxycholate), TE and 10 mM Tris pH8. Beads and input control samples were then tagmented in tagmentation buffer (50 mM Tris pH 8, 25 mM MgCl2, 50% Dimethylformamide) with Tn5 transposase (Illumina, cat # 20034197) for 10 minutes at 37°C and immediately cooled down. Beads were immediately washed. Library preparation was then conducted with Nextera-based sequencing primers[277]. qPCR and fragmentation analysis were performed.

2-10 Whole genome sequencing

2-10.1 Library preparation

Whole genome sequencing (WGS) was performed on paired platelet DNA (pDNA) and cfDNA isolated simultaneously from the same peripheral blood samples of 13 patients with a recent diagnosis of gastrointestinal adenocarcinoma. Libraries were prepared from samples that were confirmed using the Agilent TapeStation have both short DNA fragments of approximately 160 bp in addition to larger peaks of ~12,000 bp. Details of samples used for WGS are provided in Appendix Data Table A10.

i) Platelet DNA size selection

I performed size selection on the pDNA using AMPure XP beads to separate short DNA fragments (s-pDNA; under 600 bp) from large fragments (l-pDNA; over 600 bp). The ratio of AMPure XP beads to DNA solution determines the size range of DNA fragments that bind to the beads. Lower ratios (e.g., 0.5x) preferentially bind larger fragments, while higher ratios (e.g. 1.8x) capture both larger and smaller fragments (>100 bp). Therefore, I used a 0.5x bead-to-DNA ratio to selectively bind longer platelet DNA (l-pDNA) to the magnetic beads, leaving the shorter platelet DNA fragments in solution. After collecting the supernatant, the short fragments were further cleaned to remove <100 bp fragments by incubating with beads at a 1.8:1 bead ratio. Prior to library prep, l-pDNA was fragmented via sonication.

ii) Genomic DNA fragmentation

15 µl of l-pDNA diluted in TE buffer (1mM Tris-HCl, pH 8.0, 0.1 mM EDTA) was added to a Covaris microtube-15 (Covaris, cat # 520145) and briefly centrifuged at 3000 x g for 1 minute. The microtube was loaded onto the Covaris ME220 Focused-ultrasonicator and the protocol run using the treatment conditions required for a 150 bp target peak. Fragment size was determined using the Agilent TapeStation system as previously described, and the sonication was repeated if DNA fragments were > 150 bp.

iii) NEBNext® UltraTM II DNA Library Prep

DNA-Seq libraries were prepared using the NEBNext Ultra II DNA Sample Preparation Kit for Illumina (New England BioLabs, Ipswich, MA, USA) according to the manufacturer's protocol. Following end repair and adapter ligation, adapter-ligated DNA fragments were amplified using the following cycling conditions to generate final libraries: initial denaturation for 30 seconds at 98°C, 11 cycles of denaturation for 10 seconds at 98°C, annealing/extension for 75 seconds at 65°C and final extension for 5 minutes at 65°C. Cleaned up libraries were then multiplexed, and analysed on an Illumina NextSeq 500 (300 cycle PE) at low-pass (mean target coverage of 1X), and then 10X for the cfDNA and s-pDNA, using four lanes in each sample with 4% PhiX to monitor sequencing performance. This amounted to 240 fastq files.

2-11 Bioinformatic analyses

WGS analysis was performed by Jeanne Inchauspé, Benjamin Schuster-Böeckler and Zohar Etzioni.

2-11.1 Data pre-processing

Quality control of all fastq files was conducted by running FastQC v0.11.8[278]. Reads were adaptor- and quality-trimmed using TrimGalore[279] v0.6.5 and aligned to the GATK Genome Reference Consortium Human Build 38 (GRCh38)[280] using bwa-mem v0.7.17[281].

Reads were aligned to alternate contigs to represent common complex variation using bwa_postalt.js (https://github.com/lh3/bwa/blob/master/bwakit/README.md)[281]. Resulting BAM files were merged, sorted and indexed with SAMtools v1.13.0[282].

GATK toolkit v4.1.7.0 was used to mark optical and PCR duplicates, estimate library complexity, and calculate summary metrics on insert sizes[283]. Mapping rate was evaluated with SAMtools flagstat and the number of reads mapped to each chromosome and the mitochondrial genome with idxstats. Repetitive elements in the ENCODE blacklist[284] were excluded using bedtools intersect v2.30.0[285].

2-11.2 Insert size distribution

For all uniquely mapped, non-duplicated and properly paired read pairs, the frequency of insert size values was counted across all autosomes and chrX using RSAMtools. The distributions were plotted using ggplot2[286].

2-11.3 Peak quantification

A chi-square test of independence was performed in R with a simulated p-value to examine the relation between DNA type (cfDNA and s-pDNA) and the proportion of di-nucleosomal fragments. We separated the fragments into (i) fragments below 250 bp representing mono-nucleosomal fragments; and (ii) fragments above 250 bp representing di-nucleosomal fragments. The proportion of di-nucleosomal fragments was significantly higher in s-pDNA than in cfDNA ($p < 0.0005$) in all samples.

2-11.4 Coverage plotting

Coverage was calculated using SAMtools bedcov, using a bed file of 10 kb non-overlapping windows for all main chromosomes, but excluding reads with mapQ <1. Position with mappability (as defined by umap: https://bismap.hoffmanlab.org/) in the lowest 8 percentile were removed[287]. The Coverage was then corrected for mappability and GC content bias using a linear regression model and visualized with karyoplotR[288] (Gel B, Serra E, 2017).

2-11.5 Gini index

After filtering for reads that are first in pair, uniquely mapped, mapped in proper pair, primary alignments, and non-duplicates, (SAMtools view parameters: -f 2 -F 3972 -q 1), we calculated the coverage with SAMtools depth. Evenness of coverage was evaluated by calculating the Gini index[289] on the short pDNA and cfDNA's coverage, which was previously binned into adjacent 10 kb bins.

2-11.6 Read depth around transcription start sites

Transcription start sites were defined by refTSS v3.3[290]. We used the nearest refTSS entry to the 5' coding sequence of all protein coding genes. Coverage per base in a 2 kb region around each TSS was extracted with RSAMtools, counting only uniquely mapped, non-duplicate, correctly paired reads with insert sizes between 150 and 170 bp ("mono-nucleosome") or between 280 and 350 ("di-nucleosome"). PBMC gene expression values were taken from Blueprint Epigenome experiment EGAX00001327129 (http://dcc.blueprint-epigenome.eu/#/experiments/ERX1123729). Briefly, genes with posterior mean estimates of transcripts per million > 15 were defined as "highly expressed" in PBMC.

2-11.7 ichorCNA

Copy number alterations in the 10X and low-pass WGS were evaluated using ichorCNA v0.2.0[291] (github: https://github.com/broadinstitute/ichorCNA/releases/tag/v0.2.0).

2-11.8 Targeted mutational analysis

i) Tumour tissue DNA sequencing and analysis

DNA extraction from tumour and healthy tissue, as well as library preparation for Novogene sequencing was carried out by Aleksandra Dzhoneva, a postdoctoral scientist from the Centre for Immuno-Oncology. DNA from resected tumour tissue and adjacent tumour-free colonic mucosa was extracted using the Monarch Genomic DNA Purification Kit (Monarch, cat # T3010S). For sequencing, gDNA was prepared as follows: 500 ng per sample at a concentration of 25 ng/µl. The tumour samples were sequenced at 75X and the normal samples at 30X by Novogene UK Ltd. The complete NextFlow pipeline for processing sequencing output to mutation calls is provided in the Zenodo code repository. Briefly, reads were trimmed using TrimGalore (v0.6.5), requiring >= 2 bp adapter overlap and quality-trimming bases with Phred score below 20, and aligned against the complete hg38 genome, including alt alleles, using bwa-mem2 using default parameters. Mutations were called independently using Mutect2 (v4.1.7.0), Strelka (v2.9.10) and Octopus (v0.7.0). Mutations called by only one caller were excluded.

ii) Estimation of observed and expected tumour fragments

99 sets of random single-base mutations, each matching the unique mutation count identified in the tumour tissue of patient CRC_012, were generated by sampling from all SNVs detected in any WGS-sequenced colorectal cancer from TCGA. Any SNV overlapping a SNP (dbSNP v155) with > 0.5% allele frequency in 1000Genomes, HapMap, dbGaP_PopFreq, GnomAD_exomes, TOPMED or GnomAD were excluded, as well as variants identified as SNPs in the non-cancer control sample for patient CRC_012. Together with the original CRC_12 mutation set, this amounted to 100 mutation sets. For each set, reads covering the mutation positions were extracted, excluding improperly paired reads or reads with mapQ < 25. Detection rate was then calculated by dividing the count of reads containing the variant allele (min base quality: 10) by the total number of reads covering the mutation sites. Positions that exhibited an allele fraction of >20% in plasma or platelet derived DNA were excluded as potential SNPs. The likelihood of observing a detection rate as high or higher than that of CRC_012 tissue mutations in that patient's plasma and platelet-derived DNA was calculated using a normal distribution parameterised to the observed mean and standard deviation of detection rates for random mutation sets. Code and intermediate files are deposited in the publication's Zenodo repository.

2-11.9 Data availability

Raw whole genome sequencing data has been deposited in the European Genome-phenome Archive (EGA) under accession number EGAS00001006854 (Study: EGA00001006854; Dataset EGAD00001009856; Data Access Committee: EGAC00001003034).

2-11.10 Code availability

Code used in these studies is available from Zenodo under the DOI 10.5281/zenodo.7412109.

2-11.11 Statistical analysis

Parametric tests, such as the paired t-test, were performed for comparisons within the same group when the data visually appeared to follow a normal distribution. Nonparametric tests, such as the Wilcoxon

signed-rank test, were used for paired data that did not follow a normal distribution. For comparisons between different groups, the Mann-Whitney U test was used to determine statistical significance.

Chapter 3: Platelets contain DNA

3-1 Introduction

In this chapter, I explore whether platelets contain DNA.

3-1.1 Indications that platelets may contain DNA

Although prior studies of platelet nucleic acid content have focused on RNA, the presence of DNA in platelets has been indirectly shown by other groups[104,125,292,293]. For instance, in a study conducted by Frydman, G. H. *et al.*, it was revealed that while neutrophils were traditionally believed to be the primary contributors of circulating histones during sepsis, extranuclear histones are also present in megakaryocytes and platelets. Further examination of the histone proteins in these platelets showed that despite being anucleate, 5 - 35% of platelets were positive for the DNA-specific marker DRAQ5[292].

A study by Thon *et al.*, indicated that platelets can sequester bacterial/viral DNA fragments[53]. Similarly, immunofluorescence staining of blood samples taken from influenza infected patients, revealed the presence of DNA-platelet aggregates, with some platelets having a distinct DNA content at their centre[104]. The same group also published data demonstrating platelet uptake and digestion of pine tree pollen DNA following *in vitro* incubation[294]. These observations prompted Koupenova, M *et al.*, to speculate about a potential yet undiscovered role for platelets in the clearance of exogenous nucleic acids encountered during circulation.

3-1.2 Platelets express nucleic acid sensing receptors

As highlighted in chapter 1, platelets play a significant role in inflammation and immunity. Supported by emerging evidence, there is a growing opinion that platelets should also be recognised as immune cells. For instance, like professional immune cells, platelets express numerous pattern recognition receptors (PRRs), that mediate their interaction with viral particles, bacteria and pathogen derived nucleic acids[84,120]. The following section outlines two DNA sensing receptors expressed by platelets.

i) Toll-Like Receptor 9

Toll-like receptors (TLRs) are a group of 10 transmembrane PRRs that are responsible for recognising molecules commonly found on pathogens, known as pathogen-associated molecular patterns (PAMPs). TLRs are typically expressed on the surface of immune cells such as neutrophils, macrophages, and dendritic cells, but are also found in endosomes where they recognise and bind intracellular nucleic acids. Human platelets express all 10 TLRs, although expression levels vary[83].

TLR9 is a specific example of a Toll-Like receptor that primarily senses nucleic acids. Its primary ligand is unmethylated CpG sequences present in bacterial and viral DNA. In nucleated cells, TLR9 is mainly located in the endoplasmic reticulum (ER) and requires endosome shuttling to the nucleic acid containing structures such as endosomes, lysosomes and endolysosomes[53,83,295]. Here, TLR9 binds with captured CpG DNA which results in its activation and initiation of the MyD88- dependent signalling cascade, leading to NF-κB mediated transcription of proinflammatory factors and cytokines[296,297].

As well as CpG DNA, recent research has shown that TLR9 in red blood cells, dendritic cells, and colorectal tumour cells can engage with other species of DNA including free foetal DNA[94], mitochondrial DNA[298], and tumour-derived DNA[14,15]. Unlike the majority of the mammalian genome, these DNA species are rich in unmethylated CpG motifs.

TLR9 has also been shown to bind cfDNA[299] and has been implicated in numerous autoimmune and inflammatory disorders. In these conditions, elevated levels of self-DNA cause dysregulated activation

of TLR9, subsequently triggering the production of pro-inflammatory cytokines. For example, DNA binding to TLR9 in macrophages has been associated with insulin resistance[300], while its binding to TLR9 in plasmacytoid dendritic cells (PDCs) has been linked to systemic lupus erythematosus (SLE)[301].

The mechanism by which exogenous DNA enters platelets and engages TLR9 remains unclear. Unlike nucleated cells, platelet TLR9 is localised in T-granules within the cytosol[53]. The specific signalling pathways activated upon DNA binding to platelet TLR9 are also not fully understood. However, it is known that platelet TLR9 binding to proteins associated with oxidative stress leads to the recruitment of MyD88 and activation of interleukin-1 receptor-associated kinase 1 (IRAK1)[302]. This process subsequently triggers PI3K/AKT and Src kinase activation[302,303], two signalling pathways involved in platelet activation and aggregation.

Despite being primarily localised to T-granules, research by Thon *et al.,* suggests that upon platelet activation with thrombotic agonists or exposure to synthetic DNA, some TLR9 relocates from intracellular vesicles to the platelet surface[53]. They observed that increased surface expression of TLR9 following activation led to enhanced capture and internalisation of CpG DNA. Their studies using TLR9 knockout (KO) mice corroborated this and showed reduced levels of oligonucleotide sequestration. However, TLR9 KO mice still exhibited some platelet aggregation in response to CpG DNA and retained some acute inflammatory responses to certain stimuli, albeit significantly decreased. This suggests that while TLR9 plays a significant role in platelet CpG DNA sequestration, there is likely at least one yet uncharacterised platelet surface receptor that also facilitates DNA uptake[53,83].

ii) Receptor for Advanced Glycation End products

Another DNA sensing receptor platelets express is the surface receptor for advanced glycation end products (RAGE) and like TLR9, expression of RAGE increases upon platelet activation[304,305,306,307]. RAGE binds a variety of ligands including mRNA, DNA and High Mobility Group B1 (HMGB1).

HMGB1 is a DNA binding protein that readily forms complexes with DNA. HMGB1 can be released passively from necrotic cells or actively secreted[308], including from platelets[309-312]. HMGB1 serves dual

roles, participating in various intracellular DNA-related processes such as transcriptional regulation, while also acting as an inflammatory cytokine outside of cells, recognised as a damage associated molecular pattern. Several studies have also demonstrated that when HMGB1-DNA complexes engage with the RAGE receptor, for example on the surface of PDCs, they are internalised into the cytosol via dynamin- dependent endocytosis[296], where they then interact with, and signal through intracellular TLRs such as TLR9[313-315].

Overall, despite the initial assumption that TLR9 was only expressed by immune cells, TLR9 has now been identified in platelets. While it was originally thought to exclusively bind endocytosed microbial DNA, TLR9 has demonstrated the ability to engage with circulating mammalian DNA, cfDNA and tumour-derived DNA. Given that platelets also express the RAGE receptor and actively secrete the DNA-binding protein, HMGB1, they seem well equipped to sense and bind extracellular DNA. Based on these observations, Figure 3.1 illustrates a hypothetical model depicting the process of DNA sensing and internalisation by platelets.

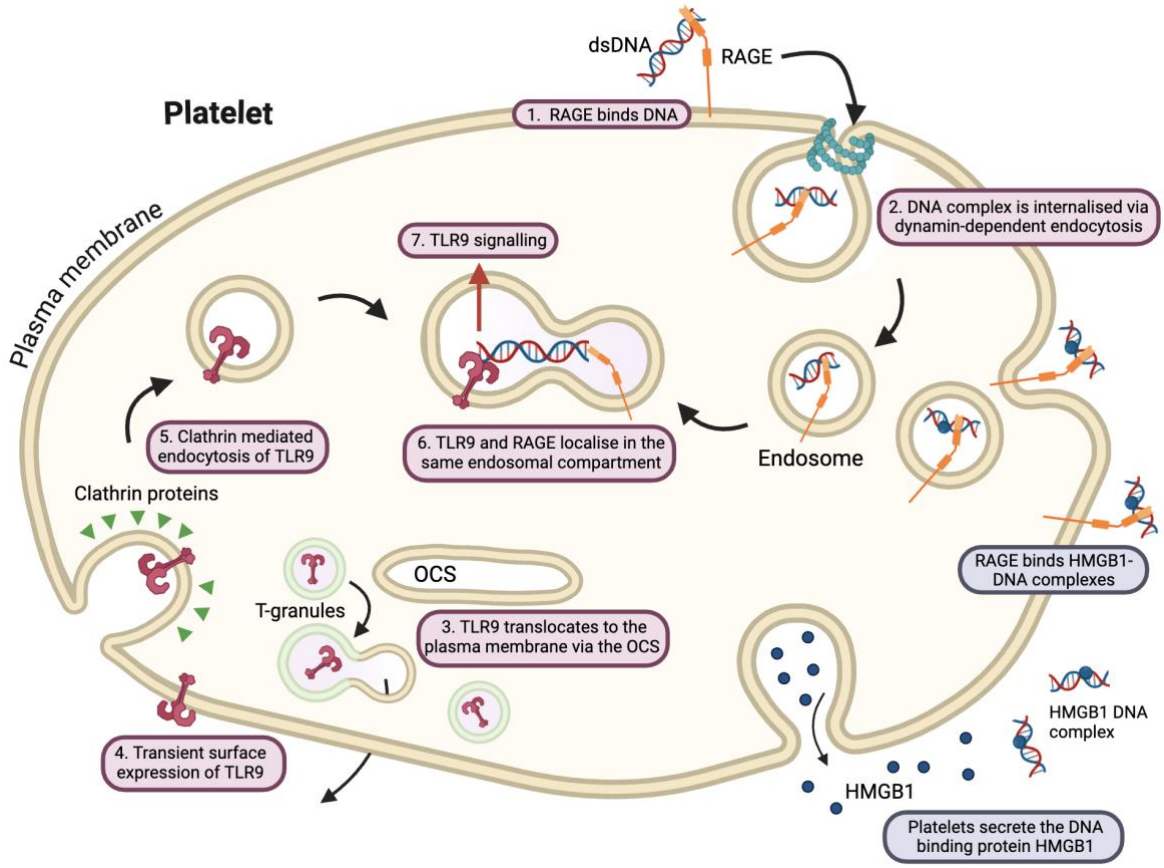


Figure 3-1. Hypothetical role for platelet RAGE and TLR9 in DNA sensing and internalisation based on published literature. 1) Platelets express the surface receptor RAGE which facilitates the binding of extracellular DNA either independently or when complexed with HMGB1. 2) Subsequently, the RAGE-DNA complex undergoes internalisation through dynamin-mediated endocytosis, where it is encapsulated within endosomal compartments. 3) TLR9, stored in T-granules is released through fusion with the open canalicular system (OCS). 4-5) Upon release, TLR9 relocates to the plasma membrane where it exhibits transient expression before undergoing re-internalisation via clathrin-mediated endocytosis. 6) Eventually, RAGE and TLR9 converge within the same endosomal compartment, facilitating the binding of TLR9 to DNA and 7) triggering TLR9 signalling. Created using Biorender.com.

3-1.3 Anucleate red blood cells bind DNA via Toll-Like Receptor 9

Red blood cells, followed by platelets, are the most abundant cell type in circulation. Like platelets, red blood cells are anucleate and have long been considered immunologically inert. However, in line with evolving platelet biology, the assumption that red blood cells are limited to their primary role in gas exchange, is changing. In 2018, Hotz *et al.,* demonstrated that red blood cells bind mitochondrial DNA (mtDNA) and suggest that DNA scavenging by red blood cells mitigates against lung injury[316]. The group speculated that because excess circulating DNA is harmful, red blood cells bind DNA to regulate lung inflammation during disease[316]. In 2021, the same group demonstrated that red blood cells bind DNA through the surface expression of the nucleic acid-sensing receptor TLR9. In addition to mtDNA, red blood cells use TLR9 to bind CpG-containing DNA from bacteria and parasites. This binding triggers erythrophagocytosis (clearance of red blood cells) and activates innate immune responses[298]. Building on their previous hypothesis, the group suggest that red blood cells play a protective role in scavenging harmful DNA that has escaped routine clearance. Later findings confirmed this hypothesis when in 2024, the group revealed that tumour derived DNA is detectable in the red blood cells of patients with early-stage lung cancer[317].

These exciting observations, coupled with my understanding that platelets also express nucleic acid receptors such as TLR9, led me to hypothesise that platelets may play a previously undescribed role in the clearance of cfDNA from circulation.

3-1.4 Hypothesis and aims

Given platelets' expression of nucleic acid sensing receptors and their ability to sequester various molecules, including proteins, RNA, and vesicles, I hypothesised that platelets also sequester cfDNA from the plasma. Overall, I sought to evaluate whether, despite lacking a nucleus, platelets contain a significant content of DNA, and whether this was in part, acquired during peripheral circulation.

The specific sub-aims for this section of my thesis were:

Aim 1.1 To confirm whether, irrespective of platelet preparation or source, platelets contain genomic DNA

Aim 1.2 To investigate potential correlations between DNA uptake, platelet activation and age

Aim 1.3 To determine the origin of platelet DNA (megakaryocyte derived vs. sequestered from the plasma)

To achieve these aims I first used immunofluorescence microscopy and flow cytometry to confirm DNA staining of platelets and characterise the abundance and phenotype of DNA-containing platelets. Following this, I investigated platelet DNA content in a larger cohort by isolating platelets from the peripheral blood of 76 patients. This included mothers carrying male babies, allowing me to confirm the presence of sequestered foetal DNA to robustly distinguish between DNA passed on to platelets from parent megakaryocytes vs. that sequestered during peripheral circulation. Finally, I used a mouse model of immune thrombocytopenia to correlate platelet number with plasma cfDNA concentration.

3-2 Results

3-2.1 Healthy donor platelets associate with DNA

To determine whether DNA was detectable within platelets isolated from the peripheral blood of human donors, platelets were purified by multiple different methods: (Fig. 3-2A) sequential centrifugation of peripheral blood samples collected in EDTA or Cell-Free DNA blood collection tubes; (Fig. 3-2B) centrifugation of clinical-grade healthy donor plateletpheresis concentrates, and (Fig. 3-2C) fluorescence-activated cell sorting (FACS) of whole blood collected into EDTA blood tubes.

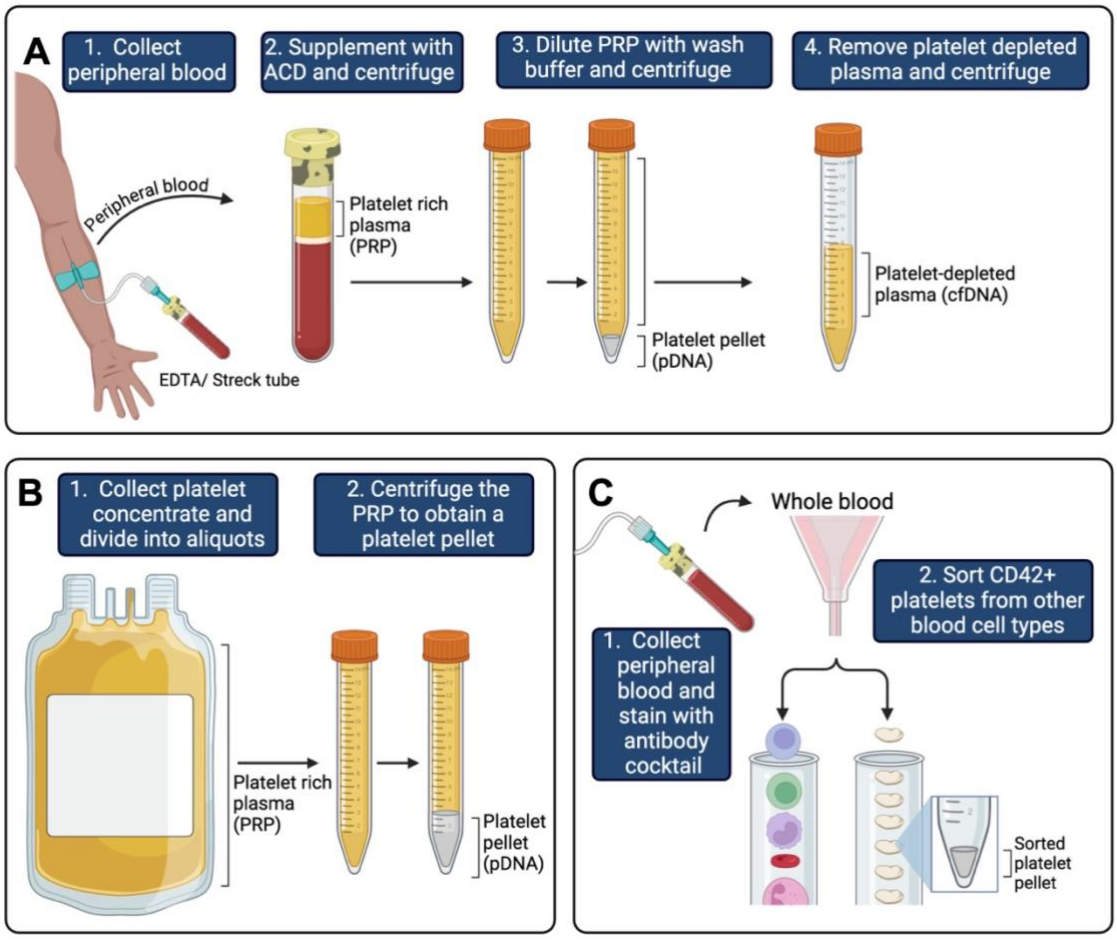


Figure 3-2. Schematic showing sources of purified platelets. (A) sequential centrifugation of peripheral blood to simultaneously extract DNA from platelet pellet (pDNA) and platelet-depleted plasma (cfDNA). **(B)** Centrifugation of healthy donor plateletpheresis concentrates to obtain a platelet pellet. **(C)** Fluorescence-activated cell sorting (FACS) of whole blood. Created using Biorender.com.

i) Platelets from peripheral blood

I first investigated the DNA content of platelets pelleted from peripheral blood of healthy donors. As this would be my primary method of platelet isolation, I confirmed high purity of the platelet pellets by flow cytometry analysis and cytospin preparations (Fig. 3-3A & B). Flow cytometry data analysis showed that contamination of nuclear cells within the isolated platelet population was 0.0033% (12 cells per 365,454 platelets) while myeloid cell contamination was calculated at 0.0022% (8 cells per 365,454 platelets). Cytospin preparations also confirmed minimal leukocyte contamination in the isolated platelet population.

After confirming that the isolation process yielded a high quantity of platelets with minimal contamination, I investigated whether DNA could be extracted from platelet pellets in a larger cohort of human donors, and its relative abundance compared to that extracted from platelet-depleted plasma (i.e. cfDNA). DNA was obtained from both the platelet pellet and platelet-depleted plasma (cfDNA) from the peripheral blood of 76 patients. This cohort comprised of individuals undergoing colonoscopy screening for cancer surveillance or inflammatory bowel disease (n = 48), and patients with known gastrointestinal cancers (n = 28), including colorectal [CRC], oesophageal and pancreatic cancer (Appendix Data Tables A7-A9).

DNA was obtained from the platelets and plasma in all cases, with a median abundance of 7.18 genomic copies per µl of plasma, or approximately 0.000012 genomic equivalents per platelet (Fig. 3-3C). This was higher than the abundance of cfDNA at 2.372 genomic copies per µl of plasma.

Using the optimised platelet isolation protocol (section 2-2.1), I next examined platelet DNA by fluorescence microscopy. I isolated healthy donor platelets and labelled them using NUCLEAR-ID Red DNA, a highly specific, cell permeable dye that only intercalates with double stranded DNA. A subpopulation of platelets identified by their positivity for the platelet cell surface integrin CD42 showed a clear fluorescent signal for the DNA probe (Fig. 3-3D).

Given the sensitivity of platelets to external factors, and their readiness to form aggregates and sequester plasma content, I wanted to be certain that the DNA detected in/on the platelets was a natural occurrence and not due to the isolation protocol itself. To exclude the possibility of platelets taking up or associating with DNA during centrifugation or isolation, I performed imaging of platelets in a peripheral blood film made from whole fresh blood (i.e. unmanipulated). The platelets shown in Figure 3-3E, show clear staining for the DNA marker Hoechst, confirming that platelets associate with DNA *in vivo* and are therefore not reliant on the addition of buffers, changes in pH or multiple rounds of centrifugation to bind to/ sequester DNA fragments.

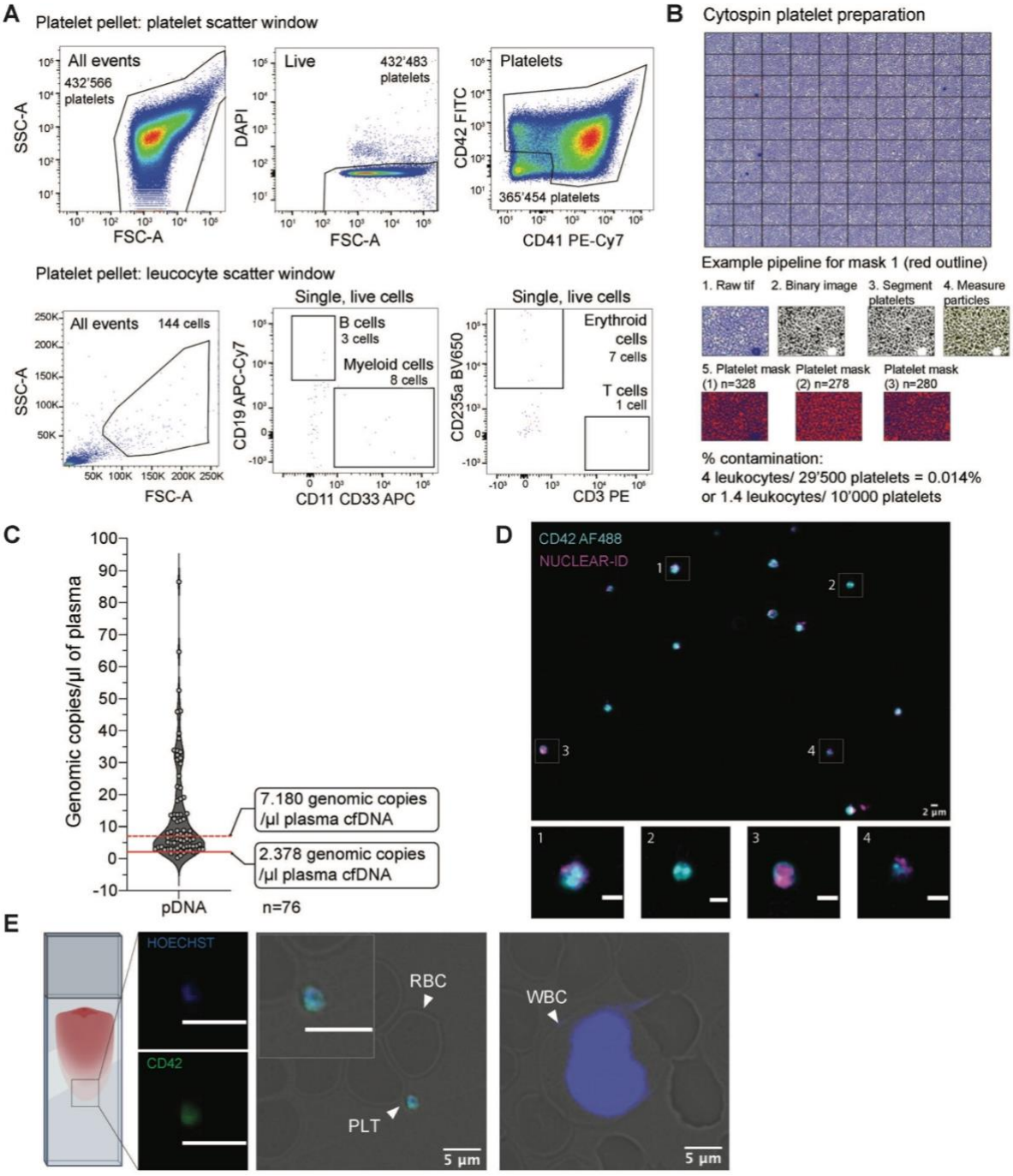


Figure 3-3. Detection of DNA from peripheral blood. (A) Flow cytometry analysis for contamination of the isolated platelet population with erythroid, myeloid, and lymphoid cells. **(B)** Cytospin with Wright-Giemsa stain and quantification of leukocyte contamination in a representative platelet pellet. **(C)** Violin plot showing yield of DNA isolated from platelet pellets and platelet-depleted plasma, calculated as genomic equivalents detected per microliter (µl) of plasma. Dashed line indicates median yield of DNA from platelet pellets (7.18 genomic copies per µl of platelet-rich plasma), solid line indicates median yield of DNA (2.378 genomic copies/µl plasma) for paired platelet-depleted plasma (cfDNA) (cohort size n=76). **(D)** Healthy donor-derived platelets identified by CD42 488 (cyan) show an internal fluorescent signal for NUCLEAR-ID, a cell permeable dye that intercalates with double stranded DNA (magenta). White boxes show magnified regions, scale bars represent 2 µm. **(E)** Peripheral blood film from a healthy human donor. Platelets, identified by CD42 AF488 (green), show a fluorescent signal for the DNA stain Hoechst (blue). Red cells (RBC) and white cells (WBC) also

indicated. White box shows magnified region, scale bars represent 5 μm, representative image of 5 experiments shown. Imaged using a Leica SPE. Created using Biorender.com.

ii) Plateletpheresis and fluorescently sorted platelets

Although isolating platelets via the sequential centrifugation of peripheral blood yielded a high purity of platelets, I wanted to confirm that the DNA observed in the platelets represented nuclear DNA. To do this, I improved platelet purity further and extracted DNA from clinical-grade healthy donor plateletpheresis concentrates and platelets sorted from whole blood using fluorescence-activated cell sorting (FACS). Details of the sorting strategy are described in the Materials and Methods (section 2-6.3).

As expected, extremely high purity of the plateletpheresis sample was confirmed using flow cytometry with a near-total absence of other blood cell types (Fig. 3-4A). Purity of the sorted platelets was also assessed by re-running an aliquot of the sample back through the BD FACSymphony™ S6 (Fig. 3-4B).

Sorter-induced cell stress (SICS) is a term used to describe the potential negative effects of sorting on cell viability and function[318]. Given platelets' sensitivity to external factors, susceptibility to rupture and therefore possible loss of sequestered DNA, I wanted to ensure their integrity during the sorting process. To verify this, sorted platelets were carefully collected onto slides and stained with CD42 AF488. Imaging of the slides confirmed that the sorted platelets remained intact (Fig. 3-4C).

Despite the absence of nucleated cells in both samples, I was still able to extract genomic DNA from both the plateletpheresis samples and sorted platelets, as demonstrated by the detection of genomic wild-type *TP53* alleles by ddPCR (Fig. 3-4D & E).

Next, I was interested to understand the size distribution of the DNA I was isolating from the plateletpheresis samples. Fragmentomic analysis revealed multiple lengths of platelet DNA per sample, with peaks at ~160 bp and > 600 bp (Fig. 3-4F).

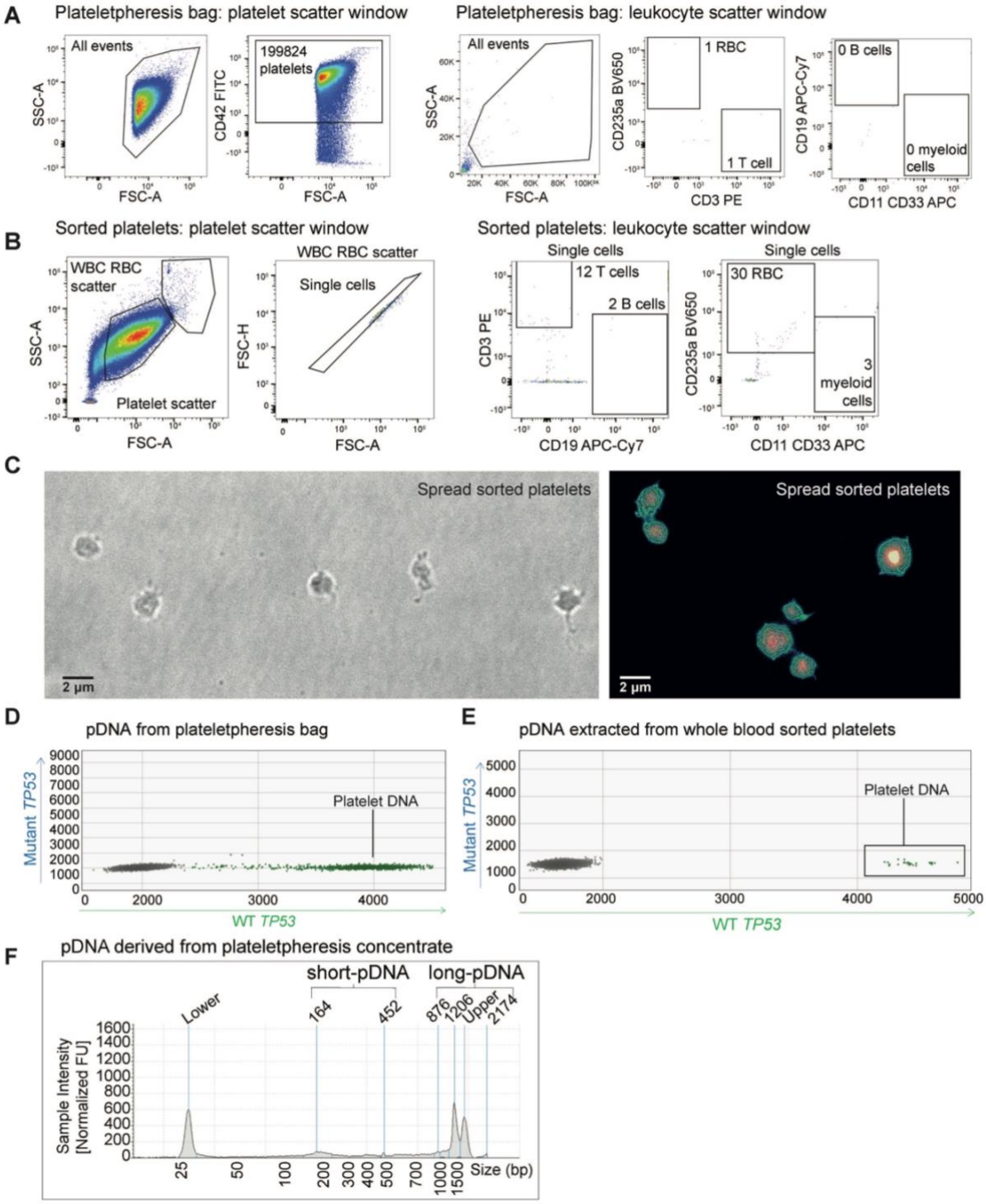


Figure 3-4. DNA extraction from plateletpheresis samples and platelets sorted from whole blood. **(A-B)** Flow cytometric analysis confirms very high platelet purity with near-total absence of other blood cell types. Plots show platelet and leukocyte scatter windows from the analysis of representative plateletpheresis **(A)** and sorted platelet samples **(B)**. Plots are annotated with cell counts. **(C)** Platelets maintain their structural integrity following sorting from whole blood. The left image depicts transmitted light, while the right utilizes CD42 AF88 fluorescence, pseudo-coloured with a Lookup Table (LUT) to enhance the visibility of platelet outlines. Scale bars are approximate. **(D-E)** Detection of WT *TP53* gene copies by ddPCR of DNA extracted from **(D)** platelets isolated from healthy donor

plateletpheresis concentrates and **(E)** 20.7 x10^6 whole blood sorted, CD42+ platelets following rigorous gating to exclude contaminating nucleated blood cell types and erythrocytes. **(F)** Representative electrophoresis of platelet DNA extracted from a plateletpheresis sample showing a peak at ~160 bp as well as larger DNA fragments.

3-2.2 Assessment of DNA associated platelets using flow cytometry

i) Labelling of platelet DNA with DRAQ5

After confirming that platelets associate with DNA during circulation, my next step was to quantify this population using flow cytometry. I isolated platelets from 20 healthy donors and labelled them with the platelet marker CD42, as well as the nucleic acid stain DRAQ5 (Fig. 3-5A). As an additional negative control and to confirm that DRAQ5 binding was specific to platelet DNA, I also incubated MACS compensation beads with DRAQ5 (Fig. 3-5B). I identified platelets using their unique size, scatter and CD42 expression and then set the DRAQ5+ gate based on autofluorescence from the MACS compensation beads and unstained platelets. The majority of platelets showed low-level DRAQ5 positivity, while ~8% were strongly positive.

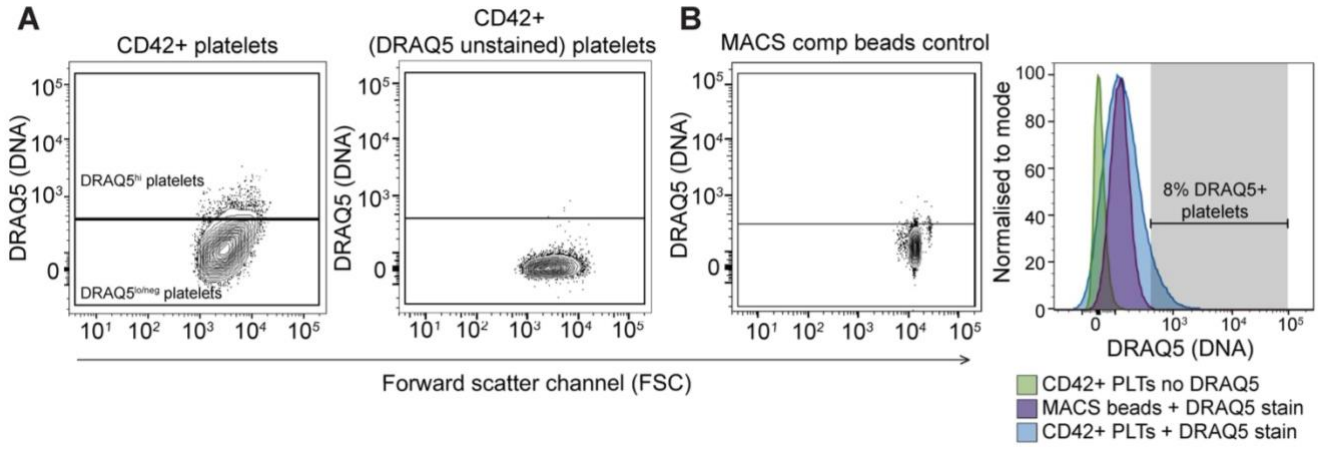


Figure 3-5. Detection of DNA in circulating platelets using DRAQ5. (A) Flow cytometric analysis of CD42+ healthy donor-derived platelets stained with/without the DNA marker DRAQ5. Left, ~8% of circulating platelets stain strongly positive for DRAQ5. Plots are a concatenation of healthy donors: CD42+ DRAQ5+ n=20, CD42+ DRAQ5- n=10. **(B)** Flow cytometric analysis of MACS compensation beads stained with DRAQ5 to adjust for possible non-specific binding of DRAQ5. Right, thresholding to determine strongly DRAQ5+ platelets.

ii) Labelling of platelet RNA with Syto-13

Next, I asked whether there was a correlation between DNA content (DRAQ5+) and RNA content of platelets, using Syto-13 to label RNA. I found that ~75% of DRAQ5^{hi} platelets were negative for RNA.

However, approximately a quarter (24.3%) of the DRAQ5^{hi} platelets had a high RNA content, compared to less than 10% of the DRAQ5$^{lo/neg}$ platelets (Fig. 3-6A). As platelets receive most of their RNA from parent megakaryocytes and their RNA content declines with time after platelet biogenesis, Syto-13 positivity is often used to distinguish 'young' and 'old' platelets[56-58]. This therefore implies that newly produced platelets also have a higher DNA content and that some of the DNA content may derive from parent megakaryocytes. However, the majority of DRAQ5^{hi} platelets were low or negative for RNA (Fig. 3-6A), meaning that DNA is also present in 'older' platelets that have been in circulation for several days. Is this because platelets supplement themselves with plasma cfDNA as they circulate?

iii) DNA containing platelets show increased expression of activation markers

Further analysis of the DRAQ5^{hi} platelets' immunophenotype revealed significantly higher expression of activation markers such as P-selectin and CD63 compared to DRAQ5$^{lo/neg}$ platelets (Fig. 3-6B). Additionally, the DRAQ5^{hi} platelets appeared slightly larger and more granular than the DRAQ5$^{lo/neg}$ platelets (Fig. 3-6C). These findings support the previous data indicating that the DNA-positive platelets are younger, larger and more active.

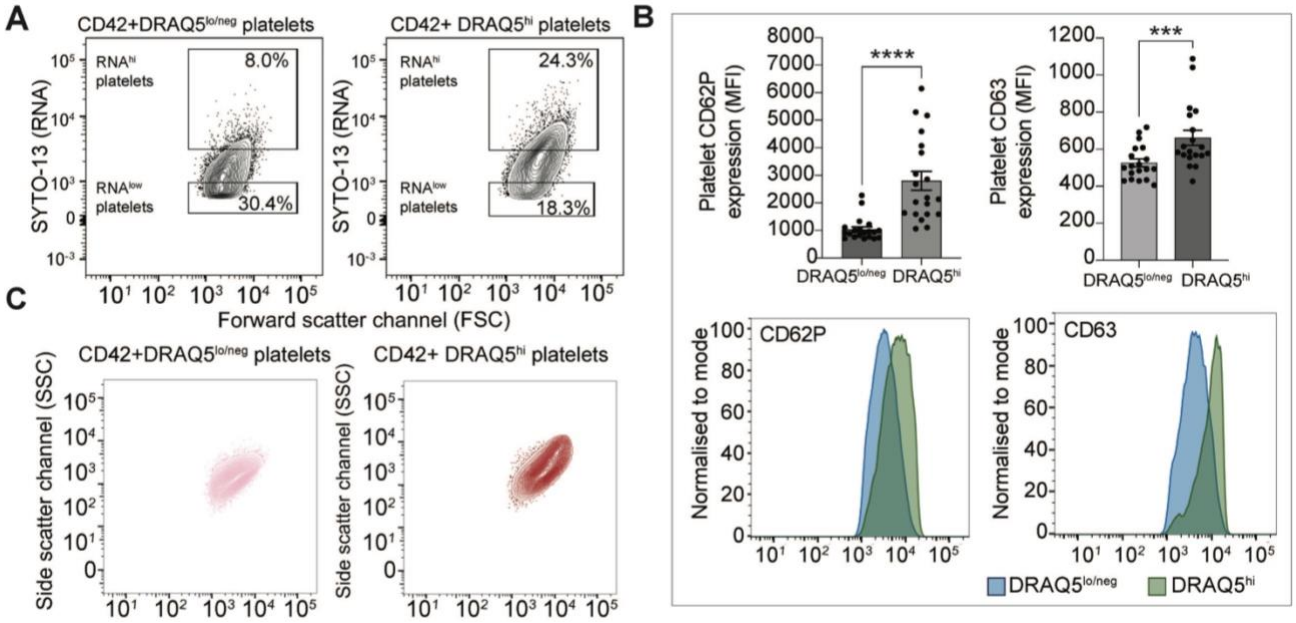


Figure 3-6. DNA containing platelets are younger and more activated. (A) Flow cytometric analysis quantifying RNA content (Syto-13 positivity) of CD42+, DRAQ5^{hi} and DRAQ5$^{lo/neg}$ platelets. Plots are a concatenation of 10 healthy donors. **(B)** Platelets with a higher DNA content (DRAQ5^{hi}) showed higher levels of activation as determined by P-selectin (CD62P) and CD63 expression. Top- plots show mean ± SEM, *** $p<0.001$, **** $p< 0.0001$ for Wilcoxon paired signed rank test, n=20 healthy donors.

Below- histograms showing increased expression of activation markers in DRAQ5^{hi} platelets (green). **(C)** Flow cytometric analysis showing a small increase in the size and granularity of DRAQ5^{hi} platelets (red) compared to DRAQ5$^{lo/neg}$ platelets (pink). Plots are a concatenation of 20 healthy donors.

3-2.3 Platelets capture DNA during circulation

i) Maternal platelets sequester foetal DNA

To determine whether the DNA detected in platelets was captured during peripheral circulation or solely derived from parent megakaryocytes, I collected antenatal blood samples and looked for fragments of the Y-chromosome in the platelets of mothers carrying male babies (Appendix Data Table A11). Using a Y-chromosome fluorescence in-situ hybridization (FISH) probe and ddPCR, Y-chromosome fragments were visualized in the platelets of mothers carrying male babies (Fig. 3-7A & B, Appendix Video 1). In 100% (20/20) of samples, I correctly ascertained the sex of the foetus by the presence or absence of *SRY* alleles in maternal platelets using ddPCR (Fig. 3-7A & B). *SRY* remained detectable in platelets at 24 and 48 hours after delivery of the baby (Fig. 3-7C) and was not detected in mononuclear cells or red blood cells (Fig. 3-7B) from the same blood samples, indicating that free foetal DNA can exclusively be detected in maternal platelets and is not due to 'contaminating' cfDNA in the cell pellets. While some of the DNA found in platelets may originate from megakaryocytes, these observations suggest that not all of the DNA content in platelets is exclusively derived from the parent cell. Instead, it appears that platelets acquire DNA fragments during circulation.

ii) Rise in plasma cell free DNA after acute platelet depletion in healthy mice

Given the detection of extracellular foetal DNA associating with maternal platelets, I reasoned that the abundance of cell/platelet-free DNA in plasma would increase if the platelet count was reduced. To test this, in collaboration with Rong Li, a former postdoctoral researcher in Beth Psaila's group, I induced acute and specific depletion of platelets in mice by treatment with an anti-CD42b anti-platelet antibody. Consistent with my hypothesis, the induction of immune thrombocytopenia led to an acute rise in plasma cfDNA concentration, in contrast to the control group where platelet number and cfDNA concentration remained stable (Fig. 3-7D). While these data suggest a relationship between platelets

and plasma cfDNA, it is also possible that the anti-platelet antibody may be inducing a rise in cfDNA, potentially through inflammation or increased cell death.

iii) Increased plasma cell free DNA in patients with ITP

To further verify the relevance of this observation in the human setting, I next investigated plasma cfDNA concentration in patients with immune thrombocytopenic purpura (ITP). Similar to my findings with the mouse model, I found significantly higher concentrations of plasma cfDNA in patients with immune thrombocytopenic purpura (ITP) who had severely low platelet counts ($< 20 \times 10^9$/L), as compared to those with normal platelet counts (Fig. 3-7E, Appendix Data Table A12, * $p<0.05$, n=23).

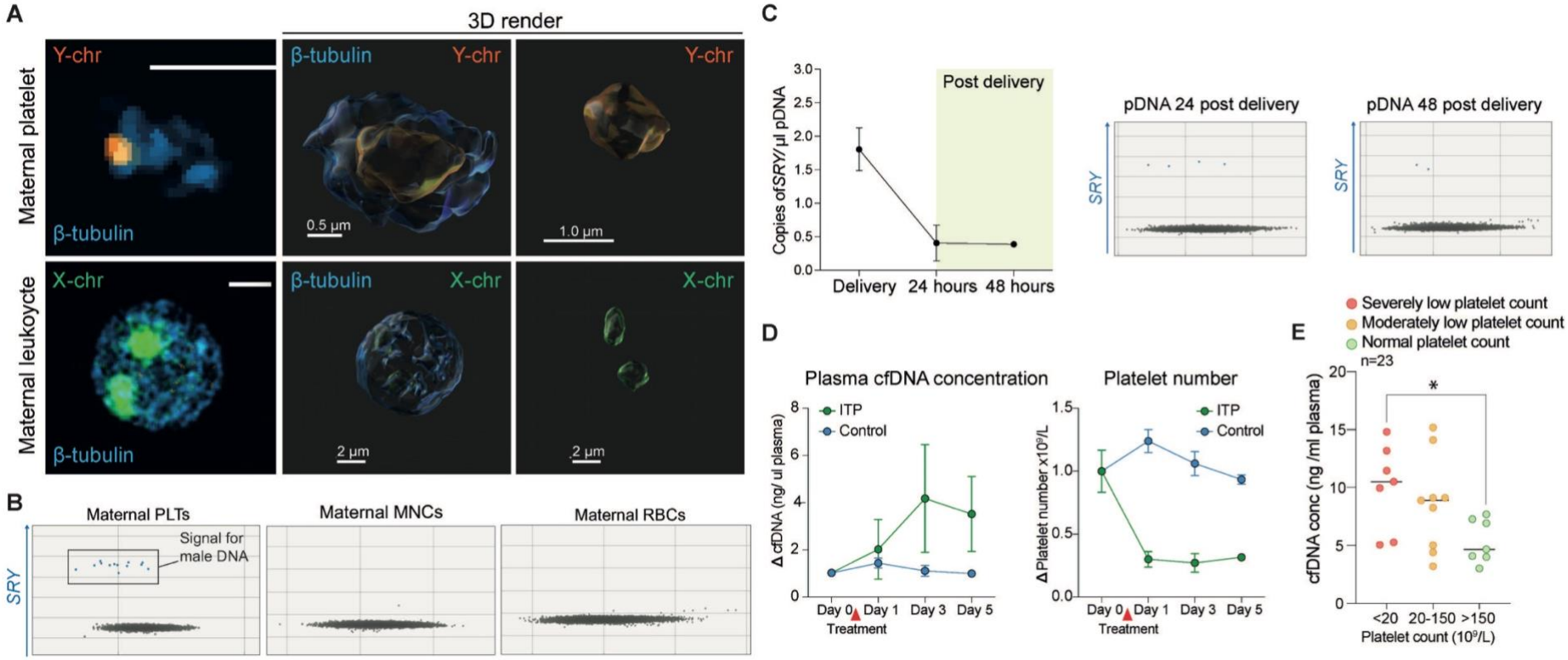


Figure 3-7. Platelets capture DNA during circulation. (A) Fluorescence in-situ hybridization chromosome paint showing detection of the Y-chromosome gene *SRY* in maternal platelets sampled from mothers of male neonates prior to delivery. Platelets and MNCs were counterstained with β-tubulin (blue) and imaged using the Airyscan detector of a ZEISS LSM900, 63X magnification. Representative images shown. **(B)** The Y-chromosome gene SRY was detected in maternal platelets but not maternal red blood cells (RBCs) or mononuclear cells (MNCs) using droplet digital PCR (ddPCR). **(C)** Detection of SRY gene copies by ddPCR of DNA isolated from maternal platelets 24 and 48 hours after caesarean section delivery of a male infant (at delivery: n=9, 24 hours after delivery: n=5 and 48 hours after delivery: n=2). Mean ± SEM shown. **(D)** Rise in cfDNA following acute depletion of platelets in healthy mice following administration of an anti-platelet antibody (n=20 for each isotype control and anti-platelet antibody group). Plots show mean ± SEM fold change at Day 1, 3 and 5 compared to baseline (Day 0, untreated mice). **(E)** Plasma cfDNA concentrations (ng/ml) for patients with immune thrombocytopenic purpura (ITP) and severely (< 20 $x10^9$/L) or moderately (20 – 150 $x10^9$/L) low platelet counts or counts in the normal range (> 150 $x10^9$/L) n=23, * $p<0.05$ for a Mann-Whitney test, plot shows individual data points with line at the median.

3-2.4 Platelets sequester DNA from nucleated cells

i) Platelet- tumour cell incubation

To confirm that platelets sequester chromosomal fragments released from nucleated cells, I used live cell imaging to visualize DNA uptake *in vitro*. Colorectal adenocarcinoma cells (COLO205) were labelled with cell-permeable, fluorescent DNA probes that intercalate with double stranded DNA (NUCLEAR ID and SiR-DNA). I washed the tumour cells twice to remove any non-internalised DNA stain prior to co-incubation with platelets. Acquisition of COLO205 cell-derived, (magenta) labelled DNA by platelets (cyan) was observed (Fig. 3-8A, Appendix Videos 2 & 3, Appendix Data Figure 1).

Uptake of chromosomal DNA released from nucleated cells by platelets was also confirmed using FISH probes. Fragments of both X- and Y-chromosomes were visualised at high resolution in a subfraction of female platelets following co-incubation with male HEL cells (Fig. 3-8B). For this imaging I used the Airyscan detector of a ZEISS LSM900 confocal microscope to generate a 3D reconstruction using Z stack acquisition.

Using the Spinning Disk Confocal microscope to image platelets in real time, I observed platelets physically interacting with the tumour cells and migrating along their outer membrane. CD42 staining of the platelets highlighted distinct filopodia extending towards the cancer cell (Fig. 3-8C, Appendix Video 4A and 4B). Over the 90-minute time course, platelets appear to actively "sample" from the colorectal tumour cells and acquire tumour-derived material (Fig. 3-8D, Appendix Video 4A and 4B).

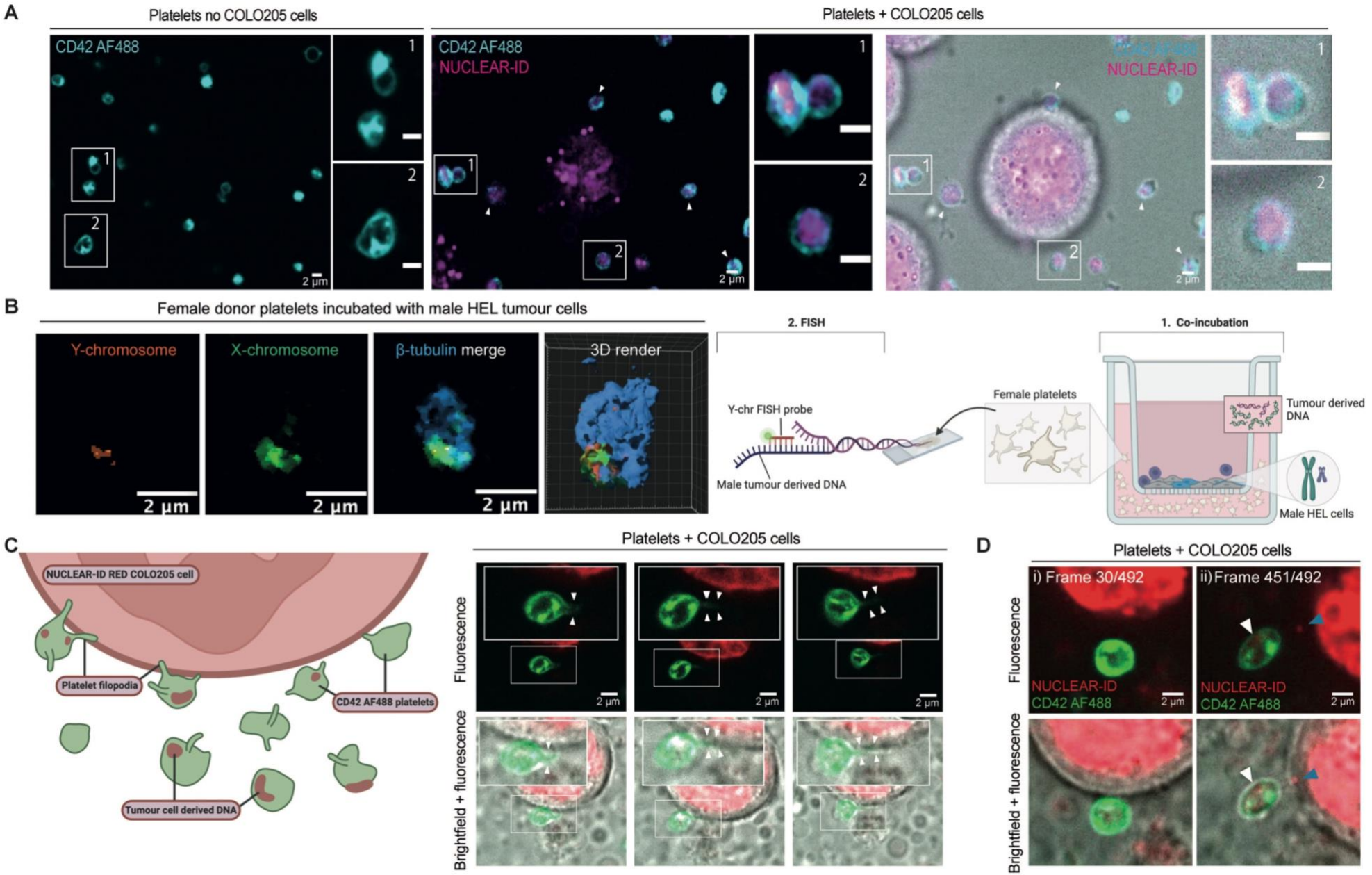

A
Platelets no COLO205 cells
Platelets + COLO205 cells
CD42 AF488
NUCLEAR-ID
2 µm
B
Female donor platelets incubated with male HEL tumour cells
Y-chromosome
X-chromosome
β-tubulin merge
3D render
2. FISH
Y-chr FISH probe
Male tumour derived DNA
Female platelets
1. Co-incubation
Tumour derived DNA
Male HEL cells
C
NUCLEAR-ID RED COLO205 cell
Platelet filopodia
CD42 AF488 platelets
Tumour cell derived DNA
Platelets + COLO205 cells
Fluorescence
Brightfield + fluorescence
D
Platelets + COLO205 cells
i) Frame 30/492
ii) Frame 451/492
NUCLEAR-ID
CD42 AF488

Figure 3-8. Platelet sequestration of DNA released from nucleated tumour cells. (A) Healthy donor-derived CD42 488 (cyan)-labelled platelets before (left) and after (middle and right) co-incubation with COLO205 cells labelled with NUCLEAR-ID, to enable tracking of DNA uptake (magenta). White arrows highlight platelet uptake of COLO205 DNA. Middle and right images are the same, with the brightfield view shown on the right to highlight membrane of COLO205 cells. Imaged using a Zeiss Spinning Disk Confocal with a 63X magnification. **(B)** Fluorescence in-situ hybridisation micrographs and 3D render (right) demonstrating fragments of X- and Y- chromosomes present in female donor platelets following exposure to male HEL cells. Platelets counterstained with β-tubulin (blue). Representative images shown. Imaged using the Airyscan function of a ZEISS LSM900, 63X magnification. **(C)** Left- schematic demonstrating observed platelet interaction with COLO205 cells. Right- healthy donor platelets (green) extend filopodia towards the COLO205 cell (red) as indicated by white arrows. Right-healthy donor platelets (green) extend filopodia towards the COLO205 cell (red). **(D)** The platelet interacting with the tumour cell in (C) acquires tumour derived DNA over the 90-minute time course as indicated by the white arrows. Blue arrows show a potential DNA containing vesicle within the cytosol of the tumour cell. i) frame 30/492 and ii) frame 451/492. Representative images shown. Imaged using a Zeiss Spinning Disk Confocal with a 63X magnification. All images were analysed using ImageJ and Imaris Viewer. Unlabelled scale bars represent 2 μm. Created using Biorender.com.

Circulating cfDNA typically consists of chromatin, which includes both DNA and histone components. Therefore, in addition to imaging platelets and tumour cells labelled with nucleic acid stains, I incubated platelets with genetically engineered HEL cells expressing exogenous mCherry-histones (Fig. 3-9A). This not only allowed me to visualise the uptake of tumour derived nucleosomes, but as the cells already contained fluorescently tagged histones, there was no need to stain with commercial dyes, thereby reducing the risk of unbound dye non-specifically labelling the platelets. Despite this, fluorescently tagged tumour derived histone proteins were observed co-localising with the platelets and co-staining with DAPI confirmed the presence of nucleosomes (Fig. 3-9B & C, Appendix Video 5).

ChIPmentation data generated from platelets by Jeanne Inchauspé, a DPhil student co-supervised by Jim Hughes and Beth Psaila, support the idea that platelets take up circulating nucleosomes. ChIPmentation is a technique that combines chromatin immunoprecipitation (ChIP) with tagmentation to study DNA-protein interactions (Fig 3-9D)[276]. The process involves lysing cells and incubating them with an antibody specific to a protein of interest, often a histone modification, to pull down nucleosomes; DNA wrapped around histone proteins. The immunoprecipitated DNA is then purified in a way that simultaneously fragments and tags it while still bound to the proteins. This tagged DNA is subsequently amplified and prepared for sequencing.

TapeStation analysis of DNA purified from immunoprecipitated proteins confirms that platelets internalise both nucleosomes and their associated DNA (Fig. 3-9E). Notably, DNA was still detected even when *only* chromatin associated proteins were targeted and pulled down, demonstrating its co-precipitation alongside the protein of interest. This finding is significant, as the absence of DNA peaks in the immunoprecipitated material would be expected if platelets exclusively sequestered nucleosome-free DNA fragments. Instead, the detection of DNA peaks strongly suggests that the DNA remains bound to histones when sequestered and stored within platelets.

Analysis of fragment coverage in DNA isolated from sequestered nucleosomes provides further support for these observations. Previous studies have shown that sequencing reads are typically depleted around transcriptional start sites (TSS), exhibiting a periodic pattern of coverage relative to these sites[319]. This distinctive coverage pattern is a result of nucleosome positioning and the protection it provides to cfDNA (Fig. 3-9F). In this experiment, nucleosomes were isolated through immunoprecipitation, and the Tn5 enzyme used to cleave accessible chromatin regions between nucleosomes. As a result, open chromatin sites were largely undetected, leading to a noticeable decrease in signal intensity, evidenced by a pronounced dip in fragment coverage at the TSS (Fig. 3-9G).

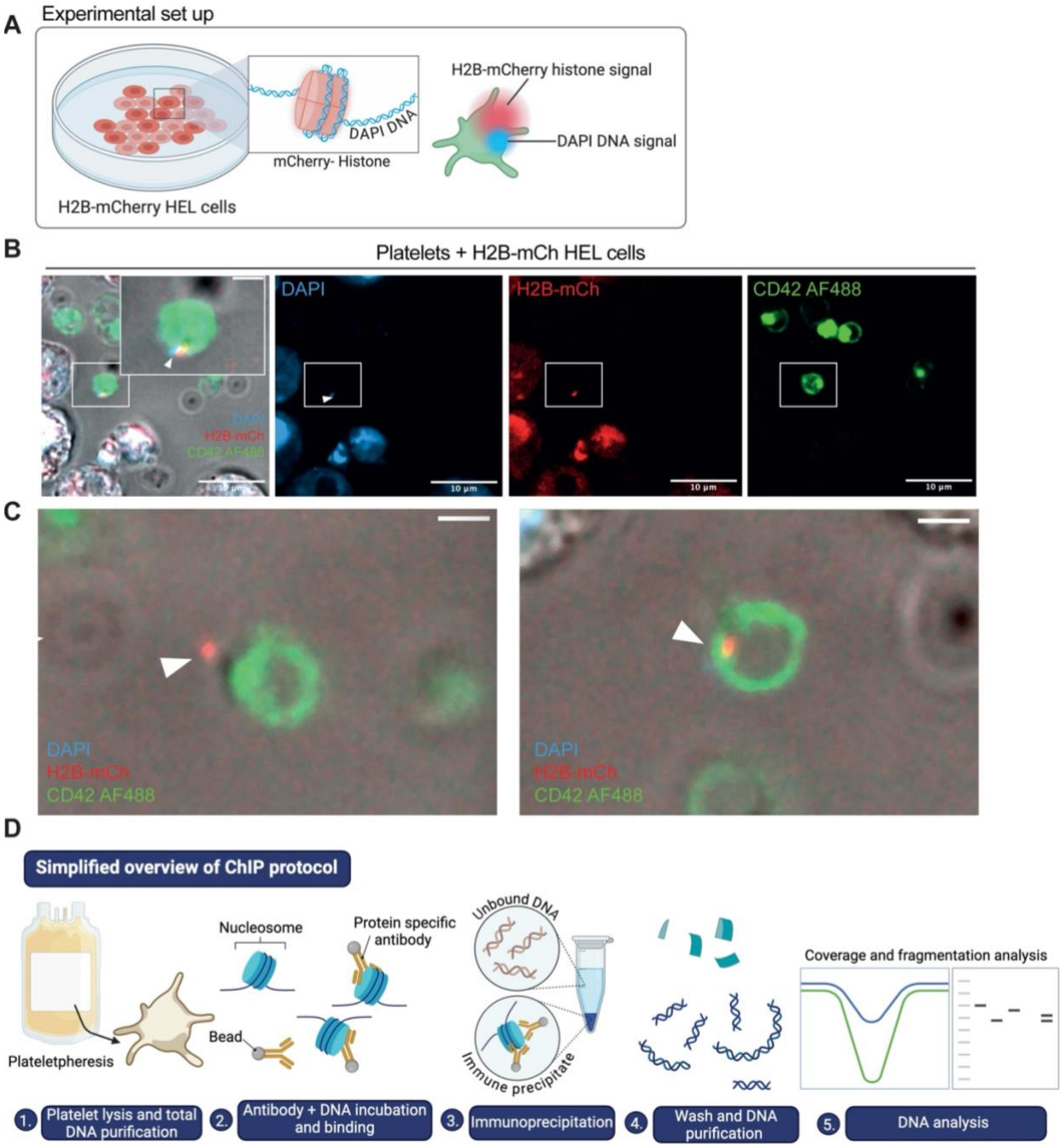


Figure 3-9 (1/2). Platelets sequester nucleosomes. (A) HEL cells are genetically engineered to express exogenous mCherry-histones (red). Platelets (green) are incubated with engineered HEL cells and sequester tumour derived histones (red) and DNA (blue). **(B)** A healthy donor platelet incubated with H2B-mChr HEL cells sequesters tumour derived histones and DNA as shown by the white arrows. Left to right, brightfield, DNA-DAPI, histone-mCherry, CD42 AF88. **(C)** Additional frames of the same platelet acquiring HEL derived histones. For all images, white boxes show magnified regions and unless otherwise stated, scale bars represent 2 µm. Imaged using a Zeiss Spinning Disk Confocal with a 63X magnification. **(D)** Schematic outlining the main steps of platelet chromatin immunoprecipitation. Created using Biorender.com. *Figure continued on the next page.*

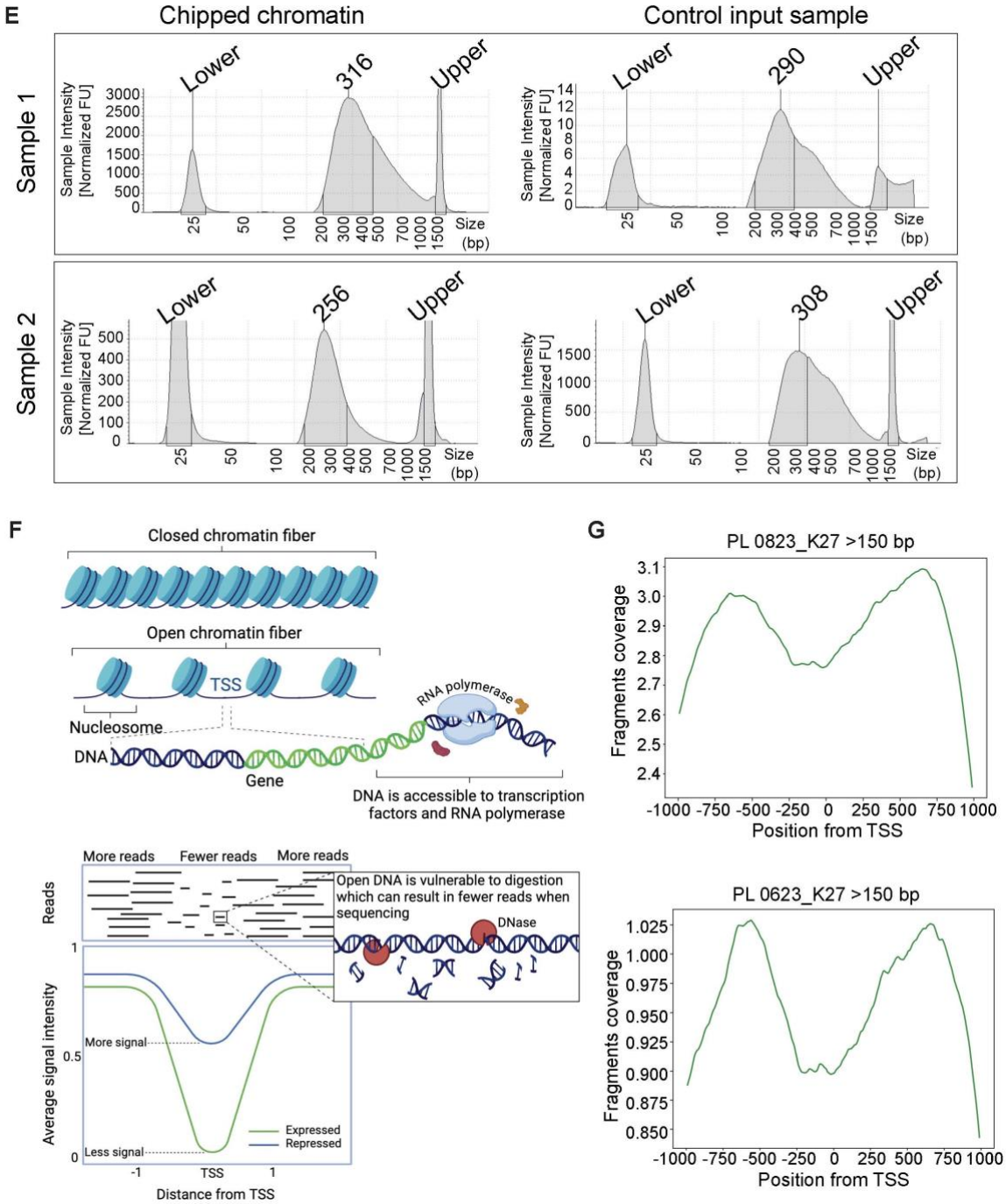


Figure 3-9 (2/2). Platelets sequester nucleosomes. (E) TapeStation of the H3K27ac ChIPmentation DNA libraries from platelet's chromatin. Left, chipped chromatin, right, control input sample of randomly tagmented DNA. **(F)** Top- a schematic illustrating the differences in nucleosome positioning between closed and open chromatin. Genes located in open chromatin regions are accessible to transcription factors and RNA polymerase, facilitating their transcription into messenger RNA. Bottom- a schematic showing the coverage patterns caused by nucleosomal protection of cfDNA. Regions of open chromatin and active gene transcription are more susceptible to digestion due to the absence of protective nucleosomes, leading to reduced sequencing coverage depth, as indicated by the green dip in the plot. Conversely, genes that are not actively transcribed are shielded by nucleosomes, resulting in higher average signal intensity and a less pronounced reduction in reads over the transcriptional start site, as shown by the blue line. **(G)** Coverage of the H3K27ac ChIP-seq reads at transcription start sites

(TSS), for nucleosomal reads (bioinformatically size selected to >= 150 bp). The loss of signal at TSS indicates the presence of open chromatin, and the signal's shoulders indicate the presence of flanking nucleosomes in platelets. The signal was smoothed with a Savitzky–Golay filter. n=2 for ChIPmentation data. Created using Biorender.com.

ii) Platelet- tumour cell conditioned media incubation

To understand whether platelets require physical contact to sequester DNA from nucleated cells and to also evaluate the time course of DNA capture, platelets were added to media conditioned by DNA-labelled COLO205 cells. Platelet uptake of fluorescently tagged DNA was measured at 16 second intervals over a 10-minute time course using the Spinning Disk Confocal microscope. Figure 3-10A outlines the image analysis pipeline used to measure DNA fluorescence in multiple platelets per frame. AF647 (DNA) intensity was then averaged and plotted against control platelets (no exposure to conditioned media) and background fluorescence.

DNA was rapidly visible in platelets within minutes (Fig. 3-10B, Appendix Video 2 & 3), and the average fluorescence intensity of the 168 platelets imaged plateaued at ~6 minutes, suggestive of saturation of DNA uptake (Fig. 3-10C). Similar results were observed in when the fluorescence signal of five randomly selected individual platelets was tracked over time, following addition of platelets to labelled, COLO205-conditioned media (Fig. 3-10D).

Together, these data reveal that DNA fragments released by nucleated cells are internalised by platelets, and that DNA uptake is not dependent on physical contact between platelets and nucleated cells.

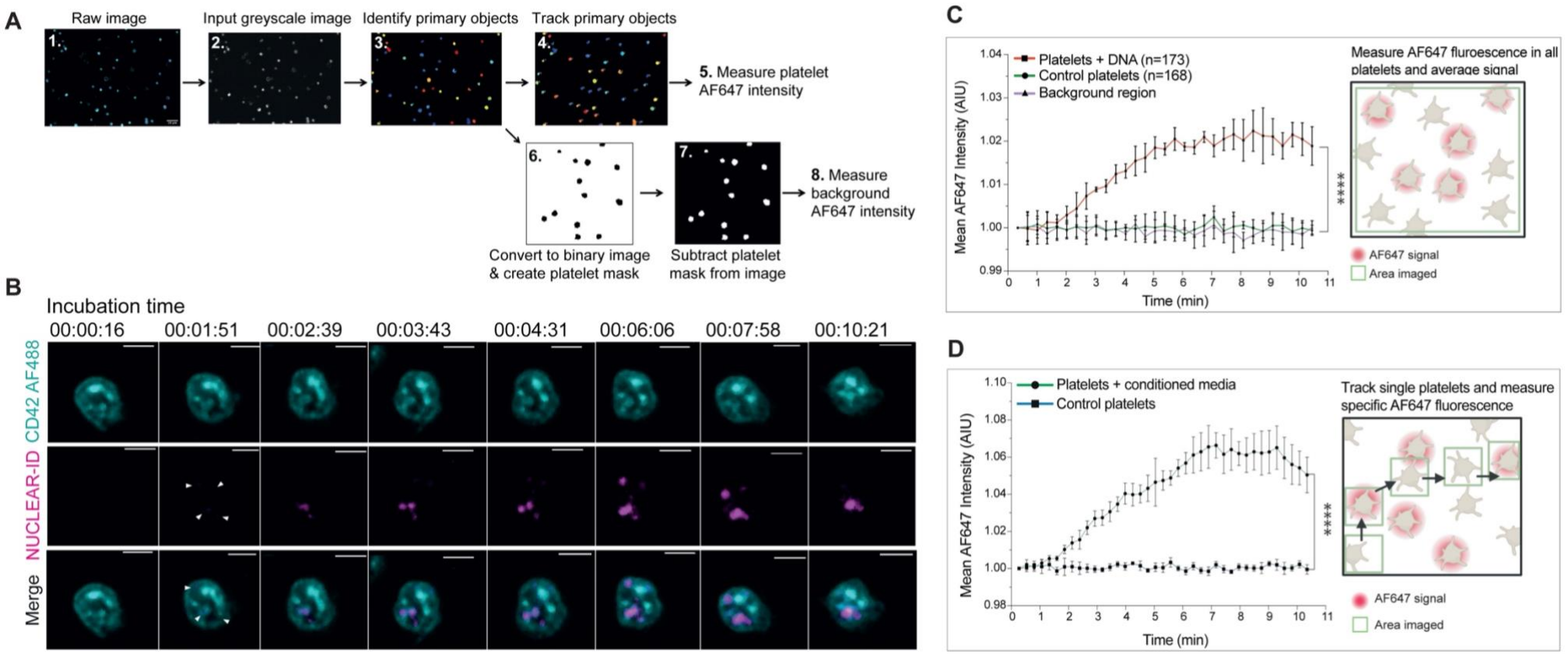


Figure 3-10. Platelet uptake of tumour derived DNA is rapid. (A) Method to quantify fluorescently labelled DNA uptake by platelets over time by: (1) converting raw image files to (2) greyscale images; (3) Segmentation of platelets; (4) tracking of individual platelets over a 10-minute time course; (5) The average platelet DNA (AF647) signal in each frame was calculated and (6-8) background intensity subtracted. **(B)** Live cell imaging time lapse showing internalisation of fluorescently labelled DNA by platelets. Scale bars represent 3 μm. **(C)** Quantification of platelet DNA fluorescence intensity over time (minutes). AF647 signal was also measured in the background regions of each image to detect any fluctuation in background signal (purple line). Tracking shown for platelets incubated with control media (n=168 platelets, green line) or media conditioned by NUCLEAR-ID-labelled COLO205 cells (n=173 platelets, red line). **(D)** DNA uptake by platelets over 10 minutes following addition to COLO205-conditioned media (without COLO205 cells), following 5 randomly selected platelets over time, and normalizing their AF647 signal to frame 1. Plots show mean ± SD, **** $p < 0.0001$ for a Mann-Whitney test. Imaged using a Zeiss Spinning Disk Confocal with a 63X magnification. Created using Biorender.com.

3-2.5 Box 1. Summary of findings in Aim 1

1. Despite lacking a nucleus, data from imaging, FISH, flow cytometry and ddPCR suggest that platelets contain DNA.
2. On average, platelets contain 1/22'000th genomic equivalents of a 2N nucleated cell.
3. Platelet DNA comprises both short (~160 bp) and long (>600 bp) fragment lengths.
4. Platelets sequester circulating nucleosomes as shown by imaging and ChIPmentation data.
5. Platelets with the highest DNA content are also younger, larger and show higher expression of activation markers P-selectin and CD63.
6. Platelets sequester DNA after thrombopoiesis– as confirmed by the detection of Y-chromosome DNA in maternal platelets during pregnancy with male babies and *in vitro* experiments showing update of tumour cell-derived DNA by platelets.
7. cfDNA levels rise in thrombocytopenia, suggesting that platelet DNA sequestration maintains low cfDNA levels in plasma.

3-3 Discussion

I show that despite lacking a nucleus, approximately 8% of circulating platelets contain DNA, and similar to mRNA, platelets likely obtain a portion of this DNA from their parent megakaryocytes, with additional DNA fragments deriving from the plasma.

Plasma cfDNA is increased in malignancy, inflammation and following tissue damage. Several physiological mechanisms exist to limit its abundance, as excess extrachromosomal DNA in the cytosol and in plasma is pro-inflammatory[320,321]. Here, I show that like red blood cells, platelets play a protective role in regulating the cfDNA content of plasma, supported by the observed higher, and more variable levels of cfDNA in plasma in the setting of severe thrombocytopenia.

However, while I have demonstrated this in both mice and humans, I cannot exclude the possibility that the higher levels of plasma cfDNA may be attributable to other factors. For example, the rise in human cfDNA levels could be linked to increased platelet destruction, potentially leading to DNA release rather than a decrease in platelet DNA sequestration. Although beyond the scope of this project, future studies are therefore required to investigate patients that produce low platelet numbers rather than those like ITP, that have increased platelet turnover. Such patients could include those with aplastic anaemia or inherited thrombocytopenia where the bone marrow's ability to produce platelets is compromised.

Similarly, in mice, the elevated levels of plasma cfDNA might stem from other consequences of antibody-mediated platelet clearance. To investigate this, in collaboration with Ian Hitchcock from the University of York, I conducted preliminary research to explore cfDNA concentrations in MPL-null mice that have chronic thrombocytopenia. This approach eliminated the need to use an anti-platelet antibody allowing us to investigate the relationship between platelet levels and cfDNA without the confounding effects of antibody treatment. As these mice have ~5-10% the total number of megakaryocytes and circulating platelets compared to wild-type mice, I hypothesised that reduced platelet production would increase plasma cfDNA. However, I saw no difference in the amount of DNA per μl of plasma when comparing MPL-null mice to wild-type mice.

This unexpected observation may be explained by several factors. Firstly, there could be an upregulation of compensatory cfDNA clearance mechanisms, such as increased urinary excretion, enhanced clearance by Kupffer cells in the liver, or increased activity of splenic macrophages. Given that the liver is the primary organ for nucleosome clearance, future investigations into whether the liver's role in cfDNA clearance is upregulated in the setting of thrombocytopenia, could provide valuable insights into platelet-independent mechanisms of DNA removal from circulation.

Secondly, MPL-null mice might have reduced cfDNA production. Recent evidence from Moss *et al.,* suggests that megakaryocytes contribute approximately 26% of the total cfDNA pool[293]. Given that MPL-null mice have significantly fewer megakaryocytes compared to wild-type, they likely have lower baseline plasma cfDNA levels. The combination of these factors probably contributed to the observed results, masking the expected increase in plasma DNA due to reduced platelet-mediated clearance in MPL-null mice.

Despite the number of questions that remain, the ITP data presented in this chapter do indicate a previously unappreciated role for platelets- in the sequestration and clearance of cfDNA from plasma. This is further supported by observations of tumour-derived and free foetal DNA uptake by platelets. Although I've shown platelets to sequester extracellular DNA, I've not yet established the specific percentage of platelet DNA originating from megakaryocytes. However, data shown by Moss, J. *et al.,* suggest that megakaryocytes account for as much as ~80% of total platelet DNA[293]. The group used targeted bisulphite sequencing to examine methylation markers in DNA extracted from platelet concentrates. The findings revealed multiple regions with distinct unmethylated patterns shared between megakaryocytes and platelets, leading to the conclusion that megakaryocytes serve as the primary source of platelet nucleic acid content.

However, as previously mentioned, this study also found that megakaryocytes significantly contribute to the plasma cfDNA pool. Therefore, it remains unclear whether the observed 80% of megakaryocyte-derived DNA in platelets is derived directly through thrombopoiesis as they suggest or during circulation.

Imaging of pro-platelet formations (PPF) from *in vitro* cultured mouse megakaryocytes challenges the conclusions drawn by Moss, J. *et al,.* For example, data collected in collaboration with Daniela Freire, from the Boston Children's Hospital (data not shown) show that the majority of PPF exhibit minimal labelling with the

nucleic acid stain, SiR-DNA in comparison to peripheral blood platelets. Although preliminary, it indicates that while some DNA may indeed originate directly from megakaryocytes, a substantial portion of platelet DNA (>20%) is extracellularly derived.

Similar to the techniques used in this study, future research will involve methylation sequencing (TAPS) of platelet DNA and megakaryocyte DNA to 'deconvolute' the cellular origin of platelet DNA by looking for lineage-specific methylation marks. Additionally, I aim to further investigate the DNA content of nascent platelets through continued imaging of pro-platelet forming megakaryocytes. If I'm able to confirm megakaryocyte-mediated delivery of DNA into platelets, I'd also like to explore the utility of platelet DNA for interrogating changes to the megakaryocyte genome, for example in clonal haematopoiesis or myeloproliferative neoplasms.

Recent analyses using single-cell RNA sequencing have revealed the existence of megakaryocytes exhibiting immune cell characteristics[322]. Further investigation into this subpopulation indicates a greater heterogeneity than previously understood, with diverse identities including thrombopoietic, immune, and niche megakaryocytes. These observations provide an interesting avenue for future research to explore whether distinct subtypes of megakaryocytes contribute to the generation of heterogeneous platelets with varying DNA content or DNA uptake abilities.

In summary, the data outlined in this chapter strongly indicate two novel scientific observations: (1) Platelets, despite lacking a nucleus, contain DNA, and (2) at least some of this DNA is sequestered during peripheral circulation. I also showed *in vitro* that platelets rapidly sequester nucleated cell-derived DNA from their surroundings without requiring physical contact. However, future investigation is required to understand the relative proportion of megakaryocyte-derived vs. peripherally sequestered DNA in platelets. I hypothesise that platelets acquire DNA from various sources through multiple mechanisms. The approaches I used to investigate this are detailed in the next chapter of this thesis.

Chapter 4: Mechanisms of DNA uptake by platelets

4-1 Introduction

In this chapter, I explore the mechanisms of DNA uptake and release by platelets and its intracellular localisation.

4-1.1 Platelet endocytosis

Platelets are highly efficient at exchanging biomolecules with their surroundings. Cargo trafficking in platelets allows for the uptake, storage, and release of molecules essential for the regulation of platelet function and response to stimuli. Like other cell types, platelets utilize a variety of endocytic pathways, including phagocytosis, pinocytosis and receptor-mediated endocytosis, to internalise a range of extracellular cargo[323]. In this introduction, I provide a concise summary of platelet endocytic pathways, focusing on those relevant to DNA fragment uptake and their potential pharmacological manipulation.

Phagocytosis

As outlined in chapters 1 and 3, like macrophages, neutrophils, and dendritic cells, platelets express pathogen recognition receptors (PRRs) that bind complementary molecular patterns on bacterial and viral particles[104,103,111]. Platelets have been observed to phagocytose immune complexes via FcγRIIa[324], bacteria such as *P. gingivalis*[325] and *S. aureus*[101,107] and viruses such as HIV-1 and influenza[101,104]. Upon binding, platelet actin polymerization is triggered, leading to the formation of cytoplasmic extensions

around the pathogen known as a phagosome. Once formed, the phagosome, containing the ingested particle, is internalised within the platelet (Fig. 4-1A)[112,326]. Although the exact trafficking of the ingested material is unclear, as described in chapter 1.3-1, there is evidence suggesting that bacterial and viral particles are held within endocytic vesicles and membrane compartments similar to the open canalicular system (OCS)[112,327,328]. Platelets can also phagocytose inert molecules such as latex beads, that cause platelet aggregation due to the release of ADP[329].

Phagocytosis can be inhibited by Cytochalasin D (cyto D) - a drug that disrupts actin polymerization by binding to F-actin filaments, thus preventing the addition of new actin monomers.

Pinocytosis

Pinocytosis refers to the process by which cells take up extracellular fluid. There are two main types: micropinocytosis and macropinocytosis, which differ in vesicle size and uptake mechanisms. Micropinocytosis occurs through the invagination of the plasma membrane, forming small vesicles often via clathrin- or caveolin-mediated pathways. In contrast, macropinocytosis is a non-receptor-mediated process that involves the formation of large, actin-driven membrane ruffles that engulf extracellular fluid to form macropinosomes (Fig. 4-1B). While evidence supporting pinocytosis in platelets is somewhat limited, there are indications that platelets may acquire plasma proteins such as IgG, IgA, and albumin through fluid-phase endocytosis[330,331].

Because macropinocytosis, like phagocytosis, is heavily dependent on actin polymerization, drugs that impair actin dynamics can effectively inhibit this pathway. For example, amiloride inhibits macropinocytosis by targeting the Na^+/H^+ exchanger (NHE) membrane protein[332,333]. The NHE protein regulates intracellular pH by exchanging Na^+ ions for extracellular H^+ ions. Inhibition of NHE leads to intracellular acidification which causes a decrease in the pH close to the membrane thus impairing the activity of actin-binding proteins such as Rac which are required for actin polymerization and depolymerization[333,334]. In addition to amiloride, studies have demonstrated that the drug imipramine

also inhibits membrane ruffling during macropinocytosis although this mechanism is not completely understood[335].

Clathrin-dependent endocytosis/ clathrin mediated endocytosis (CME)

During clathrin-mediated endocytosis, at the plasma membrane of cells including platelets, specific receptor-ligand interactions initiate the recruitment of adaptor proteins such as AP2 and clathrin to the cargo site. This assembly triggers the activation of adaptor proteins, leading to membrane invagination, clathrin binding, and polymerization. This results in the formation of a protective, lattice-like structure around the internalised cargo. Upon completion, dynamin, a protein that forms a helical structure around the neck of budding vesicles within the cytosol of the cell, binds GTP and undergoes a conformational change. This rearrangement generates the mechanical force required to detach the clathrin-coated vesicle from the membrane of the cell (Fig. 4-1C)[336,337]. There is evidence to suggest that the platelet integrin, αIIbβ3 is trafficked and recycled via clathrin- mediated endocytosis[338].

Pitstop2 is a drug commonly used to investigate CME. It disrupts the assembly of clathrin-coated vesicles by competitively binding clathrin thus preventing access from the adaptor proteins needed to form the clathrin coat[332,339,340]. For example, Pistop2 has been shown to inhibit the recycling of αIIbβ3 to the platelet plasma membrane[338]. Since the completion of this pathway relies on dynamin-mediated membrane fission, inhibition of dynamin also effectively blocks clathrin-mediated endoyctosis[341]. For example, dynamin inhibitors such as Dynole, bind to the GTPase domain of dynamin, preventing it from hydrolyzing GTP to GDP and thereby blocking the mechanical force required to pinch off the internalised vesicle from the membrane (Fig. 4-1D)[337].

Caveolae-dependent endocytosis

Caveolae-mediated endocytosis is an example of dynamin and cholesterol dependent, but clathrin independent endocytosis. Unlike clathrin-mediated endocytosis, where clathrin proteins are recruited to the membrane, caveolin-1 is permanently embedded in the plasma membrane. Upon the binding of ligands to the plasma membrane, caveolae invaginate inward from the plasma membrane and with the

assistance of cavin proteins, form flask-shaped vesicles (Fig. 4-1E). Cholesterol helps maintain the structural integrity of caveolae during this process by stabilising lipid raft microdomains, which serve as platforms for the assembly and clustering of caveolin proteins[342]. Like CME, these vesicles are then cleaved from the membrane via dynamin and are released into the cytosol of the cell. While platelets express all three caveolae proteins, it remains unclear whether platelets use this pathway to internalise molecules[323,327,343].

Nystatin is an inhibitor used to study caveolae-mediated endocytosis. It's an antifungal medication that binds ergosterol, a key component of fungal cell membranes. Binding of nystatin to ergosterol leads to pore formation, resulting in membrane destabilisation and cell death[344]. While nystatin primarily targets fungal ergosterol, it also binds to and sequesters cholesterol in the plasma membrane of mammalian cells[344,345]. Since cholesterol is vital for caveolae-mediated endocytosis, its removal by nystatin significantly impacts membrane stability leading to inhibition of endocytosis.

Open canalicular system

As described in chapter 1, unlike other cell types, platelets possess a continuous and highly complex internal membrane known as the open canalicular system (OCS, Fig. 4-1F). This unique structure comprises surface connected and interconnected channels that facilitate both the rapid release of molecules during secretion (exocytosis) and the uptake of extracellular molecules *into* the platelet cytoplasm (endocytosis) such as tissue factor (TF), fibrinogen and platelet microparticles (PMPs)[346,347]. PMPs have also been shown to bud from the OCS as well as the plasma membrane.

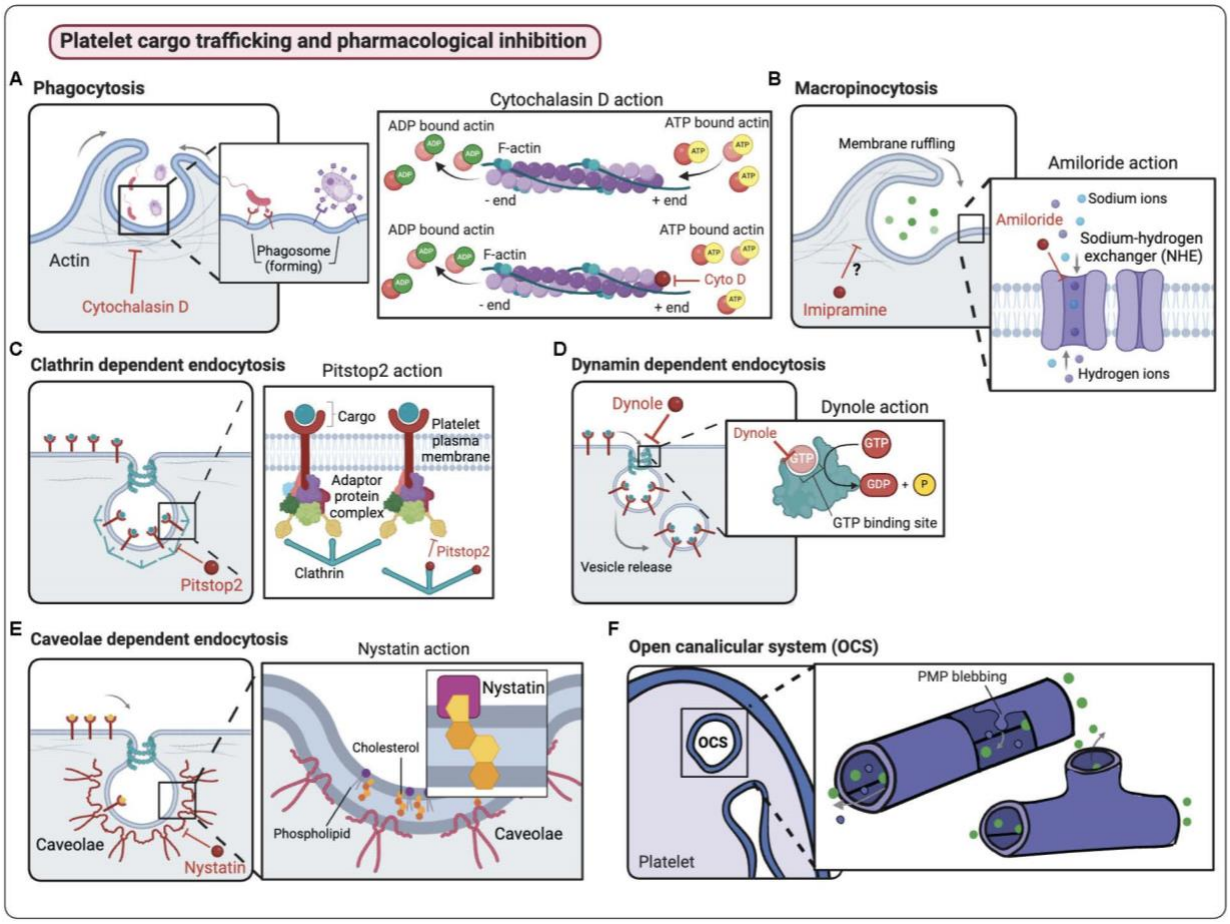


Figure 4-1. Cargo trafficking in platelets and common drugs used to inhibit them. Schematic representation of cargo trafficking within platelets and the common pharmacological agents used to inhibit the main pathways through which extracellular materials are internalised. Created using Biorender.com.

4-1.2 Platelets sequester extracellular vesicles

Extracellular vesicles (EVs) are small membrane-bound structures released by cells into the extracellular environment. They are heterogeneous in nature and can vary in size, content, and biogenesis pathway (Fig. 4-2). EVs are generated during both physiological and pathological conditions and because they are packaged with proteins, nucleic acids, lipids and metabolites, play a key role in mediating intercellular communication[348]. Microvesicles are larger and form from the blebbing of the plasma membrane, whereas exosomes are smaller and derive intracellularly, from the endosomal pathway. Apoptotic bodies are a distinct class of extracellular vesicle that are released through blebbing by cells undergoing apoptosis. Like microvesicles and exosomes, apoptotic bodies inherit organelles,

nucleic acids, lipids and proteins[349] and therefore also mediate intercellular communication (Fig. 4-2)[350-352].

The presence of double stranded DNA (dsDNA) within EVs was first reported in 2014[353]. Subsequent studies have revealed a range of DNA fragment sizes in EVs, from small DNA fragments around 100 bp to larger fragments exceeding 10 kb. In larger vesicles known as oncosomes, DNA fragments as large as 2 Mb have been observed[354-356]. While both viable and apoptotic cells release DNA-containing EVs, the precise mechanisms by which living cells package DNA into these vesicles remain unclear.

Exosomes

Nuclear content may be released into the cytoplasm of viable cells through various mechanisms, including aberrant mitosis, chromosomal instability, and micronuclear breakdown[353,354,357-359,360]. Once in the cytoplasm, DNA can be incorporated into exosomes during their biogenesis[361]. This process involves the maturation of early endosomes into late endosomes and subsequently into multivesicular bodies (MVBs)[362]. As MVBs form, they selectively incorporate cytosolic components, including DNA fragments, into intraluminal vesicles (ILVs). These ILVs are then released as exosomes when MVBs fuse with the cell membrane. Notably, research by Fernando *et al.,* in 2017 suggested that over 90% of cfDNA is associated with exosomes rather than larger microvesicles[356,361].

Microvesicles

The delivery of DNA into the microvesicles of viable cells is less well understood compared to exosomes. Given that microvesicles form from the outward budding and fission of the plasma membrane, it is hypothesised that cytoplasmic components, including DNA are passively trapped within the developing vesicle[361].

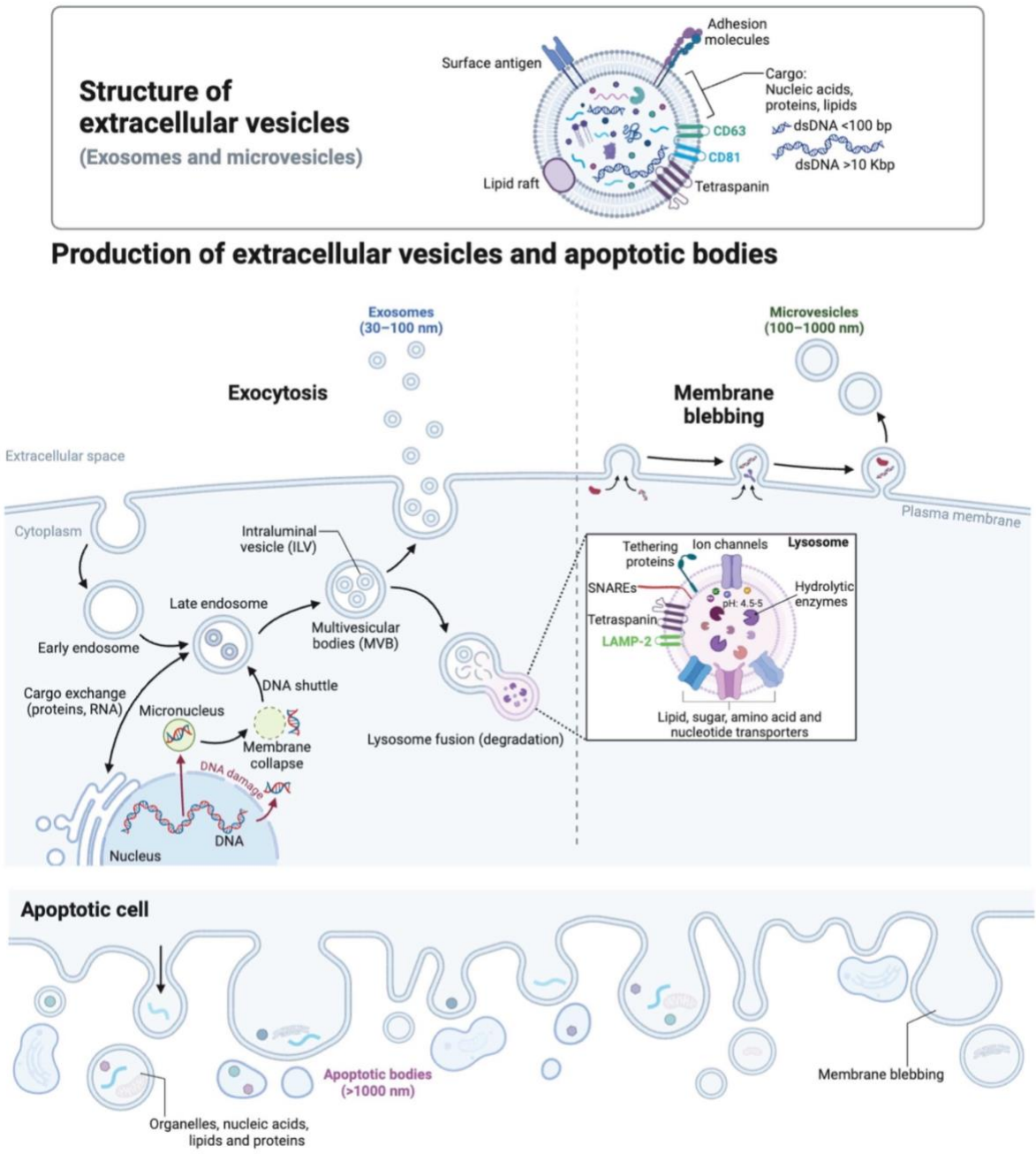


Figure 4-2. Production of extracellular vesicles and apoptotic bodies. DNA damage resulting from cellular stress can induce the formation of unstable micronuclei, which are prone to collapse and expose DNA to the cytoplasm. During exosome biogenesis, cytosolic DNA may be incorporated into intraluminal vesicles (ILVs) within multivesicular bodies (MVBs). These vesicles are subsequently released as exosomes upon fusion of MVBs with the plasma membrane. MVBs that do not fuse with the plasma membrane may undergo degradation by fusing with lysosomes, where LAMP-2 serves as a marker. Larger microvesicles are formed through outward budding and blebbing of the plasma membrane, which may also integrate cytosolic DNA released from the nucleus. Markers such as tetraspanins CD81 and CD63 are indicative of these microvesicles. Apoptotic bodies, released during cell death, represent another mode of cellular vesicle release. Adapted from J. Elzanowska *et al.,* 2021[361]. Created using Biorender.com.

Platelets have been shown to readily take up EVs, including those derived from tumour cells. This uptake process has been described as 'educating' platelets through the transfer of cancer cell-derived proteins and mRNA transcripts[363,364]. As described in chapter 1, these observations have led to numerous studies exploring the platelet transcriptome as a potential biomarker for various malignancies[60,205,230,365].

While platelet uptake of EVs is well-documented, the specific mechanisms remain unclear. EVs can interact with cells in several ways: by binding to surface receptors to trigger signalling cascades, directly fusing with the plasma membrane to release their contents, or being internalised through endocytic pathways[362]. In platelets, the mechanism of EV uptake likely depends on both the vesicle type and the activation state of the platelet. Recent research has shed light on a couple of potential mechanisms. For instance in 2016, clathrin was shown to mediate platelet internalisation of neutrophil-derived EVs[366]. Whereas, more recently in 2023, a study by Dudiki *et al.,* suggested that uptake of tumour-derived EVs, was mediated by the interaction between vesicular CD63 and platelet receptor-linked tyrosine phosphatase alpha (RPTPα)[364,367,368].

Another receptor likely involved in EV uptake by platelets is P-selectin, a cell adhesion molecule stored in platelet alpha granules. Upon activation, P-selectin is expressed at the platelet surface, where it can bind its complementary receptor, P-selectin glycoprotein ligand-1 (PSGL-1). Like CD63, PSGL-1 is expressed on EVs, which may aid in the uptake of EVs by platelets (Fig. 4-3).

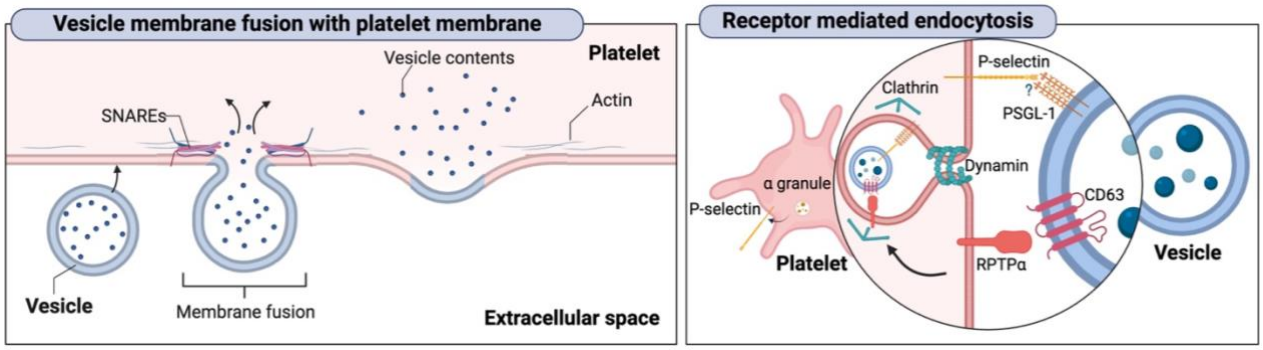


Figure 4-3. Proposed mechanisms of platelet uptake of extracellular vesicles. Extracellular vesicles can interact with platelets through two main pathways. Left- direct fusion with the platelet plasma membrane, releasing vesicle contents into the cytosol. Right- receptor-mediated internalisation, such as

binding to RPTPα, followed by processes like clathrin-mediated endocytosis. This model is based on published literature describing exosome interactions with recipient cells. Created using Biorender.com.

In summary, while vesicles are known to contain nucleic acids, EV-mediated specific transfer of DNA fragments from nucleated cells to platelets has not previously been explored. However, platelet uptake of tumour cell-derived EVs has previously been shown to transfer cancer cell-derived protein cargo and mRNA transcripts – and this inspired my hypothesis that platelets might also acquire DNA through this mechanism[363].

4-1.3 Platelet exocytosis

Upon activation, platelets release proteins and small biomolecules from their alpha granules, dense granules, and lysosomes[369]. Additionally, platelets secrete microvesicles that bud from their surface, as well as smaller exosomes generated through the endosomal pathway. Platelet granule cargo is released via several pathways. Upon activation, granules collect in the centre of the platelet and fuse with the OCS[370,371] or directly with the plasma membrane[372,373]. At high agonist concentrations, alpha granules may fuse with each other to form larger multigranular bodies before fusing with the plasma membrane. Granule fusing can potentially concentrate signalling molecules and enhance intracellular signalling cascades[41,374].

Platelet secretion is tightly regulated to prevent inappropriate release of pro-thrombogenic or inflammatory mediators. This regulation includes the selective packaging and release of granular contents in response to specific agonists. For example, platelets can release either proangiogenic factors, such as VEGF, or antiangiogenic factors, like angiostatin, depending on the agonist[41,375,376]. However, the exact mechanism behind this differential release of cargo from the same type of granule remains unclear[376]. The timing of release also varies among granule types, with dense granules releasing their contents most rapidly, followed by alpha granules and then lysosomes[375].

In addition to external agonists, granule secretion is governed by intrinsic regulatory mechanisms that control the fusion of granules with the plasma membrane. Central to this process are SNARE (SNAp REceptor) proteins, which drive the fusion of lipid bilayers[41,377,378]. SNARE proteins fall into two categories based on their location: vesicle SNAREs (vSNAREs) on the vesicle or granule membranes, and target SNAREs (tSNAREs), located on the target membrane, such as the OCS or plasma membrane in platelets[41,378]. SNARE-mediated fusion involves the transport of the granule to the target membrane, where a conformational change in the SNARE complex brings the membranes into close proximity, facilitating membrane fusion and the release of granule contents (Fig. 4-4)[378]. This process is further regulated by chaperone proteins, cytoskeletal dynamins, and intracellular calcium[41].

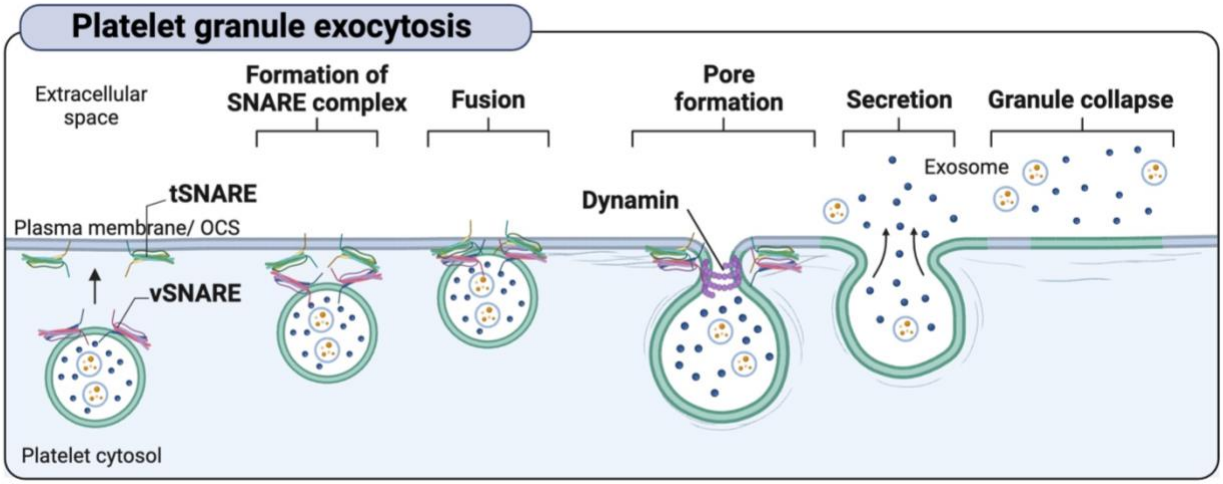


Figure 4-4. Platelet exocytosis via fusion pore formation. A granule is transported toward the target membrane, where SNARE proteins mediate docking. A conformational change in the SNARE complex brings the membranes into close proximity, enabling fusion and the release of granular contents. Created using Biorender.com.

4-1.4 Platelet activation

As described in the introduction (section 1-2), a primary role of platelets is to sense vascular damage and prevent bleeding by initiating haemostasis. To effectively perform this role, platelets must become activated. Platelet reactivity is determined by the interaction of their surface receptors with endogenous inhibitory and stimulatory mediators.

Inhibitory prostacyclin (PGI2) and nitric oxide (NO) are released from healthy endothelial cells to maintain platelets in a quiescent state[379-381]. However, upon vessel injury, platelets are exposed to extracellular matrix proteins such as collagen which induce their activation. Platelet surface receptors mediate the initial tethering of platelets to the injury site, allowing for the subsequent binding of additional platelet receptors. This triggers platelet activation, leading to increased cytosolic calcium levels. The rapid rise in calcium promotes the secretion of secondary mediators, such as ADP and thromboxane A_2 (TxA_2) from intracellular stores, resulting in cytoskeletal rearrangement and shape change.

Several assays can be used to investigate platelet activation and their reactivity to agonists. In research settings, flow cytometry is commonly employed due to its high sensitivity and ability to simultaneously measure multiple activation markers. For example, upon activation, CD63 and CD62P are expressed on the platelet surface following intracellular granule release. Additionally, the αIIbβ3 membrane integrin undergoes a conformational change from its resting to activated state. Flow cytometric antibodies targeting these activation markers can be used to assess platelet reactivity, as demonstrated in Figure 4-5.

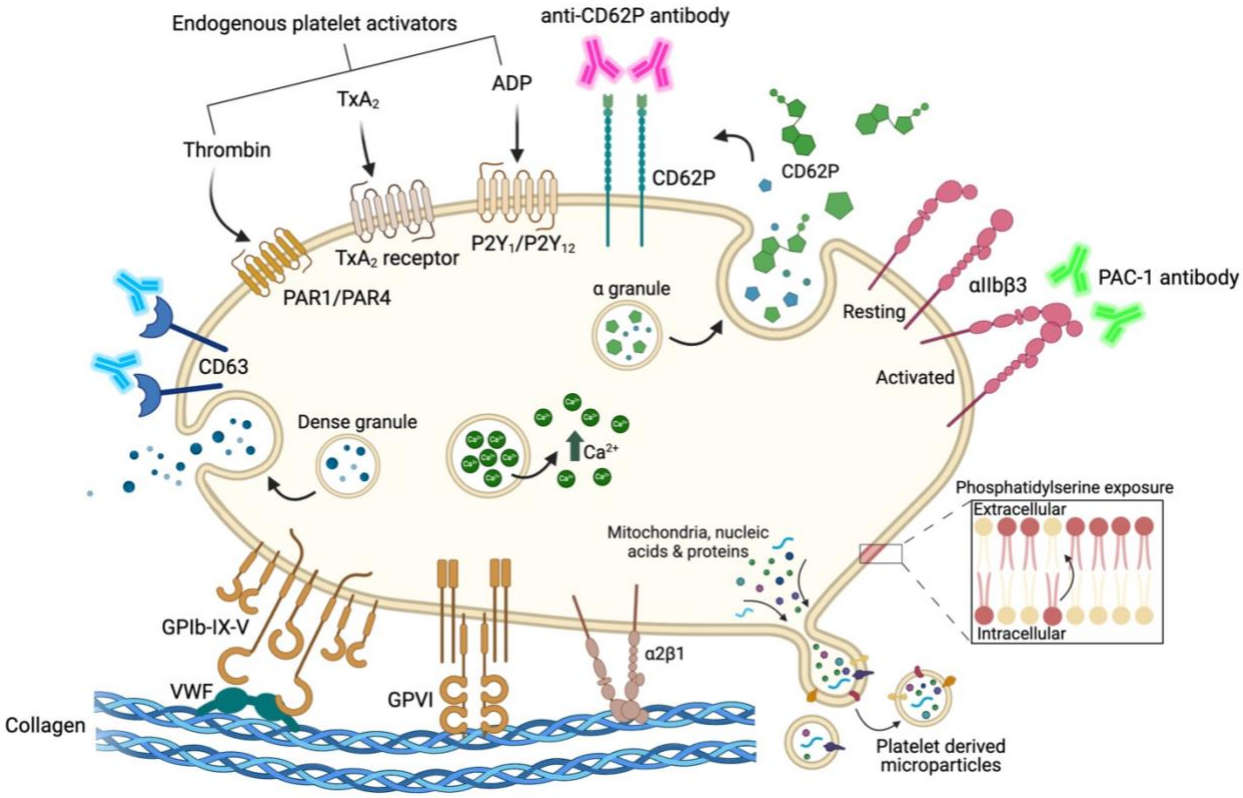


Figure 4-5. Schematic of platelet activation. Initial tethering and adhesion processes involve vWF and collagen binding to the GPIb-V-IX complex. Stable adhesion is facilitated by collagen binding to GPVI and integrin α2β1. Extracellular mediators, such as thrombin and TxA_2, trigger activation by binding to their respective receptors on the platelet surface. This activation leads to degranulation, releasing secondary mediators like ADP. ADP, secreted from dense granules, binds to $P2Y_{12}/P2Y_1$ receptors, amplifying the activation process. During activation, CD62P and CD63 are released from alpha and dense granules and translocate to the outer membrane. Thus, flow cytometric antibodies targeting these markers can be used to assess platelet activation. Here, anti-CD62P is pink and anti-CD63 is blue. Additionally, during activation, αIIbβ3 undergoes a conformational change from its resting to activated state. PAC-1, shown in green, specifically recognises the activated form of αIIbβ3. Platelet activation also causes disruption of the platelet plasma membrane structure, leading to phosphatidylserine (PS) exposure and the release of platelet microparticles. Created using Biorender.com.

i) Pharmacological inhibition of platelet activation

<u>Aspirin</u>

Due to the multiple activation pathways in platelets, a range of pharmacological agents have been designed to selectively target specific pathways. One such example is acetylsalicylic acid, more commonly known as aspirin, taken by approximately one billion people worldwide to prevent heart attacks and strokes. Aspirin inhibits platelet function by irreversibly acetylating the amino acid serine 529 in cyclooxygenase-1 (COX-1), the enzyme responsible for metabolising its substrate, arachidonic

acid (AA) into thromboxane A_2 (TxA_2) (Fig. 4-6)[382-384]. TxA_2 is a potent platelet activator and vasoconstrictor. Reduced levels of circulating TxA_2 lower platelet activation and aggregation, thereby decreasing the risk of harmful blood clot formation.

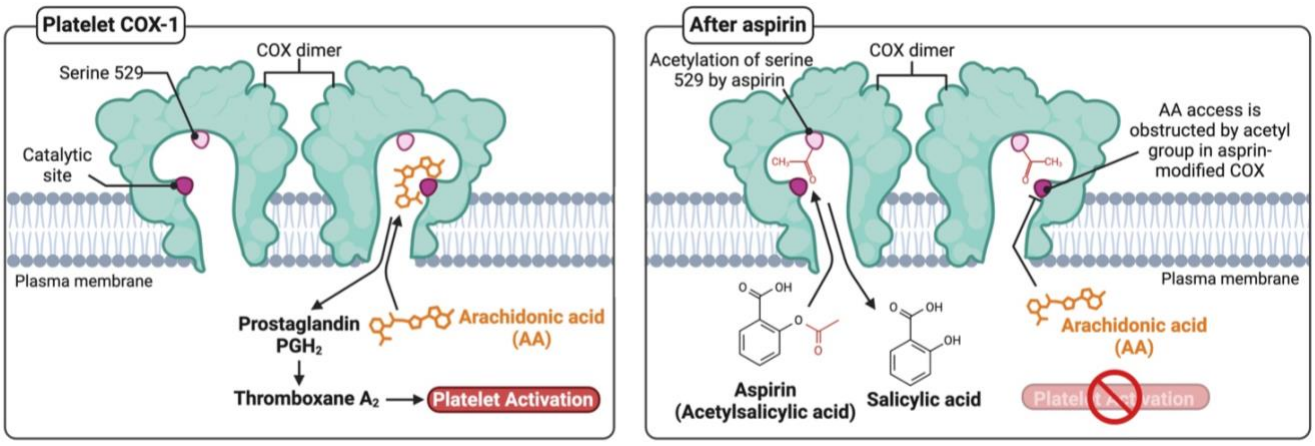


Figure 4-6. Mechanism of aspirin inhibition. Irreversible acetylation of serine 529 by aspirin physically prevents the substrate, arachidonic acid (AA) from accessing the catalytic site of cyclooxygenase-1 (COX-1). This results in inhibition of thromboxane A_2 formation and platelet activation. Adapted from Fitzgerald & FitzGerald (2013)[385]. Created using Biorender.com.

Ibrutinib

In this chapter, I also investigate the impact of ibrutinib, a Bruton tyrosine kinase (Btk) inhibitor, on platelet activation and how this, along with aspirin, impacts platelet DNA content. Ibrutinib is used in the clinic for the treatment of B cell malignancies, in particular chronic lymphocytic leukaemia. However, treatment with ibrutinib is associated with an increased risk of bleeding due to its effect on platelet signalling, specifically its inhibition of collagen-mediated platelet aggregation[386,387].

Btk is crucial for platelet activation by mediating signals from various receptors, including GPVI, the collagen receptor, and the GPIb-IX-V complex, which facilitates binding to vWF. Btk phosphorylates and activates phospholipase C gamma 2 (PLCγ2). This results in the production of inositol 1,4,5-trisphosphate (IP_3) and diacylglycerol (DAG), which are crucial secondary messengers that lead to the release of calcium ions from intracellular platelet stores[388]. This cascade ultimately promotes platelet activation, secretion, and aggregation (Fig. 4-7). Ibrutinib inhibits Btk by covalently binding to the cysteine 481 residue within its active site[389]. This irreversible binding prevents Btk from

phosphorylating its downstream target PLCγ2, leading to dysregulated calcium influx and reduced platelet activation and aggregation.

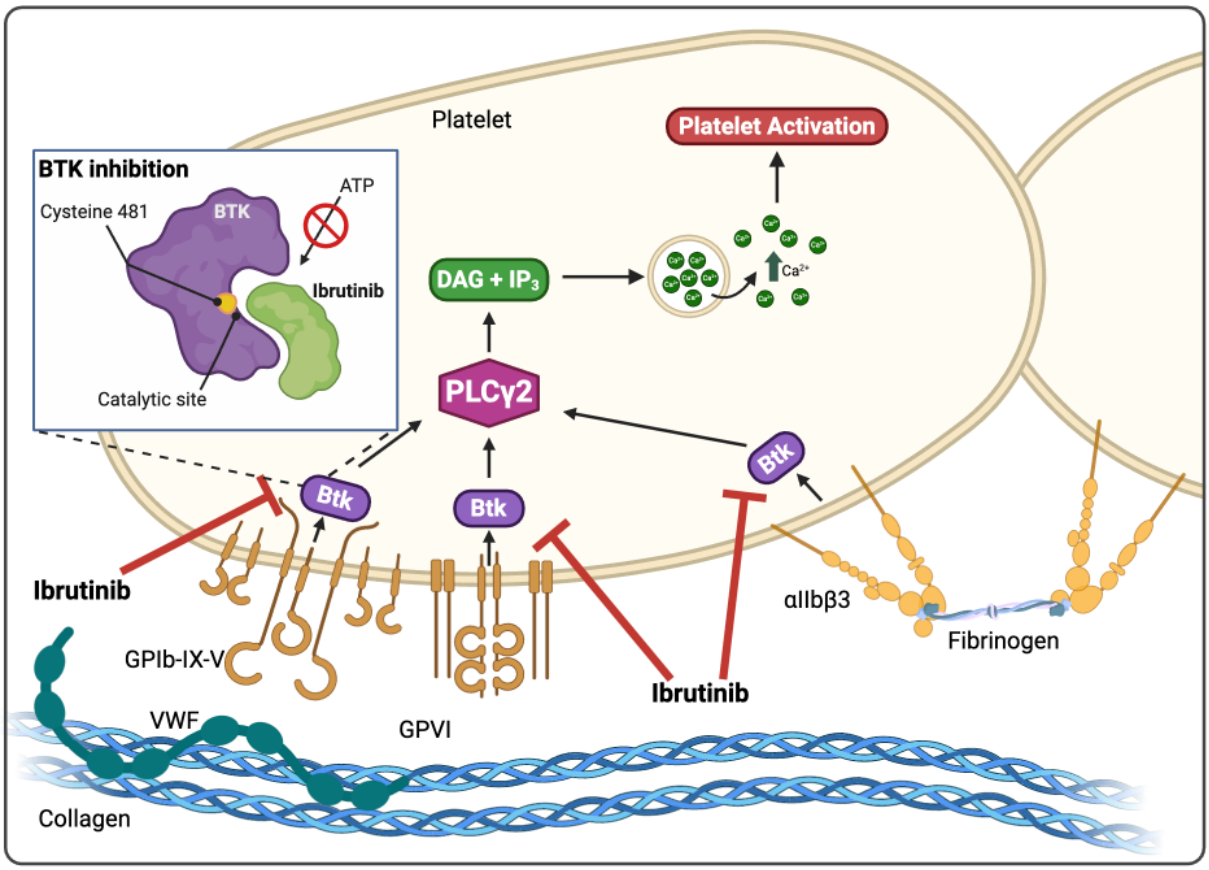


Figure 4-7. The effects of ibrutinib on platelet function. Bruton tyrosine kinase (Btk) sits downstream of multiple platelet signalling pathways. Activated Btk phosphorylates and activates phospholipase C gamma 2 (PLCγ2). Activation of PLCγ2 results in the production of inositol 1,4,5-trisphosphate (IP_3) and diacylglycerol (DAG), which leads to the release of calcium ions from intracellular stores resulting in platelet activation. Ibrutinib inhibits Btk by covalently binding to the amino acid cysteine 481 in the active site of the enzyme. This effectively blocks signalling through Btk which ultimately results in reduced platelet activation and aggregation. Created using Biorender.com.

4-1.5 Platelet lifespan

Platelet production and clearance is tightly controlled to maintain a healthy platelet count between 150'000-400'000 platelets per microliter of blood[390]. While approximately 100 billion platelets are produced daily, only a small fraction are used for haemostasis[391]. The remaining platelets continue to circulate for up to 10 days before being cleared by macrophages in the liver and spleen[392]. Several

mechanisms have been proposed for initiating platelet clearance under normal, physiological conditions.

As platelets circulate, their membrane glycoproteins become desialylated[393]. Desialylation is one of several mechanisms thought to regulate platelet lifespan. Sialic acid coats the extracellular domains of platelet membrane proteins[394]. When sialic acid is removed by the enzyme sialidase, the underlying sugar, β-galactose is exposed. This exposed β-galactose is recognised by Ashwell-Morell receptors (AMR) on hepatocytes and liver macrophages, ultimately leading to platelet phagocytosis (Fig. 4-8A) [394,395].

Another regulatory mechanism is the intrinsic (or 'mitochondrial') apoptosis pathway, mediated by anti-apoptotic and pro-apoptotic proteins. As platelets age, the degradation of the pro-survival protein Bcl-X_L, triggers Bak and Bax-mediated mitochondrial permeabilization[396]. Mitochondrial damage initiates the apoptotic cascade, resulting in the release of caspase 3, exposure of phosphatidylserine, and the subsequent clearance of platelets from circulation (Fig. 4-8B)[391,397].

However, platelet aging and the consequent loss of Bcl-X_L is likely not the only trigger for Bak and Bax activation[14]. For example, in nucleated cells, BH3-only proteins sense and transmit pro-death signals to Bak and Bax in response to stress, overriding the function of the pro-survival proteins (e.g. Bcl-X_L)[396]. The detection of BH3-only proteins in platelets supports the recent hypothesis that these proteins may provide an additional mechanism for regulating platelet lifespan.

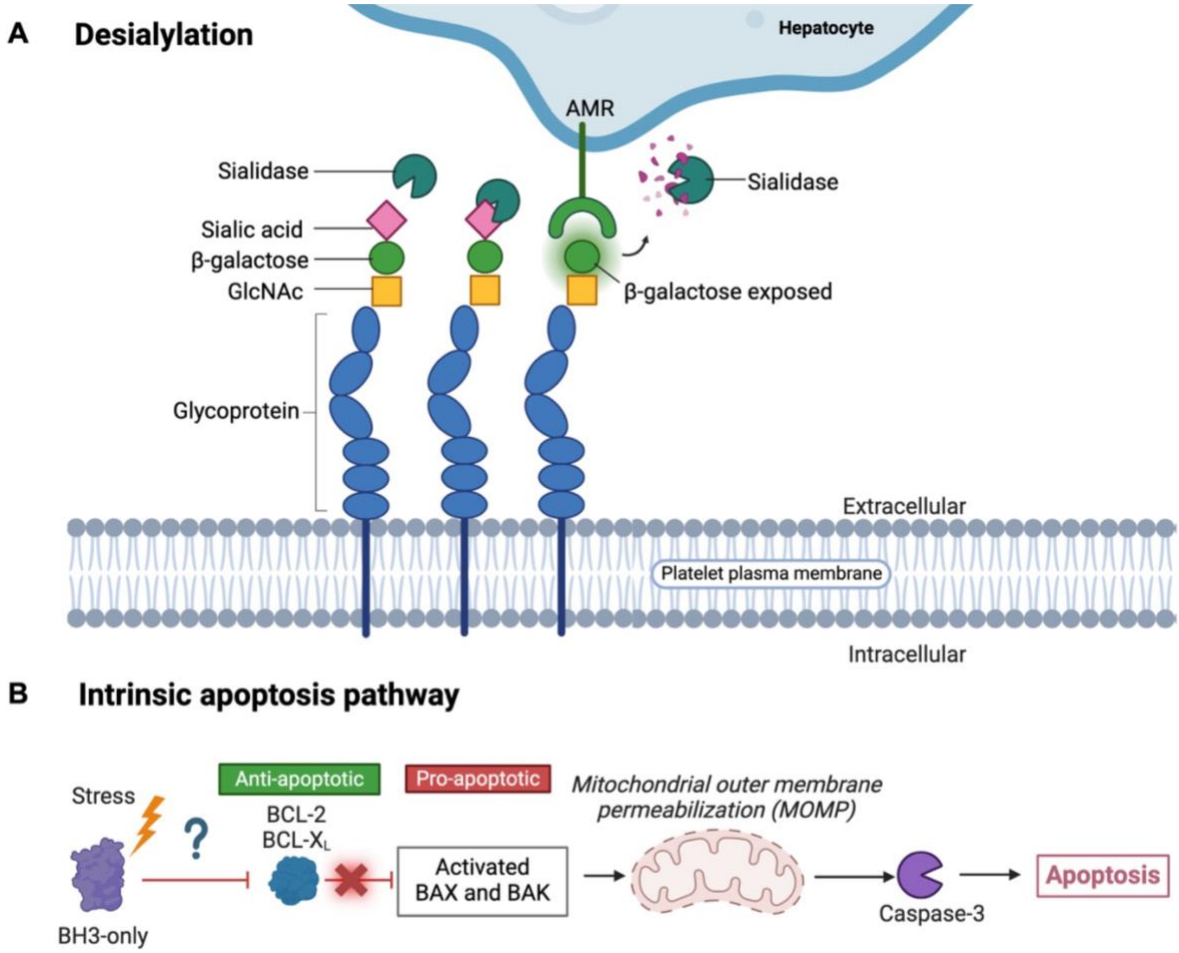


Figure 4-8. Proposed mechanisms of platelet clearance. (A) As platelets age, sialidase enzymes remove sialic acid sugars from their membrane glycoproteins. This desialylation exposes β-galactose, which is recognised by the Ashwell-Morell receptor (AMR) on hepatocytes. **(B)** Platelet survival depends on the balance between pro-survival and pro-apoptotic proteins. As platelets age, the degradation of the pro-survival protein BCL-X_L can shift the balance towards pro-apoptotic proteins. This activates Bax and Bak, resulting in mitochondrial damage and the initiation of the apoptotic cascade. Although platelets contain BH3-only proteins, it's currently unclear whether stress signals activate these proteins leading to activation of Bak and Bax. Created using Biorender.com.

Cells undergoing apoptosis express engulfment signals that are recognised by scavenger receptors on phagocytes. For example, platelet calreticulin expression activates the internalisation receptor, LRP/CD91[398,399], and externalized phosphatidylserine (PS) on the surface of apoptotic platelets, binds to complementary PS receptors on phagocytes, such as BAI1 and TIM-4 (Fig. 4-9)[400,401,402,403].

Platelet homeostasis is also regulated by the activation of inhibitory mechanisms. For instance, the pro-phagocytic signal of calreticulin is counterbalanced by 'don't eat me' signals, such as CD47. Platelet

CD47 prevents unintentional ingestion by binding to the inhibitory receptor SIRPα on macrophages, thereby inhibiting macrophage activation and phagocytosis[399,401,402,404].

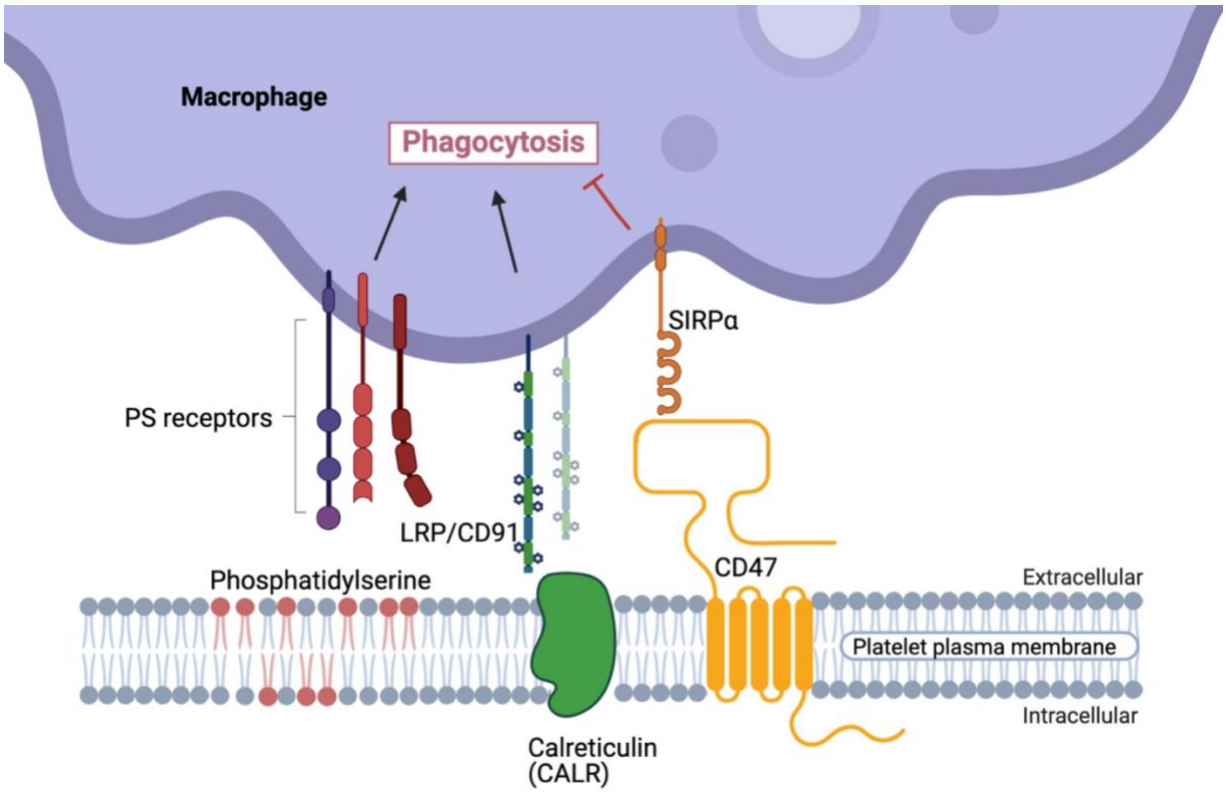


Figure 4-9. Apoptotic platelets communicate with circulating phagocytes. The redistribution of phosphatidylserine (PS) from the inner – to the outer membrane leaflet of apoptotic platelets acts as an 'eat me' signal for circulating phagocytes. Binding of calreticulin to macrophage CD91/LRP1 also promotes engulfment of the apoptotic platelets. However, CD47 is a marker of self and binds to SIRPα, an inhibitory receptor expressed on the surface of macrophages. This binding triggers a signalling pathway that results in the inhibition of phagocytosis. Created using Biorender.com.

4-1.6 Hypothesis and aims

Given platelets' ability to acquire various tumour-derived proteins and mRNA via the uptake of EVs, I hypothesised that platelets also sequester tumour-derived DNA via the uptake of EVs. My overarching goal with Aim 2 was to investigate the various mechanisms platelets use to sequester DNA and determine whether their uptake is restricted to membrane-bound (i.e. EV encapsulated) DNA, or if platelets may also take up 'free' DNA fragments.

The specific sub-aims for this section of my thesis were:

Aim 2.1 To confirm whether platelets sequester DNA-loaded EVs

Aim 2.2 To determine whether DNA uptake by platelets is an active or a passive process and investigate the impact of inhibitors on platelet cargo trafficking, DNA uptake and release

Aim 2.3 To investigate the trafficking and location of DNA following platelet internalisation

To achieve these aims I first used immunofluorescence microscopy and droplet digital (dd)PCR to confirm platelet uptake of DNA containing apoptotic and non-apoptotic extracellular vesicles. Following this, I investigated the uptake of single and double-stranded synthetic DNA fragments by platelets and used flow cytometry to assess the effects of DNA uptake on platelet immunophenotype, specifically activation state and the expression of anti-phagocytic signals. Finally, I used Airyscan imaging to gain a clearer understanding of DNA location within platelets. I aimed to determine whether the DNA was internalised by the platelet or retained within the membrane tunnels of the OCS.

4-2 Results

4-2.1 Nucleic acid transfer via DNA-loaded extracellular vesicles

i) Extracellular vesicles contain DNA

The generation, purification and amine labelling of extracellular vesicles (EVs) from BL2 and BL2-bcl-2 cells was carried out by Pamela Holland from the University of Edinburgh. Details of these procedures are described in chapter 2.

To determine if EVs are mediators of DNA transfer to platelets, and the role of tumour cell apoptosis in DNA release, platelets were isolated from female donors and incubated for 3 hours with EVs isolated from BL2 cells – a human B-cell lymphoma cell line originating from a male donor – or isogenic BL2 cells engineered to overexpress the apoptosis-suppressing gene Bcl-2 (termed BL2-Bcl-2 cells). Both apo-EVs (from BL2 cells) and non-apoptotic EVs (from engineered BL2-Bcl-2 cells) were treated with DNase to remove any non-internalised DNA that might be present on the outer membrane. EVs were then frozen and posted to Oxford.

Upon thawing, EVs were stained with the nucleic acid stain DAPI and imaged. Imaging confirmed internalised DNA (yellow) within EVs (red) (Fig. 4-10A & B). Notably, no fluorescence signal was visible in the PBS control suggesting that the observed vesicles were genuine and not attributed to auto fluorescent debris or noise (Appendix Data Figure 2). I next used ddPCR to more precisely quantify the amount of DNA in each vesicle type (Fig. 4-10C). As the vesicles were derived from male cell lines, I looked for the presence of the Y-chromosome, *SRY* gene. ddPCR confirmed copies of this gene, indicating that the vesicles were packaged with DNA.

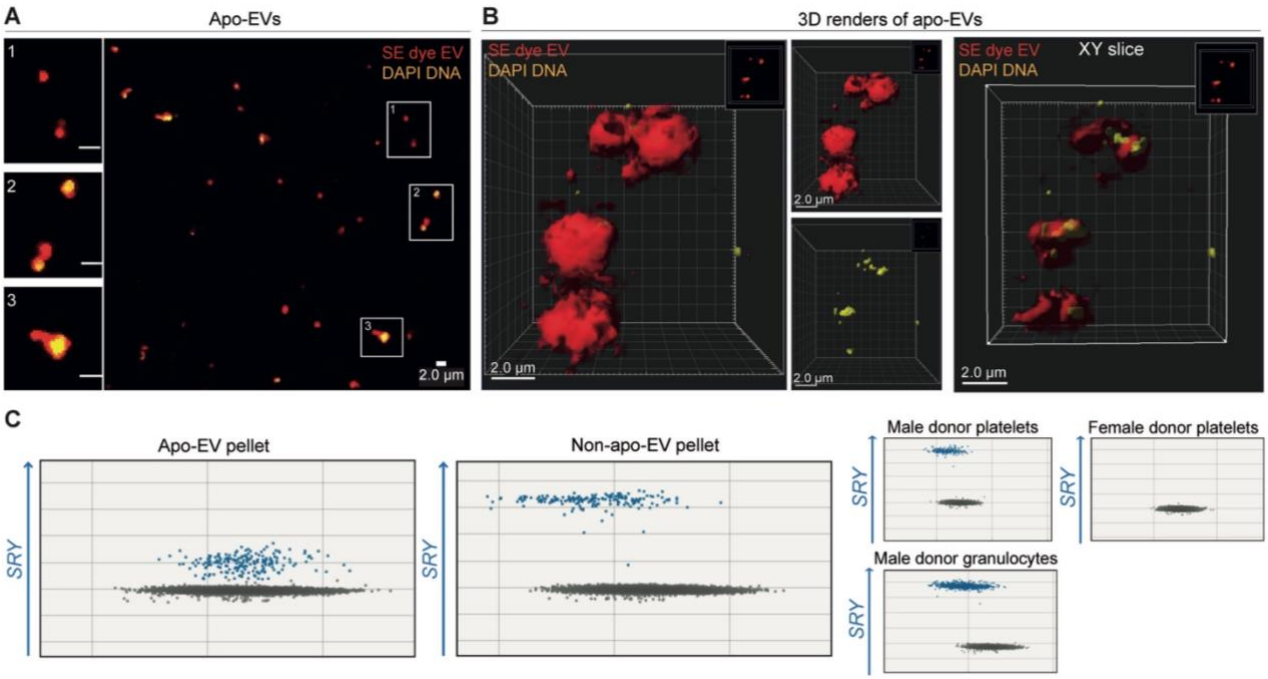


Figure 4-10. Extracellular vesicles contain genomic DNA. (A) Internalised DNA observed in extracellular vesicles (EVs) isolated from apoptotic (apo) Burkitt's Lymphoma (BL2) cells labelled with an amine-reactive, succinimidyl ester (SE) EV membrane dye (CF658, red) and DNA stain (DAPI, yellow). Insets show magnified regions, scale bars represent 2 µm. **(B)** Left- 3D reconstruction of a cluster of EVs released by apoptotic BL2 cells labelled with SE membrane dye (CF658, red) and DNA stain (DAPI, yellow) reveals internalised DNA. Right- DAPI labelled DNA is visible throughout the vesicles as shown by the cross section. Imaged using a ZEISS LSM900, 63X magnification. Representative vesicles shown. **(C)** Representative droplet digital (dd)PCR for the Y-chromosome gene *SRY* in DNA extracted from pelleted apoptotic and non-apoptotic EVs. n=3 independent EV generation and DNA extractions. Control samples are shown on the right, human platelets from a male donor, granulocytes from a male donor and platelets from a female donor.

ii) Platelets internalise DNA loaded apoptotic extracellular vesicles

I next sought to explore platelet uptake of these DNA containing vesicles. To do this I incubated healthy donor platelets (stained with CD42 AF488) with apoptotic and non-apoptotic EVs labelled with the amine-reactive, succinimidyl ester membrane dye. EVs were visible adherent to and within platelets following co-incubation (Fig. 4-11A). Co-staining the EVs with DAPI, prior to incubating with platelets confirmed the presence of DNA within the EVs, confirming that platelets *are* able to acquire DNA via the uptake of DNA loaded vesicles (Fig. 4-11B, Appendix Videos 6 & 7).

To track DNA transfer more specifically, ddPCR was used to quantify *SRY* alleles. Copies of *SRY* were detectable in platelets from female donors following incubation with EVs, and in significantly higher abundance following co-incubation with apo-EVs compared to non-apo-EVs (Fig. 4-11C). To confirm that *SRY* was specifically detected within internalised EVs from female platelets, I applied the platelet pelleting and washing protocol to the EV suspension (in the absence of platelets) to ensure EVs were not inadvertently co-pelleted with platelets. Encouragingly, DNA extracted from the pelleted material showed no *SRY* signal using ddPCR, indicating that the low centrifugation speeds used for platelet pelleting were inadequate for also pelleting EVs (Fig. 4-11C). EV cargo transfer to healthy human female platelets was further assessed using a polymerase chain reaction (PCR). Like the ddPCR data, *SRY* gDNA expression was observed only in platelets incubated with apo-EVs (white box). Male BL2 cells were used as the positive control (Fig. 4-11D). This PCR was carried out by Pamela Holland from the University of Edinburgh.

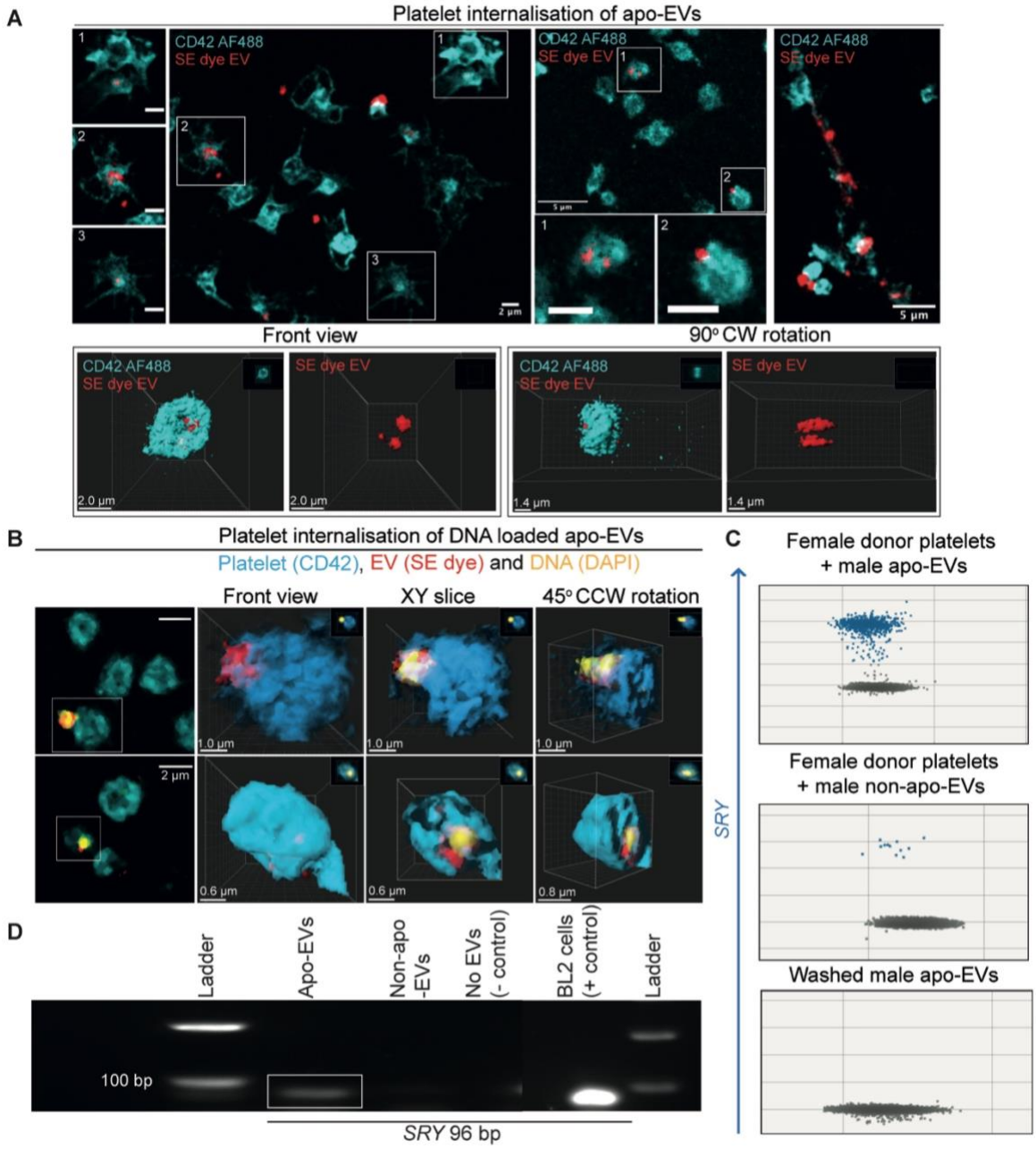


Figure 4-11. Platelets sequester DNA containing vesicles. (A) Top- following incubation with labelled EVs, platelets were stained with CD42 AF488 (cyan). EVs (red) were visualized in platelets, confirming platelet uptake of apo-EVs. White boxes show magnified regions, scale bars represent 2 µm. Bottom-3D modelling shows 90° rotation of platelet. **(B)** 3D reconstruction of platelet internalisation of DNA (yellow)-loaded apo-EVs (red). Two representative platelets shown. **(C)** Representative droplet digital (dd)PCR quantification of the Y-chromosome gene *SRY* in DNA derived from platelets of a female donor after incubation with EVs derived from male apoptotic BL2 cells (apo-EVs) vs. EVs from male apoptotic resistant BL2 cells (non-apo-EVs). No *SRY* was detected in washed apo-EVs. n=3 independent co-incubation experiments. **(D)** *SRY* gDNA was detected in female platelets following incubation with apo-EVs as indicated by the band at 96 base pairs (white box).

Overall, these data show that platelets can internalise exogenous DNA via the uptake of DNA-containing EVs. Next, I wanted to understand whether platelets could also internalise 'free' DNA fragments not encapsulated by a membrane i.e. not contained within EVs.

4-2.2 Platelet uptake of 'membrane free' DNA fragments of different lengths

To test whether platelets can sequester 'free' DNA fragments that are not contained within EVs, I exposed healthy donor platelets to synthetic DNA fragments ranging from 90 – 657 bp. I chose to incubate the DNA fragments with platelets at the physiologically relevant concentration of 10 ng/ml[405]. Following incubation, DNA was extracted from the platelets and PCR amplified using a universal primer pair. Automated gel electrophoresis showed that platelets efficiently internalised all tested DNA fragments, confirming that platelets can sequester non-membrane bound DNA of varying lengths (Fig. 4-12A).

4-2.3 Impact of DNA exposure on platelet immunophenotype and response to agonists

In a 2021 study by Lam *et al.,* it was discovered that upon binding with DNA, red blood cells exhibit decreased expression levels of the 'don't eat me' signal, CD47, leading to increased erythrophagocytosis[298]. Considering that platelets also bind DNA, I next wanted to investigate whether DNA internalisation influenced the immunophenotype and clearance of platelets. To explore this, I incubated platelets overnight with synthetic DNA fragments and used flow cytometry to measure surface expression of CD47 and the 'eat me' signal, calreticulin (CALR).

Unlike Lam *et al.,* I saw a small increase in CD47 expression for platelets incubated with DNA compared to controls, rather than a decrease. Although this increase loosely hints at a possible protective role by platelets, no decrease in surface expression of CALR was observed (Fig. 4-12B). Taken together, these data suggest that following platelet incubation with DNA, there is no immediate and obvious upregulation of pathways leading to increased platelet clearance.

I was also interested to understand whether DNA has a priming effect on platelets, particularly whether exposure to DNA causes the platelets to be hyperreactive in response to platelet agonists. To explore this, I isolated platelets from healthy donors and incubated washed platelets with and without synthetic DNA fragments. I then treated the platelets to increasing concentrations of the potent platelet agonist, TRAP-6. TRAP-6 is a synthetic thrombin analogue that activates platelets through binding to the main thrombin receptor, PAR-1. Using flow cytometry, I measured the expression levels of the platelet activation markers, CD63, P-selectin (CD62P) and PAC-1, to approximate for dense granule release, alpha granule release, and αIIbβ3 integrin activation, respectively. A one-hour incubation of platelets with 10 mg/ml DNA, prior to TRAP-6 activation did not result in any increase of platelet activation markers indicating no significant hyperreactivity compared to control platelets (Fig. 4-12C). The gating strategy of platelets incubated with resting buffer is shown in Appendix Data Figure 3.

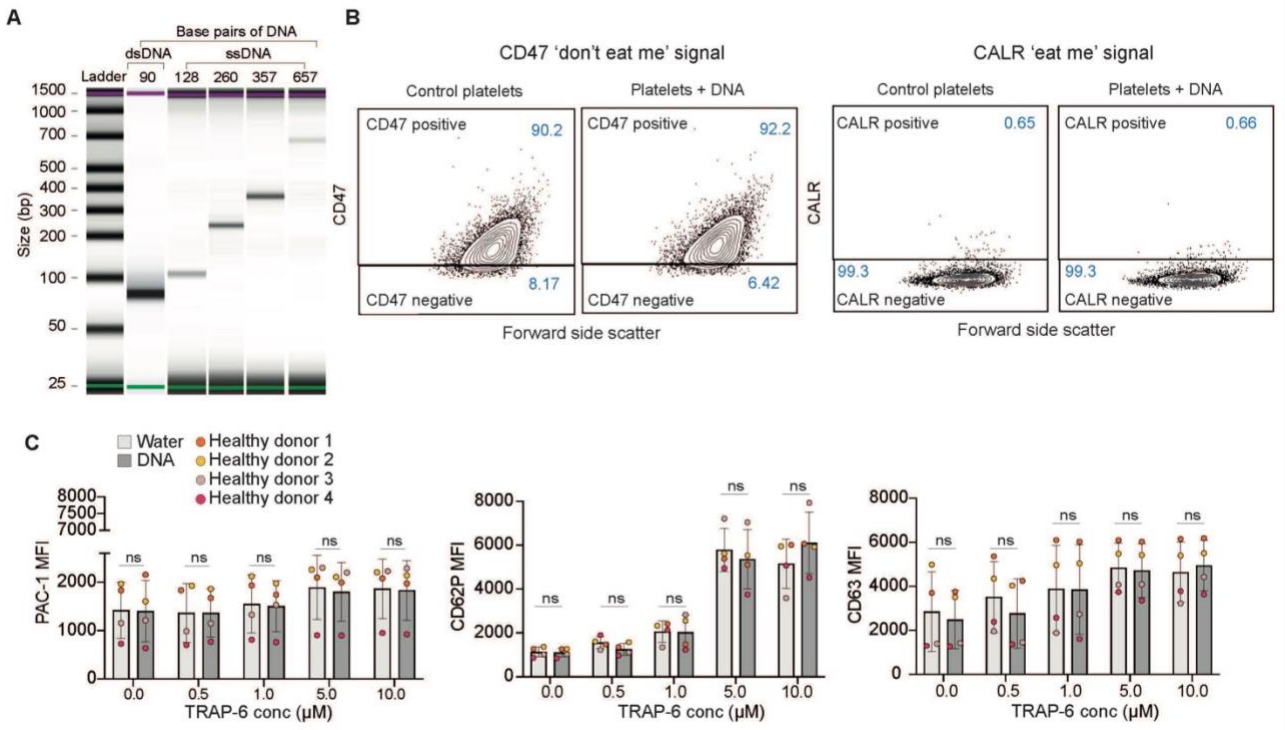


Figure 4-12. Platelet uptake of 'free' DNA fragments. (A) Representative electrophoresis analysis showing recovery of 90-657 bp synthetic DNA fragments from washed healthy donor derived platelets following overnight incubation with DNA fragments. **(B)** Flow cytometric data showing a small increase in CD47 positivity in platelets incubated with synthetic DNA fragments vs. without, n=10 donors. **(C)** Platelets were incubated with DNA or water and treated with 0, 0.5, 1, 5 and 10 μM TRAP-6. Flow cytometry was used to assess platelet activation. MFI for each activation marker is shown (n=4 healthy donors). Plot shows mean ± SD.

4-2.4 Inhibition of platelet cargo trafficking

To better understand how DNA fragments enter platelets, I treated platelets with a range of inhibitors known to block specific components of cargo trafficking including, inhibitors of actin (cytochalasin D), membrane ruffling/ macropinocytosis (imipramine), Na+/H+ exchange/ macropinocytosis (amiloride), clathrin (Pitstop 2), caveolae-dependent endocytosis (nystatin) and dynamin (Dynole) (Fig. 4-1).

Platelets were treated with inhibitors prior to exposure to either DNA-containing EVs from apoptotic BL2 cells or 'free' synthetic DNA fragments and washed prior to DNA extraction from the platelet pellet. I found that the DNA content of platelets following their exposure to apo-EVs was reduced by the dynamin inhibitor, Dynole. This indicates that the uptake of DNA-loaded apo-EVs is at least partially dynamin dependent, suggesting a role for clathrin- or caveolae-mediated endocytosis (Fig. 4-13A).

In contrast to the reduced platelet content of apo-EV-DNA following dynamin inhibition, I found that inhibition of platelets with both Dynole and amiloride significantly *increased* the amount of DNA obtained from the platelet pellet following exposure to synthetic DNA fragments that were not encapsulated in EVs (Fig. 4-13B). This was an unexpected observation and indicates that EV-associated and 'free' DNA fragments are taken up and processed by platelets using different endocytic routes.

Next, I sought to confirm whether this difference was due to the inhibitors blocking DNA release. To do this, I extracted and measured the amount of synthetic DNA secreted from platelets following treatment with or without Dynole. Interestingly, I found that Dynole treatment significantly reduced the release of DNA by platelets, into their media (Fig. 4-13C).

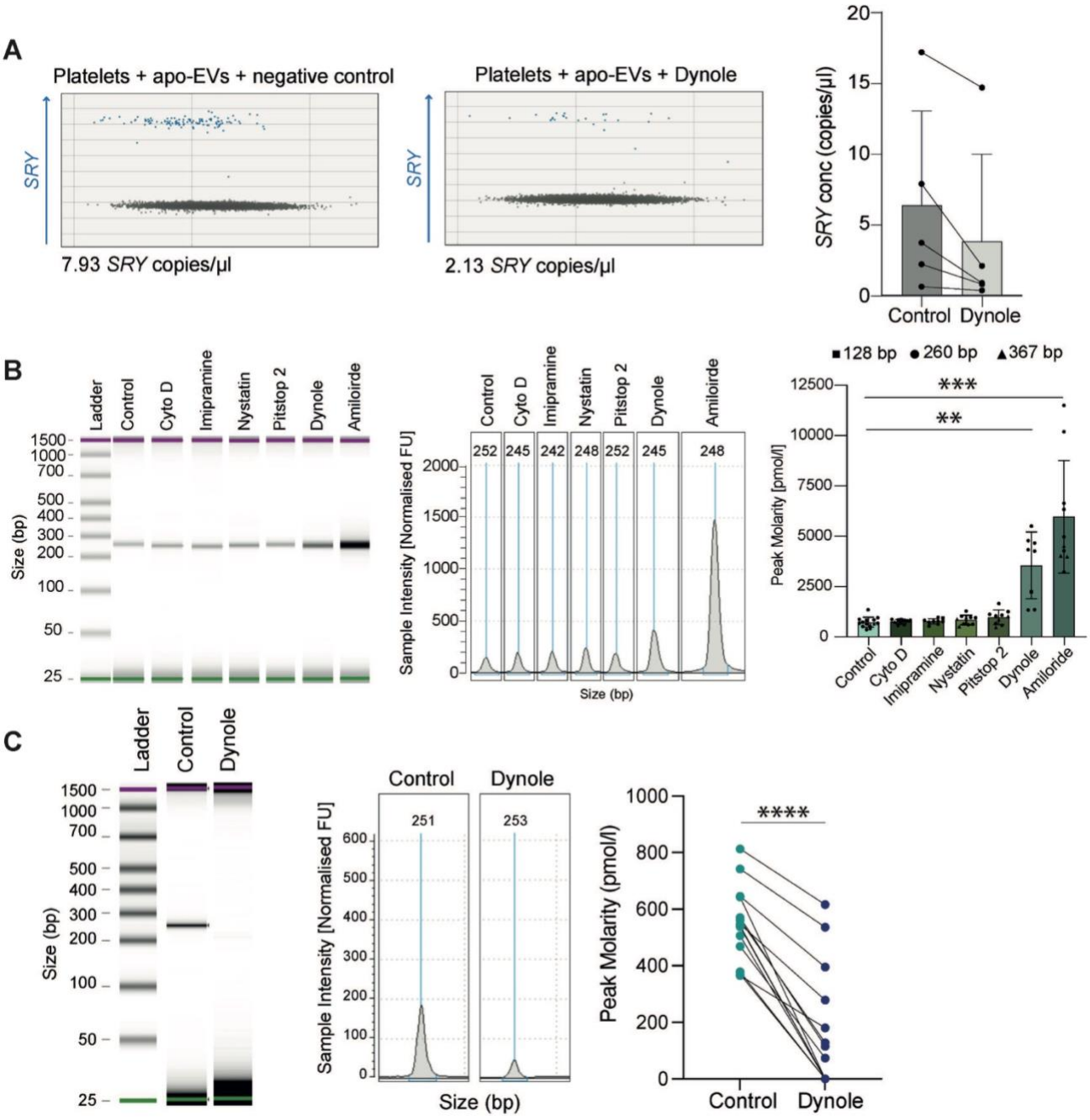


Figure 4-13. Platelet uptake of DNA-loaded extracellular vesicles and 'free' DNA fragments can be pharmacologically modulated. (A) Droplet digital PCR quantification of the Y-chromosome gene *SRY* in DNA derived from platelets of female donors after incubation with apo-EVs +/- a dynamin inhibitor (Dynole). Fewer copies of *SRY* were detected in dynamin-inhibited platelets than paired control (no inhibition). Plot shows mean ± SD, n=5. **(B)** Representative electrophoresis showing recovery of 260 bp synthetic DNA fragments from platelets treated with inhibitors known to block components of cargo trafficking (left and middle). More DNA was extracted from platelets treated with Dynole and amiloride (right). Summary plot shows mean ± SD peak molarity corresponding to DNA TapeStation peaks for all DNA fragment lengths (128 – 367 bp) following treatment with inhibitors. n=4, ** $p<0.01$, *** $p< 0.001$ for a paired t test. **(C)** Representative electrophoresis showing significant inhibition of DNA release from platelets into the buffer after dynamin inhibition. n=5 independent experiments. **** $p< 0.0001$ for a paired t test.

The findings presented thus far indicate that blocking cargo trafficking, which in turn inhibits platelet secretion, results in elevated platelet DNA content. To validate this hypothesis, I examined how Dynole and amiloride affect platelet CD62P expression. CD62P is stored inside the alpha granules of resting platelets, therefore its expression on the surface following activation, indicates granule secretion.

As expected, pre-treatment of healthy donor platelets with Dynole and amiloride, prior to activation with low dose agonists, reduced CD62P expression (Fig. 4-14). This strongly indicates that these cargo inhibitors *are* blocking DNA release resulting in increased DNA recovery. Ibrutinib was used as a positive control. This flow cytometry was performed by Natalie Jooss, a postdoctoral researcher in Beth Psaila's lab.

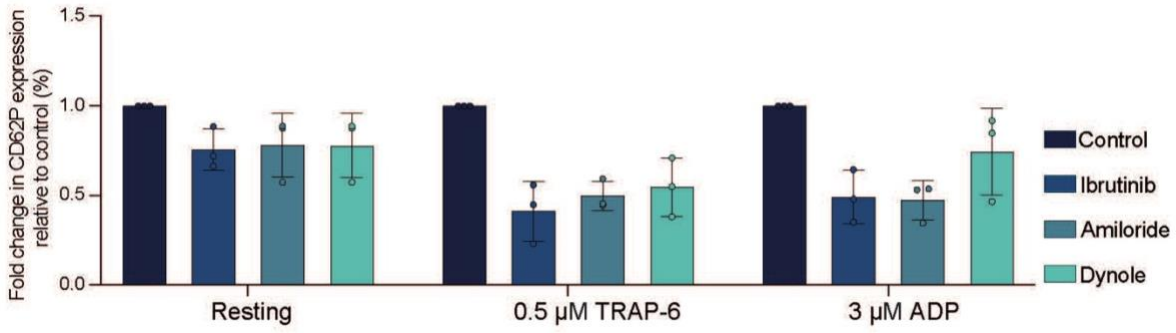


Figure 4-14. Inhibition of alpha granule secretion by Dynole and amiloride. Platelets from healthy donors were pre-treated with ibrutinib (positive control), amiloride, Dynole, or a vehicle control before activation with low doses of TRAP-6 (0.5 µM) and ADP (3 µM). CD62P expression levels were quantified using flow cytometry. Additionally, resting platelets were also analysed to ensure that ibrutinib, amiloride, Dynole, and the media in which they were resuspended did not cause platelet activation. The graph shows the fold change in CD62P expression relative to control platelets, mean ± SD, n=3 healthy donors.

4-2.5 Inhibition of platelet activation

Given that activated platelets secrete their granular content, I aimed to investigate the effect of activation inhibitors on platelet DNA levels. Specifically, I wanted to determine if inhibiting platelet activation, similar to inhibiting cargo trafficking, would result in increased platelet DNA content.

As described in the introduction, aspirin is considered the 'gold-standard' of antiplatelet therapies and works by inhibiting the formation of TxA_2. In addition to this, there is evidence to suggest that aspirin also impacts platelet secretion[406,407]. To investigate the impact of aspirin on platelet DNA content, I treated healthy donor platelets with increasing concentrations of aspirin (0, 500, 1000 and 2000 μM) before incubating them overnight with synthetic DNA oligos. Interestingly, I observed a significant increase in the amount of DNA extracted from platelets treated with the highest concentration of aspirin (2000 μM) compared to control platelets (Fig. 4-15A).

As well as aspirin, I tested the effect of ibrutinib on platelet DNA content. Ibrutinib is a powerful platelet activation inhibitor that covalently binds to the enzyme Btk, thereby blocking its ability to amplify platelet activation signals. Like aspirin, treatment with ibrutinib resulted in a concentration-dependent increase in the amount of DNA recovered from the platelets (0, 5, 50, 100 and 200 μM, Fig. 4-15B). The inhibition of platelet activation by ibrutinib and subsequent reduction in granule secretion, as indicated by the expression levels of CD62P is shown above in Figure 4-14.

Together, these data support my hypothesis that the DNA content of platelets is largely influenced by their activation status and their ability to secrete captured DNA. Specifically, activated platelets undergo secretion, leading to a reduction in DNA content, whereas resting platelets retain a higher DNA content as they are not triggered to secrete it.

This hypothesis is further strengthened by additional flow cytometry, performed by Camelia Benlabioid, a postdoctoral researcher in Beth Psaila's lab. Here we show a *decrease* in platelet DRAQ5 expression upon activation with 10 μM TRAP-6 compared to unstimulated platelets (Fig. 4-15C & D). Additionally, it's worth highlighting the significantly higher baseline level of DRAQ5 staining in the healthy donors shown in here, compared to those reported earlier in this thesis (DRAQ5+ population: 19.1 % vs 8.0 % in chapter 3).

This significant difference in DNA staining can be explained by the activation state of the platelets studied. The platelets analysed in earlier experiments, such as those in Figure 3-5, were likely pre-

activated, as they were isolated from blood samples that were not handled in a way that minimised activation. As a result, the DNA content measured, likely reflects the residual amount remaining after platelet activation and granule secretion.

Subsequent flow cytometry, including the data presented in this chapter (Fig. 4-15D), used a protocol optimised to maintain platelets in their resting state. This involved using fresh blood (< 1 hour old) collected in citrate tubes rather than EDTA-treated blood that was approximately 24 hours old. As expected, these analyses revealed that fresh platelets contain approximately twice the DNA content of platelets isolated from excess clinical samples such as those used in chapter 3. This finding underscores the importance of platelet preparation methods for accurate DNA content assessment and highlights the dynamic nature of platelet DNA in response to activation.

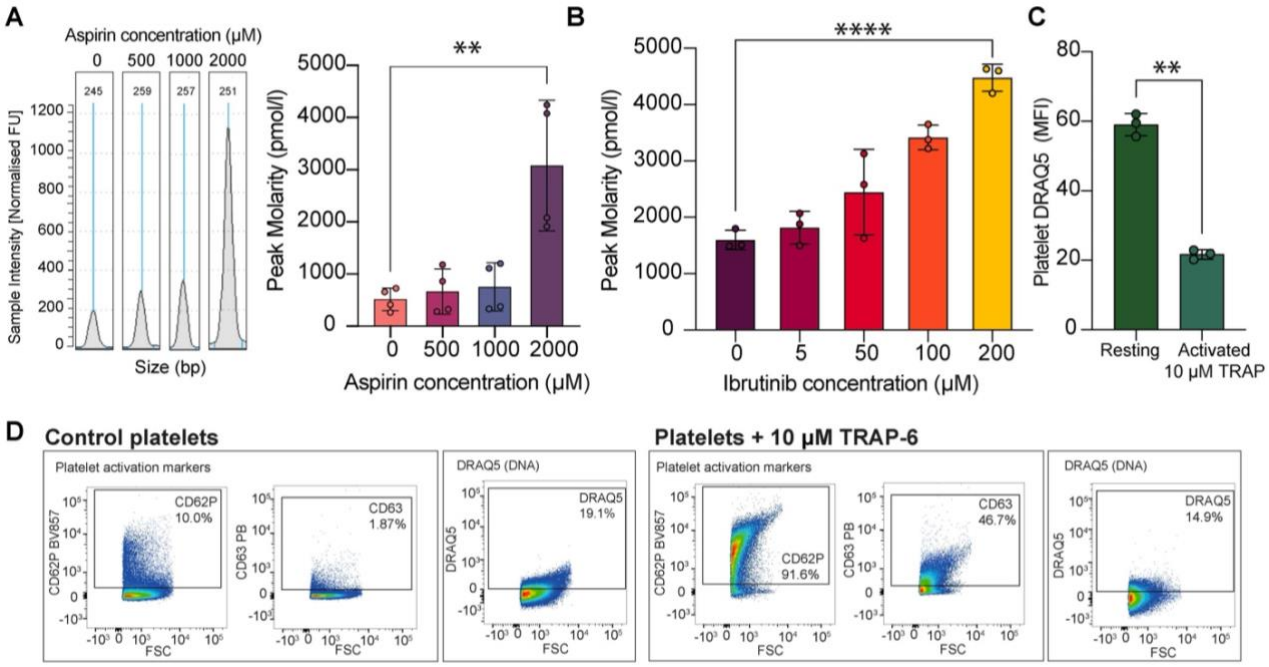


Figure 4-15. Inhibition of platelet activation increases platelet DNA content. (A left) Representative electrophoresis showing recovery of 260 bp synthetic DNA fragments from platelets treated with increasing concentrations of aspirin. ***(A right, B***) Inhibition of platelet activation with **(A)** aspirin or **(B)** ibrutinib increases the yield of DNA from platelet pellets. Plots show mean ± SD peak molarity corresponding to DNA TapeStation peaks for synthetic DNA fragments co-incubated with platelets prior to washing and DNA extraction. ** $p<0.01$ and **** $p<0.0001$ for an unpaired t test, n=3-4. **(C)** Flow cytometric analysis of CD42+ healthy donor-derived platelets, stained with the DNA marker DRAQ5 +/- activation with 10 μM TRAP-6, ** $p<0.01$ for a paired t test, n=3 experiments, mean ± SD. **(D)** Activation of healthy donor platelets with 10 μM TRAP-6 increases the expression of the CD42+ platelet activation markers CD62P and CD63, while decreasing the percentage of platelets showing a positive DRAQ5 signal, n=3 healthy donors, plots show samples concatenated.

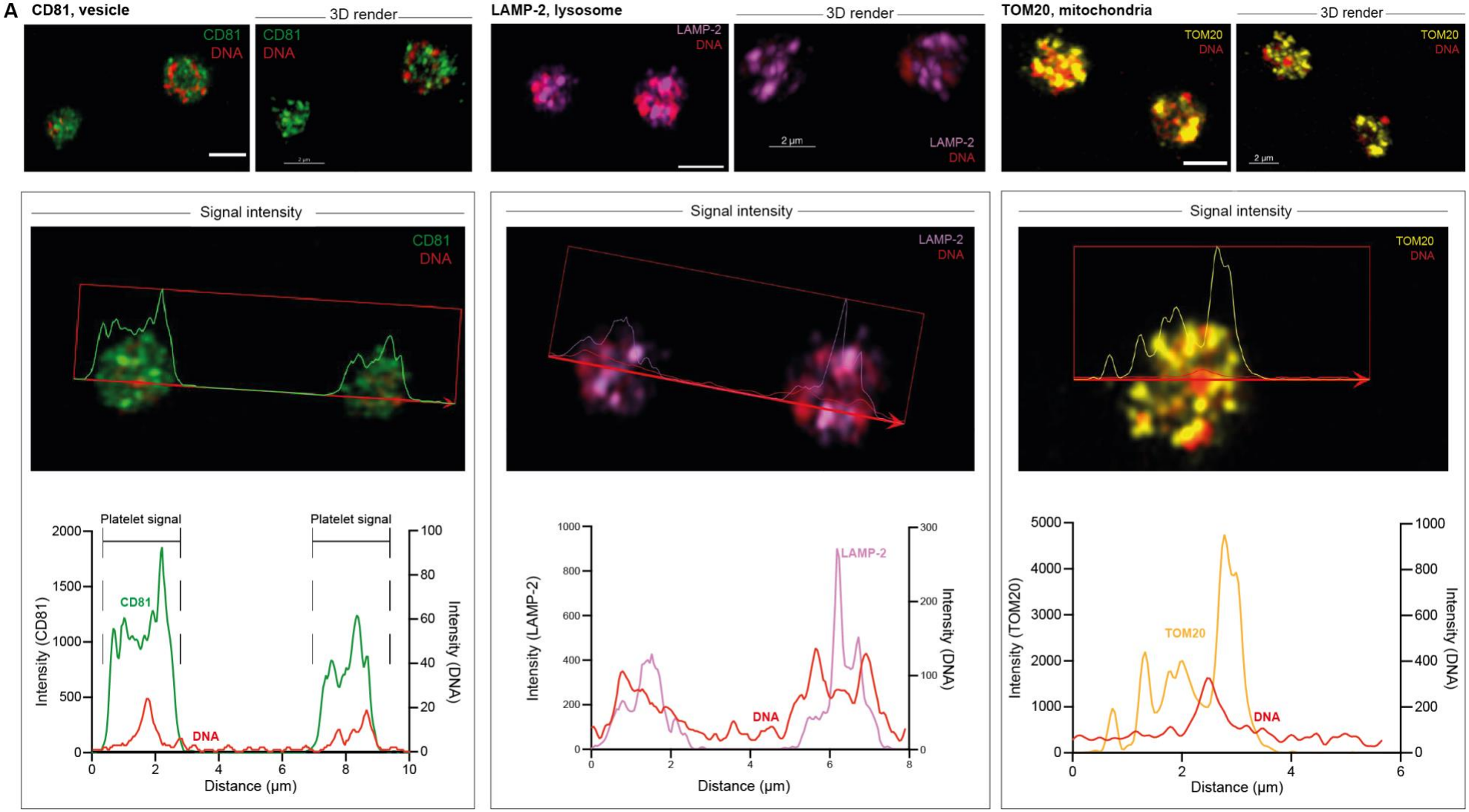
4-2.6 DNA is internalised by the platelets

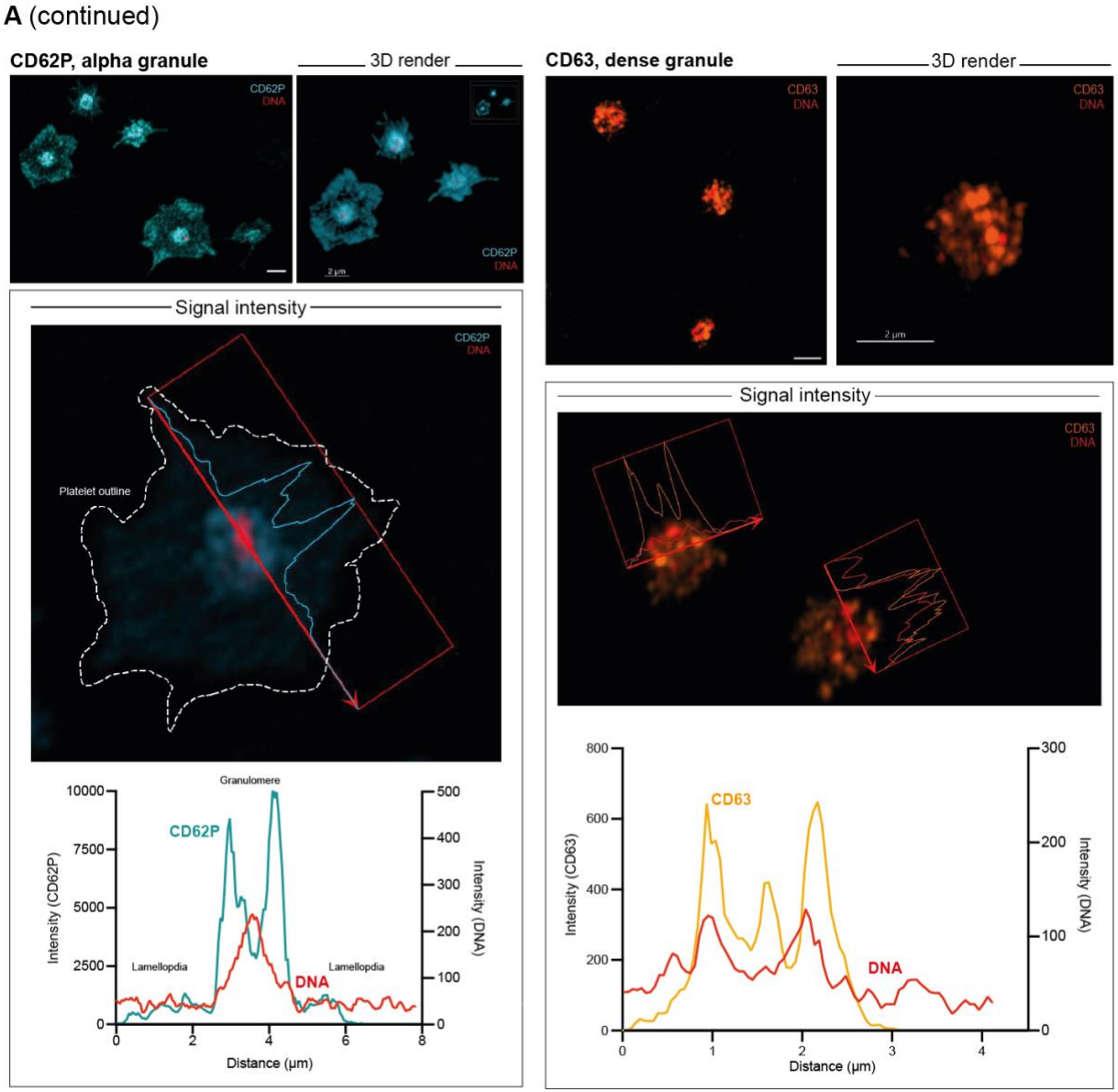
The data presented thus far indicate that platelets take up DNA. However, it is currently unclear where the DNA is located, and whether it is internalised into the platelet or remains stuck to their outer membrane. Of note, the definition of 'inside' the cell is more complex for platelets than for other cell types, due to their unique morphology that includes the open canalicular system (OCS) –a network of surface-connected membrane channels that run through the platelet interior and plays an important role in the uptake and release of molecules, but also acts as a 'reserve' of additional membrane during platelet spreading. Therefore, molecules contained within the OCS are in the platelet interior but not actually intracellular.

As described in the introduction, the trafficking of molecules into the platelet interior can occur via multiple mechanisms, including endocytosis (both clathrin-dependent and independent) and phagocytosis[111,327,329]. Once internalised, cargo undergoes sorting processes. It may be directed to intracellular storage granules, recycled back to the cell surface or transported to lysosomes for degredation[327]. To examine whether DNA is transported into the interior of the cell and determine whether sequestered DNA is directed to specific granular compartments, I performed Airyscan imaging on platelets stained with the DNA marker DRAQ5 (red) and either LAMP-2 (lysosomes, pink), CD63 (dense granules, orange), CD62P (alpha granules, blue), TOM20 (mitochondria, yellow) or the commonly recognised vesicle marker, CD81 (exosomes, green).

DNA was clearly visible in the platelet interior, adjacent to the intracellular organelles and vesicles (Fig. 4-16A). The pixel intensity distributions for DRAQ5, CD81, and LAMP-2 indicate strong colocalization among DNA, vesicles, and lysosomes within platelets. The DRAQ5 fluorescence pattern closely resembles those of CD81 (green) and LAMP-2 (pink), suggesting that DNA and granules are similarly distributed throughout the platelet. In contrast, the mitochondrial marker TOM20 exhibits a distinct pattern. Increases in TOM20 intensity (yellow) do not correspond with increases in DRAQ5 signal, indicating that the mitochondrial distribution differs from that of DNA.

Co-localisation analyses, performed by Paul Rees from Swansea University, confirmed no significant correlation between DNA localisation and mitochondria (Mander's coefficient of 0.2148 and Pearson correlation of -0.1742 for 10 platelets, Fig. 4-16B). However, the same analysis confirmed a strong correlation between DRAQ5 and CD81 and DRAQ5 and LAMP-2 (Mander's coefficient >0.5 for both markers). Overall, these data suggest that platelet DNA is not restricted to mitochondrial DNA and is instead contained within vesicles, and/or upon internalisation, is trafficked to degradative lysosomal compartments.


A
CD81, vesicle
3D render
CD81
DNA
LAMP-2, lysosome
LAMP-2
TOM20, mitochondria
TOM20
2 µm
Signal intensity
Platelet signal
Intensity (CD81)
Intensity (LAMP-2)
Intensity (TOM20)
Intensity (DNA)
Distance (µm)


A (continued)
CD62P, alpha granule
3D render
CD62P
DNA
Signal intensity
Platelet outline
Granulomere
Lamellopdia
Lamellopdia
Intensity (CD62P)
Intensity (DNA)
Distance (µm)
CD63, dense granule
CD63
Intensity (CD63)

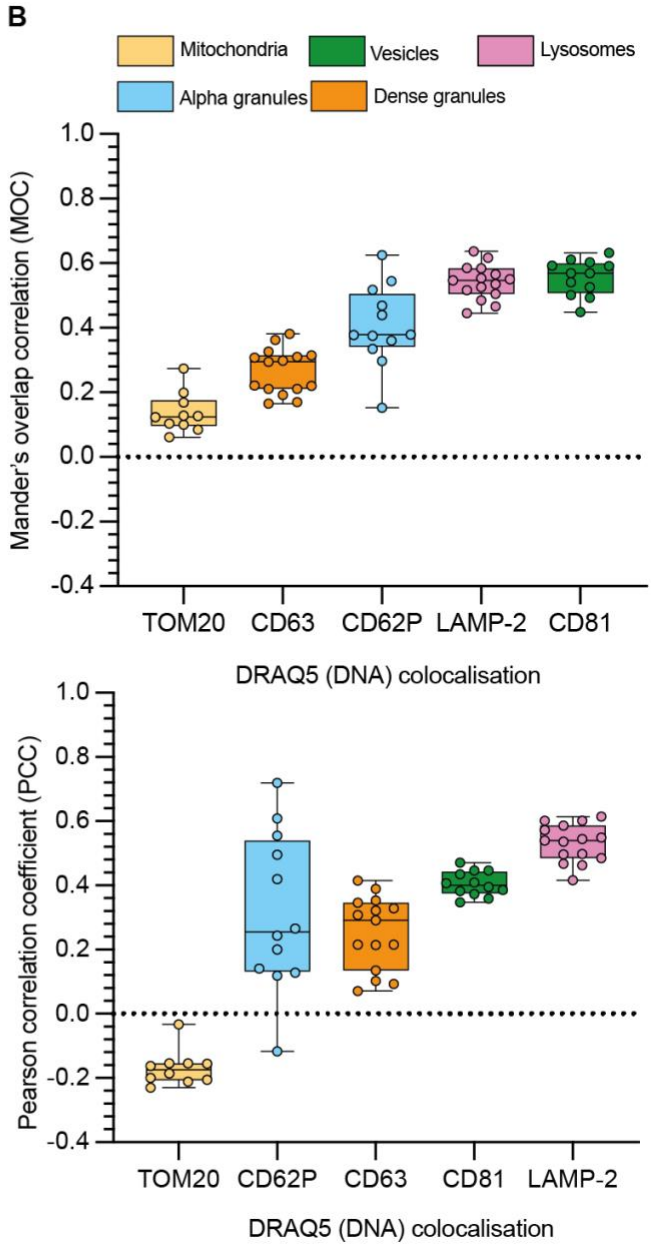

B
Mitochondria
Vesicles
Lysosomes
Alpha granules
Dense granules
Mander's overlap correlation (MOC)
TOM20
CD63
CD62P
LAMP-2
CD81
DRAQ5 (DNA) colocalisation
Pearson correlation coefficient (PCC)

Figure 4-16. Platelets internalise DNA. Healthy donor washed platelets were permeabilised, fixed and stained with DRAQ5 (DNA), TOM20 (mitochondria) LAMP-2 (lysosomes), CD63 (dense granules), CD81 (exosomes) and CD62P (alpha granules). **(A)** Representative high-resolution images demonstrating the intracellular localisation of platelet DNA (DRAQ5, red) and either LAMP-2 (lysosomes, pink), CD63 (dense granules, orange), CD62P (alpha granules, blue), TOM20 (mitochondria, yellow) or CD81 (vesicles, green). ZEISS, Zen Microscopy Software was used to process images and analyse pixel intensity (signal intensity, y axis) along defined lines (distance μm, x axis). Imaris Viewer was used to generate 3D renders of representative platelets. Images were acquired using the Airyscan detector of a ZEISS LSM980. Scale bars represent 2 μm. All images within the same channel were captured using identical exposure times and laser intensities to ensure comparability. For representative image generation, brightness and contrast were adjusted individually to optimize visibility of key features. However, all quantitative analyses were performed on the unmodified raw data to maintain accuracy and consistency. **(B)** Box plots showing the correlation between platelet DNA and platelet organelles and intracellular granules, using Manders' (left) and Pearson's (right) coefficients. The central line in each box represents the median value, with the upper and lower edges of the box indicating the first (Q1) and third (Q3) quartiles, respectively. Whiskers extend to the smallest and largest values within 1.5 times the interquartile range (IQR) from Q1 and Q3. Mander's correlation offers a more reliable assessment of correlation when dealing with signals of varying intensities[408]. The variability in data points seen with CD62P in the Pearson's correlation analysis can be attributed to the significant differences in signal intensities between DNA and alpha granules. The number of platelets analysed for each marker is as follows: TOM20 (10), LAMP-2 (15), CD63 (15), CD81 (12), and CD62P (12).

During platelet activation, CD62P is expressed on the platelet membrane where it acts as a reliable indicator of the platelet perimeter. Using Airyscan imaging of CD62P labelled platelets, I created a 3D mask to better understand the location of platelet DNA in relation to the platelet membrane. DRAQ5 stained DNA was clearly visible within the interior of the platelet and was largely concentrated within the granulomere (centre) of the platelet (Fig. 4-17A). During platelet spreading, tension causes the OCS to collapse, leading to the complete evagination of the membrane reserve onto the plasma membrane surface[33,409]. This process externalizes cargo retained in the OCS, meaning any DNA within these channels would be lost[48]. However, DRAQ5 DNA remains visible at the centre of the platelets even after spreading, suggesting that the DNA is in the 'true' interior of the platelet and not held within the OCS.

DNA internalisation was confirmed through the analysis of DRAQ5 pixel intensity, performed by Paul Rees from Swansea University. Briefly, DNA intensity was measured within a 3D mask of the platelet, generated by thresholding CD62P. The mask was subsequently computationally eroded pixel by pixel from the edge of the platelet towards the centre. DNA intensity was re-calculated as each new (smaller) mask was generated. This was repeated until one pixel remained and then plotted as DNA intensity (y axis) against eroded distance from the centre of the platelet (x axis, Fig. 4-17B). The plot clearly shows that DNA intensity is strongly localised in the centre of the platelet.

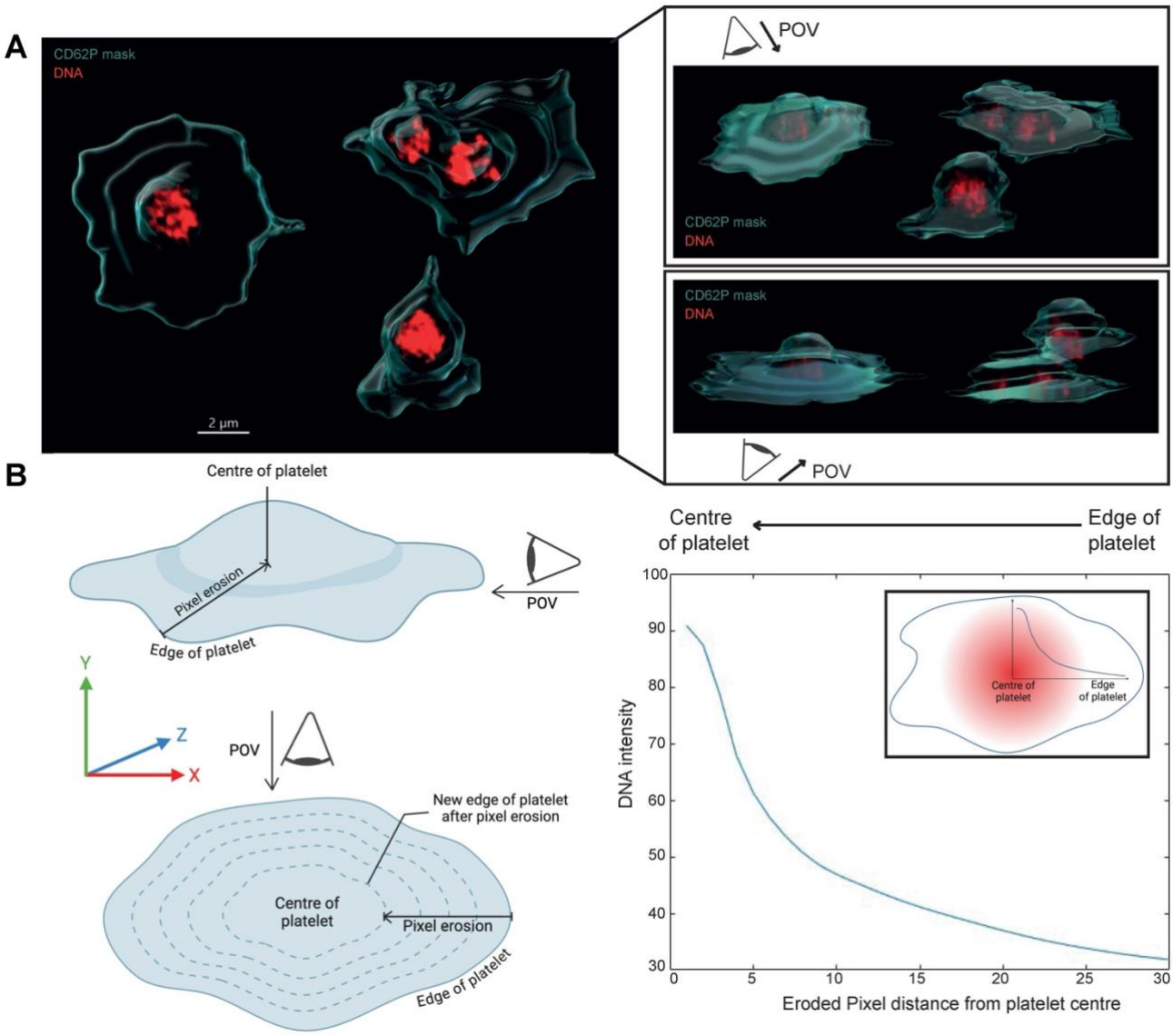


Figure 4-17. Platelet DNA is localised at the centre of platelets. (A) 3D renders of CD62P labelled, healthy donor platelets spread on collagen. The turquoise, translucent CD62P mask clearly shows red, DRAQ5 labelled DNA at the centre of three platelets. Right panel shows alternate views of the same platelets from above (top) and below (bottom). Imaris Viewer was used to generate 3D renders of representative platelets. Images were acquired using the Airyscan detector of a ZEISS LSM980. Scale bar represents 2 µm. **(B)** Left, schematic outlining the method used by Paul Rees to measure DRAQ5 pixel intensity. CD62P was used to generate a 3D platelet mask which was subsequently eroded pixel by pixel towards the centre of the platelet. Intensities along the X, Y, and Z planes were calculated. Right, pixel intensity (y axis) was plotted against distance from platelet centre (x axis). DNA (DRAQ5) signal is strongest at the centre of the platelet. Created using Biorender.com.

Overall, these imaging data suggest that platelet DNA is largely internalised into the platelet, rather than adherent to the outer membrane or held within the membrane tunnels of the OCS.

i) DNA fragments are protected from enzymatic degradation

To confirm complete internalisation of DNA by platelets, I tested whether the sequestered DNA was protected by the platelet membrane from external nuclease digestion. To do this, platelets were incubated with synthetic DNA fragments and then treated with DNase. The experimental set up is outlined in Figure 4-18A. Briefly, platelets and buffer (serving as an analogue for cfDNA) were incubated with synthetic DNA fragments overnight. After incubation, DNase was added to degrade free DNA fragments, and the remaining DNA in the platelets and conditioned media was extracted using the QIAamp Circulating Nucleic Acid Kit. Target-specific primers were used to amplify the extracted DNA, and the fragments were detected using the TapeStation. Platelet-sequestered DNA was successfully recovered even after DNase treatment, whereas DNA fragments incubated in the buffer without platelets were rapidly degraded and became undetectable (Fig. 4-18B).

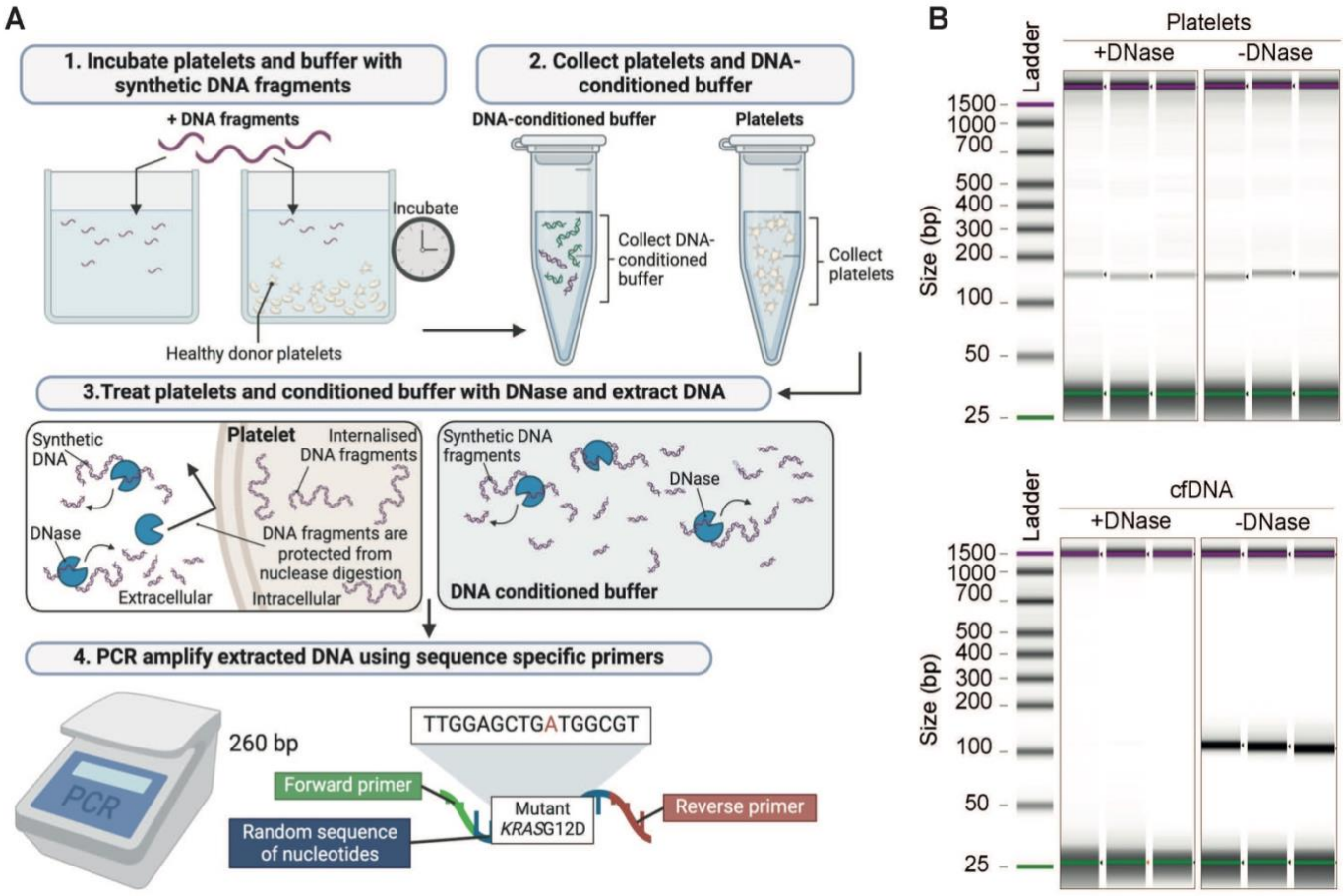


Figure 4-18. Platelet DNA is protected from nucleases. (A) Platelets and buffer (analogous to cfDNA) were incubated with synthetic DNA fragments overnight, followed by DNase treatment to degrade free DNA. The remaining DNA as then extracted, amplified with target-specific primers, and detected using the TapeStation. **(B)** Representative electrophoresis showing recovery of synthetic, 128 base pair (bp) DNA fragments from buffer with (top) and without (bottom) healthy donor derived platelets after treatment +/- DNase, n=3. Created using Biorender.com.

4-2.7 Box 2. Summary of findings in Aim 2:

1. Platelets sequester DNA by at least two mechanisms – uptake of DNA-loaded EVs released by apoptotic cells, and uptake of 'free' DNA fragments.
2. Platelet uptake of DNA-loaded EVs is partially dynamin-dependent.
3. Dynamin inhibition does not impact the uptake of 'free' DNA fragments but does block the secretion of DNA fragments by platelets.
4. DNA fragments are internalised by platelets and not held within the OCS.
5. DNA colocalises with CD81- and LAMP-2- positive intracellular platelet compartments.
6. Platelets protect DNA fragments from nuclease digestion.

4-3 Discussion

The primary aim of this chapter was to understand the mechanism(s) by which platelets interact with and internalise DNA. The data presented here demonstrate that both EV-mediated and 'free' DNA fragments are taken up by platelets and processed by dynamin-dependent and independent routes. I show that these pathways can be pharmacologically modulated, and that inhibition of exocytosis increases the abundance of DNA preserved within the platelets. This latter finding is particularly exciting as it could provide an interesting avenue for future research, exploring whether platelet inhibition improves DNA recovery in liquid biopsies – we have filed a patent protecting this discovery, on which I am listed as a co-inventor.

Flow cytometry to assess platelet immunophenotype

After confirming the uptake of 'free' DNA fragments, I set out to explore the effect of DNA internalisation on platelets. In section 4-2.3, I investigated how the immunophenotype of platelets changed following exposure to synthetic DNA by examining platelet activation markers and the phagocytosis regulatory signals, CD47 and CALR.

These initial experiments revealed no significant change in CALR, but a small increase in CD47 expression. Although these data suggest an intriguing theory that platelets are not cleared more rapidly after DNA uptake, there are some limitations to my approach.

Firstly, my analysis encompassed the entire platelet population exposed to DNA, rather than specifically focusing on DNA-binding platelets and comparing these to control platelets incubated with buffer. Based on the data presented in section 3-2.2, it's likely that only a small fraction of platelets actually take up DNA (~8%). Consequently, any subtle changes in the immunophenotype of DNA-interacting platelets may have been obscured, by the much larger percentage of platelets not binding DNA and therefore presenting a 'normal' immunophenotype. To address this limitation, future experiments should utilize fresh platelets to increase the proportion of DRAQ5-positive events and focus analysis specifically on those platelets demonstrating DNA association. This could potentially reveal immunophenotypic changes that were previously masked.

Another factor to consider is whether CALR alone, is the most appropriate marker to use alongside CD47 to infer platelet survival. CALR is a very strong 'eat me' signal and is typically expressed in response to cellular stress during apoptosis or as a result of cellular damage or injury[399]. Incubation of platelets with pure, synthetic DNA may not be stressful enough to induce CALR expression but might result in the activation of other, more easily tiggered, platelet clearance signals. Therefore, future work exploring platelet clearance in response to DNA should also include other markers of apoptosis such as desialylation and phosphatidylserine (PS) externalization (Fig. 4-8A & 4-9). It is also important to highlight that all platelets generally circulate with high levels of CD47, as demonstrated by the control platelets in Figure 4-12. This makes detecting subtle changes in CD47 surface expression challenging, underscoring the need to explore alternative markers of platelet clearance in future studies.

Inhibition of platelet cargo trafficking

Although the six chemical inhibitors discussed in this chapter targeted the main endocytic pathways in platelets, there are additional clathrin-independent routes that I did not investigate. These pathways include the dynamin-dependent RhoA GTPase pathway and the dynamin-independent CDC42 and Arf 6 GTPase pathways. Considering that RhoA is essential for platelet secretion of alpha and dense granules, exploring its role in DNA trafficking could be a promising avenue for future research[410]. It's also important to note that the inhibitors chosen for these experiments were not the only drugs commercially available. It's possible that other chemicals may be more effective in inhibiting platelet endocytosis, leading to more pronounced effects on platelet DNA uptake and secretion.

However, determining the specific endocytic pathway(s) platelets use to process internalised DNA is likely to remain challenging if relying solely on pharmacological approaches, regardless of the number of inhibitors tested. This difficulty arises from two main factors. Firstly, many endocytic pathways share the same cellular machinery. For instance, actin remodeling, dynamin hydrolysis and membrane cholesterol are essential for multiple endocytic routes[411]. Overlaps such as these make it difficult to selectively inhibit a pathway of interest as inhibitors lack specificity and exert off-target effects. For example, Pitstop2, initially identified as a clathrin

inhibitor, has been shown to potently block the uptake of proteins that typically enter cells through clathrin-independent routes[412,413].

Secondly, platelets have many redundant and compensatory mechanisms. This ensures that if one pathway fails, numerous backup mechanisms are in place to maintain overall platelet function. Consequently, it is likely that platelet DNA uptake is mediated by multiple pathways, rather than a single pathway that can be completely inhibited by any one inhibitor. Both factors- shared cellular machinery and functional redundancy, should be taken into account when assessing the effect of inhibitors on platelet endocytosis.

Unexpected increase in platelet DNA content induced by Dynole and amiloride

As shown in Figure 4-13B, I observed a significant increase in the amount of DNA extracted from amiloride and Dynole-treated platelets. Although initially unexpected, I hypothesize that this increase in DNA recovery may stem from the platelet's inability to release the sequestered DNA in the form of granules or platelet microparticles (PMPs).

As previously described, amiloride primarily blocks the activity of the sodium-hydrogen exchanger (NHE), thereby disrupting intracellular pH regulation and sodium homeostasis. However, since NHE activity is often coupled with other ion transporters, amiloride mediated inhibition of Na^+/H^+ exchange likely indirectly impacts other signalling pathways within the platelets as well. For example, NHE activity is closely linked to the sodium-calcium exchanger (NCX). This membrane protein utilizes the sodium gradient generated by the NHE protein to export calcium ions from the cytoplasm in exchange for sodium ions[414,415,416]. Calcium is crucial for platelet activation and serves as the key signalling molecule in various pathways such as platelet aggregation, granule secretion and cytoskeletal rearrangement.

It's therefore possible, that in addition to its primary function of inhibiting NHE and disrupting intracellular pH, amiloride indirectly affects NCX-mediated calcium exchange. Dysregulated calcium transport is likely to result in impaired platelet functions, such as membrane blebbing, PMP release, and ultimately, impact DNA content (Fig. 4-19)[417].

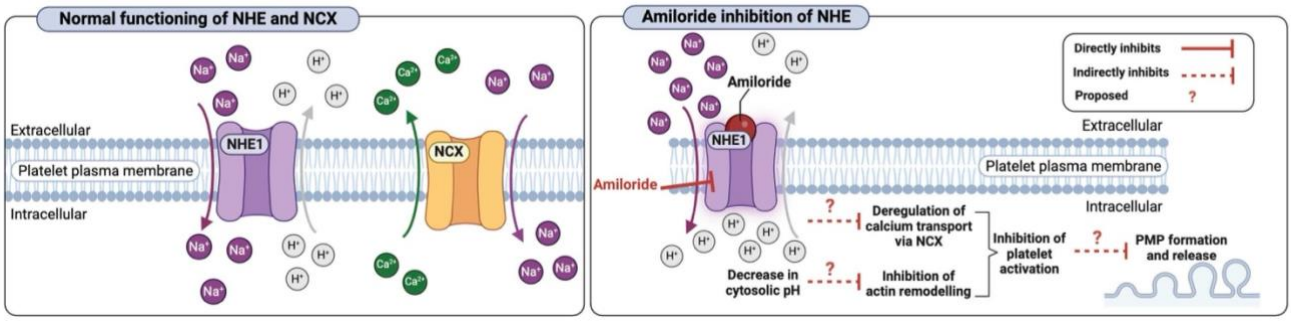


Figure 4-19. Proposed mechanism of action showing amiloride inhibition of the sodium-hydrogen exchanger (NHE) in the platelet plasma membrane. Left, the NHE protein regulates cytosolic pH by exchanging intracellular hydrogen ions for extracellular sodium in a 1:1 ratio. Right, amiloride induced inhibition of the NHE protein likely impacts intracellular pH, NCX-mediated calcium exchange and cytoskeletal rearrangement. Created using Biorender.com.

Although dynamin is primarily recognised for its role in endocytosis, there is evidence to suggest it also mediates membrane fission during platelet granule secretion[23,41,418,419]. Therefore, inhibition of dynamin likely affects the formation of the fusion pore, which facilitates the release of granule contents. If platelet-sequestered DNA is packaged within these granules for secretion, dynamin inhibition might block the release of DNA-containing granules, resulting in both DNA accumulation within the platelet as well as a reduction in the amount secreted.

While I could not find published literature verifying dynamin's direct involvement in PMP release, given that membrane fission is necessary for vesicle detachment, it's highly probable that dynamin, similar to the sodium-hydrogen exchanger, plays a role in both pathways; granule secretion and PMP release (Fig. 4-20).

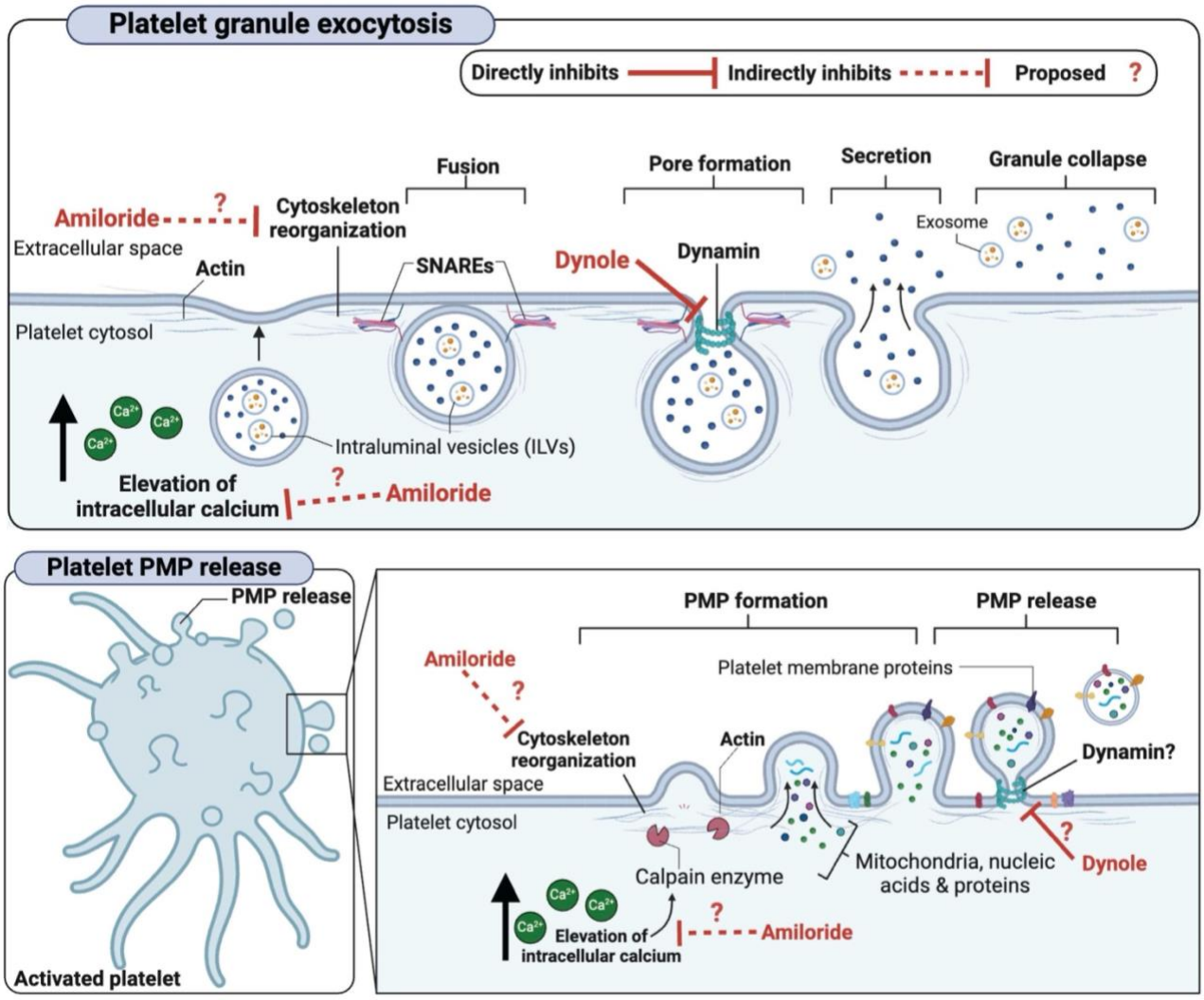


Figure 4-20. Proposed mechanism of action illustrating how treatment with Dynole and amiloride reduces platelet secretion. A summary of two secretory pathways found to be active in platelets and their proposed inhibition by Dynole and amiloride. Top shows the fusion of storage granules to the plasma membrane and eventual release of exosomes. Bottom shows the budding and release of PMPs. PMP release can occur at the plasma membrane and OCS. Both pathways rely on an increase in intracellular calcium and cytoskeletal rearrangement. During PMP release, calcium influx activates enzymes such as calpain which cleaves actin allowing it to remodel. Created using Biorender.com.

Overall, the data presented here demonstrate that the trafficking inhibitors Dynole and amiloride increase DNA recovery from platelets. Similar results were observed with activation inhibitors aspirin and ibrutinib. Collectively, these findings suggest that when treated with these drugs, the observed increase in platelet DNA is due to impaired platelet secretion. This hypothesis is further supported by flow cytometric data, which show that Dynole, amiloride, and ibrutinib all reduce CD62P expression, indicating strong inhibition of granule secretion (Fig. 4-14).

High resolution imaging of platelet ultrastructure

Fibrinogen, like CD62P, is stored in platelet alpha granules but is exclusively derived from plasma[420]. This highlights that platelet alpha granules contain both internally synthesised proteins and those acquired through endocytosis. Based on this, I questioned whether internalised DNA might follow similar intracellular trafficking pathways within platelets[421].

Co-localisation analysis of the Airyscan images, as described in section 4-2.6, showed little correlation between DNA, CD62P, and CD63, suggesting that DNA is unlikely stored in alpha or dense granules. However, the data indicate that platelet DNA is associated with CD81-positive exosomes and/or transported to LAMP-2-positive, degradative lysosomal compartments. This supports the hypothesis that platelets aid professional immune cells in clearing excess inflammatory DNA from circulation.

To explore this further, I'm currently collaborating with Christopher Millington, a postdoctoral researcher from the WIMM, to study platelet-mediated DNA digestion using mass spectrometry. This highly sensitive technique allows for the analysis of DNA fragmentation down to single labelled nucleosides.

Finally, the data presented in Figure 4-17 demonstrate the internalisation of DNA within platelets, as indicated by the DNA signal intensity relative to the CD62P-masked outline. While this provides strong indication that DNA is localised at the centre of the platelet, it is important to consider two key limitations of this approach.

Firstly, these observations were made using activated, spread platelets. In resting platelets, alpha and dense granules are randomly dispersed throughout the cytoplasm, whereas upon activation, these granules become clustered in the platelet's centre[373,422]. Given this reorganization, the localisation of internalised DNA in resting platelets may differ from what I observed given that I only imaged spread, and therefore activated platelets.

Secondly, as previously demonstrated, platelets release DNA upon activation. Consequently, the DNA observed in these spread platelets likely represents only a portion of the total DNA initially captured, as some may have been lost during the spreading process. These factors suggest that the current analysis may not provide a complete picture of DNA internalisation and localisation in platelets across different functional states.

To overcome these limitations and gain a more detailed understanding of DNA dynamics in platelets, future research should include imaging of resting platelets. Since resting platelets are smaller and more compact than activated platelets, this approach will likely require higher resolution imaging. Nevertheless, it would enable a direct comparison of DNA localisation between resting and activated platelets, providing deeper insights into how platelet activation state influences DNA internalisation and distribution.

Summary

In conclusion, the findings in this chapter reveal that platelets sequester EV derived and ‘free’ DNA fragments. My current hypothesis is that DNA-containing EVs are actively taken up by platelets through a partially dynamin-dependent mechanism. This is supported by ddPCR data, which show a reduction in EV-associated DNA in platelets following dynamin inhibition.

Regarding 'free' DNA fragments, since I haven't found an inhibitor that reduces their uptake, it seems likely that this internalisation occurs passively rather than actively. Once internalised, the DNA is trafficked into the interior of the platelet, where some is shuttled to lysosomes for degradation and some through the endosomal pathway where it is held prior to secretion upon platelet activation (Fig. 4-21). This could explain the observed increase in DNA fragments following the inhibition of platelet secretion; with less DNA being released and lost from platelets, more is recovered during DNA extraction.

Although additional work is required to fully understand the dynamics of platelet DNA uptake, the findings presented here offer new insights into platelet biology with clinical relevance. For example, using Dynole and amiloride to ‘seal’ DNA within platelets may protect it from nuclease degradation in plasma, potentially enhancing the clinical utility of platelet nucleic acid analysis in liquid biopsies. This is discussed further in chapter 6, section 6-4.3.

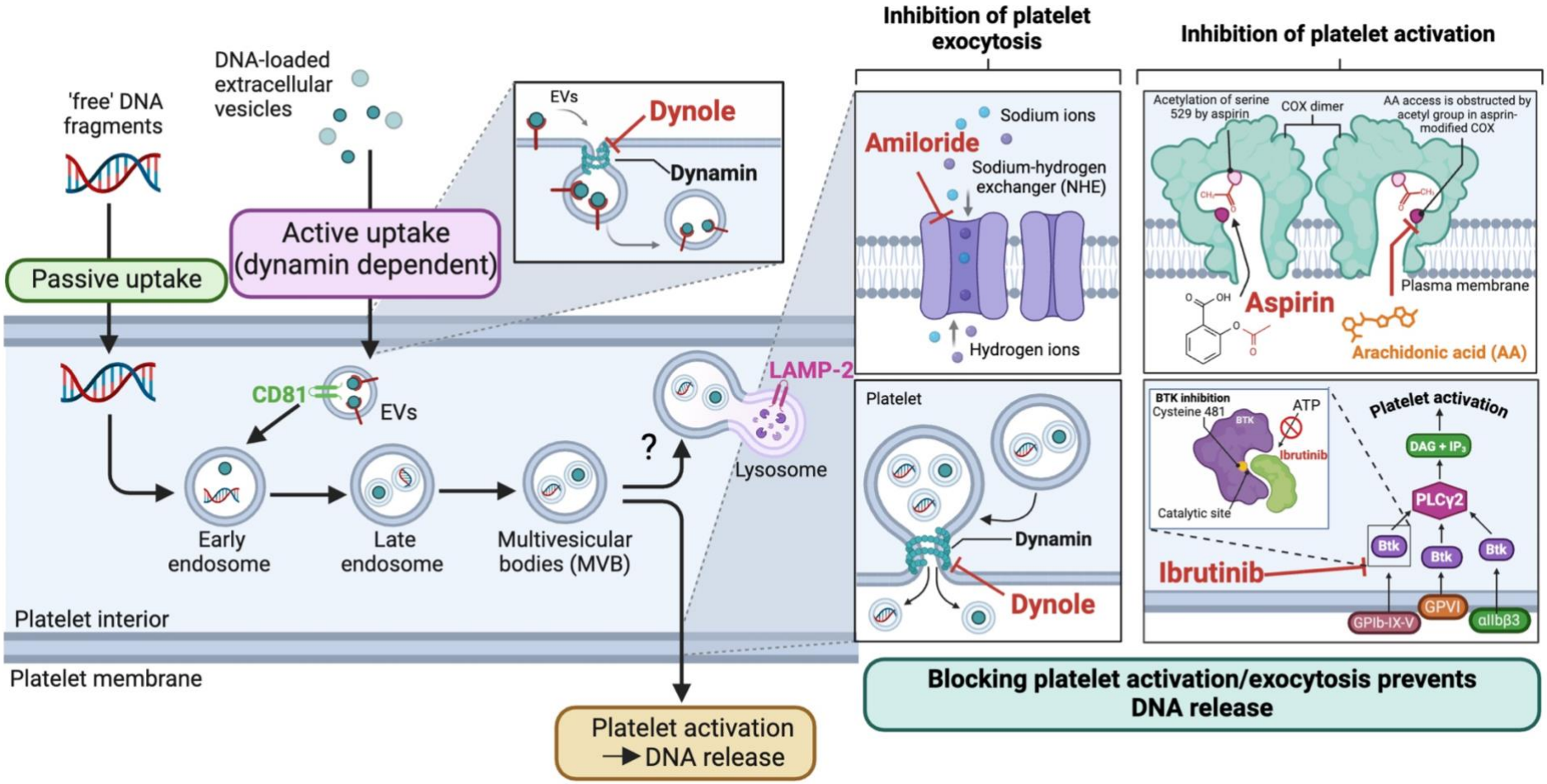


Figure 4-21. Proposed mechanism of DNA uptake by platelets. Platelets sequester DNA-containing extracellular vesicles through a mechanism that is partially mediated by dynamin. In contrast, the uptake of free DNA fragments occurs passively. Once internalised, the DNA is either trafficked to lysosomes for degradation or packaged into secretory vesicles for release. The secretion of sequestered DNA is an active process that can be pharmacologically blocked by cargo trafficking inhibitors such as amiloride and Dynole, as well as platelet activation inhibitors like aspirin and ibrutinib. Created using Biorender.com.

Chapter 5: Clinical utility of platelet DNA

5-1 Introduction

In this chapter I explore the clinical utility of platelet DNA. This introduction provides a concise overview of current liquid biopsy techniques and cell-free DNA biology, focusing on its production, fragmentation, and clearance mechanisms.

5-1.1 Liquid biopsy

Current cancer diagnostic protocols primarily rely on a combination of imaging techniques and tissue biopsies[423]. While tissue sampling is widely regarded as the 'gold standard' for mutation profiling, tissue biopsies have several significant drawbacks such as invasiveness, sample bias and limited accessibility to tumours located in hard-to-reach areas. Overall, these limitations restrict frequent and/or longitudinal monitoring. These limitations, and the fact that a single biopsy offers only a limited “snapshot” of the tissue, potentially missing the full genomic complexity of tumours or risking false negatives, has driven the search for less invasive diagnostic approaches, such as liquid biopsies[424].

Liquid biopsies are a minimally invasive diagnostic and monitoring technique that involves the analysis of biomarkers found in bodily fluids, primarily the blood. Current liquid biopsy targets include circulating tumour derived nucleic acids (ctDNA and ctRNA), circulating tumour cells (CTCs), tumour-derived extracellular vesicles (EVs), and more recently, tumour-educated platelets (TEP, Fig. 5-1). As well as being minimally invasive, the sampling of these circulating biomarkers can be performed repeatedly, providing a more comprehensive and dynamic picture of disease progression[425].



Biomarker	✗	✗	✗	✓	✓
TEPs	Platelet RNA profiles can be influenced by various non-cancerous conditions, complicating interpretation	Platelets are easy to activate leading to granule secretion and potential loss of information	Abundant and easy to isolate	Information possibly protected by membrane	Dynamic tumour interactions leads to a variety of tumour derived information
EVs	Lack of standardized protocols for sample handling and EV isolation	Lack of single EV protein expression	Very abundant	Stability of cargo is maintained and protected via membrane	Qualitative and quantitative information
ctDNA	Lack of standardised protocols for DNA isolation can lead to plasma DNA degradation	Low detection sensitivity and diluted by high WT background	Easily obtained from body fluids like blood, urine, or saliva, making it suitable for repeated sampling	Approaches to enhance the sensitivity of NGS are being developed	
ctRNA	RNA is very unstable, the naked half-life of which in plasma is ~15 seconds	The RNA profile can be influenced by non-cancerous conditions	Real time representation of gene expression	Diverse molecular information includes mRNA, miRNA, lncRNA	
CTC	Lack of standardised protocols due to physical and phenotypic heterogeneity	Extremely rare and very fragile	Direct tumour representation		

Figure 5-1. Advantages and disadvantages of current liquid biopsy biomarkers[424,426-430]. Created using Biorender.com. Abbreviations: TEP, tumour educated platelet; EVs, extracellular vesicles; ctDNA, circulating tumour DNA; ctRNA, circulating tumour RNA; CTC, circulating tumour cell.

5-1.2 Cell free DNA

Of the current liquid biopsy biomarkers, cell free-DNA (cfDNA) is the most extensively studied. Genomic material is released into body fluids by nucleated cells through numerous processes such as cell death, abnormal mitotic cycles, or regulated DNA extrusion. When extracellular DNA originates specifically from tumour cells, it is referred to as circulating tumour DNA (ctDNA). Because ctDNA carries the same genetic and epigenetic alterations as the tumour, its analysis offers significant potential for early cancer detection, monitoring of treatment responses, and disease surveillance[240,241].

The amount of circulating tumour DNA varies between tumour types. For example, ctDNA detection in patients with late stage pancreatic, ovarian and colorectal cancer is often higher than in patients with advanced brain, renal and thyroid cancers. This variability is likely due to tumour location but can also be explained by other factors such as tumour metabolism, histology and lymphovascular invasion[240,431,432].

5-1.3 Origin of cell free DNA

Several approaches have been developed to determine the tissue or cellular origin of cfDNA, including methylation profiling[264], fragmentation analysis[433,434] and nucleosome positioning[435].

The majority of cfDNA in the circulation of heathy individuals has been found to originate from cells of a haematopoietic origin (70-90 %)[436-438] with a fraction of cfDNA also derived from solid tissues such as vascular endothelial cells (~10%), neurons (~2 %) and hepatocytes (~1 %)[437,439,440].

5-1.4 Cell free DNA production

Under normal conditions, most cfDNA is believed to originate from programmed cell death (apoptosis), during which, caspase enzymes cleave DNA strands at specific sites[268]. This process creates a distinctive ladder-like pattern of DNA fragments, typically around 180-200 bp or multiples thereof, reflecting the wrapping of negatively charged DNA around positively charged core histones (147 bp) with an additional 20 bp of DNA protected by the linker histone (H1). This structure is termed a chromatosome (Fig. 5-2)[271,441,442].

Other mechanisms, such as necrosis and active release, also contribute to the cfDNA pool. However, the DNA fragments generated by these processes often exhibit different physical characteristics. For example, during necrosis, cells release DNA fragments that are usually longer (i.e., > 10 kb) and less consistent in size, contrasting with the neat, uniformly-sized DNA fragments that result from the controlled process of programmed cell death[443]. Examples of active secretion include the expulsion of nuclei by maturing erythroblasts[444], NETosis[445], and egestion of mtDNA[446,447].

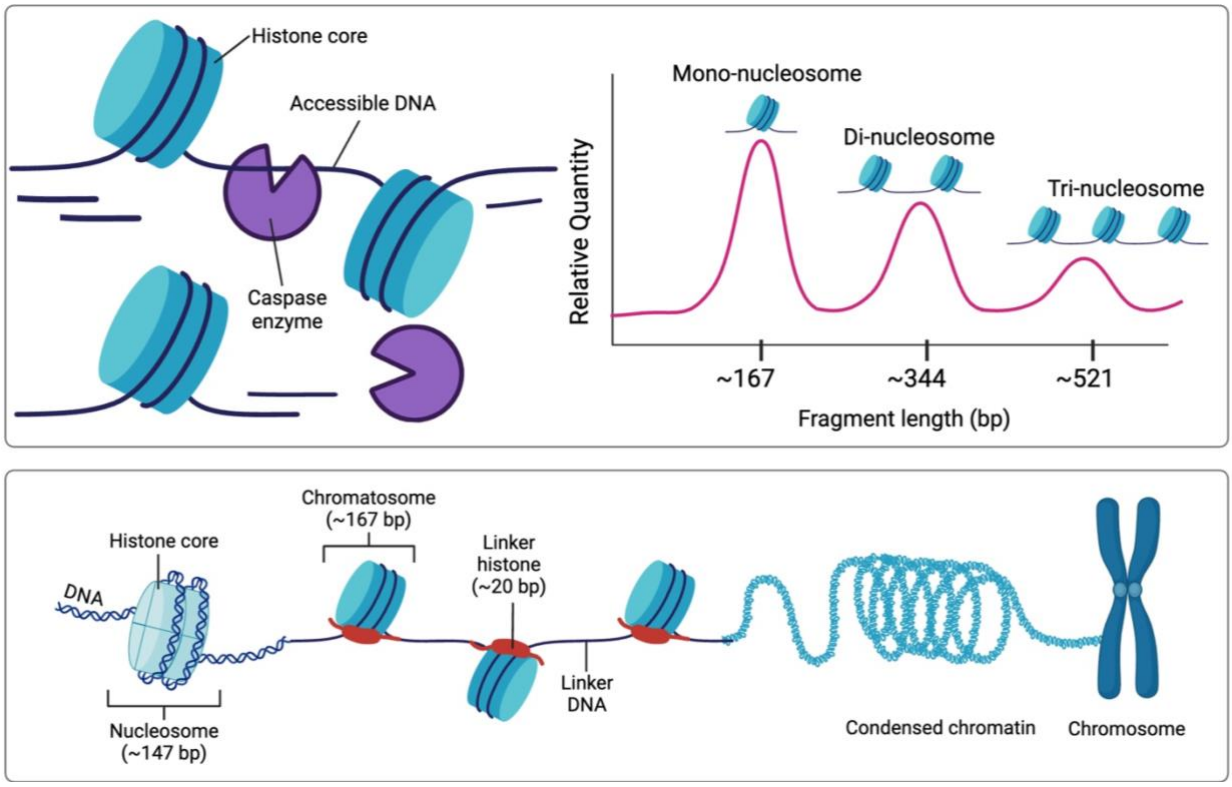


Figure 5-2. Fragmentation characteristics of cell free DNA. Top: cfDNA resulting from apoptosis is found in plasma as multiples of chromatosomes- DNA wrapped around a histone core along with a linker histone (~167 bp). Nucleosomes consist of DNA wrapped around the histone core, minus the 20 bp of DNA protected by the linker histone (~147 bp). Bottom left: During apoptosis, caspase enzymes cleave DNA at specific sites. Right: The plot displays the relative abundance and fragment length distribution of cfDNA, with the most common fragment length corresponding to that of a mono-nucleosome (~167 bp). Adapted from Underhill (2021)[448]. Created using Biorender.com.

Recent studies have shown that ctDNA is often enriched in shorter fragments, with a modal peak of 147 bp[268,269,270]. While the exact reason for this increased DNA fragmentation is not fully understood, it may be linked to changes in chromatin organization, which can create regions of open chromatin more vulnerable to enzymatic cleavage (Fig. 5-3)[449,450]. Given that a major challenge of using cfDNA for cancer surveillance is the low abundance of ctDNA, enrichment through fragment size selection has become a widely researched area[263,267,268,271-273]. Other approaches include whole genome sequencing (WGS)[262,263] and epigenetic analysis[264-267].

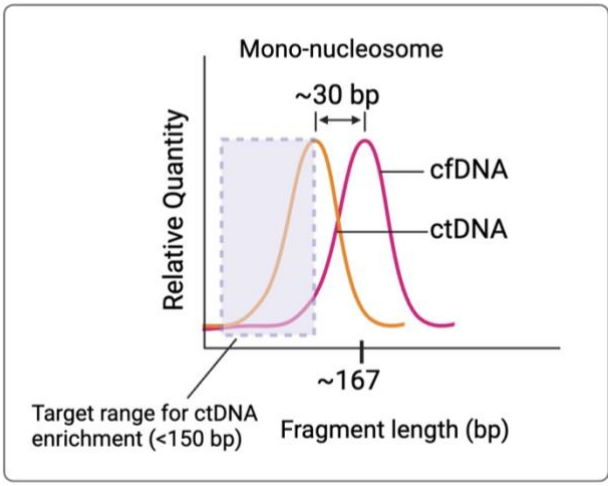


Figure 5-3. Fragmentation characteristics of circulating tumour DNA. ctDNA fragments are generally shorter than cfDNA fragments, although there is considerable overlap between the two. ctDNA enrichment strategies have typically targeted the isolation of fragments shorter than 150 bp. Adapted from Underhill (2021)[448]. Created using Biorender.com.

5-1.5 Cell free DNA clearance

cfDNA in the bloodstream has a relatively short half-life, typically ranging from 16 minutes to 2.5 hours[451]. The clearance of cfDNA from the bloodstream involves multiple mechanisms, all of which are influenced by the structure of the DNA and how it is packaged[258,428,452].

While cfDNA primarily consists of double-stranded DNA from cell nuclei and mitochondria, it can also exist as single-stranded DNA or in circular forms such as extrachromosomal DNA (eccDNA). However, cfDNA in plasma is generally not found as free-floating 'naked' DNA[453]. Due to its highly negative charge, cfDNA readily binds to plasma proteins and lipids, forming DNA complexes such as virtosomes[258,454]. Additionally, DNA is often encapsulated within vesicles, providing further protection during circulation (Fig. 5-4)[452].

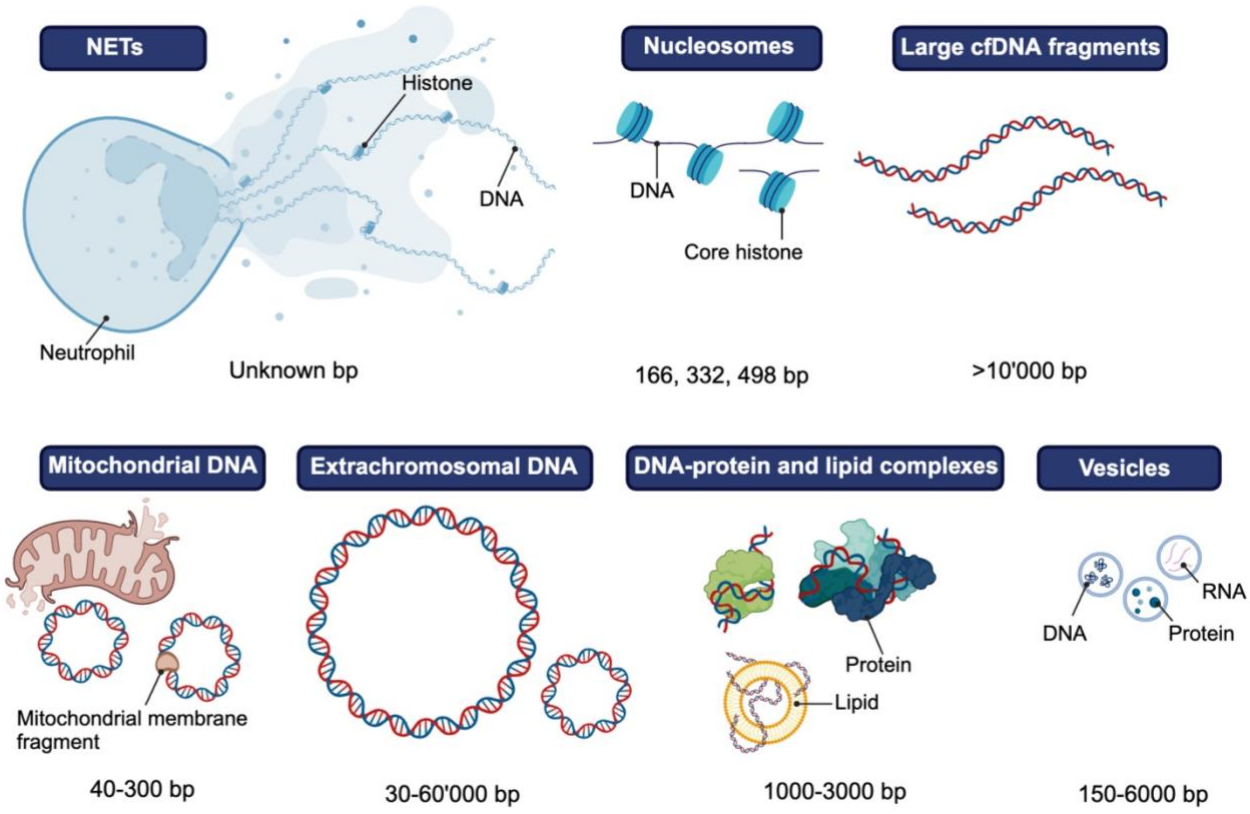


Figure 5-4. Characteristics of cell free DNA in circulation. cfDNA originates from multiple sources and exhibits considerable variation in its physical characteristics depending on the mechanism of release. Neutrophil extracellular traps (NETs), composed of DNA, histones, and antimicrobial proteins, contribute to the cfDNA pool during NETosis. Apoptosis typically produces a ladder pattern of DNA fragments (nucleosomes), while necrosis generates larger DNA fragments. Mitochondrial DNA (mtDNA), released during cell death, also adds to the cfDNA pool and is believed to circulate as either intact circular fragments or bound to mitochondrial membrane fragments[455]. Additionally, extrachromosomal circular DNA has been detected in circulation. DNA's electrostatic nature allows it to associate with proteins and lipids, forming complexes that enhance its stability, while packaging into microvesicles, exosomes, and apoptotic bodies further protects it. Adapted from Bronkhorst, A. J *et al.*, (2019) [452]. Created using Biorender.com.

These interactions help maintain the DNA's structural integrity[258], protect it from nucleases present in the circulatory system and reduce recognition by immune cells[456]. As a result, any DNA that remains unbound, particularly if linear, is rapidly degraded[457].

The liver is the main organ responsible for clearing DNA, primarily through specialized macrophages known as Kupffer cells, which capture and degrade DNA fragments. Enzymatic degradation also plays

a crucial role, occurring directly in the bloodstream where circulating nucleases break down cfDNA. Immune cells, such as neutrophils and macrophages, further aid in recognizing and removing free DNA fragments[257], while other filtering organs, including the kidneys, spleen, and lymph nodes, also contribute to cfDNA clearance.

While not a primary clearance mechanism, it's important to note that cfDNA can also be recognised and captured by specific proteins on cell surfaces[458]. These DNA-binding proteins, such as RAGE and TLR9, are found on various cell types including red blood cells[298,316,317] and platelets. This secondary process contributes to the overall removal of cfDNA from circulation, albeit to a lesser extent than the main clearance pathways.

5-1.6 Deleterious effects of excess circulating cell free DNA

As described above, under normal conditions, physiological mechanisms tightly regulate the amount of circulating cfDNA, which is typically recognised as 'self-DNA' and cleared without triggering an innate immune response. Pathogenic DNA is identified as a 'danger signal' by pattern recognition receptors (PRRs) such as TLRs and RAGE, and also through inflammasome signalling such as AIM2[296,459]. This induces production of pro-inflammatory cytokines, initiating and amplifying innate immune activation (Fig. 5-5).

Interestingly, 'self-DNA,' when present at persistently high levels in the cytosol and plasma, can provoke inflammation[320,321] by overwhelming the body's normal regulatory mechanisms. This triggers a cascade of immune responses similar to those elicited by foreign DNA derived from bacteria and viruses. Such responses can result in chronic inflammation, and has been associated with the development of autoimmune diseases, including systemic lupus erythematosus (SLE) and rheumatoid arthritis (RA)[460].

Given the negative impact that disruptions in cfDNA regulation can have on immune function and overall health, it is plausible that platelets play a role in maintaining circulating DNA homeostasis by

complementing existing clearance mechanisms and sequestering excess DNA fragments from the plasma.

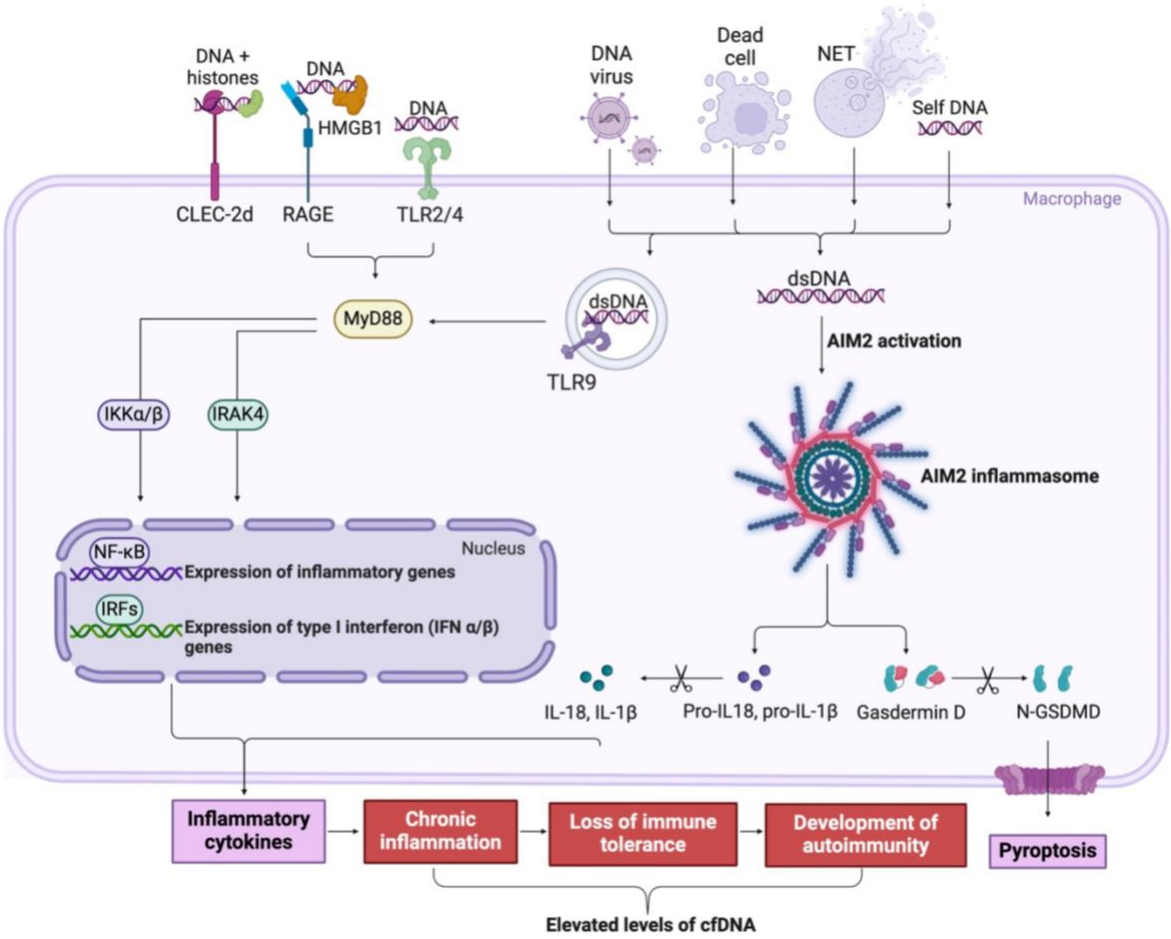


Figure 5-5. Macrophage immune sensing of cell free DNA. Circulating cfDNA binds to macrophage pattern recognition receptors (PRRs) such as RAGE, TLR2, 4 and 9, initiating a proinflammatory signalling cascade through kinases IKKα/β and IRAK4, which leads to the secretion of proinflammatory cytokines[296]. Inflammasomes, multi-protein complexes that serve as intracellular sensors, detect both damage-associated and pathogen-associated molecular patterns (DAMPs and PAMPs)[461]. AIM2, in particular, senses cytosolic double-stranded DNA[459]. Upon activation, inflammasome components assemble, activating caspase-1, which cleaves pro-inflammatory cytokines IL-1β and IL-18 into their active forms. These cytokines are then released, promoting a strong inflammatory response[461]. Additionally, active caspase-1 induces pyroptosis, a form of inflammatory cell death, by cleaving gasdermin D (GSDMD), which releases its N-terminal domain (N-GSDMD) to form pores in the plasma membrane, ultimately causing cell rupture[461]. Adapted from Soehnlein & Tall (2022)[56] and Roth *et al.*, (2023)[57].

5-1.7 Hypothesis and aims

Given their role in sensing pathogen-derived nucleic acids, I hypothesised that platelets might also clear cfDNA from plasma, and that analysing DNA fragments contained in platelets could provide clinically relevant insights. Overall, I sought to compare the abundance of mutant alleles in platelets and cfDNA from mouse models of colorectal and pancreatic cancer, as well as from patients with pre-malignant conditions and late-stage disease.

The specific sub-aims for this section of my thesis were:

Aim 3.1 To determine if mutant alleles derived from tumour cells are sequestered by platelets

Aim 3.2 To explore the genomic distribution of DNA within platelets

Aim 3.3 To assess the potential utility of platelet DNA in various cancer models and patient cohorts, including both low and high tumour burden disease

To achieve these aims, I first employed an *in vitro* co-culture system and droplet digital PCR (ddPCR) to detect tumour-derived mutant alleles in healthy donor platelets after incubation with cancer cell lines. Next, I used whole-genome sequencing to analyse the genomic distribution of platelet DNA and to assess differences in distribution between short and long DNA fragments. Finally, after confirming the uptake of tumour DNA *in vitro*, I conducted deeper sequencing of patient samples to evaluate the potential of platelets for detecting cancer-related gene aberrations in diseases with varying tumour burdens.

5-2 Results

5-2.1 Detection of mutant alleles in platelets

Given the growing importance of cfDNA detection in the setting of cancer screening and molecular profiling of malignancies, I sought to determine whether platelet uptake of tumour derived DNA fragments conferred cancer-specific genetic variants.

Platelets from healthy donors were incubated with a variety of human cancer cell lines harboring common cancer-associated gene mutations, including COLO205, HCT116 and LS180 colorectal cells and HEL erythroleukemia cells (Fig. 5-6A). Cancer cell lines were separated from platelets by inserts with 1 μm pores that facilitated exchange of biomolecules and small EVs between compartments but prevented nucleated cells from entering the lower compartment. ddPCR of DNA isolated from platelets following co-incubation with cancer cell lines detected all relevant oncogenic mutations, including *KRAS*G12D, *BRAF*V600E, *PIK3CA*H1047R and *JAK2*V617F (Fig. 5-6B & C). No cancer-specific gene mutations were identified in healthy donor platelets incubated alone, but wild-type alleles were detected as expected (Fig. 5-6C), likely indicative of sequestration of DNA from non-transformed cells encountered by platelets during circulation within the blood donor, prior to sampling.

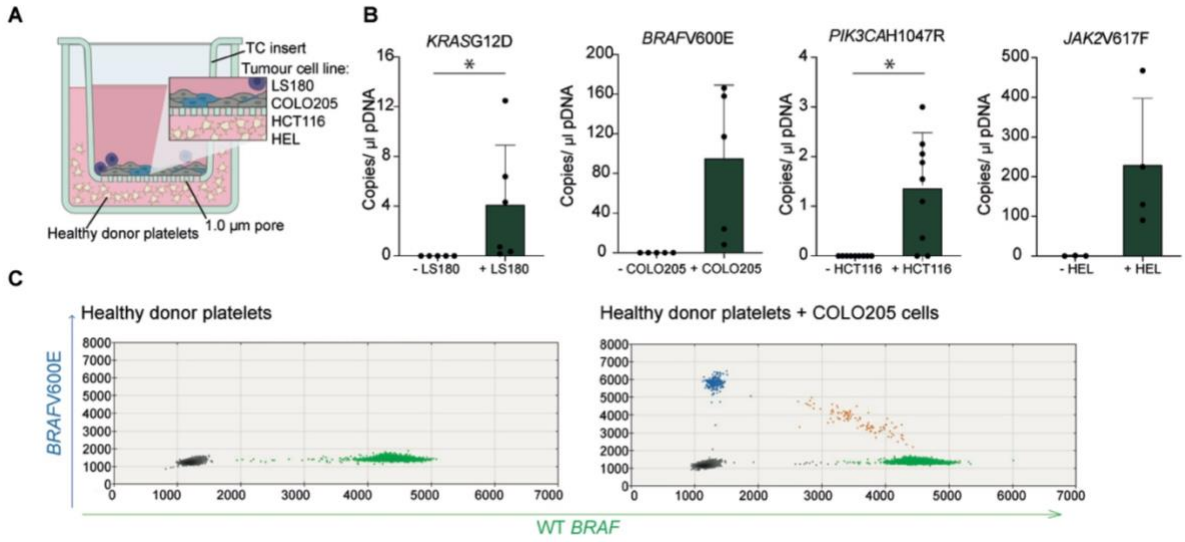


Figure 5-6. Platelets contain tumour -derived DNA bearing cancer-associated gene mutations. (A) Schematic showing experimental system for co-incubation of platelets from healthy donors with malignant cells separated by 1 µm membrane inserts. This enables the exchange of extracellular biomolecules and small EVs but not cells between compartments. Following co-incubation, platelets were removed and washed three times prior to DNA extraction from the platelet pellet. **(B)** Number of copies of mutant alleles detected per µl of DNA extracted from platelets incubated with (+) or without (-) colorectal (LS180, COLO205 and HCT116) and erythroleukemia (HEL) cell lines. Mean ± SD, n=3 independent experiments, *p <0.05 calculated using Wilcoxon paired signed rank test. **(C)** Representative droplet digital PCR analysis showing quantification of wild-type *BRAF* and *BRAF*V600E alleles in DNA isolated from healthy donor platelets before (left) and after (right) co-incubation with *BRAF*V600E positive COLO205 colorectal cancer cells. Created using Biorender.com.

5-2.2 Platelets are more efficient at capturing DNA compared to other blood cell types

To determine whether the ability to capture extracellular DNA was unique to platelets or shared by other blood cell types, I tested whether *BRAF*V600E derived from COLO205 cells was sequestered by platelets, peripheral blood mononuclear cells (MNCs) and red blood cells (RBCs) following incubation of these cells in COLO205 conditioned media. *BRAF*V600E was readily detectable in platelet DNA (pDNA) following incubation of platelets in COLO205-conditioned media as well as following direct platelet-COLO205 cell co-culture (Fig. 5-7A-D), whereas very few copies of mutant *BRAF* were detected in MNCs (*p=0.0152*) and RBCs (*p=0.0022*) (Fig. 5-7A-D). These were of negligible abundance in comparison to wild-type alleles, indicating substantially higher efficiency of detection of tumour cell-derived DNA in platelets than in other blood cell types, and confirming that the mutant isoforms detected in platelets were not due to 'contaminating' residual tumour cell-conditioned media.

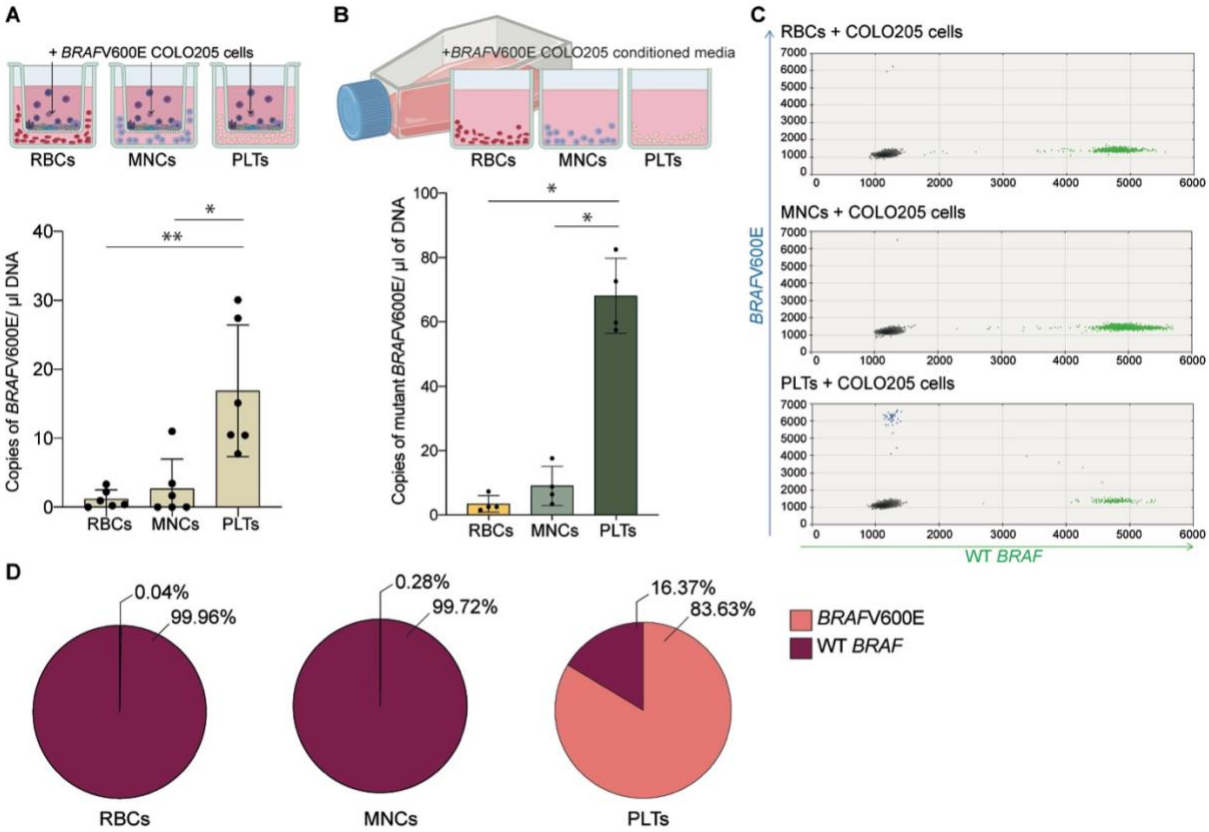


Figure 5-7. Platelets are more efficient at capturing tumour-derived DNA compared to other blood cell types. (A) Top: schematic showing co-culture of COLO205 cells with red blood cells (RBCs), mononuclear cells (MNCs) and platelets (PLTs). Lower: Quantification of *BRAF*V600E in DNA extracted from RBCs, MNCs and PLTs following co-culture with COLO205 cells. **(B)** Quantification of *BRAF*V600E in RBCs, MNCs and PLTs following incubation in media conditioned by COLO205 cells. Data for A and B represent three independent experiments, mean ± SD. *p < 0.05, using a Mann-Whitney test. **(C)** Representative ddPCR plots for *BRAF*V600E in DNA isolated from RBCs, MNCs and PLTs following incubation in COLO205 cell conditioned media. *p < 0.05 and **p < 0.01 for Mann-Whitney test. **(D)** Percentage detection of *BRAF* wild-type and mutant alleles in RBCs, MNCs and PLTs, n=3. Created using Biorender.com.

5-2.3 Mutant alleles captured by platelets are protected from degradation

Data in chapter 4 (section 4-2.6) suggest that platelets internalise and protect sequestered synthetic DNA fragments from nuclease digestion. To confirm these findings using tumour-derived DNA, I employed the co-culture set up outlined in Figure 5-8A. Briefly. conditioned media and healthy donor platelets were treated with DNase following conditioning by erythroleukemia HEL cells that carry the *JAK2*V617F mutation. The detection of *JAK2*V617F in HEL cell conditioned media (analogous to cfDNA) was significantly reduced by DNase treatment (Fig. 5-8B-D). In contrast, there was no reduction in the abundance of *JAK2*V617F in platelets following DNase treatment, indicating that the

majority of DNA is encapsulated by the platelet outer membrane and protected from enzymatic degradation. Wild-type alleles were detected in the platelets after incubation with HEL conditioned media (Fig. 5-8B-D). Given that HEL cells are homozygous for the *JAK2* mutation, the detection of wild-type *JAK2* alleles in healthy donor platelet samples suggests this DNA was present within the platelets prior to isolation.

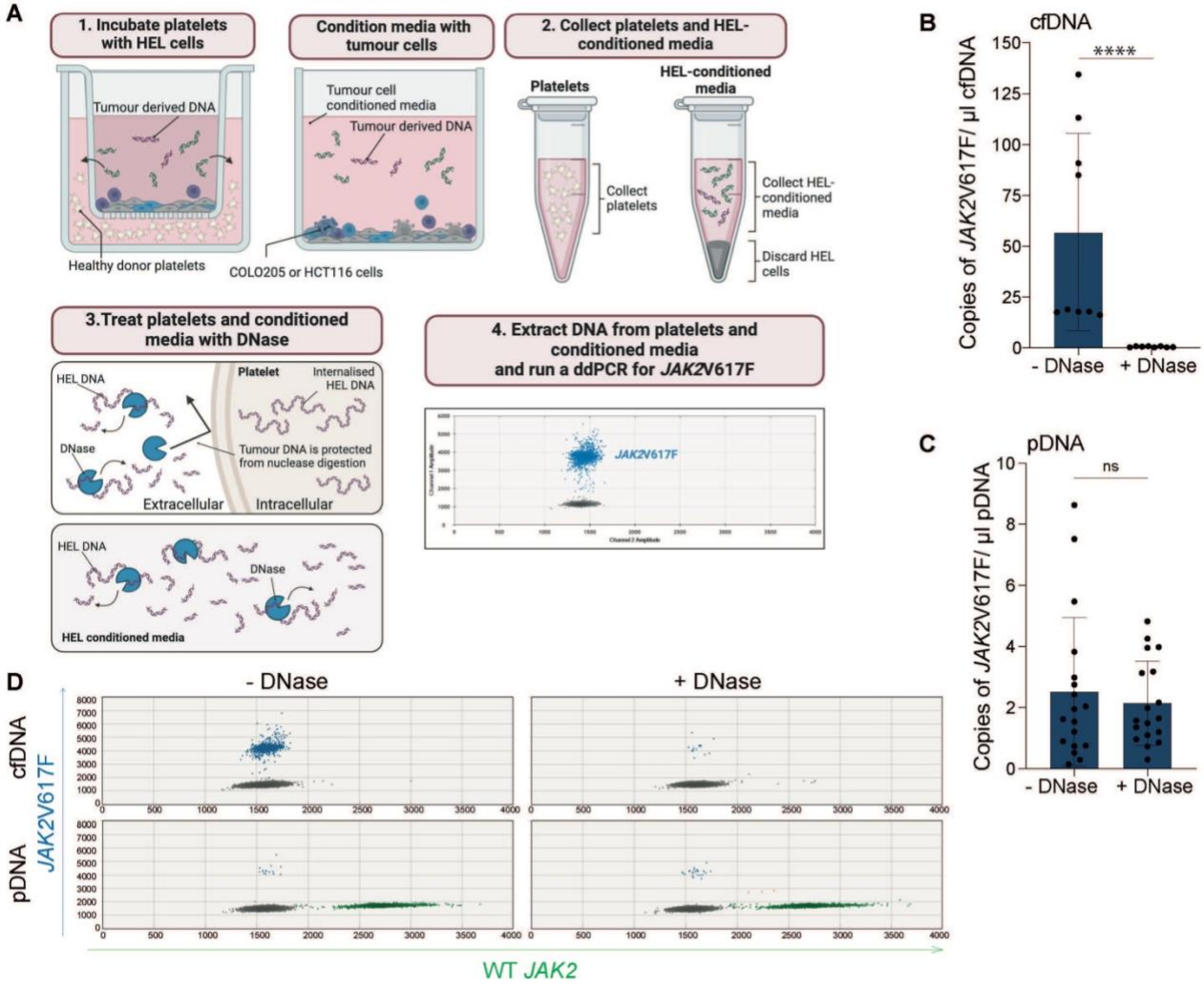


Figure 5-8. Impact of DNase treatment on the detection of *JAK2* mutant alleles. (A) HEL cells were incubated with and without platelets. Following co-incubation, platelets and HEL cell-conditioned media were collected and treated with DNase. A *JAK2* ddPCR assay was used to quantify the amount of remaining DNA in the platelets and media **(B-C).** Impact of DNase treatment on the detection of *JAK2* mutant alleles in pDNA and cfDNA (media) following co-incubation of healthy donor platelets with HEL cells. **(B)** Mutant *JAK2* is not detected in the conditioned media following DNase treatment. **(C)** Mutant *JAK2* is protected from nuclease digestion by platelets and remains detectable by ddPCR. Data represent five independent experiments, mean ± SD. ns $p > 0.05$ and ****$p < 0.0001$ for Mann-Whitney test. **(D)** Representative ddPCR plots showing mutant and wild-type *JAK2* in conditioned media and platelets -DNase (left) and +DNase (right). Plots show three samples combined from one ddPCR run. Created using Biorender.com.

5-2.4 Genomic distribution and origin of platelet DNA

i) Size distribution

Having demonstrated that platelets can take up tumour cell-derived DNA *in vitro*, I explored the utility of this phenomenon for the detection of cancer gene aberrations as a liquid biopsy approach *in vivo*, hypothesizing that analysis of platelet DNA (pDNA) might be useful for cancer screening.

I first explored the size distribution of pDNA, comparing fragment sizes to cfDNA. Electrophoretic analysis of DNA extracted from platelets isolated from peripheral blood and healthy donor plateletpheresis samples showed that pDNA contained fragments of around 12'000 – 16'000 base pairs (bp), and that many samples also showed shorter fragments of around 120 - 500 bp, with a periodicity reflecting nucleosome footprints, similar to the fragmentation profile that is classically observed in cfDNA (Fig. 5-9A & B)[242].

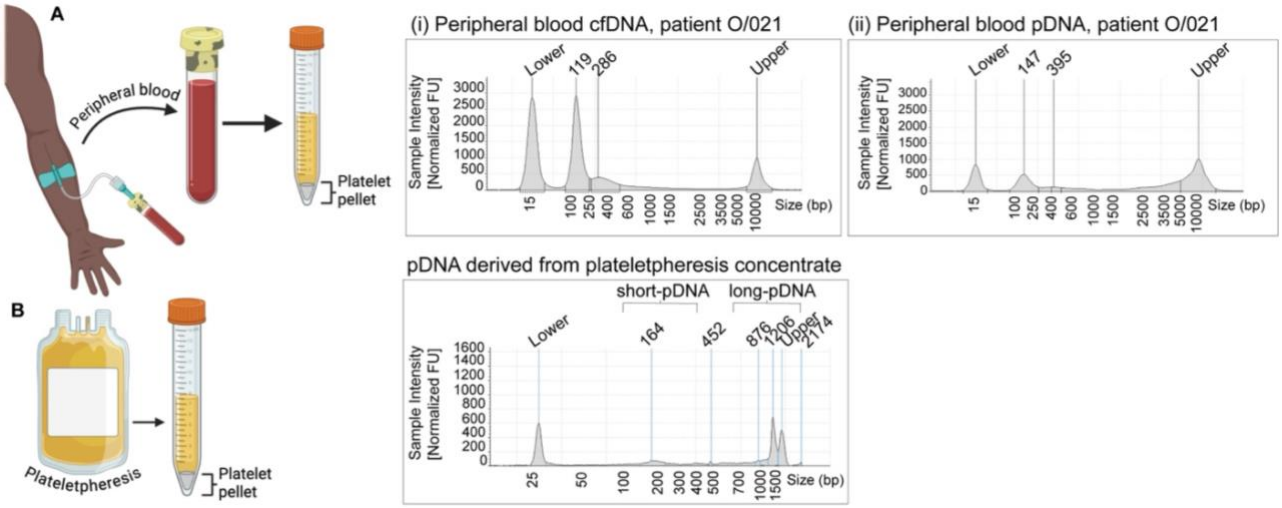


Figure 5-9. Platelets contain both short and long fragments of DNA. (A) Representative electrophoresis of DNA extracted from (i) plasma and (ii) peripheral blood platelets, showing peaks at ~150 bp and nucleosomal footprints. **(B)** Representative electrophoresis of platelet DNA (pDNA) extracted from a plateletpheresis sample showing a peak at ~160 bp as well as larger DNA fragments. Created using Biorender.com.

ii) Genomic distribution and origin of platelet DNA

To compare the genomic origin of pDNA and cfDNA, whole genome sequencing (WGS) was performed on matched pDNA and cfDNA extracted simultaneously from peripheral blood samples of 13 donors, of whom 9 had active malignancy and 4 had undergone surgery and/or chemoradiotherapy. Detailed clinical information for the patients used in WGS are listed in Appendix Data Table A10. For convenience, this table is reprinted on the following page.

Table A10: Clinical information for patients with gastrointestinal carcinoma used for whole genome sequencing study (n=13). (Reprinted from Appendix).

Patient ID	Blood collection tube	Cancer type	Platelet count ($x10^9$/L)	Tumour information (location, size)	TNM staging	Identified mutations	Therapy
C/023	Streck	Colorectal	232	Caecum	T4 N0 M0	loss of *MLH1,PMS2* IHC staining	Surgery and curative right hemicolectomy
C/026	EDTA	Colorectal	207	Rectum	T4a N1 M0	*KRAS* c.35G>A p.(Gly12Asp)	Surgery & neoadjuvant chemoradiotherapy
O/020	EDTA	Oesophageal	249	Distal oesophagus	T2 N1 M0	None identified	Surgery and neoadjuvant chemoradiotherapy
O/021	EDTA	Oesophageal	199	Distal oesophagus	T2 N0 M0	None identified	Surgery and neoadjuvant chemotherapy
O/022	EDTA	Oesophageal	304	Gastric antrum	T4a N0 M0	None identified	Surgery
P/008*	Streck	Pancreatic	266	Large 11 cm mass involving pancreatic tail, spleen, stomach and transverse colon.	T4 N1 M0	None identified	No therapy prior to blood sampling
P/017	Streck	Pancreatic	205	Pancreatic ductal adenocarcinoma	pT3 N1 (2/3) L1V1	None identified	Curative intent surgery
Combat CRC 008	Streck	Colorectal	247	Colon (ascending)	T3 N2 M0	loss of *MSH2* and *MSH6*, *KRAS* c.38G>A p.(Gly13Asp) detected in the transverse tumour	unchecked
Combat CRC 009	Streck	Colorectal	330	Colon (hepatic flexure)	T3 N0 M0	MMR immunohistochemistry not performed	unchecked
Combat CRC 010	Streck	Colorectal	235	Colon (ascending)	T3 N0 M0	loss of *MLH1* and *PMS2*, *PIK3CA* c.3140A>G p.(His1047Arf)	unchecked
Combat CRC 011	Streck	Colorectal	150	Colon (sigmoid)	Unavailable	*KRAS* c.183A>Tp.(Gln61His), *TP53* c.1024C>T p.(Arg342*)	Neo-adjuvant chemotherapy (oxaliplatin - capecitabine)
Combat CRC 012**	Streck	Colorectal	346	Colon (sigmoid)	T3 N0 M0	*NRAS* codon 12 variant detected	unchecked
Combat CRC 013	Streck	Colorectal	460	Caecum	T3 N2 M0	*KRAS* variant	unchecked

APER: Abdominoperineal excision of rectum, cm: Centimeter, FLOT: Combination of chemotherapy drugs: docetaxel, oxaliplatin, 5-fluorouracil and leucovorin,
R-CHOP: Combination of chemotherapy: rituximab, cyclophosphamide, hydroxydaunorubicin hydrochloride (doxorubicin hydrochloride), vincristine (Oncovin) and prednisone,
MMR: Mismatch repair

*Copy number variations were detected in the cfDNA and s-pDNA for this patient
** Sample used for targeted mutational analysis

To investigate the origins of short and long platelet DNA separately, I performed size selection prior to library preparation. Using Ampure XP beads, I separated shorter (less than 600 bp) “s-pDNA”, similar to the fragment lengths of cfDNA, from the longer fragments ("l-pDNA”) (Fig. 5-10).

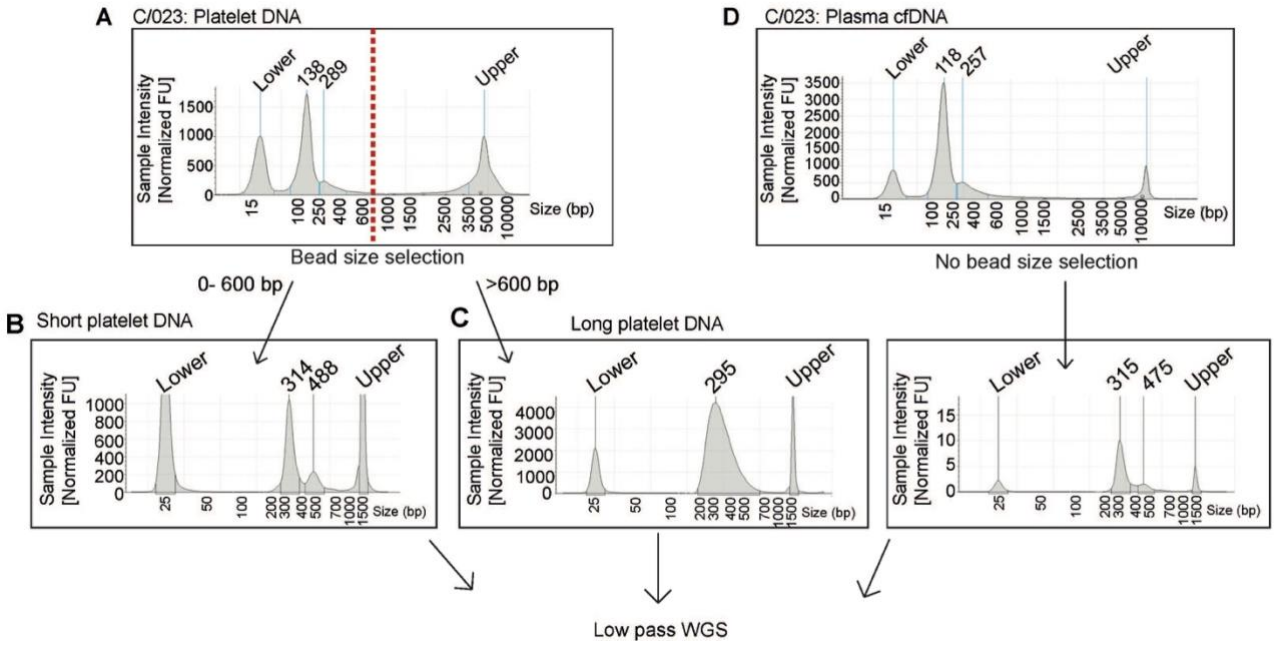


Figure 5-10. Bead separation of platelet DNA. Representative electrophoresis of DNA extracted from a colorectal tumour sample (C/023) showing size section of **(A)** platelet DNA into **(B)** short and **(C)** long fragments prior to library preparation. **(D)** Plasma cfDNA was not size selected.

I first performed low pass WGS (mean target coverage of 1X) on s-pDNA, l-pDNA and paired cfDNA (n=13). Platelets contain a small number of mitochondria, previously estimated at 4 – 6 mitochondria per cell[54,64]. As the mitochondrial genome is ~16’500 bp, I reasoned that l-pDNA fragments might be enriched for mitochondrial DNA. Indeed, a significantly higher subfraction (0.9 – 38%) of l-pDNA mapped to the mitochondrial genome, compared to <0.067 – 3.0% of the shorter fragments. However, the majority of fragments from both s- and l-pDNA mapped to the nuclear genome (97.0 - 99.9% for s-pDNA and 61.7 – 99.1% for l-pDNA, Fig. 5-11A).

Mapping across the genome revealed that the fragments in platelets (blue) covered the entire nuclear genome (Fig. 5-11B), mirroring the mapping of cfDNA (green). This exciting observation suggests that sampling pDNA could enable the detection of oncogenic variations in genes across all the

chromosomes. All computational analysis described in this chapter was carried out by Jeanne Inchauspé, a DPhil student jointly supervised by Beth Psaila and Jim Hughes (MRC WIMM), Benjamin Schuster-Böeckler, a professor at the Oxford Ludwig Institute for Cancer Research or Zohar Etzioni, a postdoctoral fellow at the Oxford Ludwig Institute for Cancer Research.

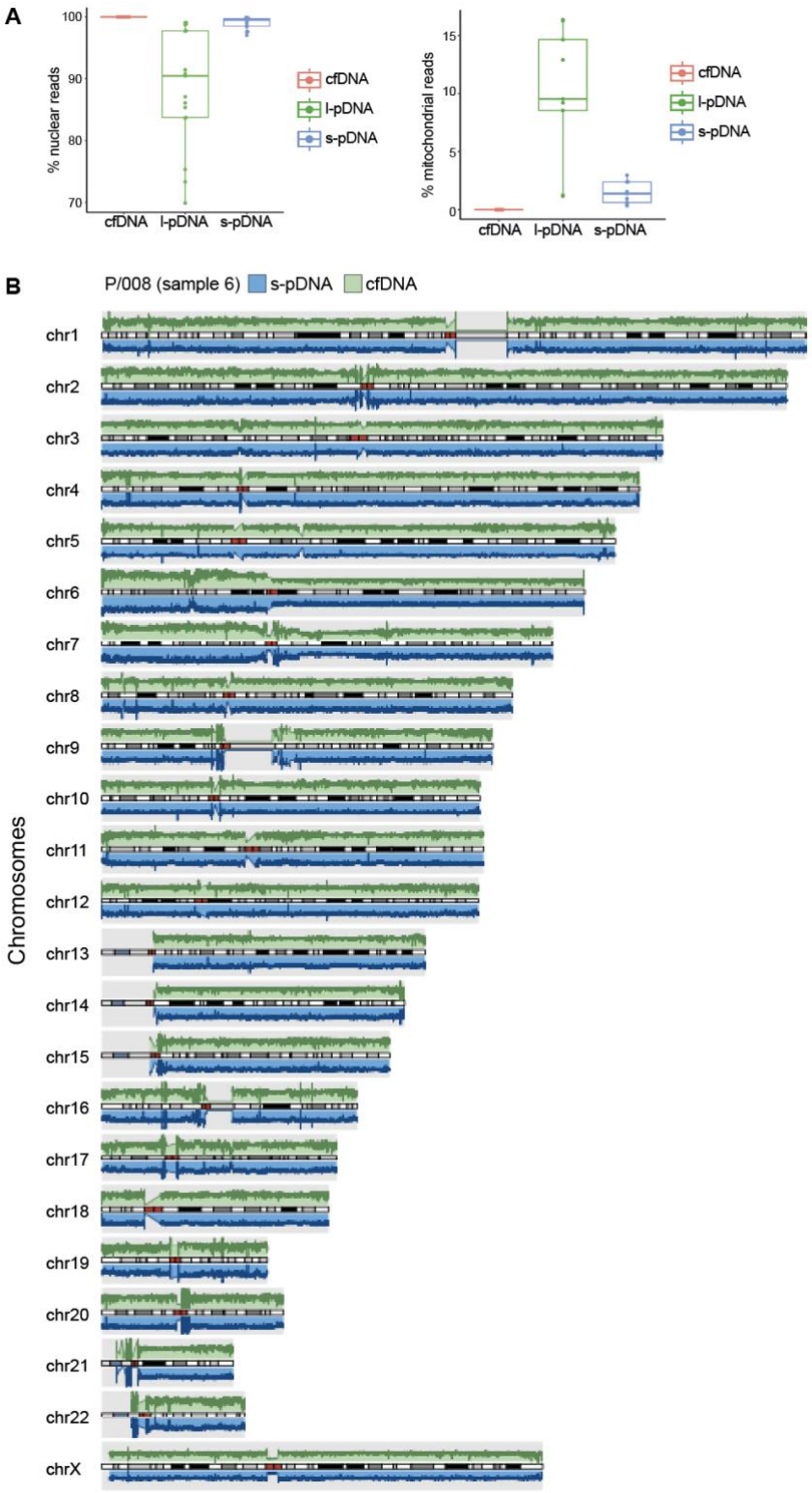


Figure 5-11. Platelets capture fragments of DNA that map across the human genome. (A) Percentage of fragments mapping to the nuclear (left) and mitochondrial (right) genomes from cell free DNA (cfDNA), short (> 100 and < 600 bp) and long (> 600 bp) platelet DNA fragments (s-pDNA and l-pDNA). Median value ± individual data points shown (n=13). **(B)** Chromosome mapping of short platelet DNA (s-pDNA, blue) and paired cell free DNA (cfDNA, green) for a representative patient with pancreatic adenocarcinoma (P/008/sample 6). Grey areas with no signal are blacklisted (highly repetitive) regions.

iii) Nuclear genomic coverage of platelet DNA mirrors cell free DNA

I then obtained deeper sequencing (mean sequencing depth 15X ± 3 / 12X ± 1 for cfDNA and s-pDNA, respectively) of the paired cfDNA and s-pDNA for a subset of samples, including 5 from donors after therapy (samples 1 – 5), and 2 from donors with active, untreated pancreatic and colorectal carcinoma (samples 6 and 7). No notable differences were detected in sequencing quality (base quality, 3' bias, mapping rate) between s-pDNA and cfDNA, except for a higher estimated PCR duplication rate (cfDNA: 3.2% ± 0.6%, pDNA: 11.3% ± 7.2%), indicating lower complexity of short pDNA libraries, presumably due to the size selection that had been performed the pDNA to separate long and short fragments (no size selection had been applied to the cfDNA).

As described in the introduction (section 5-1.5), nucleosome-bound cfDNA is more protected from degradation than nucleosome-free DNA. This leads to a characteristic fragment-length distribution of cfDNA, with mono- and di-nucleosome length peaks at approximately 167 bp and 320 bp[462]. Encouragingly, the peak mean fragment length for s-pDNA was 166 bp ± 0.8, with a second, di-nucleosome peak at approximately 328 bp (Fig. 5-12A). This strongly indicates that platelets actively sequester cfDNA fragments encountered during circulation. Furthermore, the di-nucleosome peak was fractionally, but significantly larger in s-pDNA than cfDNA ($p=<0.0005$ for a chi-squared test of independence). One explanation for this may be the increased protection of DNA fragments in platelets from nuclease digestion, as observed in my *in vitro* experiments presented in earlier in chapter 4 (section 4-2.6) and in this chapter (section 5-2.3).

Several studies have shown that cfDNA fragments of tumour cell origin are shorter in length than wild-type fragments[267,272]. Consistent with this, I observed that both mono- and di-nucleosomal fragment lengths were notably shorter in both pDNA and cfDNA in sample 6, which was obtained from a patient with an inoperable pancreatic tumour and readily detectable ctDNA in the cfDNA. In contrast, samples from patients without detectable ctDNA did not exhibit this pattern. This indicates that fragmentomic analysis may be applied to platelet DNA to detect the presence of cancer[463], and that platelets absorb DNA fragments that resemble those found in cfDNA *in vivo* (Fig. 5-12B).

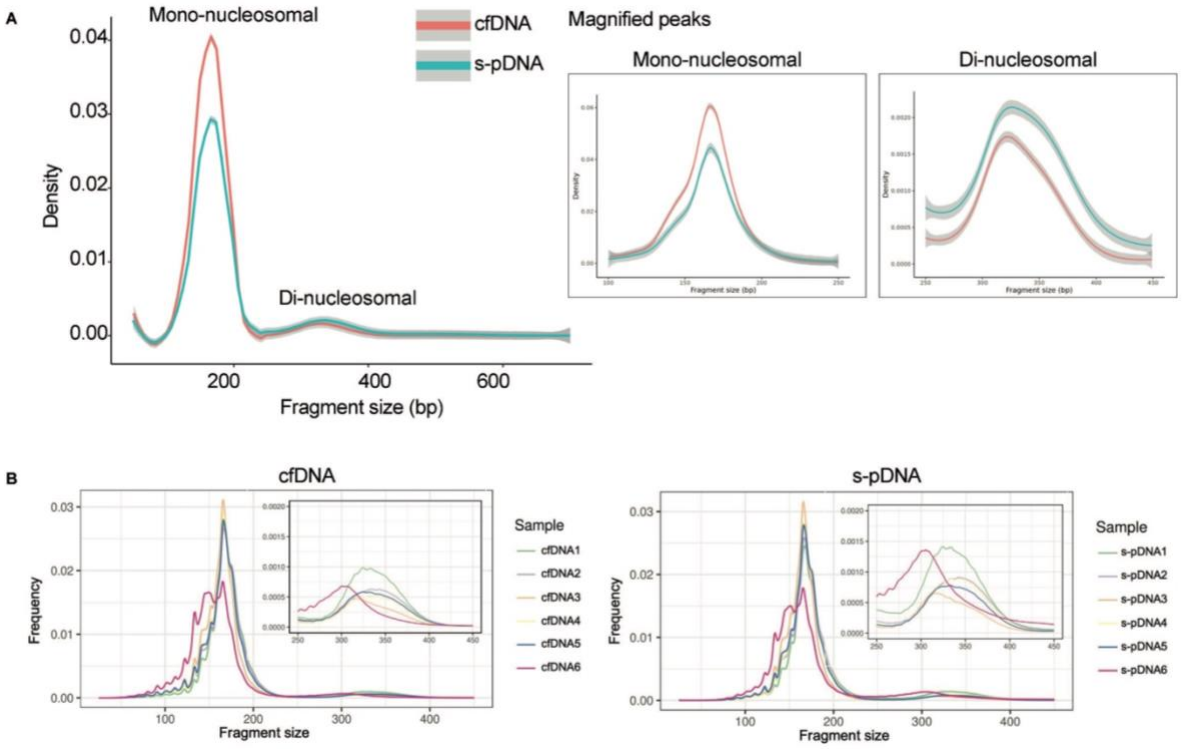


Figure 5-12. Fragmentomic analysis reveals platelets contain shorter, tumour -derived DNA. (A) Plot showing significantly higher frequency of di-nucleosomal fragments (fragments above 250 bp) in s-pDNA than cfDNA ($p < 0.0005$ for all samples with a chi-square test of independence). Insets show magnified mono- and di-nucleosomal peaks. The standard error of the mean is shown in grey. **(B)** Fragment length distribution of paired and aligned reads for cfDNA (left) and s-pDNA samples (right). Samples 1–5 have a peak fragment length of around 165 bp, representing mono-nucleosomal fragments, with a second smaller peak around 325 bp (shown in inset plot), representing di-nucleosomal fragments. However, the mono- and di-nucleosomal fragment lengths from sample 6 (red line), a patient with untreated pancreatic cancer, are notably shorter than samples 1 – 5 (from patients following anti-cancer therapy).

5-2.5 Copy number variations are detectable in platelet DNA

To confirm the capture of ctDNA by platelets *in vivo*, we used iChorCNA to look for copy number alterations (CNA) and estimate the fraction of tumour-derived DNA within the samples[291]. Clonal amplifications and deletions in chromosomes 6 and 7 as well as sub-clonal amplifications in chromosome 2 were detected in both cfDNA and s-pDNA from sample 6, a patient with pancreatic cancer and an estimated tumour fraction of 25% (Fig. 5-13A). CNAs detected in the s-pDNA of sample 6 mirrored those present in cfDNA and the estimated proportion of tumour-derived DNA was highly correlated between s-pDNA and cfDNA (Fig. 5-13B). Additionally, no CNAs were detected in either cfDNA or s-pDNA in the other 12 samples analysed by WGS (Fig. 5-13C).

Interestingly, no CNAs were detected in the l-pDNA from sample 6 (Fig. 5-13D), indicating that the large and small fragments of pDNA may have different cell and/or tissue origins. Although beyond the scope of this thesis, this is an area I am keen to explore further through additional experiments, such as DNA methylation sequencing. The difference in CNA detection between short and long fragments is also in line with previous reports that ctDNA is enriched in shorter fragments[272]. Computationally selecting DNA fragments smaller than 150 bp increased the estimated tumour content of s-pDNA from 25% to 30%, in parallel to the increase seen in cfDNA (Fig. 5-13E).

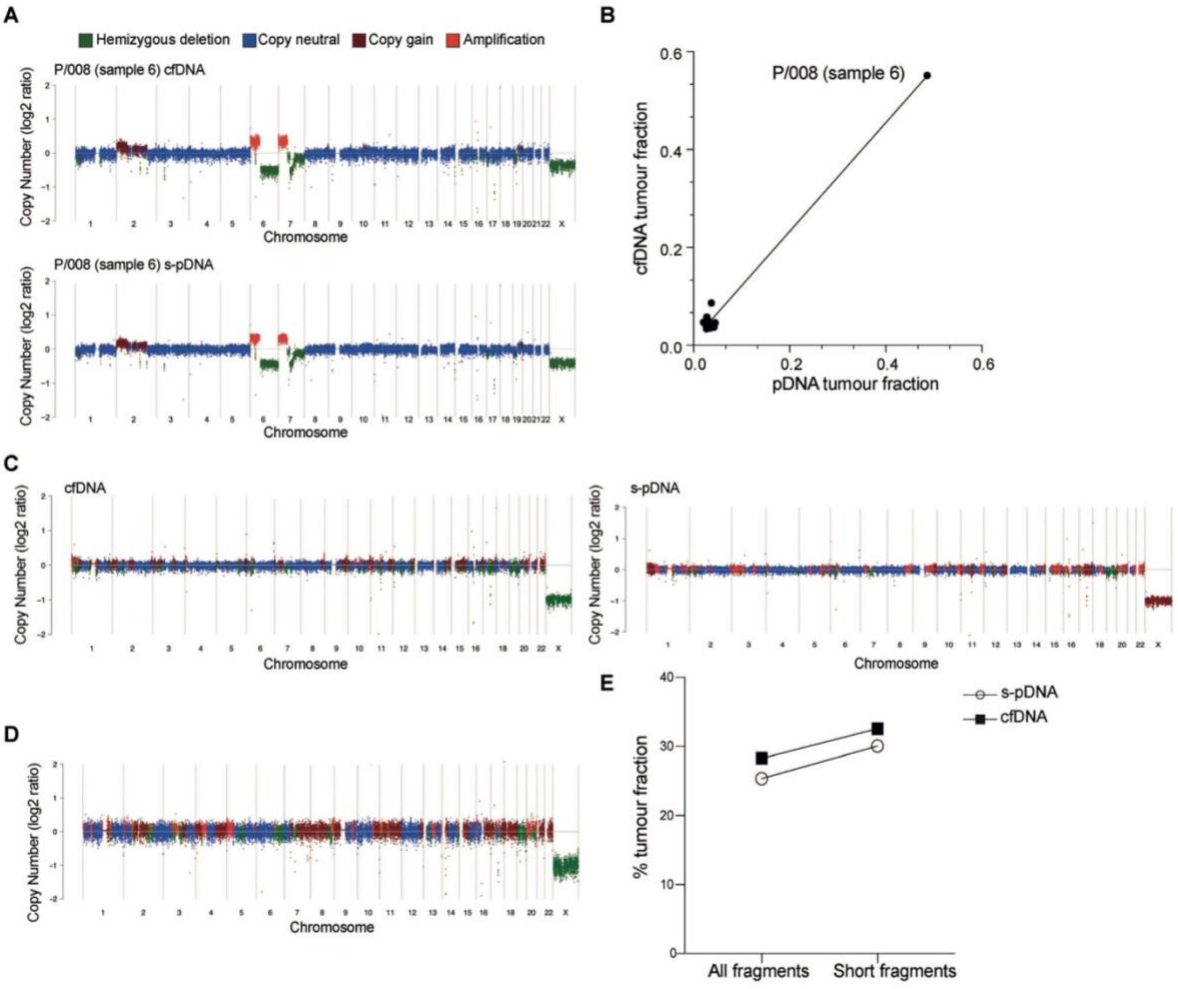


Figure 5-13. Platelet DNA analysis reveals copy number variations. (A) Deviation from median coverage in 100 kilobase (kb) windows across all chromosomes for cfDNA (top) and s-pDNA (bottom) for P/008/ sample 6, revealing chromosomal aberrations in chromosomes 2, 6 and 7 (copy number gains and amplifications shown in red, deletions in green). **(B)** CNA-based estimates of tumour-fraction in cfDNA and pDNA are highly correlated. **(C)** Deviation from median coverage in 100 kb windows across chromosomes for cfDNA (left) and s-pDNA (right) for a patient with colorectal carcinoma who had a

curative right hemicolectomy prior to blood sampling. **(D)** Copy number alterations were not observed in long platelet DNA (l-pDNA) in sample 6. **(E)** Estimated tumour fraction increases after computationally selecting DNA fragments smaller than 150 bp for both s-pDNA and cfDNA for sample 6.

5-2.6 Deeper sequencing reveals mutant alleles are detectable in platelet DNA

Matched tumour and healthy tissue samples were available for sample 7 from a patient with colorectal carcinoma. This allowed for an in-depth search for low-level ctDNA by screening for mutations found in the tumour biopsy that were not present in healthy tissue from the same patient.

The detection rate of mutations from the matched tumour sample was compared with the detection rate of randomly selected mutations from other patients with colorectal carcinoma, taken from The Cancer Genome Atlas[464]. Encouragingly, the matched tumour mutations (specific to sample 7 tumour tissue) were detected at a significantly higher rate than the random mutations in the cfDNA and s-pDNA. In contrast, these mutations were detected at a similar frequency to the random mutations (likelihood rate 8.92e-11 for cfDNA and 2.30e-07 for s-pDNA), with an overall lower-level of detection in the l-pDNA (0.000357; Fig. 5-14).

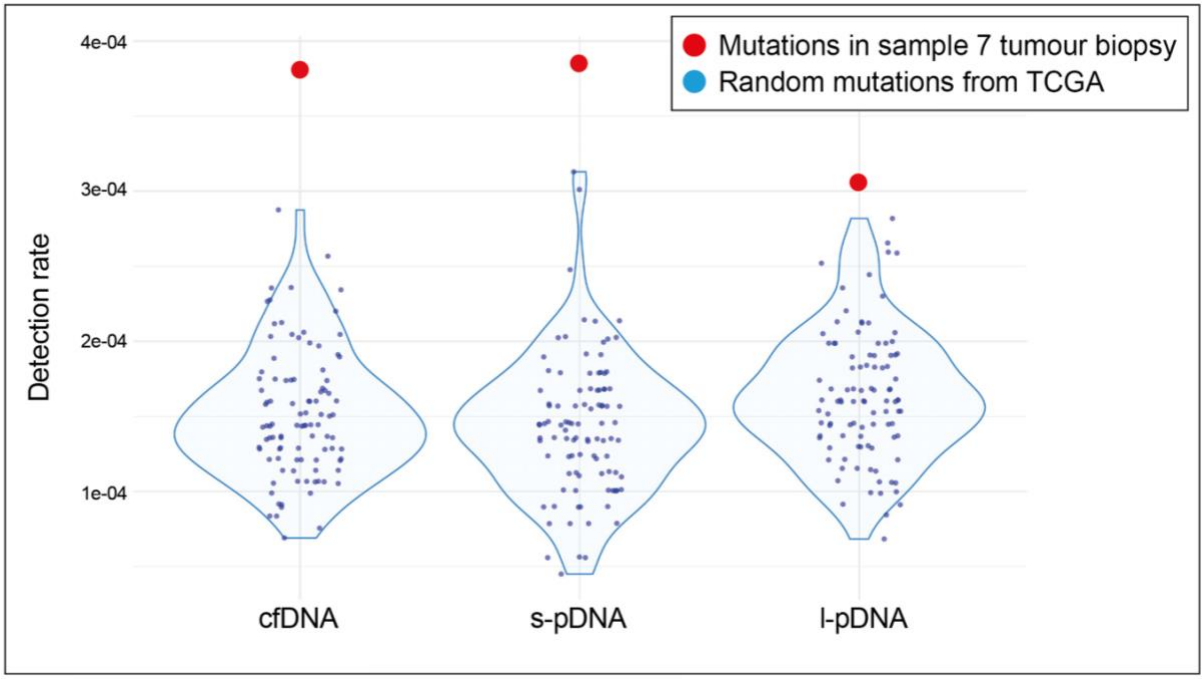


Figure 5-14. Platelets contain tumour-derived DNA bearing cancer-associated gene mutations. Detection rates of mutations in cfDNA, s-pDNA and l-pDNA for sample 7 where matched tumour biopsy was available. The red dot indicates mutations detected in the tumour biopsy; blue dots indicate 100 random samples of mutations from other patients with colorectal carcinoma from The Cancer Genome Atlas dataset (TCGA).

Together, these data indicate that ctDNA is present within platelets in similar abundance to cfDNA, both in patients with high levels of ctDNA and clear CNAs (>20%, sample 6, Fig. 5-13A) and in those with extremely low levels (<0.5%, sample 7, Fig. 5-14), where targeted analysis and matched tumour tissue was required. Overall, ctDNA was identified in both platelets and cfDNA in 20% of the pre-treatment samples either by detecting CNAs or known tumour mutations, in keeping with the sensitivity of WGS for ctDNA detection reported in large clinical cohorts[465] (2 patients / 9 patients with active malignancy).

5-2.7 Inferring gene expression in cell of origin from platelet DNA and cell free DNA

The enrichment of nucleosome-bound DNA in cfDNA has been used to gain insights into gene expression patterns and cell-of-origin. Previous reports have shown that reads are depleted over transcriptional start sites (TSS), displaying periodicity in coverage relative to the TSS[319]. This coverage pattern is attributed to nucleosome positioning and cfDNA protection (Fig. 5-15A, re-printed from chapter 3). During sequencing, fewer reads are obtained from these open chromatin regions because the enzymes digest accessible DNA more readily than nucleosome-protected DNA, resulting in lower sequencing coverage depth at the TSS for actively transcribed genes[466].

In addition, DNA methylation studies have shown that the majority (>90%) of cfDNA in healthy individuals is of haematopoietic cell origin including from neutrophils, monocytes, erythroblasts[467] and megakaryocytes[468], with a small contribution from vascular endothelial cells and hepatocytes[467]. Therefore, in cfDNA, depletion of reads over the TSS for genes highly expressed in peripheral blood mononuclear cells (PBMNCs) is observed.

A similar depletion in sequencing coverage and periodicity around TSS was observed in both s-pDNA and cfDNA for genes highly expressed in PBMNCs, consistent with previous reports on cfDNA. This suggests a shared cellular origin of pDNA and cfDNA (Fig. 5-15B). Notably, the depletion in coverage for high-expression PBMNC genes was less pronounced in sample 6, which had an estimated ctDNA fraction of 25%, compared to the other samples (Fig. 5-15B). This observation is intriguing for a couple of reasons. Firstly, it suggests that a larger proportion of the circulating DNA in this sample originates from sources other than PBMNCs. Given the high estimated tumour fraction, it is plausible that some of this DNA is derived from tumour cells. Secondly, this shift in read depth was detected in platelets at a similar level to cfDNA, further highlighting the diagnostic potential of platelets.

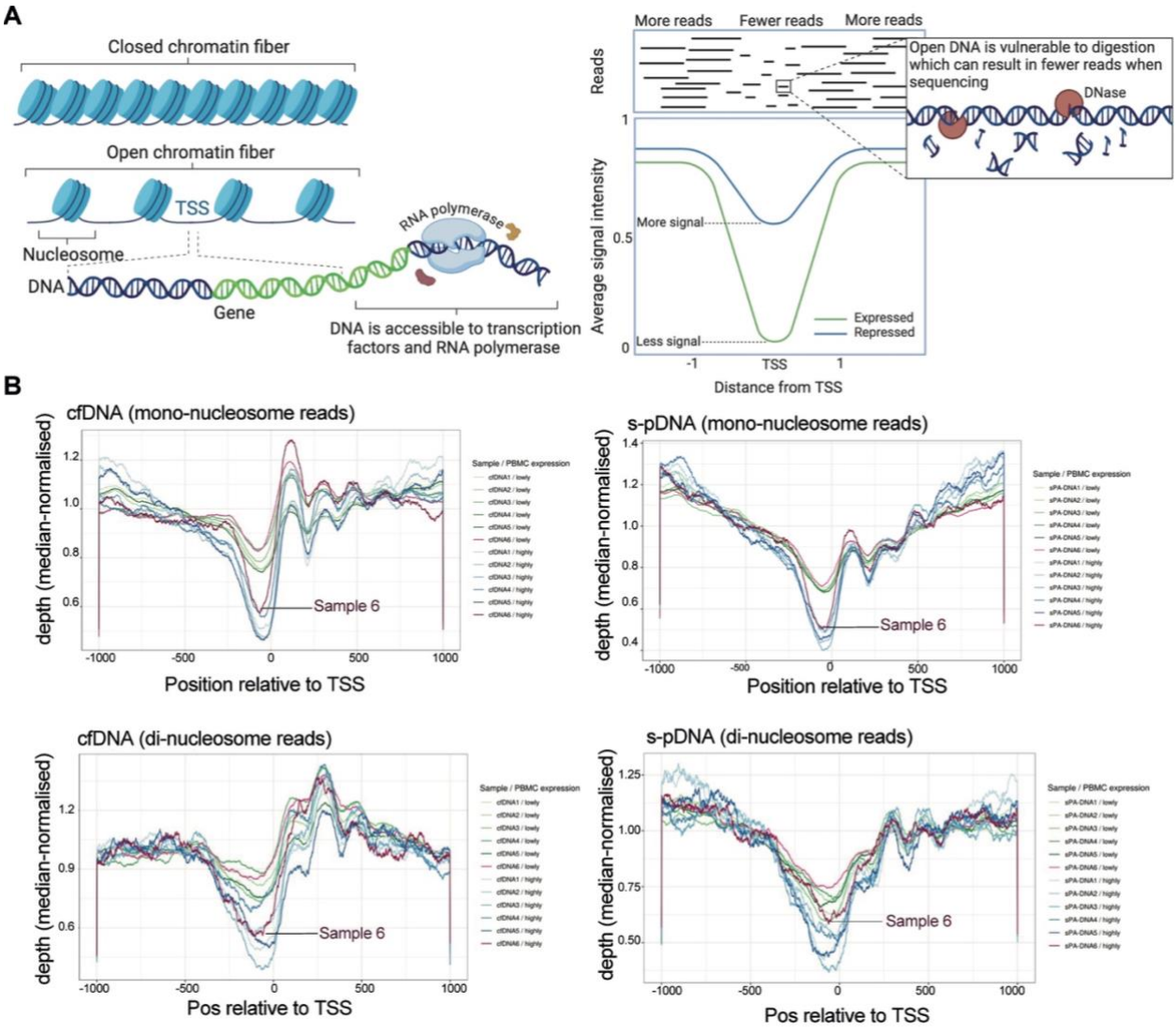


Figure 5-15. Platelet DNA analysis reveals gene activity in cell-of-origin. (A) Left- a schematic illustrating the differences in nucleosome positioning between closed and open chromatin. Genes located in open chromatin regions are accessible to transcription factors and RNA polymerase, facilitating their transcription into messenger RNA. Right- a schematic showing the coverage patterns caused by nucleosomal protection of cfDNA. Regions of open chromatin and active gene transcription are more susceptible to digestion due to the absence of protective nucleosomes, leading to reduced sequencing coverage depth, as indicated by the green dip in the plot. Conversely, genes that are not actively transcribed are shielded by nucleosomes, resulting in higher average signal intensity and a less pronounced reduction in reads over the TSS, as shown by the blue line. **(B)** Read depth distribution around TSS of genes highly (TPM>15, purple) or lowly (TPM<15, blue) expressed in PBMNCs for cfDNA (left) and s-pDNA (right), mono-nucleosome reads (top), and di-nucleosome reads (bottom). Depth per position per sample was normalised to the median read depth across all genes in that expression category. Created using Biorender.com.

6-1.1 High abundance of mutant alleles in platelets in colorectal and pancreatic carcinoma

KPN mouse maintenance was carried out by Hayley Belnoue-Davis, while Giampiero Valenzano managed the KPC mice and performed p53 immunohistochemical staining.

To compare the abundance of mutant alleles in platelets and cfDNA, I first used a mouse model of colorectal carcinoma in which expression of *KRAS*G12D and *TP53* (KP) mutations are induced via the villin promoter, resulting in locally-invasive colorectal adenocarcinoma with a low incidence of metastases, and mice with *KRAS*G12D, *TP53* and *NOTCH* (KPN), with more aggressive and metastatic disease[469] (Fig. 5-16A). To determine the relative sensitivity of cfDNA and pDNA for the detection of tumour-derived mutant alleles, pDNA and cfDNA were extracted simultaneously from the same blood sample and ddPCR was used to detect mutant *KRAS*G12D alleles.

Mutant *KRAS*G12D as well as wild-type *KRAS* alleles were readily detectable in both cfDNA and platelets of mice with colorectal carcinoma. Remarkably, in just over half of the mice (13/19, 68%), copies of *KRAS*G12D per µl of DNA were in higher abundance in pDNA than in cfDNA, both in mice with locally invasive (KP) and metastatic (KPN) disease (Fig. 5-16B-D). Notably, the number of mutant alleles detected in platelets and plasma combined were significantly higher than in plasma alone (Fig. 5-16B), suggesting that including platelet DNA in liquid biopsy sampling would add value to the current standard approach of screening platelet-depleted plasma alone.

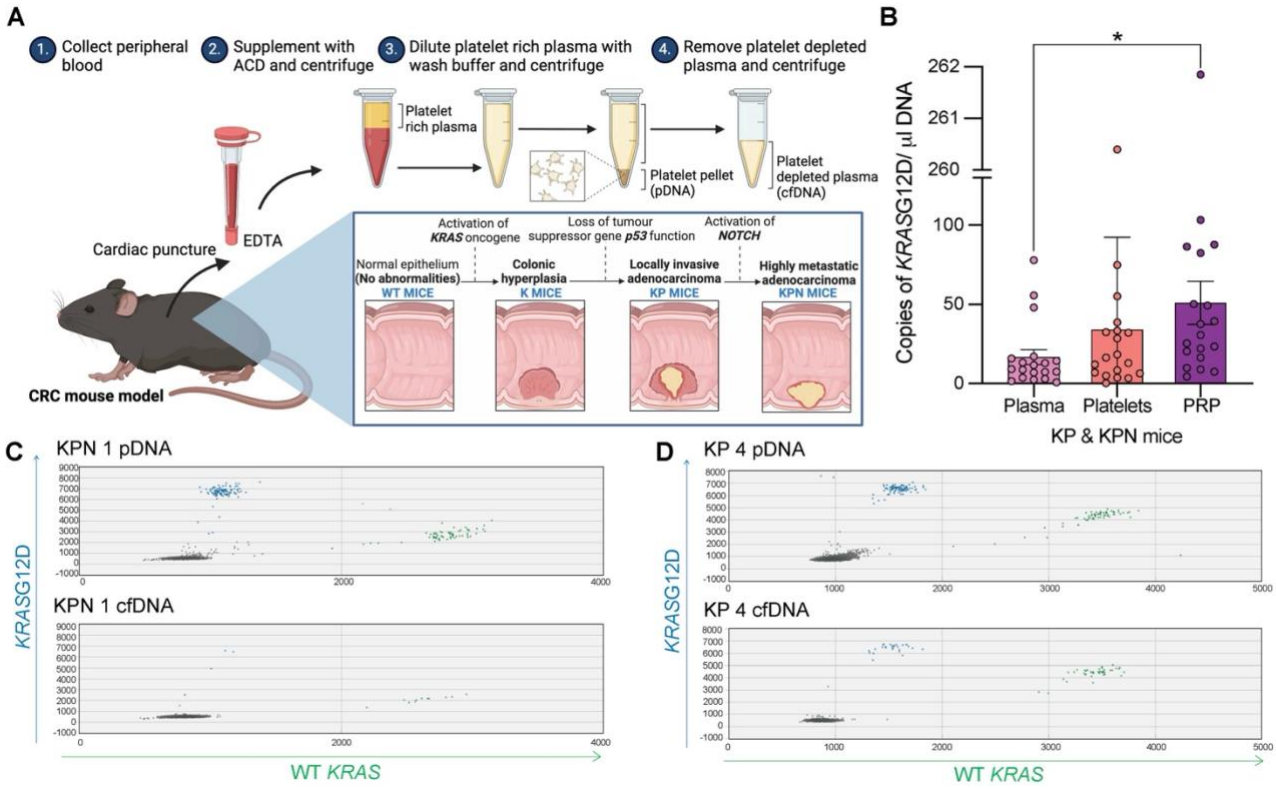


Figure 5-16. Detection of driver mutations in pDNA and cfDNA from mice with localised and metastatic colorectal adenocarcinoma. (A) Schematic showing isolation of platelet DNA (pDNA) and cell free (cfDNA) from C57BL/6 mice expressing *KRAS*G12D and *TP53* (KP) mutations via the villin promotor resulting in locally invasive colorectal adenocarcinoma, and mice with *KRAS*G12D, *TP53* and *NOTCH* (KPN) mutations with aggressive, metastatic disease. **(B)** Plot comparing the copies of *KRAS*G12D detected per µl of DNA extracted from plasma, platelets and PRP (platelet rich plasma, combined). Plot shows mean ± SD, * $p<0.05$ for a paired t test, n= 19 mice. (**C** to **D**) Representative ddPCR plots showing *KRAS*G12D (blue) in higher abundance in pDNA than in cfDNA in two representative mice, **(C),** a KPN mouse and (**D**), a KP mouse. Created using Biorender.com.

To corroborate these findings in a second model and to examine early stage tumourigenesis, prior to tumour dissemination, I used an orthotopic pancreatic cancer model, where pancreatic cancer cells were inserted within a matrigel plug into the body of the pancreas[470] (Fig. 5-17A & B). Fourteen days after implantation and prior to local tumour invasion, *KRAS*G12D alleles were readily detected in murine platelets in matching abundance to cfDNA from platelet-poor plasma (Fig. 5-17C & D).

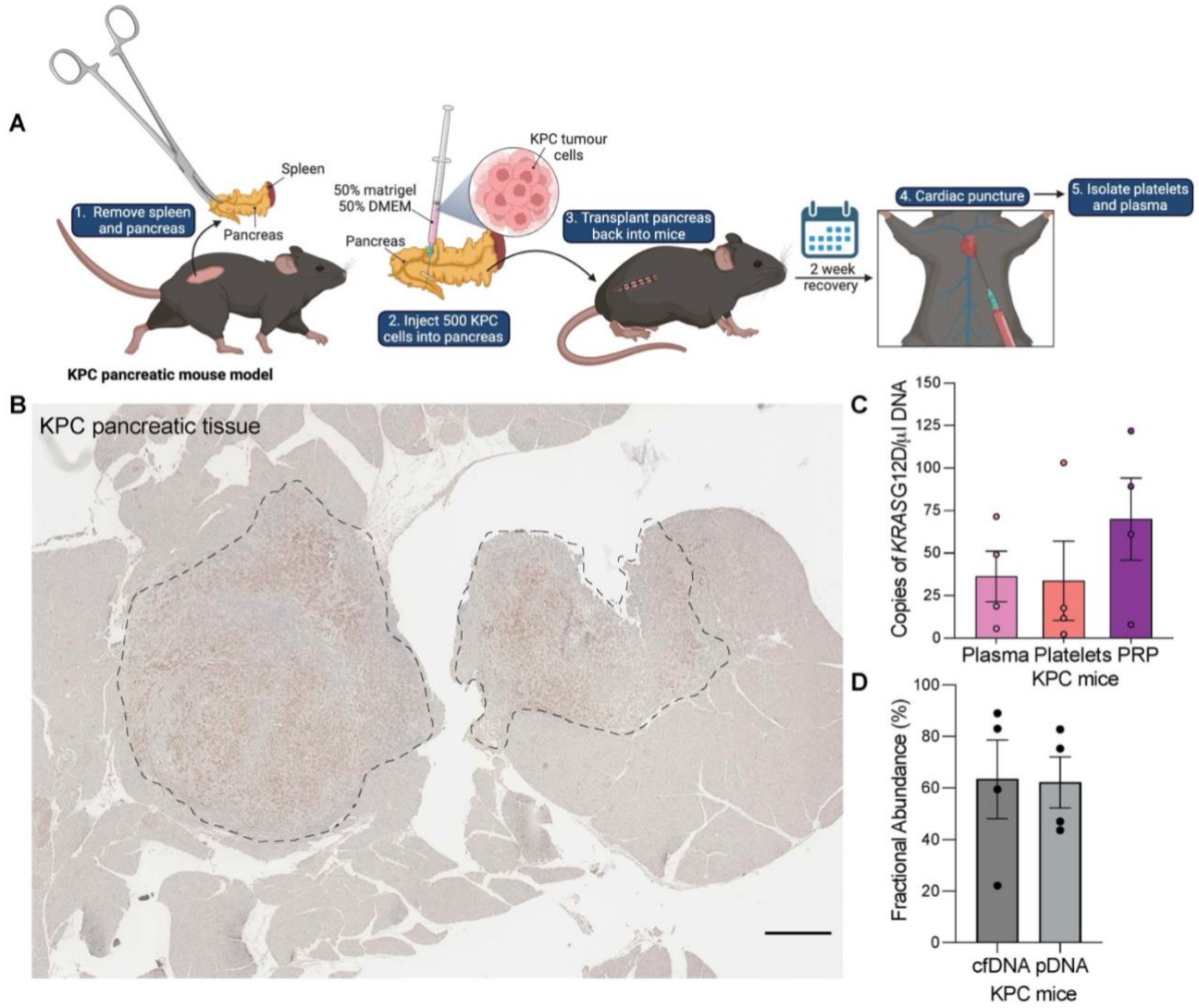


Figure 5-17. Detection of driver mutations in pDNA and cfDNA from mice with localised pancreatic cancer. (A) Schematic showing the generation of the orthotopic pancreatic cancer mouse model by Giampiero Valenzano. **(B)** Representative image shows p53 immunohistochemical staining of KPC pancreatic tissue, two weeks post engraftment. Outlined area highlights regions of contained p53 expression surrounded by healthy p53neg tissue. Scale bar represents 500 µm. **(C)** Droplet digital PCR showing number of copies of mutant *KRAS*G12D per µl of DNA extracted from the plasma, platelets and PRP (platelet rich plasma) of mice, two weeks after tumour cell implantation. **(D)** Fractional abundance of mutant *KRAS*G12D for paired cfDNA and pDNA. Plots show mean ± SD, n=4. Created using Biorender.com.

Overall, these findings confirm the clearance of tumour cell-derived DNA by circulating platelets. The results suggest that incorporating pDNA into cfDNA analysis could significantly enhance cancer detection, particularly in scenarios where tumour burden is low, such as during cancer screening or minimal residual disease (MRD) monitoring. By including pDNA, we can increase the amount of relevant (i.e. tumour-derived) genetic material available for analysis. This advantage is particularly evident when comparing the total amount of *KRAS*

mutations detected in platelet-rich plasma samples from both colorectal and pancreatic mouse models, where the inclusion of pDNA noticeably increased the detection of tumour-specific mutations.

5-2.9 Detection of *BRAF*V600E in platelets from patients with pre-malignant lesions

Improving the sensitivity for liquid biopsy screening is particularly crucial in the setting of low tumour-burden disease and in patients with pre-malignant lesions, where the abundance of ctDNA is low. Sessile serrated lesions (SSLs) are high-risk, pre-malignant colon polyps that account for around one quarter of colorectal cancers[471] (Fig. 5-18A). The majority (>75%) are driven by mutations in *BRAF*, typically *BRAF*V600E, and detection of *BRAF*V600E in cfDNA has been investigated as an SSL screening tool, with high specificity (100%) albeit low sensitivity (16.9%)[46]. To explore the utility of pDNA for detecting pre-malignant lesions, I collected platelets and cfDNA from patients found to have SSLs at colonoscopy (n = 34). Control samples (n = 14) were collected from patients with inflammatory bowel disease and from those invited for colonoscopy through the U.K. Bowel Cancer Screening Program, in whom no polyps or cancerous lesions were detected (Appendix Data Table A7).

Using ddPCR, mutant *BRAF*V600E alleles were detected in either the cfDNA and/or pDNA in 16.1% of the patients with serrated polyps (5/31, [3 samples banked did not pass QC, hence 31 not 34], Fig. 5-18B-D), a detection rate consistent with previous reports for the frequency of detectable ctDNA in this patient cohort[472,473]. Mirroring our findings in the mouse model, around half (3/5) of the patients with detectable ctDNA, had a higher number of copies of *BRAF*V600E in pDNA than in cfDNA (Fig. 5-18D). *BRAF*V600E was not detected in those in the control group that did not have serrated polyps (Fig. 5-18B), demonstrating high specificity of targeted mutational analysis of platelet DNA in this setting.

Together, these data suggest that including platelet DNA analysis in liquid biopsy methods may improve the sensitivity of cancer screening in many cases, and that current liquid biopsy approaches using only platelet-poor plasma to isolate cfDNA are missing relevant genetic information that is contained within platelets.

Collectively, these data reveal a new biological role for platelets in sequestration of cfDNA from plasma and its protection from nuclease degradation and indicate that analysis of pDNA may be useful to detect genetic aberrations in a range of clinical settings.

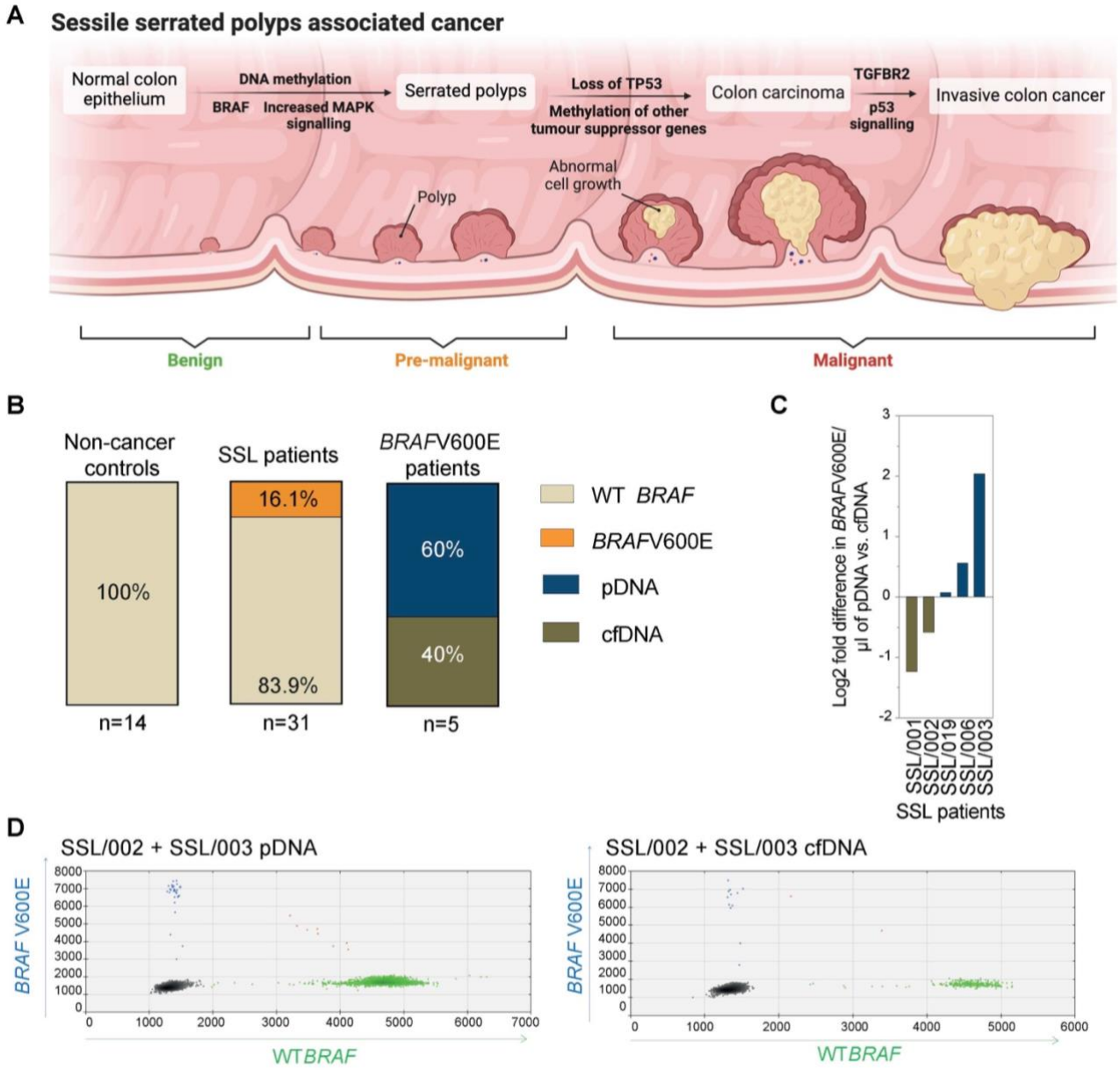


Figure 5-18. Detection of driver mutations in patients with pre-malignant colonic lesions. (A) Schematic outlining the key stages of development of sessile serrated lesions (SSLs). **(B)** Pie charts showing detection of *BRAF*V600E in patients with high-risk, premalignant colonic lesions (sessile serrated lesions, SSL) (n=31) and control individuals undergoing colonoscopy screening in whom no lesion or malignancy was detected (n=14). Mutant *BRAF* (defined as >3 positive events) was detected in 16.1% (5/31) of SSL patients and 0% (0/14) of controls. **(C)** Relative copy number of *BRAF*V600E in pDNA compared to cfDNA in the 5 patients with SSLs in whom mutant *BRAF* was detectable in either cfDNA or pDNA. Data were converted to a base-2 logarithm with a pseudo count of 1. **(D)** ddPCR plots showing *BRAF*V600E (blue) in pDNA (left) and cfDNA (right) in two SSL patients. Created using Biorender.com.

5-2.10 Box 3. Summary of findings in Aim 3:

1. Platelet DNA maps across the entire human genome and has similar coverage to cfDNA extracted from plasma.
2. Platelets capture tumour-derived DNA- as confirmed by the detection of mutant alleles in healthy donor platelets following *in vitro* co-culture with tumour cell lines and WGS of pDNA from patients with colorectal and pancreatic cancer.
3. Gene expression in cell of origin of captured DNA can be inferred from the coverage of reads from sequencing platelet DNA.
4. Mutant alleles are detectable in platelet DNA in patients with both high and low tumour burden.
5. Overall, I have demonstrated that including pDNA together with cfDNA derived from platelet-depleted plasma (which is the current source of DNA used as standard practice in liquid biopsy approaches) significantly enhances the detection of mutant alleles. This improved sensitivity is evident in both high and low tumour burden disease, therefore in addition to describing a new aspect of platelet biology, my observations offer a method to increase the sensitivity of current liquid biopsy approaches for cancer detection.

5-3 Discussion

Platelets have long been associated with carcinogenesis and metastasis, contributing to tumour angiogenesis, tumour cell extravasation and the shielding of metastasizing cancer cells from immunosurveillance[181,474]. Platelets are highly abundant and easy to isolate, and therefore ideally poised as 'sentinels' for genetic perturbations in tissues and for use in liquid biopsy approaches.

Platelet RNA has been extensively researched and shows promise as a liquid biopsy approach for hematological[475] and solid malignancies[205,365]. However, the potential of pDNA as a biomarker for disease detection remains unexplored. The main aim of this chapter was to investigate platelet DNA in the context of solid tumours, using samples from patients with pre-malignant and late-stage disease as well as mouse models of colorectal and pancreatic cancer.

In summary, the data presented here clearly highlight the utility of pDNA analysis in multiple clinical settings. A significant limitation of my dataset is the small number of patients with active cancer (n=2). However, together with the mouse models and cohort of patients with SSLs, the data from these two cases indicate that platelets contain ctDNA in quantities comparable to cfDNA. This is observed in patients with high ctDNA levels and distinct CNAs (exceeding 20%, as seen in sample 6, Fig. 5-13A), as well as those with very low ctDNA levels (below 0.5%, as observed in sample 7, Fig. 5-14), where targeted analysis and matched tumour tissue were required.

In Figure 5-7, I demonstrate that *BRAF*V600E was readily detectable in platelets following their co-incubation with both COLO205 cells and tumour cell-conditioned media. In contrast, very few copies of mutant *BRAF* were detected in peripheral blood mononuclear cells (PBMNCs) and red blood cells. From these findings, I conclude that platelets are more efficient at sequestering tumour-derived DNA compared to other blood cell types.

However, it is important to consider the composition of the PBMNC population when interpreting these results, as only a small fraction of these cells are phagocytic. Monocytes typically account for just 10-20% of the total PBMNC population[476], while the majority are lymphocytes, which generally lack significant phagocytic capacity. Therefore, a limitation of my approach here was to not specifically compare platelets to purified monocytes and neutrophils, the most abundant and efficient phagocytes in the blood. These experiments would provide a clearer understanding of how platelets compare to cells with known phagocytic capabilities.

Another potential limitation of this study concerns the DNA extraction process.

My underlying hypothesis is that platelets sequester cfDNA fragments during circulation. As discussed in the introduction, circulating DNA is typically highly fragmented, with a modal fragment size of approximately 167 bp. Therefore, to effectively capture and analyse these short DNA fragments from platelets, I selected the QIAamp Circulating Nucleic Acid Kit (Qiagen, cat # 55114) for DNA extraction. This kit is specifically optimized for isolating fragmented DNA, utilizing "advanced technology of selective binding to a silica-based membrane for improved recovery of fragmented nucleic acids," according to Qiagen. The manufacturer also highlights its efficiency in recovering DNA fragments as short as 66 bp.

Initially, this kit seemed ideal for obtaining the most efficient recovery and accurate representation of fragmented DNA. However, subsequent findings by myself and others have revealed that platelets harbour a range of DNA fragment lengths[293]. While the majority of longer platelet DNA (l-pDNA) aligns more closely with the mitochondrial genome (Fig. 5-11A), whole genome sequencing demonstrates that some of this DNA contains information similar to standard cfDNA and shorter platelet DNA (s-pDNA) (Fig. 5-14).

This suggests that by using the QIAamp Circulating Nucleic Acid Kit to process patient samples, I may be selectively enriching for shorter DNA fragments (likely captured circulating tumour DNA) while inadvertently excluding potentially important longer DNA fragments. This raises a critical question for future research: should DNA extraction protocols aim to collect the entire nucleic acid content of platelets? While this approach could allow for the detection of necrotic DNA, which is generally larger in size, it also introduces the challenge of managing contaminating white blood cell DNA[477].

Preliminary comparative analysis of DNA yields from platelet pellets using different nucleic acid extraction kits reveals significant variation (Zymo: 804 ng vs Qiagen: 266 ng, Appendix Data Figure A4). While maximizing DNA extraction might seem advantageous, a higher yield of total DNA could potentially dilute the concentration of rare mutations, making their detection more challenging against a high background of wild-type genomic DNA. In summary, additional research should be done to confirm the kit most suitable for platelet DNA extraction.

Overall, the data presented in this chapter show that a substantial proportion of ctDNA is contained within platelets, and that this information is currently being missed by standard liquid biopsy approaches that extract cfDNA from platelet-depleted plasma.

While this discovery highlights a potential improvement to current methods, further research is needed to determine whether combining cfDNA and pDNA analysis will further enhance the sensitivity of screening methods. Preliminary data indicate an increase in total DNA yield from platelet-rich plasma (PRP) compared to platelet-poor plasma (PPP), but the origin and potential informational value of DNA in these different plasma fractions remain unexplored (Appendix Data Figure A5). Moreover, future studies should investigate the potential added value of integrating DNA analysis with platelet mRNA signatures and protein cargo examinations. These avenues of research could provide a more comprehensive understanding of the information captured in platelets and further improve liquid biopsy techniques. However, such studies require a large clinical cohort and are beyond the scope and aims of my PhD.

In summary, the data presented in this chapter highlight the potential value of platelet DNA in the context of solid tumours. Given the current need for non-invasive diagnostic methods, the high abundance of platelets, their ease of isolation, and their continuous tissue perfusion, position them as ideal 'sentinels' for detecting genetic alterations, including those in early-stage or pre-malignant disease.

Chapter 6: Discussion

In this thesis I have performed the first detailed interrogation of platelet DNA content, demonstrating a new biological role for platelets that was previously unappreciated – as scavengers of endogenous extracellular cfDNA.

6-1 Outcomes of this research

6-1.1 Despite being anucleate, platelets contain DNA

Using flow cytometry, I demonstrate that ~8-20% of circulating platelets are associated with DNA, with DNA content correlating to platelet's activation state. Resting platelets tend to contain higher amounts of DNA, whereas activated, more exhausted platelets often show reduced DNA content due to degranulation and DNA secretion.

I show that platelets sequester free foetal DNA, indicating that some DNA is sequestered during peripheral circulation and therefore not solely inherited from the parent megakaryocytes during thrombopoiesis. I demonstrate higher and more variable levels of cfDNA in plasma in the setting of severe thrombocytopenia in both the murine and human setting, supportive of a role for platelets in regulating the cfDNA content of plasma.

Next, using live cell imaging, I was able to demonstrate uptake of extracellular DNA within minutes of co-incubation, independent of contact with nucleated cells.

6-1.2 Platelets sequester DNA via multiple mechanisms

I also explored the mechanism of DNA sequestration by platelets and found that this occurs by at least two mechanisms- endocytosis of DNA-laden EVs from apoptotic cells, and uptake of membrane-free DNA fragments. I found that platelets were non-selective in their sequestration of DNA fragments, internalizing all tested DNA lengths ranging from 90 to 657 bp.

I demonstrate that the uptake of DNA-containing apo-EVs by platelets is partially dynamin-dependent, as it can be reduced using the inhibitor Dynole. In contrast, Dynole had no effect on the uptake of 'free' DNA fragments, suggesting distinct mechanisms of uptake for these two types of DNA. Additionally, I show that DNA fragments are released through platelet exocytosis, and, importantly, this release can be prevented using pharmacological inhibitors, thereby preserving the DNA within platelets, where it remains protected from degradation.

Using high resolution microscopy, I confirm that DNA is internalised into the platelet interior and not held within the membrane folds of the open canalicular system. DNA strongly co-localised with CD81 expressing vesicles and LAMP-2 positive late endosomes/ lysosomes, suggesting that DNA is internalised and intentionally trafficked through the platelet for degradation or storage and release.

6-1.3 Platelets contain clinically important tumour- derived DNA

Using an *in vitro* co-culture system, I demonstrate that platelets can sequester tumour-derived DNA from a range of cancer cell lines and that this DNA is protected from enzymatic degradation within the platelets. Furthermore, platelets are more efficient at acquiring tumour-derived DNA compared to other blood cell types including red blood cells and peripheral blood mononuclear cells.

Using whole genome sequencing, we identified two distinct subpopulations of DNA within platelets: short-platelet DNA, likely sequestered genomic cell-free fragments from circulation, and long-platelet DNA, which mapped more closely to the mitochondrial genome. We then employed iChorCNA to detect copy number alterations in DNA extracted from both plasma and platelets of a patient with a high tumour burden (>20%). Clonal amplifications were detectable in both short-platelet DNA and plasma.

Furthermore, where tumour tissue from one patient with a low tumour burden (<0.5%) was available, deeper sequencing allowed us to look for low-level ctDNA by screening for mutations present in the tumour biopsy. Encouragingly, matched tumour mutations were detected at a significantly higher rate than random mutations taken from The Cancer Genome Atlas (TCGA) in both the short platelet DNA and plasma.

Next, I utilized targeted droplet digital PCR to detect mutant *BRAF* and *KRAS* in patients with high-grade colonic polyps and in mice modelling the progression from early to late stages of colorectal and pancreatic

cancer, respectively. Detection of these mutations in platelets indicates that platelet DNA might be a highly sensitive test for early-stage as well as late-stage malignancies.

6-2 Implications and wider relevance

Detection and analysis of cfDNA is rapidly being implemented in several clinical settings including cancer screening, detection of residual disease and prenatal diagnosis[478-480]. This interest is evident in the rollout of the multi-cancer early detection tests, such as GRAIL's Galleri test, which employs methylation analysis of cfDNA in platelet depleted plasma. It is estimated that implementing a genomic-based liquid biopsy test for cancer, with a 25-100% adoption rate in the U.S., could detect an additional 100,000 to 400,000 cancers beyond those identified through current screening methods[481].

However, these methods have limited sensitivity in cases of low tumour burden, where the amount of cancer cell-derived DNA in plasma is minimal[482,483]. Therefore, pre-analytical approaches to increase capture of ctDNA would be of significant interest. The data presented in my thesis suggest that a substantial proportion of ctDNA is contained within platelets, and that this information is currently being missed by standard sampling protocols that extract cfDNA from platelet-depleted plasma. This study paves the way for validation in larger clinical cohorts to test whether combining cfDNA plus platelet DNA adds value, as well as future research to further establish a role for platelets in cfDNA homeostasis. It would be particularly interesting for future research to study the 'added value' of platelet DNA combined with standard cfDNA approaches in patients following anti-cancer therapy, where the detection of tumour-derived DNA may influence intensity of further therapy or monitoring requirements.

Platelets are well-established as crucial players in infection and inflammation, engaging in pathogen engulfment, antimicrobial protein release, and promotion of inflammation through pro-inflammatory mediator secretion and immune cell recruitment. My findings in chapter 3, that demonstrate elevated and more variable levels of cfDNA in plasma during severe thrombocytopenia in both murine models and human patients, support the hypothesis that platelets also contribute to clearance of endogenous cfDNA, as well as pathogen-derived nucleic acids, from circulation.

These observations raise an intriguing question: Are patients with chronically low platelet counts such as that caused by chronic immune thrombocytopenia (ITP) at increased risk of infection or autoimmune disease? The significantly reduced number of circulating platelets might impair the immune system's capacity to combat infections. Simultaneously, prolonged elevation of plasma cfDNA levels could promote inflammation and immune cell activation, potentially driving autoimmune disease development[320,321].

Further investigation into the potential link between severe, chronic thrombocytopenia and increased risk of autoimmune diseases could yield valuable insights. This research direction could broaden our understanding of the complex interplay between platelets, cfDNA dynamics, and immune function, potentially informing new approaches to managing ITP and related disorders.

6-3 Limitations of this research

A significant limitation of this study is the relatively small number of samples analysed from patients with active cancer who had detectable ctDNA. While this limited cohort is not ideal, the fact that we were able to detect tumour-derived DNA in the platelets of two patients, including one with a high ctDNA burden (25%) and the other with very low-level ctDNA (<0.5%), is an encouraging finding. It suggests that platelet DNA analysis may be a sensitive method for tumour detection, even in cases with low circulating tumour content. To strengthen these findings, future studies should include a larger cohort of cancer patients to examine platelet DNA. Obtaining more paired tumour biopsies and follow-up samples from patients undergoing treatment would also be highly valuable, however new clinical sample banking infrastructure and ethical approvals would be required to conduct these studies, which are beyond the scope and resources of my PhD. Despite the limitations, the clinical data included in this thesis offer a strong proof-of-concept for the potential of platelet DNA analysis in cancer diagnostics.

Secondly, while I have demonstrated that a proportion of platelet DNA derives from the plasma, I have not yet explored what proportion of DNA originates from their parent megakaryocytes (MKs) and furthermore, the utility of this for interrogating changes to the megakaryocyte genome. This is the focus of my current experiments. If platelets incorporate DNA from their progenitor MKs, they could serve as valuable circulating

biomarkers that reflect the genomic state of MKs and haematopoietic stem cells, similarly to how ctDNA mirrors the genetic profile of tumours. This approach holds significant potential for monitoring clonal haematopoiesis (CH) and chronic blood cancers where aberrations in MK-biased stem cells drive disease – e.g. myeloproliferative neoplasms (MPNs), such as Essential Thrombocythemia, Myelofibrosis, and Polycythaemia Vera. Analysing platelet DNA could offer insights into the genetic changes underlying these disorders and enhance the detection of CH and MPNs, as well as the monitoring of high-risk co-mutations. This approach could offer greater sensitivity compared to current methods which primarily involve genetic testing of whole blood- or granulocyte-derived DNA, or invasive bone marrow biopsies.

Finally, as discussed in chapter 4, the fate of DNA after its internalisation by platelets remains incompletely understood. Although my imaging data show colocalization of platelet DNA with LAMP-2 and CD81, markers for lysosomes and exosomes respectively, the small antibody panel used in the analysis of the platelet ultrastructure, limits our ability to draw definitive conclusions.

For instance, the tetraspanin CD81, is expressed throughout the endosomal pathway involved in exosome biogenesis, including early endosomes, late endosomes, and multivesicular bodies (MVBs). Given this ubiquitous expression, the colocalization of CD81 with DNA in platelets, could have multiple implications. It may suggest that sequestered DNA is trafficked through the endosomal pathway for packaging into granules or vesicles destined for secretion, potentially indicating an active role for platelets in DNA transport and release. Alternatively, this colocalization could represent DNA-containing exosomes sequestered by the platelet, similar to the findings presented in chapter 3, where I demonstrate platelet uptake of DNA-containing apo-EVs. It is also not clear how long DNA is preserved within circulating platelets, and the extent/rate of its degradation.

Overall, this colocalization suggests potential trafficking of internalised DNA through lysosomal compartments and/or its association with exosome-related structures. However, a more comprehensive analysis using a larger panel of subcellular markers is needed to clarify the precise intracellular route and the fate of the internalised DNA.

Finally, I did not definitively look for the presence of foetal platelets in the maternal blood samples that I used for this study. I was able to correctly ascertain the sex of the baby in 20/20 of the blood samples that I studied, and foetal-maternal haemorrhage is a rare event. Furthermore, even in the unlikely scenario that some foetal platelets were captured, these data would still provide clear evidence of the presence of DNA fragments within the foetal platelets – which was the primary goal of my studies.

6-4 Future research

These studies have raised several further questions, which I plan to address in future studies.

6-4.1 Question 1: Do platelets transfer sequestered DNA to other cell types?

Platelets have been shown to mediate horizontal transfer of RNAs and transcription factors[484], either via uptake of whole platelets by phagocytes, endothelial cells and smooth muscle cells or by the release of platelet microparticles[321]. Whether platelets can similarly act as a vector for the horizontal transfer of DNA fragments should be investigated.

The concept of DNA acting as an intercellular messenger has been explored for decades. In 1994, Anker *et al.,* first demonstrated that the supernatant from a colon cancer cell line could transform recipient mouse cells, causing them to acquire mutated human *KRAS*[485]. García-Olmo *et al.,* corroborated these findings in 2010, showing that nucleic acids isolated from colorectal cancer patients' plasma could also transform the same cell line *in vitro*[486]. Further evidence came in 2012 when a study demonstrated gene transfer and cell transformation *in vivo* using a rat model of colorectal cancer[487].

These discoveries led to the relatively new, and widely debated, 'genometastasis' hypothesis, which suggests that cancer cells can metastasize via horizontal gene transfer. According to this theory, circulating nucleic acids are sequestered by recipient cells at distant sites, where the genetic information is transcribed and translated, leading to cellular transformation of wild type, recipient cells[258,488-490].

The precise mechanism by which cfDNA promotes the malignant transformation of non-tumour cells is unclear[491]. Some researchers have demonstrated that transformation occurs via the uptake of apoptotic bodies[351,352,492] and EVs[493], while others have suggested that DNA is complexed with lipids and proteins, forming stable structures termed "virtosomes"[494]. More recently, attention has focused on extrachromosomal circular DNA (eccDNA) as a potential mediator of oncogenic transformation. EccDNA, a type of circulating DNA, has been associated with poor outcomes across multiple cancer types, primarily due to its role in overexpression of oncogenes leading to malignant tumour growth[321,495-497].

Given that platelets sequester DNA, further investigation is warranted to determine whether platelets enhance the uptake of DNA, including cfDNA and eccDNA to recipient cells. Based on the data I've collected and our current understanding of platelet contributions to tumourigenesis, it seems plausible that platelets might also play a role in the oncogenic transformation of cell neighbourhoods.

My proposed experimental strategy to investigate the transfer of DNA from platelets to recipient cells consists of two key components. First, I will 'educate' platelets by exposing them to tumour-derived factors, followed by incubation with endothelial cells. This builds on previous findings that demonstrate the ability of endothelial cells to sequester tumour-derived DNA[498]. I will employ both a static co-culture system, as described in this thesis, and a vessel-on-a-chip microfluidic device to better simulate physiological conditions[499,500]. This microfluidic system mimics the structure and function of blood vessels, allowing for the flow of platelets through endothelial-lined channels. Platelet activation will be induced using either soluble or immobilized activators, or through direct stimulation of endothelial cells. After circulation, I will analyse the endothelial cells for the presence of platelet-derived DNA and assess any resulting changes in their behaviour or phenotype.

The second component of my experimental approach focuses on extrachromosomal circular DNA (eccDNA) analysis. I will use CIRCLE-seq, a specialized technique for detecting eccDNA[501], to investigate whether platelets can take up circular DNA fragments. Preliminary data from an unrelated experiment indicate that this may be feasible. In this study, healthy donor platelets were shown to internalise labelled circular DNA from *E. coli*, demonstrating their capacity to take up circular DNA structures. Additionally, it has been reported that

eccDNA is enriched with CpG regions, which can serve as ligands for TLR9, a receptor expressed by platelets[502]!

6-4.2 Question 2: Do platelets release DNA at sites of activation to elicit an immune response?

Further investigation is necessary to determine whether platelets actively deploy their DNA content at sites of activation. Flow cytometry data presented in chapter 4 demonstrate a decrease in DRAQ5 staining upon platelet activation, suggesting degranulation and potential DNA loss. This observation supports an intriguing hypothesis: platelet clearance may control the non-specific immunostimulatory activity of cfDNA in plasma, and that platelets may then release DNA cargo in a targeted manner to evoke an immune response at sites of platelet activation. This controlled release could occur through several mechanisms:

1. Enhancement of immune response: Platelets are known to support immune cells during infection and promote inflammation by actively releasing pro-inflammatory factors such as MIP-1 and IL-1β. Given that elevated levels of self-DNA can also trigger pro-inflammatory cytokine production, it's plausible that platelets may deliberately release cfDNA to further stimulate immune cells at sites of activation.
2. Contribution to NET composition: Platelets promote the formation of neutrophil extracellular traps (NETs) through TLR4 activation[85,91,127]. Some studies suggest that platelets provide mitochondrial DNA to neutrophils during this process[64]. Therefore, beyond stimulating NETosis and releasing mitochondria, activated platelets may also supply sequestered cfDNA to neutrophils. This mechanism could allow platelets to contribute directly to the chromatin structure forming the characteristic weblike DNA framework of NETs.

To investigate these hypotheses, as outlined in Question 1, I propose using the vessel-on-a-chip microfluidic device to trigger platelet activation and measure DNA release. Additionally, Silvia *et al.,*[503] describe a protocol for live-cell imaging of NET formation, which I could adapt for this study. By labelling platelet DNA and co-incubating neutrophils with platelets, I could track the release of platelet DNA and determine whether it is incorporated into the chromatin web of the NETs.

6-4.3 Question 3: Can we inhibit platelet exocytosis in whole blood?

I have demonstrated that the release of DNA fragments from washed platelets is an active process, which can be blocked using pharmacological inhibitors like Dynole and amiloride. Based on this data, I aim to explore whether it's possible to prevent nucleic acid release from platelets in whole blood. Since my data suggest that platelets protect the DNA they capture from degradation, blocking platelet secretion at the point of collection may enhance DNA recovery from platelets, potentially improving the sensitivity of tumour detection. To test this hypothesis, I will add inhibitors directly to the blood collection tubes prior to sampling, then isolate the platelets and compare the DNA yield between treated and control samples using ddPCR. The immediate preservation of platelet nucleic acids may be crucial to increasing the yield of disease- relevant biomarkers in liquid biopsy methods, including cancer and antenatal genetic screening (Fig. 6-1).

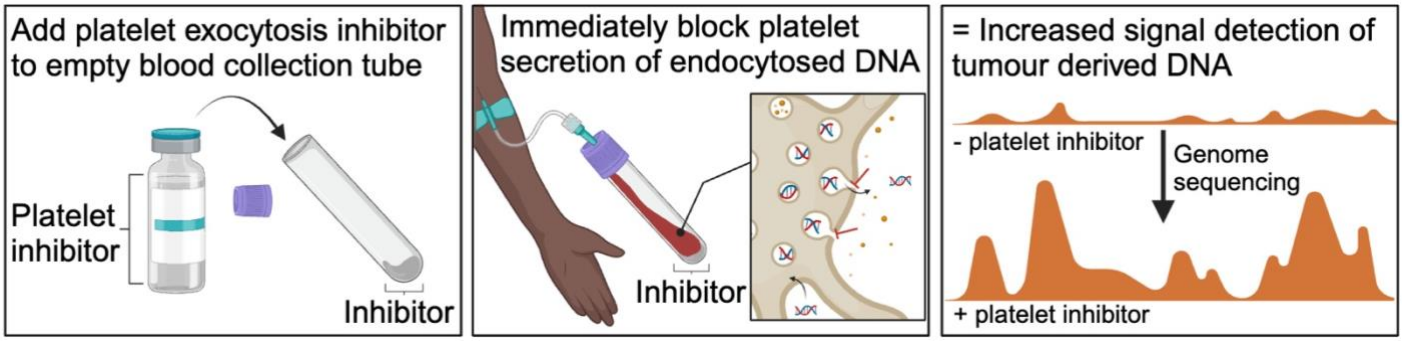


Figure 6-1. Schematic illustrating how immediate inhibition of platelet secretion may enhance the yield of tumour-derived biomarkers, thereby improving the sensitivity of tumour detection. The platelet exocytosis inhibitor is added directly to the blood collection tube and remains stable at room temperature. Blood is drawn into the tube and immediately mixes with the inhibitor, blocking platelet secretion of captured DNA. This inhibition increases the amount of DNA available within the platelets for analysis. Created using Biorender.com.

6-4.4 Question 4: Are DNA sensing receptors involved in platelet DNA uptake?

As outlined in the introduction to chapter 3 (section 3-1.2), platelets express DNA-sensing receptors, including TLR9 and RAGE. While I have demonstrated that platelets can acquire DNA through the active uptake of DNA-containing vesicles, the specific mechanisms involved in the sequestration of 'free' DNA fragments remain unclear. How do platelets detect this DNA? In 2012, Thon *et al.,* proposed that TLR9 regulates platelet uptake of unmethylated CpG DNA, showing that platelets from TLR9 knockout (KO) mice exhibit reduced

sequestration of synthetic oligonucleotides, mimicking bacterial and viral DNA[53]. Therefore, measuring platelet uptake of cfDNA in TLR9 and RAGE KO mice might provide clean, genetic evidence of a role for these receptors in mammalian DNA sequestration by circulating platelets.

6-5 Conclusion

In summary, this thesis reveals that despite lacking a nucleus, platelets acquire a repertoire of DNA fragments mapping across the nuclear genome. I demonstrate foetal DNA in maternal platelets and cancer cell-derived DNA in platelets from patients with pre-malignant and cancerous lesions. As current liquid biopsy approaches utilise platelet-depleted plasma, important genetic information contained within platelets is being missed. This work establishes a physiological role for platelets that has not previously been highlighted, with broad translational relevance.

Bibliography

1 Davis, E., Corash, L., Stenberg, P. & Levin, J. Histologic studies of splenic megakaryocytes after bone marrow ablation with strontium 90. *The Journal of Laboratory and Clinical Medicine* **120**, 767-777 (1992). https://doi.org:10.5555/uri:pii:002221439290086Z

2 Lefrançais, E. *et al.* The lung is a site of platelet biogenesis and a reservoir for haematopoietic progenitors. *Nature* **544**, 105-109 (2017). https://doi.org:10.1038/nature21706

3 Pariser, D. N. *et al.* Lung megakaryocytes are immune modulatory cells. *The Journal of Clinical Investigation* **131** (2021). https://doi.org:10.1172/JCI137377

4 Looney, M. Platelet Biogenesis in the Lung Circulation. *Blood* **132**, SCI-22-SCI-22 (2018). https://doi.org:10.1182/blood-2018-99-109544

5 Asquith, N. L. *et al.* The bone marrow is the primary site of thrombopoiesis. *Blood* **143**, 272-278 (2024). https://doi.org:10.1182/blood.2023020895

6 Machlus, K. R. & Italiano, J. E., Jr. The incredible journey: From megakaryocyte development to platelet formation. *J Cell Biol* **201**, 785-796 (2013). https://doi.org:10.1083/jcb.201304054

7 Ebbe, S. Biology of megakaryocytes. *Prog Hemost Thromb* **3**, 211-229 (1976).

8 Poulter, N. S. & Thomas, S. G. Cytoskeletal regulation of platelet formation: Coordination of F-actin and microtubules. *The International Journal of Biochemistry & Cell Biology* **66**, 69-74 (2015). https://doi.org:https://doi.org/10.1016/j.biocel.2015.07.008

9 Patel, S. R. *et al.* Differential roles of microtubule assembly and sliding in proplatelet formation by megakaryocytes. *Blood* **106**, 4076-4085 (2005). https://doi.org:10.1182/blood-2005-06-2204

10 Italiano, J. E., Jr., Lecine, P., Shivdasani, R. A. & Hartwig, J. H. Blood Platelets Are Assembled Principally at the Ends of Proplatelet Processes Produced by Differentiated Megakaryocytes. *Journal of Cell Biology* **147**, 1299-1312 (1999). https://doi.org:10.1083/jcb.147.6.1299

11 Richardson, J. L., Shivdasani, R. A., Boers, C., Hartwig, J. H. & Italiano, J. E., Jr. Mechanisms of organelle transport and capture along proplatelets during platelet production. *Blood* **106**, 4066-4075 (2005). https://doi.org:10.1182/blood-2005-06-2206

12 Thon, J. N. *et al.* Microtubule and cortical forces determine platelet size during vascular platelet production. *Nat Commun* **3**, 852 (2012). https://doi.org:10.1038/ncomms1838

13 Thon, J. N. *et al.* Cytoskeletal mechanics of proplatelet maturation and platelet release. *J Cell Biol* **191**, 861-874 (2010). https://doi.org:10.1083/jcb.201006102

14 McArthur, K., Chappaz, S. & Kile, B. T. Apoptosis in megakaryocytes and platelets: the life and death of a lineage. *Blood* **131**, 605-610 (2018). https://doi.org:https://doi.org/10.1182/blood-2017-11-742684

15 Radley, J. & Haller, C. Fate of senescent megakaryocytes in the bone marrow. *British Journal of Haematology* **53**, 277-287 (1983).

16 Quach, M. E., Chen, W. & Li, R. Mechanisms of platelet clearance and translation to improve platelet storage. *Blood, The Journal of the American Society of Hematology* **131**, 1512-1521 (2018).

17 Gaertner, F. *et al.* Plasmacytoid dendritic cells control homeostasis of megakaryopoiesis. *Nature* **631**, 645-653 (2024). https://doi.org:10.1038/s41586-024-07671-y
18 Ellis, M. L., Alwis, I., Smythe, R., Yuan, Y. & Jackson, S. P. Megakaryocyte buds are distinct from microvesicles and likely to represent platelet precursors. *Blood Adv* **7**, 982-986 (2023). https://doi.org:10.1182/bloodadvances.2022008850
19 Potts, K. S. *et al.* Membrane budding is a major mechanism of in vivo platelet biogenesis. *J Exp Med* **217** (2020). https://doi.org:10.1084/jem.20191206
20 Terreaux, A. F., Farley, A. M., Biben, C., Stonehouse, O. & Taoudi, S. (2022). https://doi.org:10.1101/2022.05.21.492939
21 Italiano, J. E. *et al.* Microvesicles, but not platelets, bud off from mouse bone marrow megakaryocytes. *Blood* **138**, 1998-2001 (2021). https://doi.org:10.1182/blood.2021012496
22 Ellis, M. L. *et al.* GPIbα–filamin A interaction regulates megakaryocyte localization and budding during platelet biogenesis. *Blood* **143**, 342-356 (2024). https://doi.org:https://doi.org/10.1182/blood.2023021292
23 Li, R. Platelet size matters. *Blood* **143**, 298-300 (2024). https://doi.org:10.1182/blood.2023023057
24 Liu, H. *et al.* Multiphoton In Vivo Microscopy of Embryonic Thrombopoiesis Reveals the Generation of Platelets through Budding. *Cells* **12**, 2411 (2023). https://doi.org:10.3390/cells12192411
25 Flaumenhaft, R. *et al.* Megakaryocyte-derived microparticles: direct visualization and distinction from platelet-derived microparticles. *Blood* **113**, 1112-1121 (2009). https://doi.org:10.1182/blood-2008-06-163832
26 Petzold, T. *et al.* Neutrophil "plucking" on megakaryocytes drives platelet production and boosts cardiovascular disease. *Immunity* **55**, 2285-2299.e2287 (2022). https://doi.org:10.1016/j.immuni.2022.10.001
27 van Grinsven, E. & Udalova, I. A. You reap what you sow: Neutrophils “plucking” platelets harvest prothrombotic effects. *Immunity* **55**, 2217-2219 (2022). https://doi.org:https://doi.org/10.1016/j.immuni.2022.11.012
28 Patel-Hett, S. *et al.* Visualization of microtubule growth in living platelets reveals a dynamic marginal band with multiple microtubules. *Blood* **111**, 4605-4616 (2008). https://doi.org:10.1182/blood-2007-10-118844
29 Mathur, A. *et al.* Cytoskeleton mechanics determine resting size and activation dynamics of platelets. *bioRxiv*, 413377 (2018). https://doi.org:10.1101/413377
30 Fox, J. E. B. The Platelet Cytoskeleton. *Thromb Haemost* **70**, 0884-0893 (1993). https://doi.org:10.1055/s-0038-1649694
31 Hartwig, J. H. & DeSisto, M. The cytoskeleton of the resting human blood platelet: structure of the membrane skeleton and its attachment to actin filaments. *Journal of Cell Biology* **112**, 407-425 (1991). https://doi.org:10.1083/jcb.112.3.407
32 Italiano, J. E., Jr *et al.* Mechanisms and implications of platelet discoid shape. *Blood* **101**, 4789-4796 (2003). https://doi.org:10.1182/blood-2002-11-3491
33 Escolar, G., Leistikow, E. & White, J. G. The Fate of the Open Canalicular System in Surface and Suspension-Activated Platelets. *Blood* **74**, 1983-1988 (1989). https://doi.org:https://doi.org/10.1182/blood.V74.6.1983.1983
34 Selvadurai, M. V. & Hamilton, J. R. Structure and function of the open canalicular system - the platelet's specialized internal membrane network. *Platelets* **29**, 319-325 (2018). https://doi.org:10.1080/09537104.2018.1431388
35 Thomas, S. G. in *Platelets (Fourth Edition)* (ed Alan D. Michelson) 47-77 (Academic Press, 2019).
36 White, J. G. Platelets are covercytes, not phagocytes: uptake of bacteria involves channels of the open canalicular system. *Platelets* **16**, 121-131 (2005).

37 Sandmann, R. & Köster, S. Topographic Cues Reveal Two Distinct Spreading Mechanisms in Blood Platelets. *Scientific Reports* **6**, 22357 (2016). https://doi.org:10.1038/srep22357

38 Liu, H. & Welburn, J. P. I. A circle of life: platelet and megakaryocyte cytoskeleton dynamics in health and disease. *Open Biology* **14**, 240041 (2024). https://doi.org:doi:10.1098/rsob.240041

39 King, S. M. & Reed, G. L. Development of platelet secretory granules. *Seminars in Cell & Developmental Biology* **13**, 293-302 (2002). https://doi.org:https://doi.org/10.1016/S1084952102000599

40 Reed, G. L., Fitzgerald, M. L. & Polgár, J. n. Molecular mechanisms of platelet exocytosis: insights into the "secrete" life of thrombocytes. *Blood* **96**, 3334-3342 (2000). https://doi.org:10.1182/blood.V96.10.3334

41 Flaumenhaft, R. & Sharda, A. in *Platelets (Fourth Edition)* (ed Alan D. Michelson) 349-370 (Academic Press, 2019).

42 Yadav, S. & Storrie, B. The cellular basis of platelet secretion: Emerging structure/function relationships. *Platelets* **28**, 108-118 (2017). https://doi.org:10.1080/09537104.2016.1257786

43 Italiano Jr, J. E. & Battinelli, E. M. Selective sorting of alpha-granule proteins. *Journal of Thrombosis and Haemostasis* **7**, 173-176 (2009). https://doi.org:10.1111/j.1538-7836.2009.03387.x

44 Heijnen, H. F. G., Schiel, A. E., Fijnheer, R., Geuze, H. J. & Sixma, J. J. Activated Platelets Release Two Types of Membrane Vesicles: Microvesicles by Surface Shedding and Exosomes Derived From Exocytosis of Multivesicular Bodies and α-Granules. *Blood* **94**, 3791-3799 (1999). https://doi.org:https://doi.org/10.1182/blood.V94.11.3791

45 Pagel, O., Walter, E., Jurk, K. & Zahedi, R. P. Taking the stock of granule cargo: Platelet releasate proteomics. *Platelets* **28**, 119-128 (2017). https://doi.org:10.1080/09537104.2016.1254762

46 McNicol, A. & Israels, S. J. Platelet Dense Granules: Structure, Function and Implications for Haemostasis. *Thrombosis Research* **95**, 1-18 (1999). https://doi.org:https://doi.org/10.1016/S0049-3848(99)00015-8

47 Sharda, A. & Flaumenhaft, R. The life cycle of platelet granules. *F1000Res* **7**, 236 (2018). https://doi.org:10.12688/f1000research.13283.1

48 Heijnen, H. & van der Sluijs, P. Platelet secretory behaviour: as diverse as the granules … or not? *Journal of Thrombosis and Haemostasis* **13**, 2141-2151 (2015). https://doi.org:https://doi.org/10.1111/jth.13147

49 Ambrosio, A. L., Boyle, J. A. & Di Pietro, S. M. Mechanism of platelet dense granule biogenesis: study of cargo transport and function of Rab32 and Rab38 in a model system. *Blood* **120**, 4072-4081 (2012). https://doi.org:10.1182/blood-2012-04-420745

50 Youssefian, T. & Cramer, E. M. Megakaryocyte dense granule components are sorted in multivesicular bodies. *Blood* **95**, 4004-4007 (2000). https://doi.org:10.1182/blood.V95.12.4004

51 Ambrosio, A. L. & Di Pietro, S. M. Storage pool diseases illuminate platelet dense granule biogenesis. *Platelets* **28**, 138-146 (2017). https://doi.org:10.1080/09537104.2016.1243789

52 Rendu, F. & Brohard-Bohn, B. The platelet release reaction: granules' constituents, secretion and functions. *Platelets* **12**, 261-273 (2001). https://doi.org:10.1080/09537100120068170

53 Thon, J. N. *et al.* T granules in human platelets function in TLR9 organization and signaling. *J Cell Biol* **198**, 561-574 (2012). https://doi.org:10.1083/jcb.201111136

54 Melchinger, H., Jain, K., Tyagi, T. & Hwa, J. Role of Platelet Mitochondria: Life in a Nucleus-Free Zone. *Front Cardiovasc Med* **6**, 153 (2019). https://doi.org:10.3389/fcvm.2019.00153

55 Lindemann, S. *et al.* Activated platelets mediate inflammatory signaling by regulated interleukin 1beta synthesis. *J Cell Biol* **154**, 485-490 (2001). https://doi.org:10.1083/jcb.200105058

56 Hille, L. *et al.* Evaluation of an Alternative Staining Method Using SYTO 13 to Determine Reticulated Platelets. *Thromb Haemost* **119**, 779-785 (2019). https://doi.org:10.1055/s-0039-1681101

57 Armstrong, P. C. *et al.* Temporal in vivo platelet labeling in mice reveals age-dependent receptor expression and conservation of specific mRNAs. *Blood Adv* **6**, 6028-6038 (2022). https://doi.org:10.1182/bloodadvances.2022007099

58 Allan, H. E. *et al.* Proteome and functional decline as platelets age in the circulation. *J Thromb Haemost* **19**, 3095-3112 (2021). https://doi.org:10.1111/jth.15496

59 D'Ambrosi, S., Nilsson, R. J. & Wurdinger, T. Platelets and tumor-associated RNA transfer. *Blood* **137**, 3181-3191 (2021). https://doi.org:10.1182/blood.2019003978

60 Nilsson, R. J. A. *et al.* Blood platelets contain tumor-derived RNA biomarkers. *Blood* **118**, 3680-3683 (2011). https://doi.org:10.1182/blood-2011-03-344408

61 Landry, P. *et al.* Existence of a microRNA pathway in anucleate platelets. *Nature structural & molecular biology* **16**, 961-966 (2009).

62 Czajka, P. *et al.* MicroRNA as potential biomarkers of platelet function on antiplatelet therapy: a review. *Frontiers in physiology* **12**, 652579 (2021).

63 Willeit, P. *et al.* Circulating microRNAs as novel biomarkers for platelet activation. *Circulation research* **112**, 595-600 (2013).

64 Boudreau, L. H. *et al.* Platelets release mitochondria serving as substrate for bactericidal group IIA-secreted phospholipase A2 to promote inflammation. *Blood* **124**, 2173-2183 (2014). https://doi.org:10.1182/blood-2014-05-573543

65 Hayashi, T. *et al.* Role of mitochondria in the maintenance of platelet function during in vitro storage. *Transfusion Medicine* **21**, 166-174 (2011). https://doi.org:https://doi.org/10.1111/j.1365-3148.2010.01065.x

66 Levoux, J. *et al.* Platelets Facilitate the Wound-Healing Capability of Mesenchymal Stem Cells by Mitochondrial Transfer and Metabolic Reprogramming. *Cell Metab* **33**, 283-299 e289 (2021). https://doi.org:10.1016/j.cmet.2020.12.006

67 Alberts, B. *et al. Molecular biology of the cell*. Vol. 3 (Garland New York, 1994).

68 Baaten, C. C. *et al.* Impaired mitochondrial activity explains platelet dysfunction in thrombocytopenic cancer patients undergoing chemotherapy. *Haematologica* **103**, 1557 (2018).

69 Bizzozero, J. Ueber einen neuen Formbestandtheil des Blutes und dessen Rolle bei der Thrombose und der Blutgerinnung. *Archiv für pathologische Anatomie und Physiologie und für klinische Medicin* **90**, 261-332 (1882). https://doi.org:10.1007/BF01931360

70 Gale, A. J. Continuing education course #2: current understanding of hemostasis. *Toxicol Pathol* **39**, 273-280 (2011). https://doi.org:10.1177/0192623310389474

71 Tomaiuolo, M., Brass, L. F. & Stalker, T. J. Regulation of Platelet Activation and Coagulation and Its Role in Vascular Injury and Arterial Thrombosis. *Interv Cardiol Clin* **6**, 1-12 (2017). https://doi.org:10.1016/j.iccl.2016.08.001

72 Clemetson, K. J. Platelets and Primary Haemostasis. *Thrombosis Research* **129**, 220-224 (2012). https://doi.org:https://doi.org/10.1016/j.thromres.2011.11.036

73 Rand, J. H. *et al.* The significance of subendothelial von Willebrand factor. *Thrombosis and haemostasis* **78**, 445-450 (1997).

74 Ruggeri, Z. M. The role of von Willebrand factor in thrombus formation. *Thrombosis Research* **120**, S5-S9 (2007). https://doi.org:https://doi.org/10.1016/j.thromres.2007.03.011

75 Nieswandt, B., Varga-Szabo, D. & Elvers, M. Integrins in platelet activation. *Journal of Thrombosis and Haemostasis* **7**, 206-209 (2009). https://doi.org:10.1111/j.1538-7836.2009.03370.x

76 Yun, S. H., Sim, E. H., Goh, R. Y., Park, J. I. & Han, J. Y. Platelet Activation: The Mechanisms and Potential Biomarkers. *Biomed Res Int* **2016**, 9060143 (2016). https://doi.org:10.1155/2016/9060143

77 WATSON, S. P., AUGER, J. M., McCARTY, O. J. T. & PEARCE, A. C. GPVI and integrin αIIbβ3 signaling in platelets. *Journal of Thrombosis and Haemostasis* **3**, 1752-1762 (2005). https://doi.org:https://doi.org/10.1111/j.1538-7836.2005.01429.x

78 Cognasse, F. *et al.* Platelets as Key Factors in Inflammation: Focus on CD40L/CD40. *Frontiers in Immunology* **13** (2022). https://doi.org:10.3389/fimmu.2022.825892

79 Swystun, L. L. & Liaw, P. C. The role of leukocytes in thrombosis. *Blood* **128**, 753-762 (2016). https://doi.org:10.1182/blood-2016-05-718114

80 Gross, P. L., Furie, B. C., Merrill-Skoloff, G., Chou, J. & Furie, B. Leukocyte-versus microparticle-mediated tissue factor transfer during arteriolar thrombus development. *Journal of Leukocyte Biology* **78**, 1318-1326 (2005). https://doi.org:10.1189/jlb.0405193

81 El Filaly, H. *et al.* Dissecting Platelet's Role in Viral Infection: A Double-Edged Effector of the Immune System. *Int J Mol Sci* **24** (2023). https://doi.org:10.3390/ijms24032009

82 Maouia, A., Rebetz, J., Kapur, R. & Semple, J. W. The immune nature of platelets revisited. *Transfusion medicine reviews* **34**, 209-220 (2020).

83 Hally, K., Fauteux-Daniel, S., Hamzeh-Cognasse, H., Larsen, P. & Cognasse, F. Revisiting Platelets and Toll-Like Receptors (TLRs): At the Interface of Vascular Immunity and Thrombosis. *Int J Mol Sci* **21** (2020). https://doi.org:10.3390/ijms21176150

84 Koupenova, M. *et al.* Platelet-TLR7 mediates host survival and platelet count during viral infection in the absence of platelet-dependent thrombosis. *Blood* **124**, 791-802 (2014). https://doi.org:10.1182/blood-2013-11-536003

85 Deppermann, C. & Kubes, P. Start a fire, kill the bug: The role of platelets in inflammation and infection. *Innate Immun* **24**, 335-348 (2018). https://doi.org:10.1177/1753425918789255

86 Zhang, G. *et al.* Lipopolysaccharide stimulates platelet secretion and potentiates platelet aggregation via TLR4/MyD88 and the cGMP-dependent protein kinase pathway. *The Journal of Immunology* **182**, 7997-8004 (2009).

87 Cognasse, F. *et al.* The Inflammatory Role of Platelets via Their TLRs and Siglec Receptors. *Frontiers in Immunology* **6**, 83 (2015). https://doi.org:10.3389/fimmu.2015.00083

88 Assinger, A. *et al.* Human Cytomegalovirus–platelet interaction triggers toll-like receptor 2–dependent proinflammatory and proangiogenic responses. *Arteriosclerosis, thrombosis, and vascular biology* **34**, 801-809 (2014).

89 Koupenova, M. *et al.* The role of platelets in mediating a response to human influenza infection. *Nature communications* **10**, 1780 (2019).

90 Koupenova, M. *et al.* Platelet-TLR7 mediates host survival and platelet count during viral infection in the absence of platelet-dependent thrombosis. *Blood, The Journal of the American Society of Hematology* **124**, 791-802 (2014).

91 Gautam, I. *et al.* From classical to unconventional: the immune receptors facilitating platelet responses to infection and inflammation. *Biology* **9**, 343 (2020).

92 Antoniak, S. & Mackman, N. Platelets and viruses. *Platelets* **32**, 325-330 (2021). https://doi.org:10.1080/09537104.2021.1887842

93 Barton, G. M., Kagan, J. C. & Medzhitov, R. Intracellular localization of Toll-like receptor 9 prevents recognition of self DNA but facilitates access to viral DNA. *Nat Immunol* **7**, 49-56 (2006). https://doi.org:10.1038/ni1280

94 Scharfe-Nugent, A. *et al.* TLR9 provokes inflammation in response to fetal DNA: mechanism for fetal loss in preterm birth and preeclampsia. *J Immunol* **188**, 5706-5712 (2012). https://doi.org:10.4049/jimmunol.1103454

95 Niu, Z. *et al.* Cell-free DNA derived from cancer cells facilitates tumor malignancy through Toll-like receptor 9 signaling-triggered interleukin-8 secretion in colorectal cancer. *Acta Biochim Biophys Sin (Shanghai)* **50**, 1007-1017 (2018). https://doi.org:10.1093/abbs/gmy104

96 Kang, T. H. *et al.* TLR9 acts as a sensor for tumor-released DNA to modulate anti-tumor immunity after chemotherapy. *J Immunother Cancer* **7**, 260 (2019). https://doi.org:10.1186/s40425-019-0738-2

97 Assinger, A. Platelets and Infection – An Emerging Role of Platelets in Viral Infection. *Frontiers in Immunology* **5** (2014). https://doi.org:10.3389/fimmu.2014.00649

98 Schrottmaier, W. C., Schmuckenschlager, A., Pirabe, A. & Assinger, A. Platelets in Viral Infections – Brave Soldiers or Trojan Horses. *Frontiers in Immunology* **13** (2022). https://doi.org:10.3389/fimmu.2022.856713

99 Hamzeh-Cognasse, H. *et al.* Platelets and infections - complex interactions with bacteria. *Front Immunol* **6**, 82 (2015). https://doi.org:10.3389/fimmu.2015.00082

100 Zucker-Franklin, D., Seremetis, S. & Zheng, Z. Y. Internalization of Human Immunodeficiency Virus Type I and Other Retroviruses by Megakaryocytes and Platelets. *Blood* **75**, 1920-1923 (1990). https://doi.org:https://doi.org/10.1182/blood.V75.10.1920.1920

101 Youssefian, T., Drouin, A., Massé, J.-M., Guichard, J. & Cramer, E. M. Host defense role of platelets: engulfment of HIV andStaphylococcus aureus occurs in a specific subcellular compartment and is enhanced by platelet activation. *Blood* **99**, 4021-4029 (2002). https://doi.org:10.1182/blood-2001-12-0191

102 Simpson, S. R., Singh, M. V., Dewhurst, S., Schifitto, G. & Maggirwar, S. B. Platelets function as an acute viral reservoir during HIV-1 infection by harboring virus and T-cell complex formation. *Blood Advances* **4**, 4512-4521 (2020). https://doi.org:10.1182/bloodadvances.2020002420

103 Bote, J., Corkrey, H. A. & Koupenova, M. Human Platelets and Influenza Virus: Internalization and Platelet Activation. *Platelets* **33**, 184-191 (2022). https://doi.org:10.1080/09537104.2021.1961710

104 Koupenova, M. *et al.* The role of platelets in mediating a response to human influenza infection. *Nat Commun* **10**, 1780 (2019). https://doi.org:10.1038/s41467-019-09607-x

105 Noisakran, S. *et al.* Detection of dengue virus in platelets isolated from dengue patients. *Southeast Asian J Trop Med Public Health* **40**, 253-262 (2009).

106 de Almeida, A. J. *et al.* Detection of hepatitis C virus in platelets: evaluating its relationship to antiviral therapy outcome. *Hepatogastroenterology* **56**, 429-436 (2009).

107 Youssefian, T., Drouin, A., Massé, J. M., Guichard, J. & Cramer, E. M. Host defense role of platelets: engulfment of HIV and Staphylococcus aureus occurs in a specific subcellular compartment and is enhanced by platelet activation. *Blood* **99**, 4021-4029 (2002). https://doi.org:10.1182/blood-2001-12-0191

108 Li, X. *et al.* An ultrastructural study of Porphyromonas gingivalis-induced platelet aggregation. *Thrombosis research* **122**, 810-819 (2008).

109 Karpman, D. *et al.* Platelet activation by Shiga toxin and circulatory factors as a pathogenetic mechanism in the hemolytic uremic syndrome. *Blood* **97**, 3100-3108 (2001). https://doi.org:10.1182/blood.V97.10.3100

110 Gaertner, F. & Massberg, S. Patrolling the vascular borders: platelets in immunity to infection and cancer. *Nat Rev Immunol* **19**, 747-760 (2019). https://doi.org:10.1038/s41577-019-0202-z

111 Youssefian, T., Drouin, A., Masse, J. M., Guichard, J. & Cramer, E. M. Host defense role of platelets: engulfment of HIV and Staphylococcus aureus occurs in a specific subcellular compartment and is enhanced by platelet activation. *Blood* **99**, 4021-4029 (2002). https://doi.org:10.1182/blood-2001-12-0191

112 Banerjee, M. *et al.* Platelets Endocytose Viral Particles and Are Activated via TLR (Toll-Like Receptor) Signaling. *Arteriosclerosis, Thrombosis, and Vascular Biology* **40**, 1635-1650 (2020). https://doi.org:doi:10.1161/ATVBAHA.120.314180

113 Ningtyas, D. C. *et al.* Platelets mediate the clearance of senescent red blood cells by forming prophagocytic platelet-cell complexes. *Blood* **143**, 535-547 (2024). https://doi.org:10.1182/blood.2023021611

114 McMorran, B. J. *et al.* Platelets Kill Intraerythrocytic Malarial Parasites and Mediate Survival to Infection. *Science* **323**, 797-800 (2009). https://doi.org:doi:10.1126/science.1166296

115 Bi, D. *et al.* Clinical characteristics of platelet-mediated killing circulating parasite of major human malaria. *Ann Med* **55**, 2221453 (2023). https://doi.org:10.1080/07853890.2023.2221453
116 Kho, S. *et al.* Platelets kill circulating parasites of all major Plasmodium species in human malaria. *Blood* **132**, 1332-1344 (2018). https://doi.org:10.1182/blood-2018-05-849307
117 Ockenhouse, C. F., Tandon, N. N., Magowan, C., Jamieson, G. & Chulay, J. D. Identification of a platelet membrane glycoprotein as a falciparum malaria sequestration receptor. *Science* **243**, 1469-1471 (1989).
118 McMorran, B. J. *et al.* Platelet Factor 4 and Duffy Antigen Required for Platelet Killing of Plasmodium falciparum. *Science* **338**, 1348-1351 (2012). https://doi.org:doi:10.1126/science.1228892
119 Engwerda, C. R. & Good, M. F. Platelets Kill the Parasite Within. *Science* **338**, 1304-1305 (2012). https://doi.org:doi:10.1126/science.1232439
120 Lam, F. W., Vijayan, K. V. & Rumbaut, R. E. Platelets and Their Interactions with Other Immune Cells. *Compr Physiol* **5**, 1265-1280 (2015). https://doi.org:10.1002/cphy.c140074
121 Krijgsveld, J. *et al.* Thrombocidins, Microbicidal Proteins from Human Blood Platelets, Are C-terminal Deletion Products of CXC Chemokines *. *Journal of Biological Chemistry* **275**, 20374-20381 (2000). https://doi.org:10.1074/jbc.275.27.20374
122 Semple, J. W., Italiano, J. E. & Freedman, J. Platelets and the immune continuum. *Nature Reviews Immunology* **11**, 264-274 (2011). https://doi.org:10.1038/nri2956
123 Yeaman, M. R. Platelets: at the nexus of antimicrobial defence. *Nature Reviews Microbiology* **12**, 426-437 (2014). https://doi.org:10.1038/nrmicro3269
124 Gaertner, F. *et al.* Migrating Platelets Are Mechano-scavengers that Collect and Bundle Bacteria. *Cell* **171**, 1368-1382.e1323 (2017). https://doi.org:10.1016/j.cell.2017.11.001
125 Koupenova, M. & Freedman, J. E. Platelets and Immunity: Going Viral. *Arterioscler Thromb Vasc Biol* **40**, 1605-1607 (2020). https://doi.org:10.1161/ATVBAHA.120.314620
126 Balakrishna Pillai, A. K., Chu, J. J. H., Mariappan, V. & JeanPierre, A. R. Platelets in the pathogenesis of flavivirus disease. *Current Opinion in Virology* **52**, 220-228 (2022). https://doi.org:https://doi.org/10.1016/j.coviro.2021.12.007
127 Carmen, M.-B. & David, S.-H. in *Toll-like Receptors* (ed Rezaei Nima) Ch. 2 (IntechOpen, 2019).
128 Gros, A., Ollivier, V. & Ho-Tin-Noé, B. Platelets in Inflammation: Regulation of Leukocyte Activities and Vascular Repair. *Frontiers in Immunology* **5** (2015). https://doi.org:10.3389/fimmu.2014.00678
129 Margraf, A. & Zarbock, A. Platelets in Inflammation and Resolution. *The Journal of Immunology* **203**, 2357-2367 (2019). https://doi.org:10.4049/jimmunol.1900899
130 Koupenova, M., Clancy, L., Corkrey, H. A. & Freedman, J. E. Circulating Platelets as Mediators of Immunity, Inflammation, and Thrombosis. *Circ Res* **122**, 337-351 (2018). https://doi.org:10.1161/circresaha.117.310795
131 Ludwig, N., Hilger, A., Zarbock, A. & Rossaint, J. Platelets at the Crossroads of Pro-Inflammatory and Resolution Pathways during Inflammation. *Cells* **11** (2022). https://doi.org:10.3390/cells11121957
132 Assoian, R. K., Komoriya, A., Meyers, C. A., Miller, D. M. & Sporn, M. B. Transforming growth factor-beta in human platelets. Identification of a major storage site, purification, and characterization. *Journal of Biological Chemistry* **258**, 7155-7160 (1983).
133 Linke, B. *et al.* Activated Platelets Induce an Anti-Inflammatory Response of Monocytes/Macrophages through Cross-Regulation of PGE2 and Cytokines. *Mediators of Inflammation* **2017**, 1463216 (2017). https://doi.org:https://doi.org/10.1155/2017/1463216
134 van Loo, G. & Bertrand, M. J. M. Death by TNF: a road to inflammation. *Nature Reviews Immunology* **23**, 289-303 (2023). https://doi.org:10.1038/s41577-022-00792-3

135 Giannakeas, V. *et al.* Analysis of platelet count and new cancer diagnosis over a 10-year period. *JAMA network Open* **5**, e2141633-e2141633 (2022).

136 Zhu, Y. *et al.* Elevated platelet count appears to be causally associated with increased risk of lung cancer: A mendelian randomization analysis. *Cancer Epidemiology, Biomarkers & Prevention* **28**, 935-942 (2019).

137 Giannakeas, V. Trends in platelet count among cancer patients. *Experimental Hematology & Oncology* **11**, 16 (2022). https://doi.org:10.1186/s40164-022-00272-3

138 Li, N. Platelets in cancer metastasis: To help the "villain" to do evil. *International journal of cancer* **138**, 2078-2087 (2016).

139 Palacios-Acedo, A. L. *et al.* Platelets, Thrombo-Inflammation, and Cancer: Collaborating With the Enemy. *Frontiers in Immunology* **10** (2019). https://doi.org:10.3389/fimmu.2019.01805

140 Xu, X. R., Yousef, G. M. & Ni, H. Cancer and platelet crosstalk: opportunities and challenges for aspirin and other antiplatelet agents. *Blood* **131**, 1777-1789 (2018). https://doi.org:10.1182/blood-2017-05-743187

141 Thun, M. J., Jacobs, E. J. & Patrono, C. The role of aspirin in cancer prevention. *Nature reviews Clinical oncology* **9**, 259-267 (2012).

142 Rothwell, P. M. *et al.* Short-term effects of daily aspirin on cancer incidence, mortality, and non-vascular death: analysis of the time course of risks and benefits in 51 randomised controlled trials. *The Lancet* **379**, 1602-1612 (2012).

143 Rothwell, P. M. *et al.* Effect of daily aspirin on risk of cancer metastasis: a study of incident cancers during randomised controlled trials. *The Lancet* **379**, 1591-1601 (2012).

144 Rothwell, P. M. *et al.* Effect of daily aspirin on long-term risk of death due to cancer: analysis of individual patient data from randomised trials. *The Lancet* **377**, 31-41 (2011).

145 Rothwell, P. M. *et al.* Long-term effect of aspirin on colorectal cancer incidence and mortality: 20-year follow-up of five randomised trials. *The Lancet* **376**, 1741-1750 (2010).

146 Rachidi, S., Wallace, K., Day, T. A., Alberg, A. J. & Li, Z. Lower circulating platelet counts and antiplatelet therapy independently predict better outcomes in patients with head and neck squamous cell carcinoma. *Journal of Hematology & Oncology* **7**, 65 (2014). https://doi.org:10.1186/s13045-014-0065-5

147 Zhang, Y. *et al.* Low Platelet Counts at Diagnosis Predict Better Survival for Patients with Intermediate-Risk Acute Myeloid Leukemia. *Acta Haematologica* **143**, 9-18 (2019). https://doi.org:10.1159/000500230

148 Gasic, G. J., Gasic, T. B. & Stewart, C. C. Antimetastatic effects associated with platelet reduction. *Proceedings of the National Academy of Sciences* **61**, 46-52 (1968). https://doi.org:doi:10.1073/pnas.61.1.46

149 Zhou, L. *et al.* The critical role of platelet in cancer progression and metastasis. *European Journal of Medical Research* **28**, 385 (2023). https://doi.org:10.1186/s40001-023-01342-w

150 Blobe, G. C., Schiemann, W. P. & Lodish, H. F. Role of transforming growth factor β in human disease. *New England Journal of Medicine* **342**, 1350-1358 (2000).

151 Cho, M. S. *et al.* Platelets increase the proliferation of ovarian cancer cells. *Blood, The Journal of the American Society of Hematology* **120**, 4869-4872 (2012).

152 Liu, Z.-L., Chen, H.-H., Zheng, L.-L., Sun, L.-P. & Shi, L. Angiogenic signaling pathways and anti-angiogenic therapy for cancer. *Signal Transduction and Targeted Therapy* **8**, 198 (2023). https://doi.org:10.1038/s41392-023-01460-1

153 Braun, A., Anders, H. J., Gudermann, T. & Mammadova-Bach, E. Platelet-Cancer Interplay: Molecular Mechanisms and New Therapeutic Avenues. *Front Oncol* **11**, 665534 (2021). https://doi.org:10.3389/fonc.2021.665534

154 Italiano, J. E., Jr *et al.* Angiogenesis is regulated by a novel mechanism: pro- and antiangiogenic proteins are organized into separate platelet α granules and differentially released. *Blood* **111**, 1227-1233 (2008). https://doi.org:10.1182/blood-2007-09-113837

155 Ma, L. *et al.* Platelets modulate gastric ulcer healing: role of endostatin and vascular endothelial growth factor release. *Proceedings of the National Academy of Sciences* **98**, 6470-6475 (2001).
156 Jurasz, P., Alonso, D., Castro-Blanco, S., Murad, F. & Radomski, M. W. Generation and role of angiostatin in human platelets. *Blood* **102**, 3217-3223 (2003).
157 Maione, T. E. *et al.* Inhibition of angiogenesis by recombinant human platelet factor-4 and related peptides. *Science* **247**, 77-79 (1990).
158 McLaren, K. M. Immunohistochemical localisation of thrombospondin in human megakaryocytes and platelets. *Journal of Clinical Pathology* **36**, 197-199 (1983).
159 Chen, L. *et al.* Platelets in the tumor microenvironment and their biological effects on cancer hallmarks. *Front Oncol* **13**, 1121401 (2023). https://doi.org:10.3389/fonc.2023.1121401
160 Battinelli, E. M., Markens, B. A. & Italiano Jr, J. E. Release of angiogenesis regulatory proteins from platelet alpha granules: modulation of physiologic and pathologic angiogenesis. *Blood, The Journal of the American Society of Hematology* **118**, 1359-1369 (2011).
161 Labelle, M., Begum, S. & Hynes, R. O. Direct signaling between platelets and cancer cells induces an epithelial-mesenchymal-like transition and promotes metastasis. *Cancer cell* **20**, 576-590 (2011).
162 Lowe, K. L., Navarro-Nunez, L. & Watson, S. P. Platelet CLEC-2 and podoplanin in cancer metastasis. *Thrombosis research* **129**, S30-S37 (2012).
163 Mammadova-Bach, E. *et al.* Platelet integrin α6β1 controls lung metastasis through direct binding to cancer cell-derived ADAM9. *JCI Insight* **1**, e88245 (2016). https://doi.org:10.1172/jci.insight.88245
164 Ward, M. P. *et al.* Platelets, immune cells and the coagulation cascade; friend or foe of the circulating tumour cell? *Molecular Cancer* **20**, 59 (2021). https://doi.org:10.1186/s12943-021-01347-1
165 Guo, Y., Cui, W., Pei, Y. & Xu, D. Platelets promote invasion and induce epithelial to mesenchymal transition in ovarian cancer cells by TGF-β signaling pathway. *Gynecologic oncology* **153**, 639-650 (2019).
166 Lowe, K. L., Navarro-Nunez, L. & Watson, S. P. Platelet CLEC-2 and podoplanin in cancer metastasis. *Thromb Res* **129 Suppl 1**, S30-37 (2012). https://doi.org:10.1016/s0049-3848(12)70013-0
167 Egan, K., Cooke, N. & Kenny, D. Living in shear: platelets protect cancer cells from shear induced damage. *Clinical & experimental metastasis* **31**, 697-704 (2014).
168 Xu, X. R. *et al.* Platelets are versatile cells: New discoveries in hemostasis, thrombosis, immune responses, tumor metastasis and beyond. *Critical Reviews in Clinical Laboratory Sciences* **53**, 409-430 (2016). https://doi.org:10.1080/10408363.2016.1200008
169 Wang, S., Li, Z. & Xu, R. Human Cancer and Platelet Interaction, a Potential Therapeutic Target. *International Journal of Molecular Sciences* **19**, 1246 (2018).
170 Karpatkin, S., Ambrogio, C. & Pearlstein, E. The role of tumor-induced platelet aggregation, platelet adhesion and adhesive proteins in tumor metastasis. *Prog Clin Biol Res* **283**, 585-606 (1988).
171 Kopp, H.-G., Placke, T. & Salih, H. R. Platelet-derived transforming growth factor-β down-regulates NKG2D thereby inhibiting natural killer cell antitumor reactivity. *Cancer research* **69**, 7775-7783 (2009).
172 Nieswandt, B., Hafner, M., Echtenacher, B. & Männel, D. N. Lysis of tumor cells by natural killer cells in mice is impeded by platelets. *Cancer Res* **59**, 1295-1300 (1999).
173 Viel, S. *et al.* TGF-β inhibits the activation and functions of NK cells by repressing the mTOR pathway. *Science Signaling* **9**, ra19-ra19 (2016). https://doi.org:doi:10.1126/scisignal.aad1884

174 Placke, T. *et al.* Platelet-Derived MHC Class I Confers a Pseudonormal Phenotype to Cancer Cells That Subverts the Antitumor Reactivity of Natural Killer Immune Cells. *Cancer Research* **72**, 440-448 (2012). https://doi.org:10.1158/0008-5472.Can-11-1872

175 Placke, T., Kopp, H.-G. & Salih, H. R. The wolf in sheep's clothing. *OncoImmunology* **1**, 557-559 (2012). https://doi.org:10.4161/onci.19367

176 Franco, A. T., Corken, A. & Ware, J. Platelets at the interface of thrombosis, inflammation, and cancer. *Blood* **126**, 582-588 (2015). https://doi.org:https://doi.org/10.1182/blood-2014-08-531582

177 Gawaz, M., Langer, H. & May, A. E. Platelets in inflammation and atherogenesis. *The Journal of Clinical Investigation* **115**, 3378-3384 (2005). https://doi.org:10.1172/JCI27196

178 Papadimitriou, M. N. B., Menter, D. G., Konstantopoulos, K., Nicolson, G. L. & McIntire, L. V. Integrin α4β1/VCAM-1 pathway mediates primary adhesion of RAW117 lymphoma cells to hepatic sinusoidal endothelial cells under flow. *Clinical & Experimental Metastasis* **17**, 669-676 (1999). https://doi.org:10.1023/A:1006747106885

179 Kim, Y. J., Borsig, L., Han, H.-L., Varki, N. M. & Varki, A. Distinct selectin ligands on colon carcinoma mucins can mediate pathological interactions among platelets, leukocytes, and endothelium. *The American journal of pathology* **155**, 461-472 (1999).

180 Tozawa, K. *et al.* Positive correlation between sialyl Lewis X expression and pathologic findings in renal cell carcinoma. *Kidney International* **67**, 1391-1396 (2005). https://doi.org:https://doi.org/10.1111/j.1523-1755.2005.00216.x

181 Lucotti, S. & Muschel, R. J. Platelets and Metastasis: New Implications of an Old Interplay. *Front Oncol* **10**, 1350 (2020). https://doi.org:10.3389/fonc.2020.01350

182 Li, W. H. *et al.* P2Y2 receptor promotes cell invasion and metastasis in prostate cancer cells. *British Journal of Cancer* **109**, 1666-1675 (2013). https://doi.org:10.1038/bjc.2013.484

183 Ballerini, P., Dovizio, M., Bruno, A., Tacconelli, S. & Patrignani, P. P2Y12 Receptors in Tumorigenesis and Metastasis. *Frontiers in Pharmacology* **9** (2018). https://doi.org:10.3389/fphar.2018.00066

184 Schumacher, D., Strilic, B., Sivaraj, K. K., Wettschureck, N. & Offermanns, S. Platelet-derived nucleotides promote tumor-cell transendothelial migration and metastasis via P2Y2 receptor. *Cancer Cell* **24**, 130-137 (2013). https://doi.org:10.1016/j.ccr.2013.05.008

185 Gkolfinopoulos, S., Jones, R. L. & Constantinidou, A. The Emerging Role of Platelets in the Formation of the Micrometastatic Niche: Current Evidence and Future Perspectives. *Front Oncol* **10**, 374 (2020). https://doi.org:10.3389/fonc.2020.00374

186 Labelle, M., Begum, S. & Hynes, R. O. Platelets guide the formation of early metastatic niches. *Proceedings of the National Academy of Sciences* **111**, E3053-E3061 (2014). https://doi.org:doi:10.1073/pnas.1411082111

187 Gidlöf, O. *et al.* Platelets activated during myocardial infarction release functional miRNA, which can be taken up by endothelial cells and regulate ICAM1 expression. *Blood, The Journal of the American Society of Hematology* **121**, 3908-3917 (2013).

188 Laffont, B. *et al.* Activated platelets can deliver mRNA regulatory Ago2• microRNA complexes to endothelial cells via microparticles. *Blood, The Journal of the American Society of Hematology* **122**, 253-261 (2013).

189 Risitano, A., Beaulieu, L. M., Vitseva, O. & Freedman, J. E. Platelets and platelet-like particles mediate intercellular RNA transfer. *Blood, The Journal of the American Society of Hematology* **119**, 6288-6295 (2012).

190 Clancy, L., Beaulieu, L. M., Tanriverdi, K. & Freedman, J. E. The role of RNA uptake in platelet heterogeneity. *Thromb Haemost* **117**, 948-961 (2017). https://doi.org:10.1160/TH16-11-0873

191 Heijnen, H. F., Schiel, A. E., Fijnheer, R., Geuze, H. J. & Sixma, J. J. Activated Platelets Release Two Types of Membrane Vesicles: Microvesicles by Surface Shedding and

Exosomes Derived From Exocytosis of Multivesicular Bodies and□-Granules. *Blood, The Journal of the American Society of Hematology* **94**, 3791-3799 (1999).
192 Mezouar, S. *et al.* in *Seminars in oncology.* 346-358 (Elsevier).
193 Zarà, M. *et al.* Biology and role of extracellular vesicles (EVs) in the pathogenesis of thrombosis. *International journal of molecular sciences* **20**, 2840 (2019).
194 Yao, B. *et al.* Delivery of platelet TPM3 mRNA into breast cancer cells via microvesicles enhances metastasis. *FEBS Open Bio* **9**, 2159-2169 (2019).
195 Liang, H. *et al.* MicroRNA-223 delivered by platelet-derived microvesicles promotes lung cancer cell invasion via targeting tumor suppressor EPB41L3. *Molecular cancer* **14**, 1-13 (2015).
196 Anene, C., Graham, A. M., Boyne, J. & Roberts, W. Platelet microparticle delivered microRNA-Let-7a promotes the angiogenic switch. *Biochimica et Biophysica Acta (BBA)-Molecular Basis of Disease* **1864**, 2633-2643 (2018).
197 Yang, L. *et al.* TIMP1 mRNA in tumor-educated platelets is diagnostic biomarker for colorectal cancer. *Aging (Albany NY)* **11**, 8998 (2019).
198 Laffont, B. *et al.* Platelet microparticles reprogram macrophage gene expression and function. *Thrombosis and haemostasis* **115**, 311-323 (2016).
199 Warshaw, A. L., Laster, L. & Shulman, N. R. The stimulation by thrombin of glucose oxidation in human platelets. *J Clin Invest* **45**, 1923-1934 (1966). https://doi.org:10.1172/jci105497
200 Weyrich, A. S., Schwertz, H., Kraiss, L. W. & Zimmerman, G. A. Protein synthesis by platelets: historical and new perspectives. *J Thromb Haemost* **7**, 241-246 (2009). https://doi.org:10.1111/j.1538-7836.2008.03211.x
201 Booyse, F. M. & Rafelson, M. E., Jr. Stable messenger RNA in the synthesis of contractile protein in human platelets. *Biochim Biophys Acta* **145**, 188-190 (1967). https://doi.org:10.1016/0005-2787(67)90673-9
202 Newman, P. J. *et al.* Enzymatic amplification of platelet-specific messenger RNA using the polymerase chain reaction. *J Clin Invest* **82**, 739-743 (1988). https://doi.org:10.1172/jci113656
203 Weyrich, A. S. *et al.* Signal-dependent translation of a regulatory protein, Bcl-3, in activated human platelets. *Proc Natl Acad Sci U S A* **95**, 5556-5561 (1998). https://doi.org:10.1073/pnas.95.10.5556
204 Wurdinger, T., In 't Veld, S. & Best, M. G. Platelet RNA as Pan-Tumor Biomarker for Cancer Detection. *Cancer Res* **80**, 1371-1373 (2020). https://doi.org:10.1158/0008-5472.CAN-19-3684
205 Best, M. G. *et al.* RNA-Seq of Tumor-Educated Platelets Enables Blood-Based Pan-Cancer, Multiclass, and Molecular Pathway Cancer Diagnostics. *Cancer Cell* **28**, 666-676 (2015). https://doi.org:10.1016/j.ccell.2015.09.018
206 Best, M. G., Vancura, A. & Wurdinger, T. Platelet RNA as a circulating biomarker trove for cancer diagnostics. *J Thromb Haemost* **15**, 1295-1306 (2017). https://doi.org:10.1111/jth.13720
207 Best, M. G. *et al.* Swarm Intelligence-Enhanced Detection of Non-Small-Cell Lung Cancer Using Tumor-Educated Platelets. *Cancer Cell* **32**, 238-252.e239 (2017). https://doi.org:10.1016/j.ccell.2017.07.004
208 Best, M. G., In 't Veld, S., Sol, N. & Wurdinger, T. RNA sequencing and swarm intelligence-enhanced classification algorithm development for blood-based disease diagnostics using spliced blood platelet RNA. *Nat Protoc* **14**, 1206-1234 (2019). https://doi.org:10.1038/s41596-019-0139-5
209 Schlesinger, M. Role of platelets and platelet receptors in cancer metastasis. *Journal of Hematology & Oncology* **11**, 125 (2018). https://doi.org:10.1186/s13045-018-0669-2

210 Zhang, Q. *et al.* Patterns and functional implications of platelets upon tumor "education". *The International Journal of Biochemistry & Cell Biology* **90**, 68-80 (2017). https://doi.org:https://doi.org/10.1016/j.biocel.2017.07.018

211 Roweth, H. G. & Battinelli, E. M. Lessons to learn from tumor-educated platelets. *Blood* **137**, 3174-3180 (2021). https://doi.org:10.1182/blood.2019003976

212 Holmes, C. E. *et al.* Platelet phenotype changes associated with breast cancer and its treatment. *Platelets* **27**, 703-711 (2016).

213 Yan, M. & Jurasz, P. The role of platelets in the tumor microenvironment: from solid tumors to leukemia. *Biochimica et Biophysica Acta (BBA)-Molecular Cell Research* **1863**, 392-400 (2016).

214 Peterson, J. E. *et al.* VEGF, PF4 and PDGF are elevated in platelets of colorectal cancer patients. *Angiogenesis* **15**, 265-273 (2012).

215 Provost, P. The clinical significance of platelet microparticle-associated microRNAs. *Clinical Chemistry and Laboratory Medicine (CCLM)* **55**, 657-666 (2017).

216 Kerr, B. A., McCabe, N. P., Feng, W. & Byzova, T. V. Platelets govern pre-metastatic tumor communication to bone. *Oncogene* **32**, 4319-4324 (2013). https://doi.org:10.1038/onc.2012.447

217 Kim, H. *et al.* Elevated levels of circulating platelet microparticles, VEGF, IL-6 and RANTES in patients with gastric cancer: possible role of a metastasis predictor. *European journal of cancer* **39**, 184-191 (2003).

218 Helley, D. *et al.* Platelet microparticles: a potential predictive factor of survival in hormone-refractory prostate cancer patients treated with docetaxel-based chemotherapy. *European urology* **56**, 479-485 (2009).

219 Nadal-Wollbold, F. *et al.* Platelet ERK2 activation by thrombin is dependent on calcium and conventional protein kinases C but not Raf-1 or B-Raf. *FEBS letters* **531**, 475-482 (2002).

220 Brown, G. T. & McIntyre, T. M. Lipopolysaccharide signaling without a nucleus: kinase cascades stimulate platelet shedding of proinflammatory IL-1β–rich microparticles. *The Journal of Immunology* **186**, 5489-5496 (2011).

221 Denis, M. M. *et al.* Escaping the Nuclear Confines: Signal-Dependent Pre-mRNA Splicing in Anucleate Platelets. *Cell* **122**, 379-391 (2005). https://doi.org:10.1016/j.cell.2005.06.015

222 Calverley, D. C. *et al.* Significant downregulation of platelet gene expression in metastatic lung cancer. *Clinical and translational science* **3**, 227-232 (2010).

223 Cimmino, G. *et al.* Activating stimuli induce platelet microRNA modulation and proteome reorganisation. *Thromb Haemost* **114**, 96-108 (2015). https://doi.org:10.1160/TH14-09-0726

224 Meehan, K. & Vella, L. J. The contribution of tumour-derived exosomes to the hallmarks of cancer. *Critical reviews in clinical laboratory sciences* **53**, 121-131 (2016).

225 Fendler, A., Stephan, C., Yousef, G. M., Kristiansen, G. & Jung, K. The translational potential of microRNAs as biofluid markers of urological tumours. *Nature Reviews Urology* **13**, 734-752 (2016).

226 Skog, J. *et al.* Glioblastoma microvesicles transport RNA and proteins that promote tumour growth and provide diagnostic biomarkers. *Nature cell biology* **10**, 1470-1476 (2008).

227 Suzuki, A. *et al.* Thrombocytosis in patients with tumors producing colony-stimulating factor. *Blood* **80**, 2052-2059 (1992).

228 Salgado, R. *et al.* Circulating interleukin-6 predicts survival in patients with metastatic breast cancer. *International Journal of Cancer* **103**, 642-646 (2003). https://doi.org:https://doi.org/10.1002/ijc.10833

229 Nilsson, R. J. A. *et al.* Rearranged EML4-ALK fusion transcripts sequester in circulating blood platelets and enable blood-based crizotinib response monitoring in non-small-cell lung cancer. *Oncotarget* **7**, 1066 (2016).

230 Best, M. G. *et al.* Swarm Intelligence-Enhanced Detection of Non-Small-Cell Lung Cancer Using Tumor-Educated Platelets. *Cancer Cell* **32**, 238-252 e239 (2017). https://doi.org:10.1016/j.ccell.2017.07.004

231 Brinkman, K. *et al.* Extracellular vesicles from plasma have higher tumour RNA fraction than platelets. *Journal of Extracellular Vesicles* **9**, 1741176 (2020). https://doi.org:10.1080/20013078.2020.1741176

232 Lood, C. *et al.* Platelet transcriptional profile and protein expression in patients with systemic lupus erythematosus: up-regulation of the type I interferon system is strongly associated with vascular disease. *Blood, The Journal of the American Society of Hematology* **116**, 1951-1957 (2010).

233 Middleton, E. A. *et al.* Sepsis alters the transcriptional and translational landscape of human and murine platelets. *Blood, The Journal of the American Society of Hematology* **134**, 911-923 (2019).

234 Eicher, J. D. *et al.* Characterization of the platelet transcriptome by RNA sequencing in patients with acute myocardial infarction. *Platelets* **27**, 230-239 (2016).

235 Plé, H. *et al.* Alteration of the platelet transcriptome in chronic kidney disease. *Thrombosis and haemostasis* **108**, 605-615 (2012).

236 Ezzaty Mirhashemi, M. *et al.* The dynamic platelet transcriptome in obesity and weight loss. *Arteriosclerosis, thrombosis, and vascular biology* **41**, 854-864 (2021).

237 Edelstein, L. C. *et al.* Racial differences in human platelet PAR4 reactivity reflect expression of PCTP and miR-376c. *Nature medicine* **19**, 1609-1616 (2013).

238 Massimi, I. *et al.* Enhanced platelet MRP4 expression and correlation with platelet function in patients under chronic aspirin treatment. *Thrombosis and Haemostasis* **116**, 1100-1110 (2016).

239 Liefaard, M. C. *et al.* Tumour-educated platelets for breast cancer detection: biological and technical insights. *British Journal of Cancer* **128**, 1572-1581 (2023). https://doi.org:10.1038/s41416-023-02174-5

240 Bettegowda, C. *et al.* Detection of circulating tumor DNA in early- and late-stage human malignancies. *Sci Transl Med* **6**, 224ra224 (2014). https://doi.org:10.1126/scitranslmed.3007094

241 Bronkhorst, A. J., Ungerer, V. & Holdenrieder, S. The emerging role of cell-free DNA as a molecular marker for cancer management. *Biomol Detect Quantif* **17**, 100087 (2019). https://doi.org:10.1016/j.bdq.2019.100087

242 Cristiano, S. *et al.* Genome-wide cell-free DNA fragmentation in patients with cancer. *Nature* **570**, 385-389 (2019). https://doi.org:10.1038/s41586-019-1272-6

243 Dasari, A. *et al.* ctDNA applications and integration in colorectal cancer: an NCI Colon and Rectal-Anal Task Forces whitepaper. *Nat Rev Clin Oncol* **17**, 757-770 (2020). https://doi.org:10.1038/s41571-020-0392-0

244 Diehl, F. *et al.* Circulating mutant DNA to assess tumor dynamics. *Nat Med* **14**, 985-990 (2008). https://doi.org:10.1038/nm.1789

245 Fiala, C. & Diamandis, E. P. Utility of circulating tumor DNA in cancer diagnostics with emphasis on early detection. *BMC Med* **16**, 166 (2018). https://doi.org:10.1186/s12916-018-1157-9

246 Wan, J. C. M. *et al.* Liquid biopsies come of age: towards implementation of circulating tumour DNA. *Nat Rev Cancer* **17**, 223-238 (2017). https://doi.org:10.1038/nrc.2017.7

247 Lo, Y. M. *et al.* Presence of fetal DNA in maternal plasma and serum. *Lancet* **350**, 485-487 (1997). https://doi.org:10.1016/S0140-6736(97)02174-0

248 Lo, Y. M. D. *et al.* Presence of fetal DNA in maternal plasma and serum. *The Lancet* **350**, 485-487 (1997). https://doi.org:https://doi.org/10.1016/S0140-6736(97)02174-0

249 Lo, Y. M. D. *et al.* PRENATAL SEX DETERMINATION BY DNA AMPLIFICATION FROM MATERNAL PERIPHERAL BLOOD. *The Lancet* **334**, 1363-1365 (1989). https://doi.org:10.1016/S0140-6736(89)91969-7

250 Mahdi Mortazavipour, M., Mahdian, R. & Shahbazi, S. The current applications of cell-free fetal DNA in prenatal diagnosis of single-gene diseases: A review. *Int J Reprod Biomed* **20**, 613-626 (2022). https://doi.org:10.18502/ijrm.v20i8.11751

251 Benn, P. *et al.* Position statement from the Chromosome Abnormality Screening Committee on behalf of the Board of the International Society for Prenatal Diagnosis. *Prenatal Diagnosis* **35**, 725-734 (2015). https://doi.org:https://doi.org/10.1002/pd.4608

252 Tug, S. *et al.* Exercise-induced increases in cell free DNA in human plasma originate predominantly from cells of the haematopoietic lineage. *Exerc Immunol Rev* **21**, 164-173 (2015).

253 van der Meer, A. J. *et al.* Systemic inflammation induces release of cell-free DNA from hematopoietic and parenchymal cells in mice and humans. *Blood Advances* **3**, 724-728 (2019). https://doi.org:10.1182/bloodadvances.2018018895

254 Vajpeyee, A. *et al.* Clinical Usefulness of Cell-Free DNA as a Prognostic Marker in Acute Ischemic Stroke. *Neurologist* **25**, 11-13 (2020). https://doi.org:10.1097/nrl.0000000000000249

255 Humardani, F. M., Mulyanata, L. T. & Dwi Putra, S. E. Adipose cell-free DNA in diabetes. *Clin Chim Acta* **539**, 191-197 (2023). https://doi.org:10.1016/j.cca.2022.12.008

256 Schwarzenbach, H., Hoon, D. S. B. & Pantel, K. Cell-free nucleic acids as biomarkers in cancer patients. *Nature Reviews Cancer* **11**, 426-437 (2011). https://doi.org:10.1038/nrc3066

257 Grinshpun, A. Life and death of circulating cell-free DNA. *Cancer biology & therapy* (2019). https://doi.org:10.1080/15384047.2019.1598759.

258 Thierry, A. R., El Messaoudi, S., Gahan, P. B., Anker, P. & Stroun, M. Origins, structures, and functions of circulating DNA in oncology. *Cancer and Metastasis Reviews* **35**, 347-376 (2016). https://doi.org:10.1007/s10555-016-9629-x

259 Valpione, S. *et al.* Plasma total cell-free DNA (cfDNA) is a surrogate biomarker for tumour burden and a prognostic biomarker for survival in metastatic melanoma patients. *Eur J Cancer* **88**, 1-9 (2018). https://doi.org:10.1016/j.ejca.2017.10.029

260 Dao, J. *et al.* Using cfDNA and ctDNA as Oncologic Markers: A Path to Clinical Validation. *Int J Mol Sci* **24** (2023). https://doi.org:10.3390/ijms241713219

261 Khurram, I. *et al.* Efficacy of cell-free DNA as a diagnostic biomarker in breast cancer patients. *Scientific Reports* **13**, 15347 (2023). https://doi.org:10.1038/s41598-023-42726-6

262 Widman, A. J. *et al.* Machine learning guided signal enrichment for ultrasensitive plasma tumor burden monitoring. *bioRxiv*, 2022.2001.2017.476508 (2022). https://doi.org:10.1101/2022.01.17.476508

263 Zviran, A. *et al.* Genome-wide cell-free DNA mutational integration enables ultra-sensitive cancer monitoring. *Nature Medicine* (2020). https://doi.org:10.1038/s41591-020-0915-3

264 Siejka-Zielińska, P. *et al.* Cell-free DNA TAPS provides multimodal information for early cancer detection. *Sci Adv* **7**, eabh0534 (2021). https://doi.org:10.1126/sciadv.abh0534

265 van der Pol, Y. & Mouliere, F. Toward the Early Detection of Cancer by Decoding the Epigenetic and Environmental Fingerprints of Cell-Free DNA. *Cancer Cell* **36**, 350-368 (2019). https://doi.org:10.1016/j.ccell.2019.09.003

266 Cresswell, G. D. *et al.* Mapping the breast cancer metastatic cascade onto ctDNA using genetic and epigenetic clonal tracking. *Nat Commun* **11**, 1446 (2020). https://doi.org:10.1038/s41467-020-15047-9

267 Mouliere, F. *et al.* Enhanced detection of circulating tumor DNA by fragment size analysis. *Sci Transl Med* **10** (2018). https://doi.org:10.1126/scitranslmed.aat4921

268 Mouliere, F. & Rosenfeld, N. Circulating tumor-derived DNA is shorter than somatic DNA in plasma. *Proc Natl Acad Sci U S A* **112**, 3178-3179 (2015). https://doi.org:10.1073/pnas.1501321112

269 Mouliere, F. *et al.* Enhanced detection of circulating tumor DNA by fragment size analysis. *Sci Transl Med* **10** (2018). https://doi.org:10.1126/scitranslmed.aat4921

270 El Messaoudi, S. *et al.* Circulating DNA as a Strong Multimarker Prognostic Tool for Metastatic Colorectal Cancer Patient Management Care. *Clinical Cancer Research* **22**, 3067-3077 (2016). https://doi.org:10.1158/1078-0432.Ccr-15-0297

271 Heitzer, E., Auinger, L. & Speicher, M. R. Cell-Free DNA and Apoptosis: How Dead Cells Inform About the Living. *Trends Mol Med* **26**, 519-528 (2020). https://doi.org:10.1016/j.molmed.2020.01.012

272 Underhill, H. R. *et al.* Fragment Length of Circulating Tumor DNA. *PLoS Genet* **12**, e1006162 (2016). https://doi.org:10.1371/journal.pgen.1006162

273 Mouliere, F. *et al.* Selecting short DNA fragments in plasma improves detection of circulating tumour DNA. *bioRxiv*, 134437 (2017). https://doi.org:10.1101/134437

274 N, R., R, K., M, S., H, K. & P, B. Optimized procedure for platelet RNA profiling from blood samples with limited platelet numbers. *Clin Chem* **51**, 1078-1080 (2005). https://doi.org:10.1373/clinchem.2005.049486

275 Jung, Y., Wen, L., Altman, A. & Ley, K. CD45 pre-exclusion from the tips of T cell microvilli prior to antigen recognition. *Nat Commun* **12**, 3872 (2021). https://doi.org:10.1038/s41467-021-23792-8

276 Schmidl, C., Rendeiro, A. F., Sheffield, N. C. & Bock, C. ChIPmentation: fast, robust, low-input ChIP-seq for histones and transcription factors. *Nature Methods* **12**, 963-965 (2015). https://doi.org:10.1038/nmeth.3542

277 Buenrostro, J. D., Wu, B., Chang, H. Y. & Greenleaf, W. J. ATAC-seq: A Method for Assaying Chromatin Accessibility Genome-Wide. *Curr Protoc Mol Biol* **109**, 21.29.21-21.29.29 (2015). https://doi.org:10.1002/0471142727.mb2129s109

278 Andrews, S. (Babraham Bioinformatics, Babraham Institute, Cambridge, United Kingdom, 2010).

279 Krueger, F., James, F., Ewels, P., Afyounian, E. & Schuster-Boeckler, B. FelixKrueger/TrimGalore: v0. 6.7-DOI via Zenodo. *Zenodo https://zenodo. org/record/5127899 (Accessed February 23, 2022)* (2021).

280 Schneider, V. A. *et al.* Evaluation of GRCh38 and de novo haploid genome assemblies demonstrates the enduring quality of the reference assembly. *Genome Res* **27**, 849-864 (2017). https://doi.org:10.1101/gr.213611.116

281 Li, H. Aligning sequence reads, clone sequences and assembly contigs with BWA-MEM. *arXiv preprint arXiv:1303.3997* (2013).

282 Li, H. *et al.* The Sequence Alignment/Map format and SAMtools. *Bioinformatics* **25**, 2078-2079 (2009). https://doi.org:10.1093/bioinformatics/btp352

283 Van der Auwera, G. & O'Connor, B. Safari, an OMC Using Docker, GATK, and WDL in Terra. *Genomics in the Cloud* **300** (2020).

284 Amemiya, H. M., Kundaje, A. & Boyle, A. P. The ENCODE Blacklist: Identification of Problematic Regions of the Genome. *Sci Rep* **9**, 9354 (2019). https://doi.org:10.1038/s41598-019-45839-z

285 Quinlan, A. R. & Hall, I. M. BEDTools: a flexible suite of utilities for comparing genomic features. *Bioinformatics* **26**, 841-842 (2010). https://doi.org:10.1093/bioinformatics/btq033

286 Wickham, H. in *ggplot2* 189-201 (Springer, 2016).

287 Karimzadeh, M., Ernst, C., Kundaje, A. & Hoffman, M. M. Umap and Bismap: quantifying genome and methylome mappability. *Nucleic acids research* **46**, e120-e120 (2018).

288 Gel, B. & Serra, E. karyoploteR: an R/Bioconductor package to plot customizable genomes displaying arbitrary data. *Bioinformatics* **33**, 3088-3090 (2017). https://doi.org:10.1093/bioinformatics/btx346

289 Gini, C. On the measure of concentration with special reference to income and statistics. *Colorado College Publication, General Series* **208**, 73-79 (1936).

290 Abugessaisa, I. *et al.* refTSS: a reference data set for human and mouse transcription start sites. *Journal of molecular biology* **431**, 2407-2422 (2019).

291 Adalsteinsson, V. A. *et al.* Scalable whole-exome sequencing of cell-free DNA reveals high concordance with metastatic tumors. *Nat Commun* **8**, 1324 (2017). https://doi.org:10.1038/s41467-017-00965-y

292 Frydman, G. H. *et al.* Megakaryocytes contain extranuclear histones and may be a source of platelet-associated histones during sepsis. *Sci Rep* **10**, 4621 (2020). https://doi.org:10.1038/s41598-020-61309-3

293 Moss, J. *et al.* Megakaryocyte- and erythroblast-specific cell-free DNA patterns in plasma and platelets reflect thrombopoiesis and erythropoiesis levels. *Nat Commun* **14**, 7542 (2023). https://doi.org:10.1038/s41467-023-43310-2

294 Koupenova, M. *et al.* Pollen-derived RNAs Are Found in the Human Circulation. *iScience* **19**, 916-926 (2019). https://doi.org:10.1016/j.isci.2019.08.035

295 Latz, E., Visintin, A., Espevik, T. & Golenbock, D. T. Mechanisms of TLR9 activation. *Journal of Endotoxin Research* **10**, 406-412 (2004). https://doi.org:10.1177/09680519040100060501

296 Roth, S., Wernsdorf, S. R. & Liesz, A. The role of circulating cell-free DNA as an inflammatory mediator after stroke. *Seminars in Immunopathology* **45**, 411-425 (2023). https://doi.org:10.1007/s00281-023-00993-5

297 Shen, J., Dai, Z., Li, Y., Zhu, H. & Zhao, L. TLR9 regulates NLRP3 inflammasome activation via the NF-kB signaling pathway in diabetic nephropathy. *Diabetology & metabolic syndrome* **14**, 26 (2022).

298 Lam, L. K. M. *et al.* DNA binding to TLR9 expressed by red blood cells promotes innate immune activation and anemia. *Sci Transl Med* **13**, eabj1008 (2021). https://doi.org:10.1126/scitranslmed.abj1008

299 Vollmer, J. TLR9 in Health and Disease. *International Reviews of Immunology* **25**, 155-181 (2006). https://doi.org:10.1080/08830180600743107

300 Nishimoto, S. *et al.* Obesity-induced DNA released from adipocytes stimulates chronic adipose tissue inflammation and insulin resistance. *Sci Adv* **2**, e1501332 (2016). https://doi.org:10.1126/sciadv.1501332

301 Barrat, F. J. *et al.* Nucleic acids of mammalian origin can act as endogenous ligands for Toll-like receptors and may promote systemic lupus erythematosus. *J Exp Med* **202**, 1131-1139 (2005). https://doi.org:10.1084/jem.20050914

302 D' Atri, L. P. & Schattner, M. Platelet toll-like receptors in thromboinflammation. *Frontiers in bioscience* **22**, 1867-1883 (2017).

303 Panigrahi, S. *et al.* Engagement of Platelet Toll-Like Receptor 9 by Novel Endogenous Ligands Promotes Platelet Hyperreactivity and Thrombosis. *Circulation Research* **112**, 103–112 (2013).

304 Bertheloot, D. *et al.* RAGE Enhances TLR Responses through Binding and Internalization of RNA. *J Immunol* **197**, 4118-4126 (2016). https://doi.org:10.4049/jimmunol.1502169

305 Sims, G. P., Rowe, D. C., Rietdijk, S. T., Herbst, R. & Coyle, A. J. HMGB1 and RAGE in inflammation and cancer. *Annu Rev Immunol* **28**, 367-388 (2010). https://doi.org:10.1146/annurev.immunol.021908.132603

306 Fuentes, E., Rojas, A. & Palomo, I. Role of multiligand/RAGE axis in platelet activation. *Thromb Res* **133**, 308-314 (2014). https://doi.org:10.1016/j.thromres.2013.11.007

307 Gawlowski, T. *et al.* Advanced glycation end products strongly activate platelets. *European Journal of Nutrition* **48**, 475-481 (2009). https://doi.org:10.1007/s00394-009-0038-6

308 Yuan, S., Liu, Z., Xu, Z., Liu, J. & Zhang, J. High mobility group box 1 (HMGB1): a pivotal regulator of hematopoietic malignancies. *J Hematol Oncol* **13**, 91 (2020). https://doi.org:10.1186/s13045-020-00920-3

309 Mardente, S. *et al.* From Human Megakaryocytes to Platelets: Effects of Aspirin on High-Mobility Group Box 1/Receptor for Advanced Glycation End Products Axis. *Front Immunol* **8**, 1946 (2017). https://doi.org:10.3389/fimmu.2017.01946

310 Nomura, S. *et al.* The correlation between platelet activation markers and HMGB1 in patients with disseminated intravascular coagulation and hematologic malignancy. *Platelets* **22**, 396-397 (2011). https://doi.org:10.3109/09537104.2011.553970

311 Vogel, S. *et al.* Activated platelets interfere with recruitment of mesenchymal stem cells to apoptotic cardiac cells via high mobility group box 1/Toll-like receptor 4-mediated down-regulation of hepatocyte growth factor receptor MET. *J Biol Chem* **289**, 11068-11082 (2014). https://doi.org:10.1074/jbc.M113.530287

312 Stark, K. *et al.* Disulfide HMGB1 derived from platelets coordinates venous thrombosis in mice. *Blood* **128**, 2435-2449 (2016). https://doi.org:10.1182/blood-2016-04-710632

313 Tian, J. *et al.* Toll-like receptor 9-dependent activation by DNA-containing immune complexes is mediated by HMGB1 and RAGE. *Nat Immunol* **8**, 487-496 (2007). https://doi.org:10.1038/ni1457

314 Watanabe, H. & Son, M. The Immune Tolerance Role of the HMGB1-RAGE Axis. *Cells* **10** (2021). https://doi.org:10.3390/cells10030564

315 Ivanov, S. *et al.* A novel role for HMGB1 in TLR9-mediated inflammatory responses to CpG-DNA. *Blood* **110**, 1970-1981 (2007). https://doi.org:10.1182/blood-2006-09-044776

316 Hotz, M. J. *et al.* Red Blood Cells Homeostatically Bind Mitochondrial DNA through TLR9 to Maintain Quiescence and to Prevent Lung Injury. *Am J Respir Crit Care Med* **197**, 470-480 (2018). https://doi.org:10.1164/rccm.201706-1161OC

317 Thompson, J. C. *et al.* Red blood cells function as reservoirs of tumor DNA. *Am J Physiol Lung Cell Mol Physiol* **326**, L646-L650 (2024). https://doi.org:10.1152/ajplung.00049.2024

318 Pfister, G., Toor, S. M., Sasidharan Nair, V. & Elkord, E. An evaluation of sorter induced cell stress (SICS) on peripheral blood mononuclear cells (PBMCs) after different sort conditions - Are your sorted cells getting SICS? *J Immunol Methods* **487**, 112902 (2020). https://doi.org:10.1016/j.jim.2020.112902

319 Esfahani, M. S. *et al.* Inferring gene expression from cell-free DNA fragmentation profiles. *Nat Biotechnol* **40**, 585-597 (2022). https://doi.org:10.1038/s41587-022-01222-4

320 Vanpouille-Box, C., Demaria, S., Formenti, S. C. & Galluzzi, L. Cytosolic DNA Sensing in Organismal Tumor Control. *Cancer Cell* **34**, 361-378 (2018). https://doi.org:10.1016/j.ccell.2018.05.013

321 Wang, Y. *et al.* eccDNAs are apoptotic products with high innate immunostimulatory activity. *Nature* **599**, 308-314 (2021). https://doi.org:10.1038/s41586-021-04009-w

322 Puhm, F., Laroche, A. & Boilard, E. Diversity of Megakaryocytes. *Arterioscler Thromb Vasc Biol* **43**, 2088-2098 (2023). https://doi.org:10.1161/ATVBAHA.123.318782

323 Zhou, Y., Dong, J., Wang, M. & Liu, Y. New insights of platelet endocytosis and its implication for platelet function. *Front Cardiovasc Med* **10**, 1308170 (2023). https://doi.org:10.3389/fcvm.2023.1308170

324 Worth, R. G. *et al.* Platelet FcγRIIA binds and internalizes IgG-containing complexes. *Experimental Hematology* **34**, 1490-1495 (2006). https://doi.org:https://doi.org/10.1016/j.exphem.2006.06.015

325 Li, X. *et al.* An ultrastructural study of Porphyromonas gingivalis-induced platelet aggregation. *Thromb Res* **122**, 810-819 (2008). https://doi.org:10.1016/j.thromres.2008.03.011

326 Rennick, J. J., Johnston, A. P. R. & Parton, R. G. Key principles and methods for studying the endocytosis of biological and nanoparticle therapeutics. *Nature Nanotechnology* **16**, 266-276 (2021). https://doi.org:10.1038/s41565-021-00858-8

327 Banerjee, M. & Whiteheart, S. W. The ins and outs of endocytic trafficking in platelet functions. *Curr Opin Hematol* **24**, 467-474 (2017). https://doi.org:10.1097/MOH.0000000000000366

328 Boukour, S., Massé, J. M., Bénit, L., Dubart-Kupperschmitt, A. & Cramer, E. M. Lentivirus degradation and DC-SIGN expression by human platelets and megakaryocytes. *J Thromb Haemost* **4**, 426-435 (2006). https://doi.org:10.1111/j.1538-7836.2006.01749.x

329 Movat, H. Z., Weiser, W. J., Glynn, M. F. & Mustard, J. F. Platelet phagocytosis and aggregation. *J Cell Biol* **27**, 531-543 (1965). https://doi.org:10.1083/jcb.27.3.531

330 George, J. N. Platelet IgG: measurement, interpretation, and clinical significance. *Prog Hemost Thromb* **10**, 97-126 (1991).

331 George, J. N. Platelet immunoglobulin G: its significance for the evaluation of thrombocytopenia and for understanding the origin of alpha-granule proteins. (1990).

332 Engelberg, S., Modrejewski, J., Walter, J. G., Livney, Y. D. & Assaraf, Y. G. Cancer cell-selective, clathrin-mediated endocytosis of aptamer decorated nanoparticles. *Oncotarget* **9** (2018).

333 Kay, R. R. Macropinocytosis: Biology and mechanisms. *Cells & Development* **168**, 203713 (2021). https://doi.org:https://doi.org/10.1016/j.cdev.2021.203713

334 Koivusalo, M. *et al.* Amiloride inhibits macropinocytosis by lowering submembranous pH and preventing Rac1 and Cdc42 signaling. *Journal of Cell Biology* **188**, 547-563 (2010). https://doi.org:10.1083/jcb.200908086

335 Lin, H. P. *et al.* Identification of novel macropinocytosis inhibitors using a rational screen of Food and Drug Administration-approved drugs. *Br J Pharmacol* **175**, 3640-3655 (2018). https://doi.org:10.1111/bph.14429

336 Smith, S. M. & Smith, C. J. Capturing the mechanics of clathrin-mediated endocytosis. *Current Opinion in Structural Biology* **75**, 102427 (2022). https://doi.org:https://doi.org/10.1016/j.sbi.2022.102427

337 Morlot, S. & Roux, A. Mechanics of dynamin-mediated membrane fission. *Annu Rev Biophys* **42**, 629-649 (2013). https://doi.org:10.1146/annurev-biophys-050511-102247

338 Gao, W. *et al.* Clathrin-mediated integrin αIIbβ3 trafficking controls platelet spreading. *Platelets* **29**, 610-621 (2018). https://doi.org:10.1080/09537104.2017.1353682

339 von Kleist, L. *et al.* Role of the Clathrin Terminal Domain in Regulating Coated Pit Dynamics Revealed by Small Molecule Inhibition. *Cell* **146**, 471-484 (2011). https://doi.org:https://doi.org/10.1016/j.cell.2011.06.025

340 Smith, S. M., Baker, M., Halebian, M. & Smith, C. J. Weak Molecular Interactions in Clathrin-Mediated Endocytosis. *Frontiers in Molecular Biosciences* **4** (2017). https://doi.org:10.3389/fmolb.2017.00072

341 Kirchhausen, T., Macia, E. & Pelish, H. E. in *Methods in Enzymology* Vol. 438 77-93 (Academic Press, 2008).

342 Parton, R. G., Hanzal-Bayer, M. & Hancock, J. F. Biogenesis of caveolae: a structural model for caveolin-induced domain formation. *Journal of Cell Science* **119**, 787-796 (2006). https://doi.org:10.1242/jcs.02853

343 Jayachandran, M. & Miller, V. M. Human platelets contain estrogen receptor α, caveolin-1 and estrogen receptor associated proteins. *Platelets* **14**, 75-81 (2003). https://doi.org:10.1080/0953710031000080562

344 Sousa, F., Nascimento, C., Ferreira, D., Reis, S. & Costa, P. Reviving the interest in the versatile drug nystatin: A multitude of strategies to increase its potential as an effective and safe antifungal agent. *Advanced Drug Delivery Reviews* **199**, 114969 (2023). https://doi.org:10.1016/j.addr.2023.114969

345 Baek, S. *et al.* The Cholesterol-Binding Antibiotic Nystatin Induces Expression of Macrophage Inflammatory Protein-1 in Macrophages. *Biomolecules & Therapeutics* **21**, 42-48 (2013). https://doi.org:10.4062/biomolther.2012.082

346 Escolar, G., Lopez-Vilchez, I., Diaz-Ricart, M., White, J. G. & Galan, A. M. Internalization of tissue factor by platelets11Authorship: All authors have read and approved the final version of this manuscript and have made important contributions:G. Escolar and A. Galán have participated in the conception and design of the study, analysis and interpretation of data and and finally writing the manuscript and revising intellectual content.I. López-Vilchez and M. Díaz-Ricart have made the acquisition of data and interpretation of data.J.G. White has participated in acquisition of data and revising important intellectual content. *Thrombosis Research* **122**, S37-S41 (2008). https://doi.org:https://doi.org/10.1016/S0049-3848(08)70017-3

347 Jerez-Dolz, D. *et al.* Internalization of microparticles by platelets is partially mediated by toll-like receptor 4 and enhances platelet thrombogenicity. *Atherosclerosis* **294**, 17-24 (2020). https://doi.org:https://doi.org/10.1016/j.atherosclerosis.2019.12.017

348 Liu, Y.-J. & Wang, C. A review of the regulatory mechanisms of extracellular vesicles-mediated intercellular communication. *Cell Communication and Signaling* **21**, 77 (2023). https://doi.org:10.1186/s12964-023-01103-6

349 Zhou, M. *et al.* Apoptotic bodies for advanced drug delivery and therapy. *Journal of Controlled Release* **351**, 394-406 (2022). https://doi.org:https://doi.org/10.1016/j.jconrel.2022.09.045

350 Atkin-Smith, G. K. & Poon, I. K. H. Disassembly of the Dying: Mechanisms and Functions. *Trends in Cell Biology* **27**, 151-162 (2017). https://doi.org:https://doi.org/10.1016/j.tcb.2016.08.011

351 Bergsmedh, A. *et al.* Horizontal transfer of oncogenes by uptake of apoptotic bodies. *Proceedings of the National Academy of Sciences* **98**, 6407-6411 (2001).

352 Holmgren, L. *et al.* Horizontal transfer of DNA by the uptake of apoptotic bodies. *Blood, The Journal of the American Society of Hematology* **93**, 3956-3963 (1999).

353 Thakur, B. K. *et al.* Double-stranded DNA in exosomes: a novel biomarker in cancer detection. *Cell Res* **24**, 766-769 (2014). https://doi.org:10.1038/cr.2014.44

354 Kahlert, C. *et al.* Identification of double-stranded genomic DNA spanning all chromosomes with mutated KRAS and p53 DNA in the serum exosomes of patients with pancreatic cancer. *J Biol Chem* **289**, 3869-3875 (2014). https://doi.org:10.1074/jbc.C113.532267

355 Vagner, T. *et al.* Large extracellular vesicles carry most of the tumour DNA circulating in prostate cancer patient plasma. *J Extracell Vesicles* **7**, 1505403 (2018). https://doi.org:10.1080/20013078.2018.1505403

356 Fernando, M. R., Jiang, C., Krzyzanowski, G. D. & Ryan, W. L. New evidence that a large proportion of human blood plasma cell-free DNA is localized in exosomes. *PLoS One* **12**, e0183915 (2017). https://doi.org:10.1371/journal.pone.0183915

357 Balaj, L. *et al.* Tumour microvesicles contain retrotransposon elements and amplified oncogene sequences. *Nat Commun* **2**, 180 (2011). https://doi.org:10.1038/ncomms1180

358 Takahashi, A. *et al.* Exosomes maintain cellular homeostasis by excreting harmful DNA from cells. *Nat Commun* **8**, 15287 (2017). https://doi.org:10.1038/ncomms15287

359 Hu, Z., Chen, H., Long, Y., Li, P. & Gu, Y. The main sources of circulating cell-free DNA: Apoptosis, necrosis and active secretion. *Crit Rev Oncol Hematol* **157**, 103166 (2021). https://doi.org:10.1016/j.critrevonc.2020.103166

360 Yokoi, A. *et al.* Mechanisms of nuclear content loading to exosomes. *Sci Adv* **5**, eaax8849 (2019). https://doi.org:10.1126/sciadv.aax8849

361 Elzanowska, J., Semira, C. & Costa-Silva, B. DNA in extracellular vesicles: biological and clinical aspects. *Mol Oncol* **15**, 1701-1714 (2021). https://doi.org:10.1002/1878-0261.12777

362 Gurung, S., Perocheau, D., Touramanidou, L. & Baruteau, J. The exosome journey: from biogenesis to uptake and intracellular signalling. *Cell Communication and Signaling* **19**, 47 (2021). https://doi.org:10.1186/s12964-021-00730-1

363 Nilsson, R. J. *et al.* Rearranged EML4-ALK fusion transcripts sequester in circulating blood platelets and enable blood-based crizotinib response monitoring in non-small-cell lung cancer. *Oncotarget* **7**, 1066-1075 (2016). https://doi.org:10.18632/oncotarget.6279

364 Dudiki, T. *et al.* Mechanism of Tumor-Platelet Communications in Cancer. *Circulation Research* **132**, 1447-1461 (2023). https://doi.org:10.1161/CIRCRESAHA.122.321861

365 In 't Veld, S. *et al.* Detection and localization of early- and late-stage cancers using platelet RNA. *Cancer Cell* **40**, 999-1009 e1006 (2022). https://doi.org:10.1016/j.ccell.2022.08.006

366 Rossaint, J. *et al.* Directed transport of neutrophil-derived extracellular vesicles enables platelet-mediated innate immune response. *Nature Communications* **7**, 13464 (2016). https://doi.org:10.1038/ncomms13464

367 Hearn, J. I. & Gardiner, E. E. Tumor Cell EnVoys Advance the Education of Platelets. *Circulation Research* **132**, 1462-1464 (2023). https://doi.org:10.1161/CIRCRESAHA.123.322781

368 Lin, D. *et al.* Expression of Tetraspan Protein CD63 Activates Protein-tyrosine Kinase (PTK) and Enhances the PTK-induced Inhibition of ROMK Channels *. *Journal of Biological Chemistry* **283**, 7674-7681 (2008). https://doi.org:10.1074/jbc.M705574200

369 Coppinger, J. A. *et al.* Characterization of the proteins released from activated platelets leads to localization of novel platelet proteins in human atherosclerotic lesions. *Blood* **103**, 2096-2104 (2004). https://doi.org:10.1182/blood-2003-08-2804

370 Escolar, G. & White, J. The platelet open canalicular system: a final common pathway. *Blood cells* **17**, 467-485; discussion 486 (1991).

371 Stenberg, P. E., Shuman, M. A., Levine, S. P. & Bainton, D. F. Redistribution of alpha-granules and their contents in thrombin-stimulated platelets. *The Journal of cell biology* **98**, 748-760 (1984).

372 Morgenstern, E., Neumann, K. & Patscheke, H. The exocytosis of human blood platelets. A fast freezing and freeze-substitution analysis. *European journal of cell biology* **43**, 273-282 (1987).

373 Flaumenhaft, R. Molecular Basis of Platelet Granule Secretion. *Arteriosclerosis, Thrombosis, and Vascular Biology* **23**, 1152-1160 (2003). https://doi.org:10.1161/01.ATV.0000075965.88456.48

374 Eckly, A. *et al.* Respective contributions of single and compound granule fusion to secretion by activated platelets. *Blood, The Journal of the American Society of Hematology* **128**, 2538-2549 (2016).

375 Jonnalagadda, D., Izu, L. T. & Whiteheart, S. W. Platelet secretion is kinetically heterogeneous in an agonist-responsive manner. *Blood* **120**, 5209-5216 (2012). https://doi.org:10.1182/blood-2012-07-445080

376 Whiteheart, S. W. Platelet granules: surprise packages. *Blood* **118**, 1190-1191 (2011). https://doi.org:10.1182/blood-2011-06-359836

377 D'Agostino, M., Risselada, H. J., Lürick, A., Ungermann, C. & Mayer, A. A tethering complex drives the terminal stage of SNARE-dependent membrane fusion. *Nature* **551**, 634-638 (2017).

378 Golebiewska, E. M. & Poole, A. W. Secrets of platelet exocytosis - what do we really know about platelet secretion mechanisms? *Br J Haematol* **165**, 204-216 (2013). https://doi.org:10.1111/bjh.12682

379 Bye, A. P., Unsworth, A. J. & Gibbins, J. M. Platelet signaling: a complex interplay between inhibitory and activatory networks. *J Thromb Haemost* **14**, 918-930 (2016). https://doi.org:10.1111/jth.13302

380 Nagy, Z. & Smolenski, A. Cyclic nucleotide-dependent inhibitory signaling interweaves with activating pathways to determine platelet responses. *Res Pract Thromb Haemost* **2**, 558-571 (2018). https://doi.org:10.1002/rth2.12122

381 Mitchell, J. A., Ali, F., Bailey, L., Moreno, L. & Harrington, L. S. Role of nitric oxide and prostacyclin as vasoactive hormones released by the endothelium. *Exp Physiol* **93**, 141-147 (2008). https://doi.org:10.1113/expphysiol.2007.038588

382 Schrör, K. Aspirin and platelets: the antiplatelet action of aspirin and its role in thrombosis treatment and prophylaxis. *Semin Thromb Hemost* **23**, 349-356 (1997). https://doi.org:10.1055/s-2007-996108

383 Theken, K. N. & Grosser, T. Weight-adjusted aspirin for cardiovascular prevention. *Lancet* **392**, 361-362 (2018). https://doi.org:10.1016/S0140-6736(18)31307-2

384 Corrigan, T. *et al.* Changes in the Physical and Mechanical Properties of Human Blood with Sustained Prophylactic Use of Acetylsalicylic Acid (Aspirin)—A Rheological Study. *Open Journal of Fluid Dynamics* **11**, 167-176 (2021). https://doi.org:10.4236/ojfd.2021.114010

385 Fitzgerald, D. J. & Fitzgerald, G. A. Historical lessons in translational medicine: cyclooxygenase inhibition and P2Y12 antagonism. *Circ Res* **112**, 174-194 (2013). https://doi.org:10.1161/circresaha.111.300271

386 Kamel, S. *et al.* Ibrutinib inhibits collagen-mediated but not ADP-mediated platelet aggregation. *Leukemia* **29**, 783-787 (2015). https://doi.org:10.1038/leu.2014.247

387 Levade, M. *et al.* Ibrutinib treatment affects collagen and von Willebrand factor-dependent platelet functions. *Blood* **124**, 3991-3995 (2014). https://doi.org:10.1182/blood-2014-06-583294

388 Kraft, P., De Meyer, S. F. & Kleinschnitz, C. Next-generation antithrombotics in ischemic stroke: preclinical perspective on 'bleeding-free antithrombosis'. *J Cereb Blood Flow Metab* **32**, 1831-1840 (2012). https://doi.org:10.1038/jcbfm.2012.108

389 Davids, M. S. & Brown, J. R. Ibrutinib: a first in class covalent inhibitor of Bruton's tyrosine kinase. *Future Oncol* **10**, 957-967 (2014). https://doi.org:10.2217/fon.14.51

390 Li, R., Hoffmeister, K. M. & Falet, H. Glycans and the platelet life cycle. *Platelets* **27**, 505-511 (2016). https://doi.org:10.3109/09537104.2016.1171304

391 Josefsson, E. C., Dowling, M. R., Lebois, M. & Kile, B. T. in *Platelets (Third Edition)* (ed Alan D. Michelson) 51-65 (Academic Press, 2013).

392 Josefsson, E. C., Vainchenker, W. & James, C. Regulation of Platelet Production and Life Span: Role of Bcl-xL and Potential Implications for Human Platelet Diseases. *Int J Mol Sci* **21** (2020). https://doi.org:10.3390/ijms21207591

393 Grozovsky, R. *et al.* The Ashwell-Morell receptor regulates hepatic thrombopoietin production via JAK2-STAT3 signaling. *Nat Med* **21**, 47-54 (2015). https://doi.org:10.1038/nm.3770

394 Li, M. F. *et al.* Platelet desialylation is a novel mechanism and a therapeutic target in thrombocytopenia during sepsis: an open-label, multicenter, randomized controlled trial. *J Hematol Oncol* **10**, 104 (2017). https://doi.org:10.1186/s13045-017-0476-1

395 Quach, M. E., Chen, W. & Li, R. Mechanisms of platelet clearance and translation to improve platelet storage. *Blood* **131**, 1512-1521 (2018). https://doi.org:10.1182/blood-2017-08-743229

396 Mason, K. D. *et al.* Programmed Anuclear Cell Death Delimits Platelet Life Span. *Cell* **128**, 1173-1186 (2007). https://doi.org:https://doi.org/10.1016/j.cell.2007.01.037

397 Mason, K. D. *et al.* Programmed anuclear cell death delimits platelet life span. *Cell* **128**, 1173-1186 (2007). https://doi.org:10.1016/j.cell.2007.01.037

398 Gregory, C. D. & Brown, S. B. Apoptosis: eating sensibly. *Nature Cell Biology* **7**, 1161-1163 (2005). https://doi.org:10.1038/ncb1205-1161

399 Gardai, S. J. *et al.* Cell-Surface Calreticulin Initiates Clearance of Viable or Apoptotic Cells through trans-Activation of LRP on the Phagocyte. *Cell* **123**, 321-334 (2005). https://doi.org:https://doi.org/10.1016/j.cell.2005.08.032

400 Min, C. *et al.* Tim-4 functions as a scavenger receptor for phagocytosis of exogenous particles. *Cell Death & Disease* **11**, 561 (2020). https://doi.org:10.1038/s41419-020-02773-7

401 Li, W. Eat-me signals: keys to molecular phagocyte biology and "appetite" control. *J Cell Physiol* **227**, 1291-1297 (2012). https://doi.org:10.1002/jcp.22815

402 Naeini, M. B., Bianconi, V., Pirro, M. & Sahebkar, A. The role of phosphatidylserine recognition receptors in multiple biological functions. *Cellular & Molecular Biology Letters* **25**, 23 (2020). https://doi.org:10.1186/s11658-020-00214-z

403 Ravichandran, K. S. Find-me and eat-me signals in apoptotic cell clearance: progress and conundrums. *J Exp Med* **207**, 1807-1817 (2010). https://doi.org:10.1084/jem.20101157

404 Olsson, M., Bruhns, P., Frazier, W. A., Ravetch, J. V. & Oldenborg, P. A. Platelet homeostasis is regulated by platelet expression of CD47 under normal conditions and in passive immune thrombocytopenia. *Blood* **105**, 3577-3582 (2005). https://doi.org:10.1182/blood-2004-08-2980

405 Zhong, Y. *et al.* Plasma cfDNA as a Potential Biomarker to Evaluate the Efficacy of Chemotherapy in Gastric Cancer. *Cancer Manag Res* **12**, 3099-3106 (2020). https://doi.org:10.2147/cmar.S243320

406 Coppinger, J. A. *et al.* Moderation of the platelet releasate response by aspirin. *Blood* **109**, 4786-4792 (2007). https://doi.org:10.1182/blood-2006-07-038539

407 McKenzie, M. E. *et al.* Aspirin inhibits surface glycoprotein IIb/IIIa, P-selectin, CD63, and CD107a receptor expression on human platelets. *Blood Coagulation & Fibrinolysis* **14**, 249-253 (2003). https://doi.org:10.1097/01.mbc.0000046182.72384.ab

408 Zinchuk, V., Zinchuk, O. & Okada, T. Quantitative Colocalization Analysis of Multicolor Confocal Immunofluorescence Microscopy Images: Pushing Pixels to Explore Biological Phenomena. *ACTA HISTOCHEMICA ET CYTOCHEMICA* **40**, 101-111 (2007). https://doi.org:10.1267/ahc.07002

409 Mountford, J. K. *et al.* The class II PI 3-kinase, PI3KC2α, links platelet internal membrane structure to shear-dependent adhesive function. *Nature Communications* **6**, 6535 (2015). https://doi.org:10.1038/ncomms7535

410 Pleines, I. *et al.* Megakaryocyte-specific RhoA deficiency causes macrothrombocytopenia and defective platelet activation in hemostasis and thrombosis. *Blood* **119**, 1054-1063 (2012). https://doi.org:10.1182/blood-2011-08-372193

411 Grimmer, S., van Deurs, B. & Sandvig, K. Membrane ruffling and macropinocytosis in A431 cells require cholesterol. *Journal of Cell Science* **115**, 2953-2962 (2002). https://doi.org:10.1242/jcs.115.14.2953

412 Dutta, D., Williamson, C. D., Cole, N. B. & Donaldson, J. G. Pitstop 2 Is a Potent Inhibitor of Clathrin-Independent Endocytosis. *PLOS ONE* **7**, e45799 (2012). https://doi.org:10.1371/journal.pone.0045799

413 Willox, A. K., Sahraoui, Y. M. E. & Royle, S. J. Non-specificity of Pitstop 2 in clathrin-mediated endocytosis. *Biology Open* **3**, 326-331 (2014). https://doi.org:10.1242/bio.20147955

414 Mentzer, R. M., Jr., Lasley, R. D., Jessel, A. & Karmazyn, M. Intracellular sodium hydrogen exchange inhibition and clinical myocardial protection. *The Annals of Thoracic Surgery* **75**, S700-S708 (2003). https://doi.org:10.1016/S0003-4975(02)04700-8

415 Theroux, P. *et al.* Design of a trial evaluating myocardial cell protection with cariporide, an inhibitor of the transmembrane sodium-hydrogen exchanger: the Guard During Ischemia Against Necrosis (GUARDIAN) trial. *Curr Control Trials Cardiovasc Med* **1**, 59-67 (2000). https://doi.org:10.1186/cvm-1-1-059

416 Madonna, R. & De Caterina, R. Sodium–hydrogen exchangers (NHE) in human cardiovascular diseases: Interfering strategies and their therapeutic applications. *Vascular Pharmacology* **59**, 127-130 (2013). https://doi.org:https://doi.org/10.1016/j.vph.2013.10.001

417 Antwi-Baffour, S. *et al.* Understanding the biosynthesis of platelets-derived extracellular vesicles. *Immun Inflamm Dis* **3**, 133-140 (2015). https://doi.org:10.1002/iid3.66

418 Wei, K., Huang, H., Liu, M., Shi, D. & Ma, X. Platelet-Derived Exosomes and Atherothrombosis. *Frontiers in Cardiovascular Medicine* **9** (2022). https://doi.org:10.3389/fcvm.2022.886132

419 Koseoglu, S. *et al.* Dynamin-Related Protein-1 Controls Fusion Pore Dynamics During Platelet Granule Exocytosis. *Arteriosclerosis, Thrombosis, and Vascular Biology* **33**, 481-488 (2013). https://doi.org:doi:10.1161/ATVBAHA.112.255737

420 Harrison, P. *et al.* Uptake of plasma fibrinogen into the alpha granules of human megakaryocytes and platelets. *The Journal of Clinical Investigation* **84**, 1320-1324 (1989). https://doi.org:10.1172/JCI114300

421 Heijnen, H. F. G. *et al.* Multivesicular Bodies Are an Intermediate Stage in the Formation of Platelet α-Granules. *Blood* **91**, 2313-2325 (1998). https://doi.org:https://doi.org/10.1182/blood.V91.7.2313

422 Stenberg, P. E., Shuman, M. A., Levine, S. P. & Bainton, D. F. Redistribution of alpha-granules and their contents in thrombin-stimulated platelets. *Journal of Cell Biology* **98**, 748-760 (1984). https://doi.org:10.1083/jcb.98.2.748

423 Antunes-Ferreira, M., Koppers-Lalic, D. & Wurdinger, T. Circulating platelets as liquid biopsy sources for cancer detection. *Mol Oncol* (2020). https://doi.org:10.1002/1878-0261.12859

424 De Rubis, G., Rajeev Krishnan, S. & Bebawy, M. Liquid Biopsies in Cancer Diagnosis, Monitoring, and Prognosis. *Trends Pharmacol Sci* **40**, 172-186 (2019). https://doi.org:10.1016/j.tips.2019.01.006

425 De Rubis, G., Krishnan, S. R. & Bebawy, M. Circulating tumor DNA - Current state of play and future perspectives. *Pharmacol Res* **136**, 35-44 (2018). https://doi.org:10.1016/j.phrs.2018.08.017

426 Tsui, N. B., Ng, E. K. & Lo, Y. D. Stability of Endogenous and Added RNA in Blood Specimens, Serum, and Plasma. *Clinical Chemistry* **48**, 1647-1653 (2002). https://doi.org:10.1093/clinchem/48.10.1647

427 Sharma, S. *et al.* Circulating tumor cell isolation, culture, and downstream molecular analysis. *Biotechnology Advances* **36**, 1063-1078 (2018). https://doi.org:https://doi.org/10.1016/j.biotechadv.2018.03.007

428 Fleischhacker, M. & Schmidt, B. Circulating nucleic acids (CNAs) and cancer—A survey. *Biochimica et Biophysica Acta (BBA) - Reviews on Cancer* **1775**, 181-232 (2007). https://doi.org:https://doi.org/10.1016/j.bbcan.2006.10.001

429 Garcia-Romero, N. *et al.* Extracellular vesicles compartment in liquid biopsies: Clinical application. *Molecular Aspects of Medicine* **60**, 27-37 (2018). https://doi.org:https://doi.org/10.1016/j.mam.2017.11.009

430 Armstrong, D. & Wildman, D. E. Extracellular vesicles and the promise of continuous liquid biopsies. *Journal of Pathology and Translational Medicine* **52**, 1-8 (2018). https://doi.org:10.4132/jptm.2017.05.21

431 Abbosh, C. *et al.* Phylogenetic ctDNA analysis depicts early-stage lung cancer evolution. *Nature* **545**, 446-451 (2017). https://doi.org:10.1038/nature22364

432 Zhang, Y. *et al.* Pan-cancer circulating tumor DNA detection in over 10,000 Chinese patients. *Nature Communications* **12**, 11 (2021). https://doi.org:10.1038/s41467-020-20162-8

433 Ivanov, M., Baranova, A., Butler, T., Spellman, P. & Mileyko, V. Non-random fragmentation patterns in circulating cell-free DNA reflect epigenetic regulation. *BMC Genomics* **16**, S1 (2015). https://doi.org:10.1186/1471-2164-16-S13-S1

434 Stanley, K. E. *et al.* Cell type signatures in cell-free DNA fragmentation profiles reveal disease biology. *Nature Communications* **15**, 2220 (2024). https://doi.org:10.1038/s41467-024-46435-0

435 Lo, Y. M. D., Han, D. S. C., Jiang, P. & Chiu, R. W. K. Epigenetics, fragmentomics, and topology of cell-free DNA in liquid biopsies. *Science* **372** (2021). https://doi.org:10.1126/science.aaw3616

436 Lam, W. K. J. *et al.* DNA of Erythroid Origin Is Present in Human Plasma and Informs the Types of Anemia. *Clinical Chemistry* **63**, 1614-1623 (2017). https://doi.org:10.1373/clinchem.2017.272401

437 Moss, J. *et al.* Comprehensive human cell-type methylation atlas reveals origins of circulating cell-free DNA in health and disease. *Nature Communications* **9**, 5068 (2018). https://doi.org:10.1038/s41467-018-07466-6

438 Moss, J. *et al.* Megakaryocyte- and erythroblast-specific cell-free DNA patterns in plasma and platelets reflect thrombopoiesis and erythropoiesis levels. *Nature Communications* **14**, 7542 (2023). https://doi.org:10.1038/s41467-023-43310-2

439 Sun, K. *et al.* Plasma DNA tissue mapping by genome-wide methylation sequencing for noninvasive prenatal, cancer, and transplantation assessments. *Proceedings of the National Academy of Sciences* **112**, E5503-E5512 (2015). https://doi.org:doi:10.1073/pnas.1508736112

440 Wong, F. C. K. *et al.* Cell-free DNA in maternal plasma and serum: A comparison of quantity, quality and tissue origin using genomic and epigenomic approaches. *Clinical Biochemistry* **49**, 1379-1386 (2016). https://doi.org:https://doi.org/10.1016/j.clinbiochem.2016.09.009

441 Vanderstichele, A. *et al.* Nucleosome footprinting in plasma cell-free DNA for the pre-surgical diagnosis of ovarian cancer. *npj Genomic Medicine* **7**, 30 (2022). https://doi.org:10.1038/s41525-022-00300-5

442 Fyodorov, D. V., Zhou, B.-R., Skoultchi, A. I. & Bai, Y. Emerging roles of linker histones in regulating chromatin structure and function. *Nature Reviews Molecular Cell Biology* **19**, 192-206 (2018). https://doi.org:10.1038/nrm.2017.94

443 Beyer, C. *et al.* The extracellular release of DNA and HMGB1 from Jurkat T cells during in vitro necrotic cell death. *Innate Immun* **18**, 727-737 (2012). https://doi.org:10.1177/1753425912437981

444 Moras, M., Lefevre, S. D. & Ostuni, M. A. From Erythroblasts to Mature Red Blood Cells: Organelle Clearance in Mammals. *Frontiers in Physiology* **8** (2017). https://doi.org:10.3389/fphys.2017.01076

445 Yipp, B. G. *et al.* Infection-induced NETosis is a dynamic process involving neutrophil multitasking in vivo. *Nature Medicine* **18**, 1386-1393 (2012). https://doi.org:10.1038/nm.2847

446 Ingelsson, B. *et al.* Lymphocytes eject interferogenic mitochondrial DNA webs in response to CpG and non-CpG oligodeoxynucleotides of class C. *Proceedings of the National Academy of Sciences* **115**, E478-E487 (2018). https://doi.org:doi:10.1073/pnas.1711950115

447 Sansone, P. *et al.* Packaging and transfer of mitochondrial DNA via exosomes regulate escape from dormancy in hormonal therapy-resistant breast cancer. *Proceedings of the National Academy of Sciences* **114**, E9066-E9075 (2017). https://doi.org:doi:10.1073/pnas.1704862114

448 Underhill, H. R. Leveraging the Fragment Length of Circulating Tumour DNA to Improve Molecular Profiling of Solid Tumour Malignancies with Next-Generation Sequencing: A Pathway to Advanced Non-invasive Diagnostics in Precision Oncology? *Molecular Diagnosis & Therapy* **25**, 389-408 (2021). https://doi.org:10.1007/s40291-021-00534-6

449 Markus, H. *et al.* Refined characterization of circulating tumor DNA through biological feature integration. *Scientific Reports* **12**, 1928 (2022). https://doi.org:10.1038/s41598-022-05606-z

450 Keller, L., Belloum, Y., Wikman, H. & Pantel, K. Clinical relevance of blood-based ctDNA analysis: mutation detection and beyond. *British Journal of Cancer* **124**, 345-358 (2021). https://doi.org:10.1038/s41416-020-01047-5

451 Diehl, F. *et al.* Circulating mutant DNA to assess tumor dynamics. *Nature medicine* **14**, 985-990 (2008).

452 Bronkhorst, A. J., Ungerer, V. & Holdenrieder, S. The emerging role of cell-free DNA as a molecular marker for cancer management. *Biomolecular Detection and Quantification* **17**, 100087 (2019). https://doi.org:https://doi.org/10.1016/j.bdq.2019.100087

453 Fleischhacker, M. *et al.* Methods for isolation of cell-free plasma DNA strongly affect DNA yield. *Clinica Chimica Acta* **412**, 2085-2088 (2011). https://doi.org:https://doi.org/10.1016/j.cca.2011.07.011

454 Gahan, P. B. & Stroun, M. The virtosome-a novel cytosolic informative entity and intercellular messenger. *Cell Biochem Funct* **28**, 529-538 (2010). https://doi.org:10.1002/cbf.1690

455 Chiu, R. W. *et al.* Quantitative analysis of circulating mitochondrial DNA in plasma. *Clinical chemistry* **49**, 719-726 (2003).

456 Mittra, I., Nair, N. K. & Mishra, P. K. Nucleic acids in circulation: Are they harmful to the host? *Journal of Biosciences* **37**, 301-312 (2012). https://doi.org:10.1007/s12038-012-9192-8

457 Bendich, A., Wilczok, T. & Borenfreund, E. Circulating DNA as a Possible Factor in Oncogenesis. *Science* **148**, 374-376 (1965). https://doi.org:doi:10.1126/science.148.3668.374

458 Chelobanov, B. P., Laktionov, P. P. & Vlasov, V. V. Proteins involved in binding and cellular uptake of nucleic acids. *Biochemistry (Moscow)* **71**, 583-596 (2006). https://doi.org:10.1134/S0006297906060010

459 Soehnlein, O. & Tall, A. R. AIMing 2 treat atherosclerosis. *Nature Reviews Cardiology* **19**, 567-568 (2022). https://doi.org:10.1038/s41569-022-00755-0

460 Mondelo-Macía, P., Castro-Santos, P., Castillo-García, A., Muinelo-Romay, L. & Diaz-Peña, R. Circulating Free DNA and Its Emerging Role in Autoimmune Diseases. *J Pers Med* **11** (2021). https://doi.org:10.3390/jpm11020151

461 Kumari, P., Russo, A. J., Shivcharan, S. & Rathinam, V. A. AIM2 in health and disease: Inflammasome and beyond. *Immunol Rev* **297**, 83-95 (2020). https://doi.org:10.1111/imr.12903

462 Snyder, M. W., Kircher, M., Hill, A. J., Daza, R. M. & Shendure, J. Cell-free DNA Comprises an In Vivo Nucleosome Footprint that Informs Its Tissues-Of-Origin. *Cell* **164**, 57-68 (2016). https://doi.org:10.1016/j.cell.2015.11.050

463 Lo, Y. D., Han, D. S., Jiang, P. & Chiu, R. W. Epigenetics, fragmentomics, and topology of cell-free DNA in liquid biopsies. *Science* **372**, eaaw3616 (2021).

464 Kandoth, C. *et al.* Mutational landscape and significance across 12 major cancer types. *Nature* **502**, 333-339 (2013). https://doi.org:10.1038/nature12634

465 Jamshidi, A. *et al.* Evaluation of cell-free DNA approaches for multi-cancer early detection. *Cancer Cell* **40**, 1537-1549 e1512 (2022). https://doi.org:10.1016/j.ccell.2022.10.022

466 Ulz, P. *et al.* Inferring expressed genes by whole-genome sequencing of plasma DNA. *Nature Genetics* **48**, 1273-1278 (2016). https://doi.org:10.1038/ng.3648

467 Moss, J. *et al.* Comprehensive human cell-type methylation atlas reveals origins of circulating cell-free DNA in health and disease. *Nat Commun* **9**, 5068 (2018). https://doi.org:10.1038/s41467-018-07466-6

468 Sadeh, R. *et al.* ChIP-seq of plasma cell-free nucleosomes identifies gene expression programs of the cells of origin. *Nat Biotechnol* **39**, 586-598 (2021). https://doi.org:10.1038/s41587-020-00775-6

469 Jackstadt, R. *et al.* Epithelial NOTCH Signaling Rewires the Tumor Microenvironment of Colorectal Cancer to Drive Poor-Prognosis Subtypes and Metastasis. *Cancer Cell* **36**, 319-336 e317 (2019). https://doi.org:10.1016/j.ccell.2019.08.003

470 Go, S. *et al.* Tissue-resident NK cells support survival in pancreatic cancer through promotion 1 of cDC1-CD8T activity. *bioRxiv* **https://doi.org/10.1101/2023.10.14.56233** (2023).

471 East, J. E. *et al.* British Society of Gastroenterology position statement on serrated polyps in the colon and rectum. *Gut* **66**, 1181-1196 (2017). https://doi.org:10.1136/gutjnl-2017-314005

472 Junca, A. *et al.* Detection of Colorectal Cancer and Advanced Adenoma by Liquid Biopsy (Decalib Study): The ddPCR Challenge. *Cancers (Basel)* **12** (2020). https://doi.org:10.3390/cancers12061482

473 Galanopoulos, M. *et al.* Comparative Study of Mutations in Single Nucleotide Polymorphism Loci of KRAS and BRAF Genes in Patients Who Underwent Screening Colonoscopy, With and Without Premalignant Intestinal Polyps. *Anticancer Res* **37**, 651-657 (2017). https://doi.org:10.21873/anticanres.11360

474 Wojtukiewicz, M. Z., Sierko, E., Hempel, D., Tucker, S. C. & Honn, K. V. Platelets and cancer angiogenesis nexus. *Cancer Metastasis Rev* **36**, 249-262 (2017). https://doi.org:10.1007/s10555-017-9673-1

475 Shen, Z. *et al.* Platelet transcriptome identifies progressive markers and potential therapeutic targets in chronic myeloproliferative neoplasms. *Cell Rep Med* **2**, 100425 (2021). https://doi.org:10.1016/j.xcrm.2021.100425

476 Kleiveland, C. R. in *The Impact of Food Bioactives on Health* Ch. Chapter 15, 161-167 (2015).

477 Jahr, S. *et al.* DNA fragments in the blood plasma of cancer patients: quantitations and evidence for their origin from apoptotic and necrotic cells. *Cancer Res* **61**, 1659-1665 (2001).

478 Kim, E. S. *et al.* Blood-based tumor mutational burden as a biomarker for atezolizumab in non-small cell lung cancer: the phase 2 B-F1RST trial. *Nat Med* **28**, 939-945 (2022). https://doi.org:10.1038/s41591-022-01754-x

479 Rothwell, D. G. *et al.* Utility of ctDNA to support patient selection for early phase clinical trials: the TARGET study. *Nat Med* **25**, 738-743 (2019). https://doi.org:10.1038/s41591-019-0380-z

480 Merker, J. D. *et al.* Circulating Tumor DNA Analysis in Patients With Cancer: American Society of Clinical Oncology and College of American Pathologists Joint Review. *J Clin Oncol* **36**, 1631-1641 (2018). https://doi.org:10.1200/JCO.2017.76.8671

481 Hackshaw, A. *et al.* Estimating the population health impact of a multi-cancer early detection genomic blood test to complement existing screening in the US and UK. *Br J Cancer* **125**, 1432-1442 (2021). https://doi.org:10.1038/s41416-021-01498-4

482 Pons-Belda, O. D., Fernandez-Uriarte, A. & Diamandis, E. P. Multi Cancer Early Detection by Using Circulating Tumor DNA-The Galleri Test. Reply to Klein et al. The Promise of Multicancer Early Detection. Comment on "Pons-Belda et al. Can Circulating Tumor DNA Support a Successful Screening Test for Early Cancer Detection? The Grail Paradigm. Diagnostics 2021, 11, 2171". *Diagnostics (Basel)* **12** (2022). https://doi.org:10.3390/diagnostics12051244

483 Turnbull, C. *et al.* GRAIL-Galleri: why the special treatment? *The Lancet* **403**, 431-432 (2024). https://doi.org:10.1016/S0140-6736(23)02830-1

484 Hawwari, I. *et al.* Platelet-derived transcription factors licence human monocyte inflammation. *bioRxiv* (2023).

485 Anker, P., Lyautey, J., Lefort, F., Lederrey, C. & Stroun, M. Transformation of NIH/3T3 cells and SW 480 cells displaying K-ras mutation. *Comptes Rendus de L'academie des sciences. Serie III, Sciences de la vie* **317**, 869-874 (1994).

486 García-Olmo, D. C. *et al.* Cell-free nucleic acids circulating in the plasma of colorectal cancer patients induce the oncogenic transformation of susceptible cultured cells. *Cancer research* **70**, 560-567 (2010).

487 Trejo-Becerril, C. *et al.* Cancer progression mediated by horizontal gene transfer in an in vivo model. *PLoS One* **7**, e52754 (2012). https://doi.org:10.1371/journal.pone.0052754

488 Garcia-Olmo, D. C. & Garcia-Olmo, D. Biological role of cell-free nucleic acids in cancer: the theory of genometastasis. *Critical Reviews™ in Oncogenesis* **18** (2013).

489 Garcia-Olmo, D., Garcia-Olmo, D., Ontanon, J., Martinez, E. & Vallejo, M. Tumor DNA circulating in the plasma might play a role in metastasis. The hypothesis of the genometastasis. *Histology and histopathology* **14**, 1159-1164 (1999).

490 Hamam, D. *et al.* Transfer of malignant trait to BRCA1 deficient human fibroblasts following exposure to serum of cancer patients. *Journal of Experimental & Clinical Cancer Research* **35**, 1-12 (2016).

491 Souza, A. G. d. *et al.* Cell-free DNA promotes malignant transformation in non-tumor cells. *Scientific Reports* **10**, 21674 (2020). https://doi.org:10.1038/s41598-020-78766-5

492 de la Taille, A., Chen, M.-W., Burchardt, M., Chopin, D. K. & Buttyan, R. Apoptotic conversion: evidence for exchange of genetic information between prostate cancer cells mediated by apoptosis. *Cancer research* **59**, 5461-5463 (1999).

493 Cai, J. *et al.* Extracellular vesicle-mediated transfer of donor genomic DNA to recipient cells is a novel mechanism for genetic influence between cells. *Journal of molecular cell biology* **5**, 227-238 (2013).

494 Gahan, P. B. & Stroun, M. The virtosome—a novel cytosolic informative entity and intercellular messenger. *Cell biochemistry and function* **28**, 529-538 (2010).

495 Li, R., Wang, Y., Li, J. & Zhou, X. Extrachromosomal circular DNA (eccDNA): an emerging star in cancer. *Biomarker Research* **10**, 53 (2022). https://doi.org:10.1186/s40364-022-00399-9

496 Kim, H. *et al.* Extrachromosomal DNA is associated with oncogene amplification and poor outcome across multiple cancers. *Nature genetics* **52**, 891-897 (2020).

497 Zuo, S. *et al.* Extrachromosomal Circular DNA (eccDNA): From Chaos to Function. *Frontiers in Cell and Developmental Biology* **9** (2022). https://doi.org:10.3389/fcell.2021.792555

498 Ehnfors, J. *et al.* Horizontal transfer of tumor DNA to endothelial cells in vivo. *Cell Death & Differentiation* **16**, 749-757 (2009). https://doi.org:10.1038/cdd.2009.7

499 Brouns, S. L. N., Provenzale, I., van Geffen, J. P., van der Meijden, P. E. J. & Heemskerk, J. W. M. Localized endothelial-based control of platelet aggregation and coagulation under flow: A proof-of-principle vessel-on-a-chip study. *J Thromb Haemost* **18**, 931-941 (2020). https://doi.org:10.1111/jth.14719

500 Coenen, D. M., Mastenbroek, T. G. & Cosemans, J. M. E. M. Platelet interaction with activated endothelium: mechanistic insights from microfluidics. *Blood* **130**, 2819-2828 (2017). https://doi.org:10.1182/blood-2017-04-780825

501 Koche, R. P. *et al.* Extrachromosomal circular DNA drives oncogenic genome remodeling in neuroblastoma. *Nat Genet* **52**, 29-34 (2020). https://doi.org:10.1038/s41588-019-0547-z

502 Yang, L. *et al.* Extrachromosomal circular DNA: biogenesis, structure, functions and diseases. *Signal transduction and targeted therapy* **7**, 342 (2022).

503 Silva, L. M., Moutsopoulos, N., Bugge, T. H. & Doyle, A. Live Imaging and Quantification of Neutrophil Extracellular Trap Formation. *Curr Protoc* **1**, e157 (2021). https://doi.org:10.1002/cpz1.157

Appendix

Supplementary Figures

Chapter 3: Platelets contain DNA

A1 Platelet sequestration of DNA released by nucleated cells

Chapter 4: Mechanisms of DNA uptake by platelets

A2 PBS control for vesicle imaging

A3 Flow cytometric analysis of resting platelets

Chapter 5: Mechanisms of DNA uptake by platelets

A4 Comparison of total DNA isolated from platelets using two different extraction kits

A5 Comparison of DNA yield from platelet poor plasma and platelet rich plasma

Supplementary Tables

A1 Platelet wash buffer and HEPES-modified Tyrode's buffer

A2 Droplet digital PCR assays

A3 Antibodies and nucleic acid stains used for flow cytometry

A4 Platelet activation mixtures

A5 Details of synthetic DNA fragments synthesised

A6 Antibodies and nucleic acid stains used for microscopy

A7 Clinical information for the control cohort (n=14, including patients with ulcerative colitis, Crohn's disease and individuals on the bowel cancer screening programme)

A8 Clinical information for patients with pre-malignant sessile serrated lesions (n=34)

A9 Clinical information for patients with gastrointestinal carcinoma (n=15)

A10 Clinical information for patients with gastrointestinal carcinoma used for whole genome sequencing study (n=13)

A11 Clinical information for obstetric cohort (n=30)

A12 Clinical information for the immune thrombocytopenic purpura (ITP) and controls cohort (n=23)

Supplementary Videos

Video 1: Maternal platelets sequester male fetal DNA. 3D render of maternal platelet labelled with β-tubulin (blue), with positive signal for a Y-chromosome fluorescent *in situ* hybridization (FISH) probe (orange).

Video 2: A healthy donor platelet sequesters tumour- derived DNA. Live cell imaging video showing uptake of fluorescently labelled DNA (NUCLEAR-ID, magenta) from a COLO205 cell by a platelet (CD42 488, blue) from a healthy donor *in vitro*.

Video 3: Multiple platelets sequester COLO205 tumour- derived DNA. Live cell imaging video showing multiple platelets (CD42 488, blue) showing signal for fluorescently labelled DNA (NUCLEAR-ID, magenta) derived from COLO205 cells *in vitro*.

Video 4A and 4B: Healthy donor platelets physically interact with colorectal tumour cells. Live cell imaging of healthy donor platelets (CD42 488, green) extending filopodia towards the COLO205 cell (NUCLEAR-ID, red). The platelet appears to 'sample' tumour derived DNA over the 90-minute time course as indicated by the white arrows. Blue arrows show a potential DNA containing vesicle within the cytosol of the tumour cell.

Video 5: Platelets sequester tumour-derived, DNA bound histone proteins. A healthy donor platelet (CD42 AF88, green) incubated with H2B-mChr HEL cells sequesters tumour derived histones (red) and DNA (DAPI, blue) as shown by the white arrows.

Video 6: Platelets interact with DNA containing extracellular vesicles. 3D render and rotation video of a platelet (CD42 488, blue) with adherent extracellular vesicle (EV) (succinimidyl ester [SE], red) containing DNA (DAPI, yellow).

Video 7: Platelets internalise DNA containing extracellular vesicles. 3D render and rotation video of a platelet (CD42 488 blue) with internal extracellular vesicle (EV) (succinimidyl ester [SE], red) containing DNA (DAPI, yellow).

Supplementary Figures

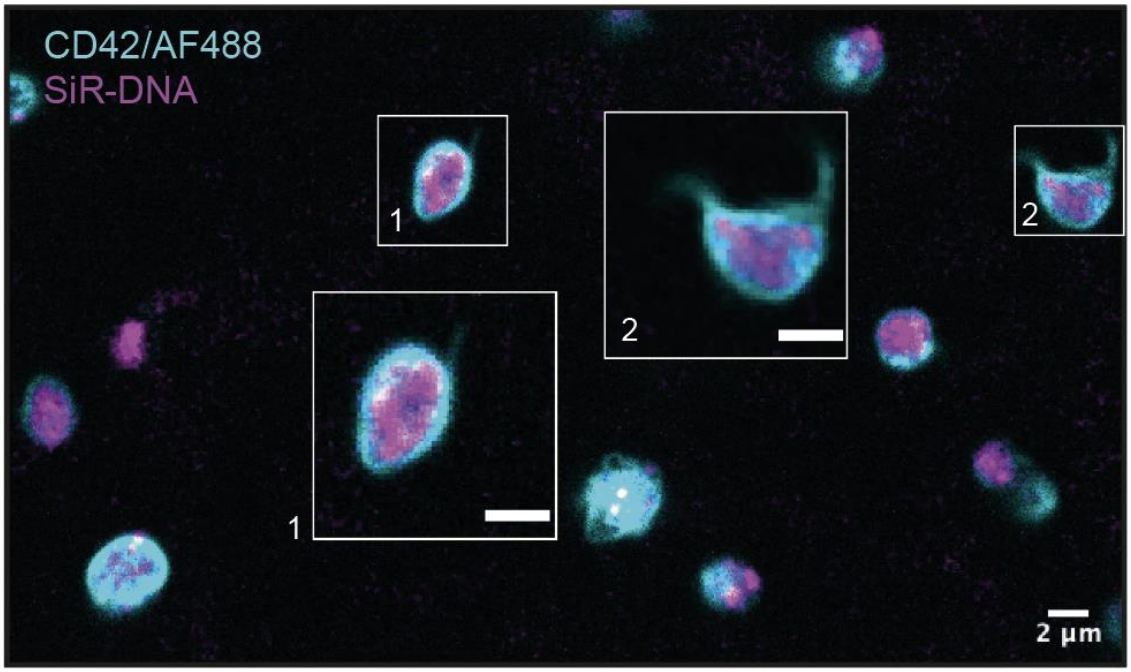


Figure A1: Platelet sequestration of DNA released by nucleated cells. COLO205 colorectal carcinoma cells were labelled with SiR-DNA (magenta), a highly specific DNA probe, washed 2x and co-incubated with healthy donor platelets labelled for CD42 (AF488, cyan). White box shows magnified region of fluorescently labelled, COLO205-derived DNA in platelets. Images acquired using a Zeiss Spinning Disk confocal, 63X magnification.

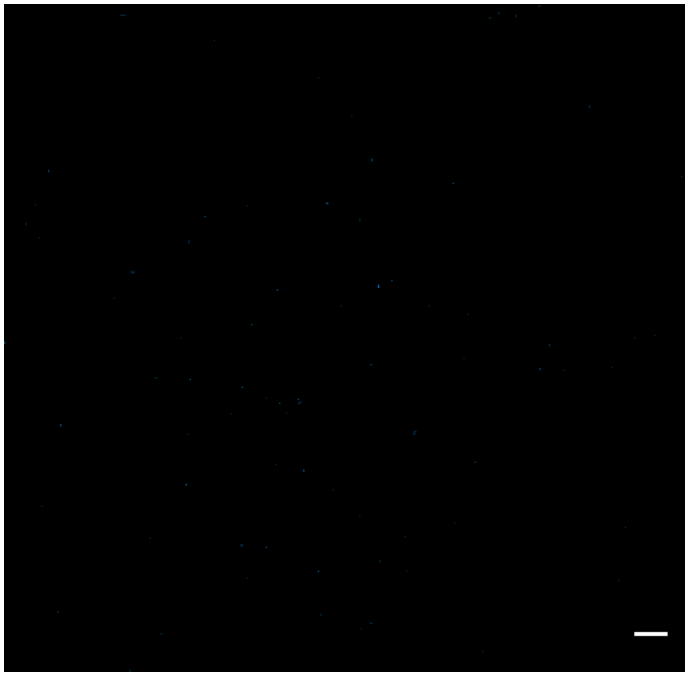


Figure A2: PBS control for vesicle imaging. PBS was used to show no autofluorescence or pelleting of debris when imaging apoptotic and non-apoptotic extracellular vesicles. Scale bar represents 2 µm.

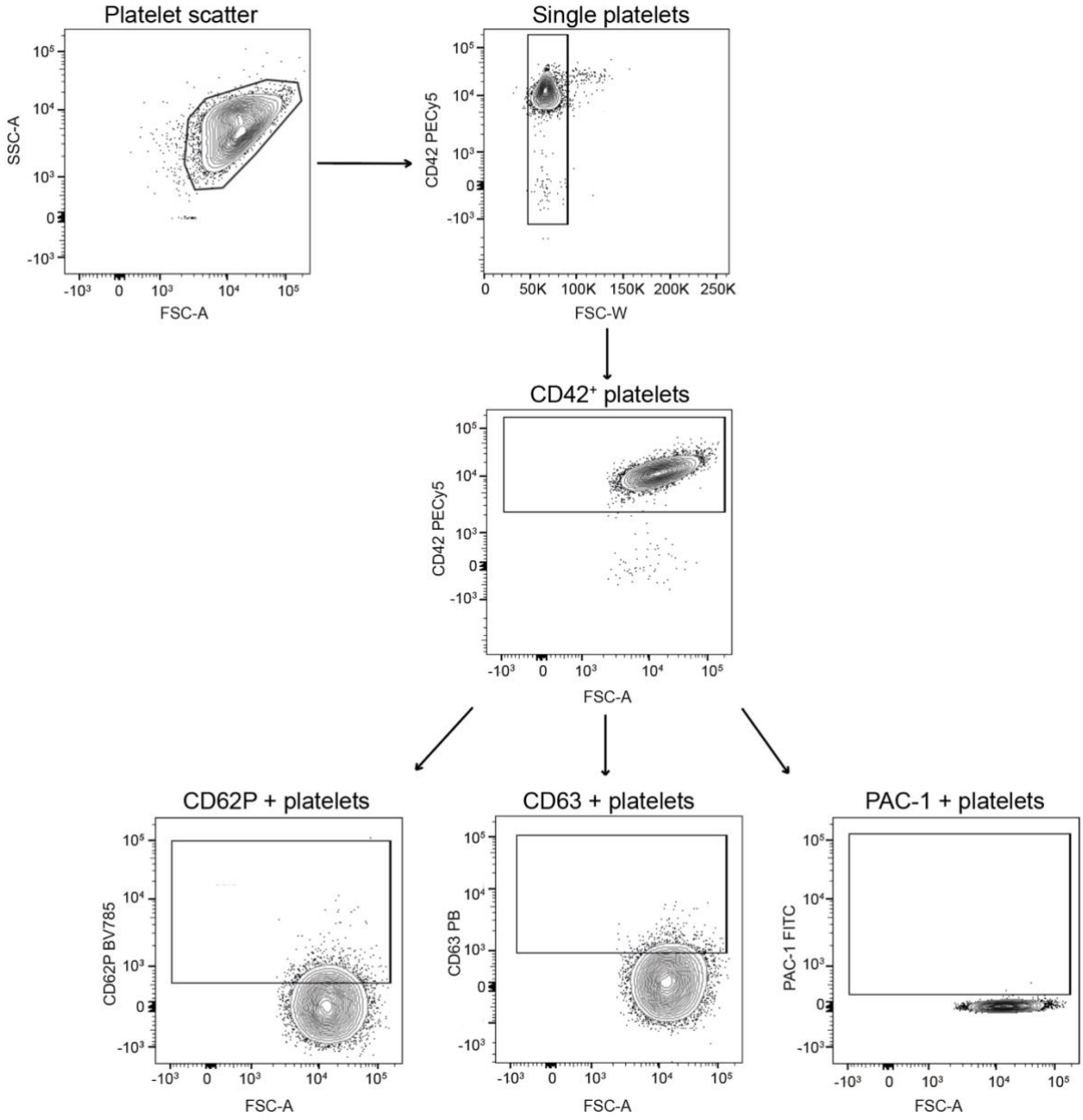


Figure A3: Flow cytometric analysis of resting platelets. CD42+ platelets show minimal CD62P, CD63 and PAC-1 staining.

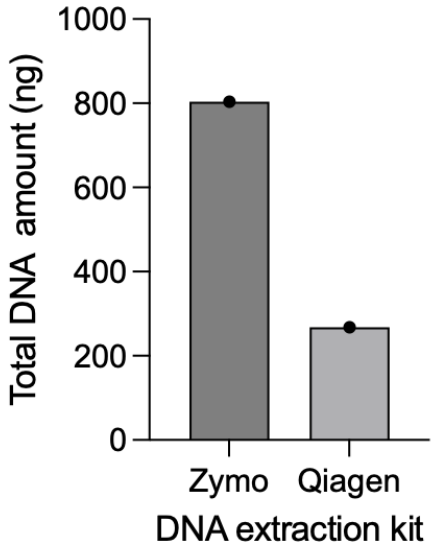


Figure A4: Comparison of total DNA isolated from platelets using two different extraction kits. Blood was taken from a healthy donor and platelet rich plasma (PRP) was collected. 2 x 1 ml aliquots of PRP were pelleted and subject to DNA extraction according to the manufacturers protocol. The kits used for DNA extraction were the Quick-DNA/RNA Microprep Plus Kit (Zymo, cat # D7005) and QIAamp Circulating Nucleic Acid Kit (Qiagen, cat # 55115). Extracted DNA was quantified using the Qubit.

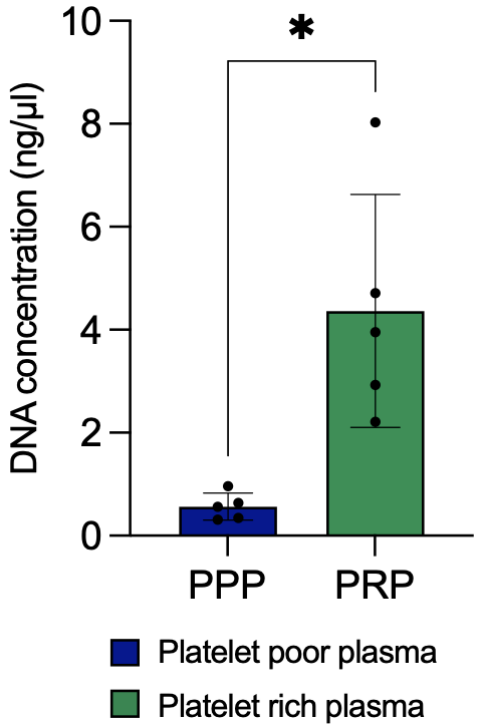


Figure A5: Comparison of DNA yield from platelet poor plasma and platelet rich plasma. Plot comparing the concentration of DNA (ng/µl) in equal volumes of platelet poor plasma (PPP) and platelet rich plasma (PRP) from 5 patients recruited to the SCAN pathway. Plot shows mean ± SD, * $p<0.05$ for a paired t test, n= 5 patients.

Supplementary Tables

Table A1: Platelet wash buffer and HEPES-modified Tyrode's buffer.

Material	Catalogue number	Company	Preparation
Prostaglandin (PGE1)	538903	Calbiochem*	Dilute 1mg of PGE1 in 1ml 100% EtOH (STOCK: 1mg/ml PGE1). Store at -20°C (Target: 100ng/ml, 0.1µl stock + 1ml PWB).
Platelet Wash Buffer (PWB) (1L)			Dilute to 1L with sterile water, ensure at pH 7.4. Store at RT. This buffer is supplemented with 100ng/ml PGE1 right before use.
10 mM sodium citrate: 2.94g	S1804-500G	Sigma Aldrich^	
150 mM sodium chloride: 8.77g	Sigma S9888-1KG	Sigma Aldrich^	
1 mM EDTA: 0.372g	Sigma EDS-100G	Sigma Aldrich^	
1% (w/v) Dextrose: 10g	Sigma D9434-250G	Sigma Aldrich^	
HEPES Buffered-Tyrode Solution (1L)			
140 mM NaCl: 8.140g	S9888-1KG	Sigma Aldrich^	Dilute to 1L with sterile water. Sterile-filter and store at 4°C. Remember to pre-warm to 37°C before use.
6.1 mM KCl: 0.456g	P9333-500G	Sigma Aldrich^	
2.4 mM MgSO4.7H2O: 0.586g	63138-250G	Sigma Aldrich^	
1.7 mM Na2HPO4: 0.241g	S7907-100G	Sigma Aldrich^	
5.8 mM NaHEPES: 1.510g	H7006-25G	Sigma Aldrich^	
Bring pH to 7.4 and add:			
0.35% BSA: 3.500g	A9418-50G	Sigma Aldrich^	
0.10% Dextrose: 1.020g	D9434-250G	Sigma Aldrich^	

* Calibiochem, San Diego, US-CA

^ Sigma Aldrich, St. Louis, US-MO

Table A2: Droplet digital PCR assays.

Assay type	**Assay name**	**Assay ID**	**Positive control DNA**	**Negative control DNA**
Mutation Detection Single Tube	*PIK3CA* p.H1047R	dHsaMDV2010077	HCT116 cells	HEL cells
Mutation Detection Single Tube	*TP53* p.R273H	dHsaMDV2010109	HT29 cells	HEL cells
Mutation Detection Single Tube	*BRAF* p.V600E c.1799T>A	dHsaMDV2010027	COLO205 cells	HEL cells
Mutation Detection Two Tube	*KRAS* p.G12D c.35G>A	dHsaCP2500596	CCRF-CEM cells	HEL cells
Copy Number Determination	ChrY	dHsaCP2500472 dHsaCP2506653	Male granulocytes	HEY cells
Designed by Nikolaos Sousos	*JAK2* p.V617F		HEL cells	MARIMO cells

Table A3: Flow cytometry antibodies used for haematopoietic lineage panel, platelet activation panel and analysis of DNA and RNA content.

Flow cytometry					
Antigen	**Clone**	**Conjugate**	**Dilution**	**Company**	**Catalogue number**
CD42b	HIP1	FITC	1:20	BioLegend‡	303903
CD42	HIP1	PeCy7	1:20	BioLegend‡	303916
CD41	HIP8	PE-Cyanine7	1:30	BioLegend‡	303718
CD3	SK7	PE	1:20	BioLegend‡	344805
CD3	OKT3	BV421	1:20	BioLegend‡	317344
CD11b	ICRF44	APC	1:20	BioLegend‡	301309
CD33	WM53	APC	1:20	BioLegend‡	303407
CD19	HIB19	APC-Cyanine7	1:20	BioLegend‡	302218
CD235a	HIR2	BV650	1:20	BD Biosciences§	740583
CD235a	HIR2	FITC	1:20	Invitrogen™#	11-9987-82
DAPI (4',6-Diamidino-2-Phenylindole, Dilactate)			1:100*	Invitrogen™#	D3571
CD63	H5C6	PB	1:20	BioLegend‡	353012
CD62P	AK4	BV785	1:20	BioLegend‡	304941
SYTO™ 13 Green Fluorescent Nucleic Acid Stain			1:20	Invitrogen™#	S7575
DRAQ5™ Fluorescent Probe Solution			1:1200	BioLegend‡	424101

*Viability stain, previously diluted 1:100 from 5mg/ml stock solution.

§Becton, Dickinson and Company, Franklin Lakes, US-NJ

‡BioLegend, San Diego, US-CA

#Thermo Fisher Scientific Inc., Waltham, US-MA

Table A4: Reagents used to assess platelet reactivity

	Resting mix	**TRAP-6 activation mix**			
Starting concentration (μM)	0	5	10	50	100
Final concentration (μM)	0	0.5	1	5	10
	Volume (μl)				
TRAP-6* (1 mM)	0	2.5	5	25	50
Calcium^ (1M)	10	10	10	10	10
HEPES-modified Tyrode's buffer	490	487.5	485	465	440
Total volume (μl)	500	500	500	500	500

* Bachem AG, cat # 4031274.0025

^ Sigma Aldrich, cat # 21115-100ML

Table A5: Details of synthetic DNA fragments synthesised.

Fragment Length (base pairs)	(ss) DNA sequence (5' → 3')
128	GCCTGCTGAAAATGACTGAGTGCCCCCACTTCCACTATGTTGT GGTGGTTGGAGCTGATGGCGTAGGCAAGAGCGCCTTGACGAT ACAGCTAATTCAGAATCACTTTGTGGATGAGTATGACCCTACG
260	GCCTGCTGAAAATGACTGAGTGCCCCCACTTCCACTATGGACA ACTTCATGAACTTTGCCCACTAAGGTAGGTACATCAAAGCTGCC CTATGGCTTCTGAAAATAACAGACACCCTAATAGATGGTTTTGG AGCTGATGGCGTTTCAGGGCCACTACAACAATTCAATCTCAATC CTTTGGACTTCATTCCTGCTGCCCAGGCCACTGGTGCCTCAGT AGGAATTTTCAAAGGTGCGGTGTGGATGAGTATGACCCTACG
367	GCCTGCTGAAAATGACTGAGTGCCCCCACTTCAAACTTTGTTTC CACTATGGACAACTTCATGAACTTTGCCCACTAAGGTAGGTACA TCAAAGCTGCCCTATGGCTTTCTTCCCCGGGACTGAAAATAAC AGACACCATAGTGGGATTTAAACTAATAGATGGTTTTGGAGCTG ATGGCGTTTCAGGGCCACTACAACAATTCAATCTCAATCCTTTG GACTTCATTCCTGCTGCCCAGGCCACTGGTGCCTCAGTAGGAA TTTTCAAAATTAGTGTGAACAGACTCAACATTTATTCAGTGCTTG TCATATTCTGGGAATTACACTAGGCACTCAGGGTGCGGTGTGG ATGAGTATGACCCTACG
657	GCCTGCTGAAAATGACTGAGTGCCAGTCTTGGGCAAATTGTGC AAGAGGTAAAATTTATATTTCAGTATCCATTCTCCCATTTCAGGA CTCCCCTCCAACATTATGCTGGCTTTCAGCCTGTCTCTCACCTG CCCATCACTTAGTGTAGTTTTAATAATTTCCCCCACTTCAAACTT TGTTTCCACTATGGACAACTTCATGAACTTTGCCCACTAAGGTA GGTACATCAAAGCTGCCCTATGGCTTTCTTCCCCGGGACTGAA AATAACAGACACCATAGTGGGATTTAAACTAATAGATGGTTTTG GAGCTGATGGCGTTTCAGGGCCACTACAACAATTCAATCTCAA TCCTTTGGACTTCATTCCTGCTGCCCAGGCCACTGGTGCCTCA GTAGGAATTTTCAAAATTAGTGTGAACAGACAGAGCACAGTCCA GTGGAAGGTGAGCTTAATCTTCATCTAGCCATCATCATGGTAAG TGATAGATTCTATTGTTTTAATAAATACAGTCTAACAATGAAAAA CACTTCGAAGTTTCAATCATAAAGCTGTCTTTTTAAAAATTTTAT TTACTCAACATTTATTCAGTGCTTGTCATATTCTGGGAATTACAC TAGGCACTCAGGGTGCGGTGTGGATGAGTATGACCCTACG

Fragment Length (base pairs)	Stand	(ds) DNA sequence (5' → 3')
90	Top	GCCTGCTGAAAATGACTGAGTGCCCCCCCCTTTG GAGCTGATGGCGTTTCAGGGCCACTACAACAACG TGTGGATGAGTATGACCCTACG
	Compliment	CGT AGG GTC ATA CTC ATC CAC ACG TTG TTG TAG TGG CCC TGA AAC GCC ATC AGC TCC AAA GGG GGG GGC ACT CAG TCA TTT TCA GCA GGC

Table A6: Antibodies and nucleic acid stains used for microscopy.

Microscopy					
Antigen	**Clone**	**Conjugate**	**Dilution**	**Company**	**Catalogue number**
SiR-DNA			1:500	Spirochromeˆ	SC007
NUCLEAR-ID Red DNA stain			1:2000	Enzo Life Sciences~	ENZ-2406
DRAQ5 Fluorescent Probe Solution			1:1000	BioLegend‡	424101
Hoechst 33342, Trihydrochloride Trihydrate			1:1000	Invitrogen™#	H3570
Primary mouse anti human CD63	MX-49.129.5	Unconjugated	1:50	Abcam†	ab193349
Primary mouse anti human LAMP-2	H4B4	Unconjugated	1:100	Abcam†	ab25631
Primary mouse anti human CD62P	AK-6	Unconjugated	1:55	Abcam†	ab6632
Primary rabbit anti human CD81	EPR21916	Unconjugated	1:100	Abcam†	ab219209
Primary rabbit IgG anti human TOM20 (D8T4N)	Recombinant (D8T4N)	Unconjugated	1:200	Cell signalling technology¦	42406S
Primary Anti-β-Tubulin, mouse monoclonal	TUB 2.1	Unconjugated	1:130	Sigma Aldrich°	T5201
Secondary Goat Anti-Mouse IgG H&L		AF568	1:500 or 1:1000	Abcam†	ab175473
Secondary Goat anti-rabbit IgG H&L		AF488	1:500	Cell signalling technology¦	4412
Secondary Donkey Anti-Mouse IgG H&L		AF405	1:1000	Abcam†	ab175658

‡BioLegend, San Diego, US-CA

#Thermo Fisher Scientific Inc., Waltham, US-MA

ˆSpirochrome, Switzerland

~Enzo Life Sciences (UK) LTD, UK

†Abcam, Cambridge, UK

¦Cell Signalling Technology, Inc., Danvers, US-MA

°Sigma Aldrich, St. Louis, US-MO

Table A7: Clinical information for the control cohort (n=14, including patients with ulcerative colitis, Crohn's disease and individuals on the bowel cancer screening programme).

Patient ID	Blood collection tube	Age (years)	Gender	Platelet count ($x10^9$/L)
NC/001	Streck	35	M	N/A
NC/003	Streck	63	M	303
NC/004	Streck	66	F	211
NC/005	Streck	65	M	330
NC/006	Streck	53	F	282
NC/007	Streck	28	F	200
NC/008	Streck	42	M	343
NC/009	Streck	61	M	255
NC/010	Streck	41	F	398
NC/011	Streck	69	F	216
NC/012	Streck	28	M	270
NC/013	Streck	47	F	398
NC/015	Streck	72	M	N/A
NC/018	Streck	81	M	137

F: Female, M: Male, N/A: Not available, NC: Non-cancer control

Table A8: Clinical information for patients with pre-malignant sessile serrated lesions (n=34).

Patient ID	Blood collection tube	Age (years)	Gender	Platelet count (x10^9/L)	Diagnosis
SSL/001	Streck	43	F	260	Confirmed SSL and on surveillance
SSL/002	Streck	38	F	N/A	Confirmed SSL and on surveillance
SSL/003	Streck	37	M	274	Confirmed SSL and on surveillance
SSL/004	Streck	73	M	205	Confirmed SSL and on surveillance
SSL/005	Streck	41	M	L 92	Confirmed SSL and on surveillance for SSLs as well as previous surgery for CRC
SSL/006	Streck	52	F	351	Confirmed SSL and on surveillance
SSL/007	Streck	75	M	270	Confirmed SSL and on surveillance
SSL/007.2	Streck	76	M	N/A	Confirmed SSL and on surveillance
SSL/008	Streck	38	M	N/A	Surveillance after previous polyps, family history of CRC and SSL
SSL/009	Streck	35	F	N/A	Confirmed SSL and on surveillance
SSL/010	Streck	43	F	188	Confirmed SSL and on surveillance
SSL/012	Streck	44	F	317	Not confirmed SSL but on surveillance
SSL/013	Streck	75	F	348	Confirmed SSL and on surveillance
SSL/018	Streck	41	F	276	Confirmed SSL and on surveillance
SSL/019	Streck	48	F	208	Confirmed SSL and on surveillance
SSL/022	Streck	43	F	N/A	Confirmed SSL and on surveillance
SSL/024	Streck	40	F	246	Confirmed SSL and on surveillance
SSL/025	Streck	43	F	N/A	Confirmed SSL and on surveillance
SSL/026	Streck	43	M	N/A	Confirmed SSL and on surveillance
SSL/027	Streck	70	F	N/A	Confirmed SSL and on surveillance
SSL/028*	Streck	73	F	N/A	Confirmed SSL and on surveillance
SSL/029*	Streck	43	M	N/A	Confirmed SSL and on surveillance
SSL/030*	Streck	42	M	N/A	Confirmed SSL and on surveillance
SSL/30.2	Streck	43	M	215	Confirmed SSL and on surveillance
SSL/031	Streck	62	F	229	Confirmed SSL and on surveillance
SSL/032	Streck	43	M	N/A	Confirmed SSL and on surveillance
SSL/033	Streck	25	F	N/A	Familial adenomatous polyposis and on surveillance
SSL/034	Streck	41	M	226	Confirmed SSL and on surveillance
SSL/035	Streck	40	M	251	Confirmed SSL and on surveillance
SSL/037	Streck	44	F	N/A	Confirmed SSL and on surveillance
SSL/038	Streck	45	M	N/A	Confirmed SSL and on surveillance
SSL/039	Streck	41	F	N/A	Confirmed SSL and on surveillance
SSL/040	Streck	56	F	278	Confirmed SSL and on surveillance
SSL/041	Streck	59	M	251	Confirmed SSL and on surveillance

* Sample did not pass QC
Note: Red text highlights SSL patients where BRAFV600E was detected in either cfDNA or pDNA
CRC: Colorectal cancer, F: Female, N/A: Not available, M: Male, SSL: Sessile serrated lesions

Table A9: Clinical information for patients with gastrointestinal carcinoma (n=15).

Patient ID	Blood collection tube	Cancer type	Platelet count (x10^9/L)	Tumour information (location, size)	TNM staging	Identified mutations	Therapy
C/024	Streck	Colorectal	332	Ascending colon, caecum with intramural lymphatic invasion. Tumour size: 5.5 cm	T4aN1aMx	None identified	N/A
C/025	Streck	Colorectal	248	Sigmoid cancer with liver metastasis	T3 N2 M1	*TP53* c.578A>G p.(His193Arg)	4 cycles of chemotherapy (Oxaliplatin/Capecitabine)
C/027	EDTA	Colorectal	235	Transverse colon	T3 N0 M0	*TP53* c.733G>A p.(Gly2455Ser)	N/A
C/028	EDTA	Colorectal	323	Ascending colon	T2N1M0	*TP53* c.659A>G p.(Tyr220Cys)	N/A
C/029	EDTA	Colorectal	183	Rectosigmoid tumour	pT4a pN1b Ly1 V1 R0 (T4a N1 Mx)	*TP53* c.742C>T p.(Arg248Trp). *KRAS* c.37G>T p.(Gly13Cys)	N/A
C/031	Streck	Colorectal	317	Ascending colon. Tumour size: 22 mm	pT2 pN0 Ly0 V0 R0 (T2N0Mx)	*KRAS*: c.34G>T p.(Gly12Cys). *PIK3CA*: c.1258T>C p.(Cys420Arg).*TP53*: c.691A>C p.(Thr231Pro)	N/A
O/030	Streck	Oesophageal	193	Proximal/mid oesophagus. Tumour size: 3.5 cm	R1 pT3 L1 V0 Pn0 N1 (2/19) M0 (T2N1M0)	None identified	Neoadjuvant chemotherapy (cisplatin and fluorouracil) 2 cycles prior to surgery.
O/019	EDTA	Oesophageal	225	Oesophagogastric junction. Tumour size: 63 mm (30 mm above + 33 mm below)	R0 ypT1a L0 V0 Pn0 N0 (T1aN0mx)	None identified	Neoadjuvant FLOT chemotherapy, 4 cycles 2 months prior to blood sampling

Table A9: Clinical information for patients with gastrointestinal carcinoma (n=15) continued.

Patient ID	Blood collection tube	Cancer type	Platelet count ($x10^9$/L)	Tumour information (location, size)	TNM staging	Identified mutations	Therapy
O/023	EDTA	Oesophageal	261	Gastric cardia just below GOJ. Tumour size: 45 mm	R1 ypT4a L1 Pn1 N2 (4/35) M1 (T4aN2M1)	None identified	Neoadjuvant FLOT chemotherapy, 4 cycles 1 month prior to blood sampling
O/024	Streck	Oesophageal	189	Tumour at GOJ, size: 30 mm	R0 ypT3 L0 V0 Pn0 N0 (0/22) M0 (T3N0M0)	None identified	Post neoadjuvant FLOT chemotherapy and radiotherapy commenced after blood sampling
O/025	Streck	Oesophageal		N/A	N/A	N/A	N/A
O/026	Streck	Oesophageal	270	Tumour at lower 3rd distal oesophagus and GOJ. Tumour size: 30 mm x 45 mm	R0 ypT3 L1 V0 Pn1 N2 (T3N2M0)	None identified	Neoadjuvant FLOT and 5FU, 4 cycles 3 months prior to blood sampling
O/027	Streck	Oesophageal	254	GOJ. No tumour present, regression from chemotherapy	R0 ypT0 L0 V0 Pn0 N0 (0/40) M0 (Original staging was T3 before chemotherapy)	None identified	Chemotherapy finished 11 weeks prior to bloods sample
O/028	Streck	Oesophageal	273	GOJ - Tumour size: 30x35 mm tumour	T3 N0 M0 at time of bloods. T3N3M0 after surgery	None identified	N/A
P/009	Streck	Pancreatic	243	Distal pancreas, tumour size: 20 mm	T1N0Mx	None identified	N/A

APER: Abdominoperineal excision of rectum, cm: Centimeter, FLOT: Combination of chemotherapy drugs: docetaxel, oxaliplatin, 5-fluorouracil and leucovorin, R-CHOP: Combination of chemotherapy: riituximab, cyclophosphamide, hydroxydaunorubicin hydrochloride (doxorubicin hydrochloride), vincristine (Oncovin) and prednisone, MMR: Mismatch repair

*Copy number variations were detected in the cfDNA and s-pDNA for this patient

** Sample used for targeted mutational analysis

Table A10: Clinical information for patients with gastrointestinal carcinoma used for whole genome sequencing study (n=13).

Patient ID	Blood collection tube	Cancer type	Platelet count (x10^9/L)	Tumour information (location, size)	TNM staging	Identified mutations	Therapy
C/023	Streck	Colorectal	232	Caecum	T4 N0 M0	loss of *MLH1,PMS2* IHC staining	Surgery and curative right hemicolectomy
C/026	EDTA	Colorectal	207	Rectum	T4a N1 M0	*KRAS* c.35G>A p.(Gly12Asp)	Surgery & neoadjuvant chemoradiotherapy
O/020	EDTA	Oesophageal	249	Distal oesophagus	T2 N1 M0	None identified	Surgery and neoadjuvant chemoradiotherapy
O/021	EDTA	Oesophageal	199	Distal oesophagus	T2 N0 M0	None identified	Surgery and neoadjuvant chemotherapy
O/022	EDTA	Oesophageal	304	Gastric antrum	T4a N0 M0	None identified	Surgery
P/008*	Streck	Pancreatic	266	Large 11 cm mass involving pancreatic tail, spleen, stomach and transverse colon	T4 N1 M0	None identified	No therapy prior to blood sampling
P/017	Streck	Pancreatic	205	Pancreatic ductal adenocarcinoma	pT3 N1 (2/3) L1V1	None identified	Curative intent surgery
Combat CRC 008	Streck	Colorectal	247	Colon (ascending)	T3 N2 M0	loss of *MSH2* and *MSH6*, *KRAS* c.38G>A p.(Gly13Asp) detected in the transverse tumour	unchecked
Combat CRC 009	Streck	Colorectal	330	Colon (hepatic flexure)	T3 N0 M0	MMR immunohistochemistry not performed	unchecked
Combat CRC 010	Streck	Colorectal	235	Colon (ascending)	T3 N0 M0	loss of *MLH1* and *PMS2*, *PIK3CA* c.3140A>G p.(His1047Arf)	unchecked
Combat CRC 011	Streck	Colorectal	150	Colon (sigmoid)	Unavailable	*KRAS* c.183A>Tp.(Gln61His), *TP53* c.1024C>T p.(Arg342*)	Neo-adjuvant chemotherapy (oxaliplatin - capecitabine)
Combat CRC 012**	Streck	Colorectal	346	Colon (sigmoid)	T3 N0 M0	*NRAS* codon 12 variant detected	unchecked
Combat CRC 013	Streck	Colorectal	460	Caecum	T3 N2 M0	*KRAS* variant	unchecked

Table A11: Clinical information for obstetric cohort (n=30).

Patient ID	Blood collection tube	Age (years)	Gender	Gestation (weeks + days)	Neonatal sex
AS/001	Streck	40	F	39 + 0	M
AS/002	Streck	32	F	39 + 3	F
AS/003	Streck	34	F	39 + 1	M
AS/004	Streck	34	F	40 + 4	F
AS/005	Streck	24	F	39 + 6	M
AS/006	Streck	39	F	40 + 4	F
AS/007	Streck	29	F	39 + 4	F
AS/008	Streck	32	F	39 + 2	M
AS/009	Streck	34	F	41 + 5	M
AS/010	Streck	32	F	35 + 4	M
AS/011	Streck	34	F	40 + 0	F
AS/012	Streck	33	F	35 + 1	F
AS/013	Streck	47	F	38 + 2	M
AS/014	Streck	40	F	39 + 0	M
AS/015	Streck	37	F	39 + 3	F
AS/016	Streck	40	F	39 + 0	M
AS/017	Streck	33	F	39 + 0	F
AS/018	Streck	29	F	41 + 3	F
AS/019	Streck	34	F	39 + 0	M
AS/020	Streck	34	F	39 + 0	M
PN/024	Streck	31	F	PD + 1	M
PN/025	Streck	36	F	PD + 2	M
PN/026	Streck	33	F	PD + 1	M
PN/027	Streck	31	F	PD + 1	F
PN/028	Streck	32	F	PD + 2	M
PN/029	Streck	40	F	PD + 1	M
PN/030	Streck	32	F	PD + 1	M
PN/031	Streck	34	F	PD + 1	M
PN/032	Streck	24	F	PD + 1	M
PN/033	Streck	31	F	PD + 2	M

AS: Antenatal sample, F: Female, M: Male, PD: Post delivery, PN: Postnatal

Table A12: Clinical information for the immune thrombocytopenic purpura (ITP) and controls cohort (n=23).

Patient ID	Blood collection tube	Platelet count (x10^9/L)
ITP/001	Streck	3
ITP/002	Streck	490
ITP/003	Streck	18
ITP/004	Streck	31
ITP/005	Streck	157
ITP/007	Streck	35
ITP/008	Streck	34
ITP/014	Streck	80
ITP/015	Streck	17
ITP/016	Streck	21
ITP/017	Streck	42
ITP/018	Streck	231
ITP/020	Streck	12
ITP/021	Streck	76
ITP/022	Streck	10
ITP/023	Streck	2
ITP/024	Streck	18
ITP/025	Streck	27
ITP/026	Streck	256
ITP/027	Streck	52
ITP/028	Streck	375
ITP/029	Streck	465
ITP/030	Streck	335

ITP: immune thrombocytopenic purpura

The End